NASA Contractor Report CR-201353

Final Report on the Evaluation of the Emergency Response Dose Assessment System (ERDAS)

Prepared By:
Applied Meteorology Unit

Prepared for:
Kennedy Space Center
Under Contract NAS10-11844

NASA
National Aeronautics and
Space Administration

Office of Management

Scientific and Technical
Information Program

1996

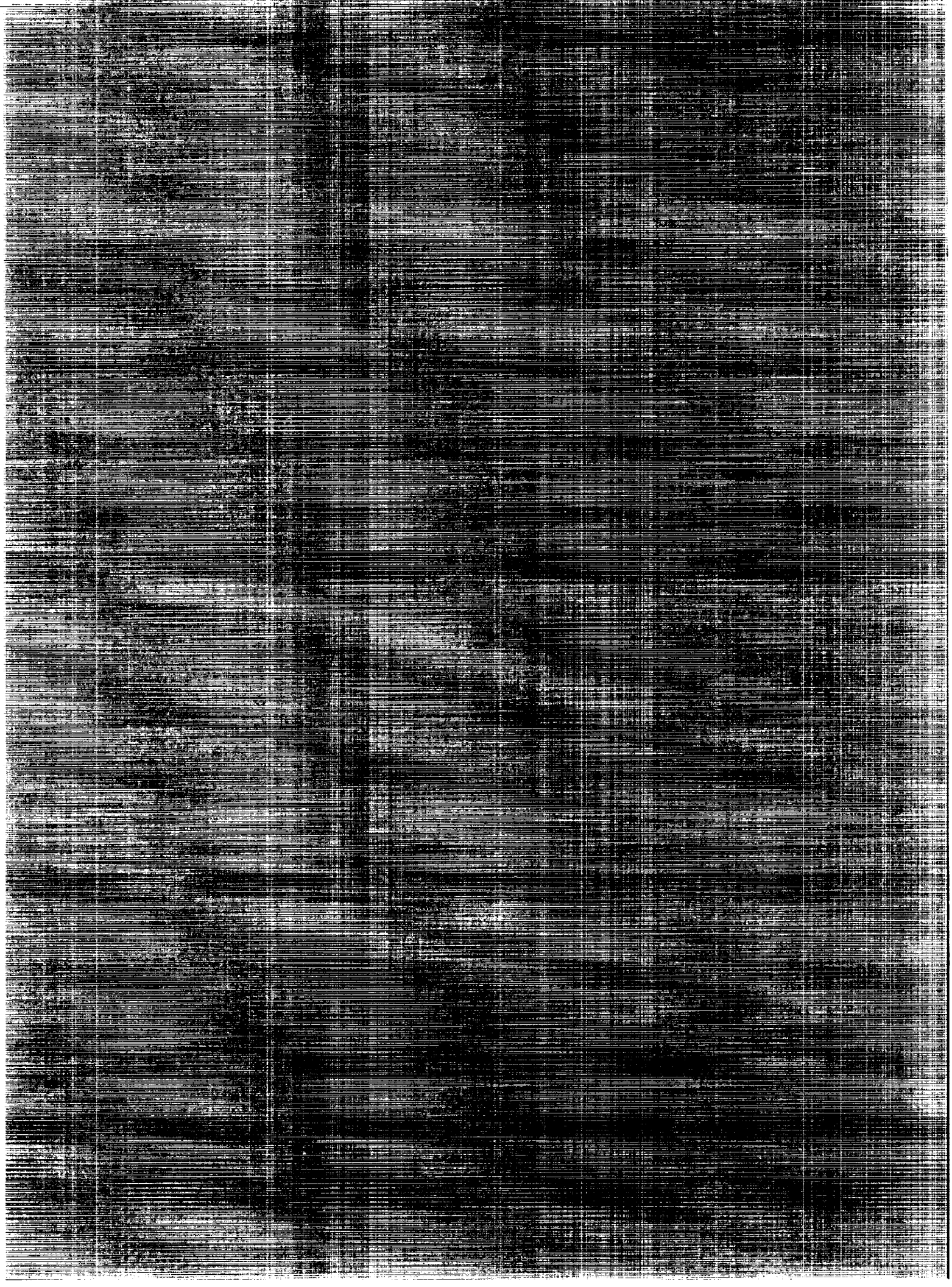

NASA Contractor Report CR-201353

Final Report on the Evaluation of the Emergency Response Dose Assessment System (ERDAS)

Prepared By:
Applied Meteorology Unit

Prepared for:
Kennedy Space Center
Under Contract NAS10-11844

NASA
National Aeronautics and
Space Administration

Office of Management

Scientific and Technical
Information Program

1996

Attributes and Acknowledgments:

NASA/KSC POC:
Dr. Francis J. Merceret
PH-B3

Applied Meteorology Unit (AMU)

Randolph J. Evans, primary author
Winifred C. Lambert
John T. Manobianco
Gregory E. Taylor
Mark M. Wheeler
Ann M. Yersavich

Table of Contents

List of Figures

List of Tables

Executive Summary

The Applied Meteorology Unit (AMU) has evaluated the Emergency Response Dose Assessment System (ERDAS) located in the Range Operations Control Center (ROCC) at CCAS/KSC since its installation in March 1994. Before the Air Force's 45th Space Wing including Range Safety (45 SW) , the Weather Squadron (45 WS) and the Eastern Range Program Office (SMC/CW-OLAK) accepts ERDAS as an operational emergency response system, they must determine its value, accuracy and reliability. In support of this requirement, the AMU has evaluated ERDAS in a near-operational environment. This will enable the 45th Space Wing to determine if and how it should be transitioned to an operational environment.

ERDAS is a prototype software and hardware system configured to produce routine mesoscale meteorological forecasts and enhanced dispersion estimates on an operational basis for the KSC/CCAS region. ERDAS includes two major software systems run and accessed through a graphical user interface. The first software system is the Regional Atmospheric Modeling System (RAMS), a three-dimensional, multiple nested grid prognostic mesoscale model. The second software system is the Hybrid Particle and Concentration Transport (HYPACT) model, a pollutant trajectory and concentration model. ERDAS also runs the Rocket Exhaust Effluent Diffusion Model (REEDM).

ASTeR, Inc. (now called Mission Research Corporation/ASTER division) developed ERDAS for the Air Force for the purpose of providing emergency response guidance to operations at KSC/CCAS in case of an accidental hazardous material release or an aborted vehicle launch. The ERDAS development occurred during the period 1989 to 1994 under Phase I and II Small Business Innovative Research contracts. ERDAS was delivered to the Air Force's Range Operations Control Center (ROCC) in March 1994. The AMU was tasked with keeping ERDAS running and with evaluating ERDAS during the period March 1994 to December 1995. The development and evaluation of ERDAS was funded by the Air Force Space and Missile Systems Center, Los Angeles Air Force Base.

The evaluation of ERDAS included:

- Evaluation of the sea breeze predictions
- Comparison of launch plume location and concentration predictions.
- Case study of a toxic release.
- Evaluation of model sensitivity to varying input parameters.
- Evaluation of the user interface.
- Assessment of ERDAS's operational capabilities.
- Comparison of ERDAS models to Ocean Breeze Dry Gulch diffusion model.

Conclusions

1. Some of the principal conclusions of the ERDAS meteorological model evaluation were:

    - RAMS predicted the 3-dimensional wind field reasonably well during non-cloudy conditions but slightly overpredicted surface wind speeds due to the height of lowest vertical grid point.

    - RAMS did reasonably well at predicting wind direction shifts due to passage of sea breeze fronts during non-cloudy conditions but not during cloudy ones. This result is not surprising since the modules used for predicting explicit cloud microphysics are disabled to allow the model to run in a reasonable time on the current computer hardware.

- RAMS was very sensitive to the soil moisture parameter for predicting the location and intensity of the sea breeze at KSC/CCAS.

- For cases where RAMS predicted a sea breeze, it predicted passage of sea breeze one to three hours earlier than observed in approximately 60% to 70% of the cases. Result may be due to parameterization of soil moisture, sea surface temperatures and/or land use classification.

2. Some of the principal conclusions of the ERDAS diffusion model evaluation were:

   - HYPACT-predicted plume trajectory from 3 May 94 Titan launch closely followed the observed trajectory with some variation over time. This launch was the only launch that significant observed plume data was available during the ERDAS evaluation.

   - Use of REEDM model to calculate the source term for HYPACT was very promising for use in launch plume modeling but some modifications to technique are needed. HYPACT should be modified to handle buoyant plumes rather than treating the plumes as passive tracers.

   - Launch plumes predicted by HYPACT overlapped the observed deposition patterns for 4 of 5 Space Shuttle launches analyzed in 1994-95. One predicted plume did not overlap but was located within 35° of the observed plume.

   - ERDAS did very well at predicting the trajectory of observed N_2O_4 release on 20 Aug 94 when modeled source was moved from LC-41 to center of Cape. The modeled source was moved to compensate for the complex land/water features which are difficult to resolve with the 3-km grid.

   - The 3-km grid spacing of current ERDAS configuration is too large to resolve all of the detailed land/water features in the KSC/CCAS area. A smaller grid spacing would improve the resolution but model run time prohibits a smaller grid configuration on the current computer hardware.

   - A special study was conducted to compare the currently certified OBDG model with the ERDAS models to determine if the ERDAS models changed launch availability. The study was limited in that it looked at dispersion during 30 two-hour periods over a 6-month period. These periods included late afternoon periods similar to the original OBDG study but it also included a higher percentage of late morning cases than the original OBDG study and included nighttime cases which were not included in the original OBDG study. The results of the study were:

     - Cases where the winds shifted over time and space were the ones where major differences existed between the OBDG model and the ERDAS model. Currently certified OBDG model did not adequately handle wind shifting situations while the ERDAS models provided a more realistic picture of dispersion when wind shifts occurred.

     - The ERDAS models could provide safety personnel with a better understanding of the three-dimensional wind field causing plume dispersion resulting from a potential toxic spill. Information on vertical

plume development is not available from the OBDG model. This information can help safety personnel in making evacuation decisions and answer questions such as:

- Will potential toxic plumes which have lofted upward eventually mix back down to surface? Are concentrations aloft large enough to pose a threat to populated areas if they reach the surface?

- Will potential toxic plumes which have moved offshore eventually move back onshore?

- Comparing diffusion model predictions made by the OBDG model and the ERDAS models in this limited comparison study produced results which showed that using the ERDAS models for non-continuous spill scenarios improves launch processing availability in 19 of 29 cases. For continuous spill scenarios, ERDAS improves launch processing availability in 2 out of 29 cases. A non-continuous spill is one that has a limited release duration (less than approximately one hour). The OBDG model assumes a continuous release.

Recommended enhancements

ERDAS is a system which provides safety personnel with mesoscale and diffusion modeling capabilities that are more advanced than the current models (e.g. OBDG). ERDAS, as it runs at the end of the evaluation phase, performs as designed for the functions that are important for dispersion prediction. Therefore, ERDAS is ready to begin the phased approach of transitioning from the AMU to Range Safety Operations. Initially, ERDAS will provide Safety with a system to assist them in day-to-day operations and decision-making. With phased improvements and enhancements, ERDAS will become a system which will provide Safety with a state-of-the-art dispersion forecast and analysis system for use in launch and day-to-day operations The phased transition of ERDAS to operations has begun and we recommend that it continue until ERDAS becomes a fully-functioning, certified dispersion system.

The following enhancements will provide ERDAS with better capabilities to support operations and can be implemented in a phased approach.

1. Immediate implementation requirements to transition system to operations:

   - Documentation on software maintenance, hardware maintenance, certification testing, and training needed to transition system to operations.

2. Short term technical enhancements:

   - System should be moved to faster, more powerful computer to provide results in less time than current platform.

   - User interface needs minor revisions to provide users full capabilities of system.

   - The Observed Data/Forecast blending feature needs additional testing since it is important for diffusion predictions.

- Current data interface to MIDDS should be modified for operations to provide smoother initialization data input.

- ERDAS should be validated against tracer data.

3. Intermediate and long term technical enhancements which should be studied and possibly implemented include:

- Activating the explicit cloud microphysics modules.

- Reducing the finest RAMS grid resolutions from the currently-implemented 3-km resolution.

- Adding near real-time input parameters for RAMS initialization such as soil moisture measurements and sea surface temperatures.

- Automate quality control of input data used to initialize RAMS.

  Implement four-dimensional data assimilation (nudging) in RAMS along with development of Local Analysis and Prediction System (LAPS). LAPS is a system which ingests and displays near real-time 3-D meteorological data from a variety of sources including wind profilers, rawinsondes, surface observations, buoys, towers, WSR-88 Doppler radar, and GOES-8 visible and infrared radiance and sounding data. The LAPS data are used to initialize and update models such as RAMS and to provide dispersion models with observed 3-D data rather than predicted data.

- HYPACT should be modified to handle deposition of solid and liquid plume particulates as well as plume rise due to bouyant plumes.

- HYPACT should be modified to allow for calculation of cumulative dosages as well as instantaneous concentrations.

The Eastern Range has validated a requirement to transition ERDAS to operational status. The results and recommendations presented here should assist in that process.

1. Introduction

This document describes the evaluation of the Emergency Response Dose Assessment System (ERDAS) conducted by the Applied Meteorology Unit's (AMU) during the period March 1994 to February 1996.

One AMU purpose is to evaluate selected new technologies and transition those which are ready into operational use by forecasters providing weather support to Shuttle, military, and commercial space flight operations (Ernst and Merceret 1995). The AMU also devises techniques to use existing technologies more effectively, and advises on matters relating to technology acquisition.

ERDAS is a prototype software and hardware system configured to produce routine mesoscale meteorological forecasts and enhanced dispersion estimates on an operational basis for the KSC/CCAS region. ERDAS includes two major software systems which are run and accessed through a graphical user interface. The first software system is the Regional Atmospheric Modeling System (RAMS), a three-dimensional, multiple nested grid prognostic mesoscale model. The second software system is the Hybrid Particle and Concentration Transport (HYPACT) model, a pollutant trajectory and concentration model. ERDAS also runs the Rocket Exhaust Effluent Diffusion Model (REEDM) to determine the source term for modeling launch plume dispersion.

ASTeR Inc. (ASTeR, Inc. merged with Mission Research Corporation on 4 Jan 1994 and is now called Mission Research Corporation/ASTER division; in this report they are referred to as MRC/ASTER) developed ERDAS for the Air Force for the purpose of providing emergency response guidance to operations at KSC/CCAS in case of an accidental hazardous material release or an aborted vehicle launch. The ERDAS development occurred during the period 1989 to 1994. under Phase I and II Small Business Innovative Research contracts with the Air Force Space and Missile Systems Center, Los Angeles AFB. ERDAS was delivered to the Air Force's Range Operations Control Center (ROCC) in March 1994. The AMU was tasked with keeping ERDAS running and with evaluating ERDAS during the period March 1994 to December 1995.

Before safety personnel and weather forecasters accept ERDAS as an operational emergency response system, they must determine its value, accuracy and reliability. In partial fulfillment of this requirement, the AMU has evaluated ERDAS in a near-operational environment to determine if and how it should be transitioned to an operational environment. The evaluation of ERDAS has included:

- Evaluation of the sea breeze predictions
- Comparison of launch plume location and concentration predictions.
- Case study of a toxic release.
- Evaluation of model sensitivity to varying input parameters.
- Evaluation of the user interface.
- Assessment of ERDAS's operational capabilities.

This document presents the results of the different facets of the AMU's evaluation of the system. The remainder of Section 1 presents an overview of ERDAS and an overview of the AMU evaluation. Section 2 presents the AMU evaluation of the ERDAS system performance. Sections 3 and 4 present the results of the meteorological model evaluation. Section 3 contains an analysis of the sensitvity of RAMS to soil moisture variations while Section 4 presents the

analysis of RAMS predictions of the sea breeze. Sections 5 through 8 present the results of the diffusion model evaluation. Section 5 presents a case study of the diffusion of a Titan launch plume while Section 6 presents case studies of the diffusion of several Shuttle launch plumes. Section 7 presents a case study of ERDAS predcitons for an accidental release of nitrogen tetroxide. Section 8 presents the results of comparing the ERDAS diffusion models and the Ocean Breeze Dry Gulch model. Graphs comparing the observed and predicted winds for July-August 1994 are presented in Appendix A.

1.1 Overview of ERDAS System

ERDAS is described in considerable detail in the Final Scientific and Technical Report compiled by Lyons and Tremback (1994) of ASTeR, Inc. at the conclusion of Phase II of the SBIR project. Much of the information in this section of this report describing ERDAS and its development history was obtained from the ASTeR, Inc. report.

1.1.1 Development of ERDAS System by ASTeR, Inc.

The ERDAS concept evolved from the results of a Department of Defense SBIR Phase I announcement for FY1989 (Lyons et al., 1991). A proposal, originally directed at modeling 3-D wind fields at the Vandenberg AFB, was submitted by ASTeR, Inc. The proposal was funded by the USAF Space System Division under contract F04701-89-C-0052 as a Phase I SBIR contract. The modeling venue was changed by mutual agreement to the Cape Canaveral Air Station and the adjacent Kennedy Space Center.

Phase I demonstrated that a mesoscale prognostic model, RAMS, could successfully simulate the complex wind flow regimes over the CCAS/KSC region. The RAMS model and its many applications have been fully described in numerous technical papers in the professional literature (Pielke et al., 1992; Lyons et al., 1993). Data from the KABLE field experiment (Taylor et al., 1990) were used to validate the model's performance. RAMS revealed that vertical motions in excess of 150 cm/sec were associated with complex boundary convergence zones (Lyons et al., 1992). A Lagrangian Particle Dispersion Model (LPDM) successfully modeled 3-D, mesoscale transport patterns associated with the sea breeze.

The development of the prototype ERDAS was funded under a Department of Defense SBIR Phase II, from the U.S. Air Force, Space and Missile Systems Center (SMC/CLN), Los Angeles AFB, CA under contract number F04701-91-C-0058. Work began on the project in September 1991 and was completed on 30 June 1994.

Phase II goals included developing a prototype Emergency Response Dose Assessment System (ERDAS) and testing the feasibility of using such a system in an operational forecasting setting. RAMS was tested, optimized for a dedicated workstation and configured for selected accident scenarios at CCAS/KSC. In order to obtain maximum use from the rich suite of observational data in the area, RAMS can be used as the template for a hybrid wind flow model incorporating both the prognostic model output and observations. A more advanced dispersion model was configured for use at CCAS/KSC. Called the HYPACT (Hybrid Particle and Concentration Transport) model, this code employs many advanced features of the Lagrangian Particle Dispersion Model (LPDM) technique. It allows determination of the impact of a source at long distances and/or wide areas. For very long ranges, it is possible to extend HYPACT to emulate Eulerian dispersion models, thus reducing the number of particles required. This reduces the computational requirements for the dispersion modeling for sources impacting large geographic areas.

The aim of the ERDAS development was defined as the design, development, evaluation and delivery of the following:

(1) mesoscale prognostic wind flow model,

(2) advanced particle dispersion model,

(3) computer display graphics and

(4) associated computer hardware for predicting 3-D wind fields and atmospheric dispersion patterns in the CCAS/KSC area

ASTeR, Inc. prepared a detailed discussion on the user needs and requirements of an ERDAS which is in their Final Report.

1.1.2 ERDAS development since AMU installation: March 94–present

During the period the AMU evaluated ERDAS, MRC/ASTER (ASTeR, Inc. merged with Mission Research Corporation on 4 Jan 1994) and the AMU were enhancing and modifying the software to improve and fix problems that were found. A discussion of these modifications was provided in the AMU Monthly Activity Reports. Some of the modifications/corrections include:

- Configuring REEDM and HYPACT diffusion models to run and display as designed.
- Changing the soil moisture parameter and analyzing the sensitivity.
- Modified code to allow for missing grids from NGM data.
- Modified ingest routine to correct wind speed speeds from rawinsondes and surface sites.
- MRC/ASTER installed new version of ERDAS software to fix deficiencies on 23 January 1995.
- Modified ERDAS software to allow the blending of tower data with forecast data for diffusion analysis.

1.1.3 System Description

1.1.3.1 General Features

The ERDAS is a turn-key software, hardware and graphics system. It is resident on a dedicated IBM RS/6000-550 workstation. ERDAS is comprised of two key software systems: a meteorological model to provide highly localized 24-hour forecasts for the KSC/CCAS area (RAMS) and dispersion modules, REEDM and HYPACT, which can be employed in the event of an emergency as well as for mission planning and research.

The RAMS code, as configured in this initial version of ERDAS, is suitable for preparing forecasts on approximately 70% of the days in a typical year (Lyons and Fisher, 1988). The model will be best suited for predicting "fair weather" mesoscale regimes such as land and sea breezes, as well as conditions associated with large scale synoptic weather systems. Because of

computational speed limitations, during periods of tropical disturbances and general deep convection, RAMS will not predict with skill the localized wind shifts that can accompany such weather systems.

RAMS is initialized using the MIDDS data resident at the CCAS/KSC. It is run twice daily, out to 24 hours. The outer domain covers the southeastern U.S., but with finer grids centered over the KSC/CCAS region in order to predict the details of such features as the land breeze, the various river breezes and the Atlantic sea breeze. In its current configuration the model runs in approximately 9 hours. A RAMS-generated forecast is always available for immediate use.

The RAMS output drives the dispersion modules, with primary reliance on the HYPACT code. It has been configured so that the REEDM module provides source terms for a suite of nominal and abort vehicle scenarios as well as the cold spill source terms resident in MARSS.

The HYPACT code allows for dispersion estimates to be made using fully three-dimensional, time-dependent wind and turbulent fields. Atmospheric phenomena such as wind shear, vertical motion, subsidence, recirculation and thermal internal boundary layers (TIBLs) can be accounted for directly. In simpler dispersion models, features such as TIBLs (Garratt, 1990; Lyons et al., 1981) have been ignored or very crudely parameterized, a short cut which can now be avoided.

ERDAS is designed to be straightforward to use. Operation of the ERDAS is via a keyboard/mouse-driven Graphical User Interface (GUI). A variety of dispersion predictions are available, many within five minutes of request. Some more advanced dispersion estimates using HYPACT require some additional computation time.

The RAMS model is initialized and run twice daily. The initialization data for RAMS originates from the mainframe data processing system serving the RWO (MIDDS). It is transferred from MIDDS to the AMU's PS/2 machine which in turn is obtained by the ERDAS RS/6000-550.

1.1.3.2. Software

The code of RAMS and HYPACT is written mostly in extended FORTRAN 77. RAMS has successfully executed on a number of machines including a Cray Y/MP, Convex, Stardent, DEC alpha, HP, Sun and SGI workstations and the IBM RS/6000 series workstations with little or no modification. ERDAS was delivered installed on an IBM-RS/6000 series machine.

In addition, C was used to supplement the FORTRAN 77 standard and to provide the functionality that FORTRAN 90 will contain. Small C routines are used for dynamic memory allocation and file I/O. The IBM AIX (Advanced Interactive Executive) XL FORTRAN 77 and ANSI C compiler are installed on the unit. The operating system for the ERDAS platform is a variant of the UNIX operating system. Currently, IBM's AIX Version 3.2 for RS/6000 is installed in the ERDAS. Also included is the IBM AIX Windows Environment/6000. Graphics is provided using the NCAR Graphics visualization software package.

The programming standards currently used with the Department of Atmospheric Sciences, Colorado State University were employed by ASTeR, Inc. in the RAMS and HYPACT code. The core of the RAMS code, which is licensed exclusively from CSU to Mission Research Corporation/ASTER Division, was developed within the university. ERDAS uses the FORTRAN 77 standard. The IEEE standard for representation of floating point numbers is implemented within AIX.

The RAMS and HYPACT codes continue to undergo testing by a wide variety of users. As many as 50 researchers are using various configurations of RAMS worldwide. This allows the code to be highly stressed under a wide variety of conditions. When any bugs or deficiencies are reported to MRC/ASTER and CSU, patches are made when necessary, or revisions are scheduled for the next release of the software.

As part of the Lake Michigan Ozone Study, a detailed audit of the core RAMS software was conducted by Richard Londergan and his staff of ENSR, Inc. No major problems were discovered. The numerics faithfully represented the equations according to the tests conducted.

1.1.3.3. Computer Hardware

The ERDAS runs software in a configuration that runs (1) essentially on a quasi-continuous basis for RAMS (two nine hour cycles daily), (2) on a demand basis in the event of required response to an emergency, (3) on a platform with a considerable fraction of a mainframe supercomputer's throughput, and (4) with immediate access to results via advanced visualization systems.

To meet the performance requirements as stated below, the platform required a speed on the order of 25 megaflops (million floating point operations per second). Central memory requirements mandate at least 64 megabytes of RAM.

External disk storage on the order of a gigabyte was required in order to handle an adequate fraction of the very large output files produced by the several software systems comprising the ERDAS. An external tape drive was not included in the hardware configuration to be delivered, but is strongly recommended for archival activities. Table 1-1 lists several of the ERDAS performance goals established by ASTeR, Inc. against which model configurations were tested.

Table 1-1. Performance Goals for the ERDAS System

Activity	Time Goal	Time Achieved
Access Initializing Data for RAMS	60 minutes	85 minutes
Initialize RAMS forecast model (ISAN)	15 minutes	28 minutes
Run 24-hour forecast	6.0 hours	9.5 hours
Time to prepare Hybrid analysis	3.0 minutes	10 minutes
Retrieve RAMS output for display	10 seconds	20 seconds
Compute single particle trajectory	1.0 seconds	1 second
Make OB/DG calculation	2.0 seconds	OBDG not implemented
Make AFTOX calculation	3.0 seconds	AFTOX not implemented
Run streak line of 1000 particles for 3 hours	1.0 minute	Not Tested
Disperse 10,000 particles for 6 hours	5.0 minutes	Not Tested

The amount of time required to execute RAMS is a function of a number of factors:

- the number of horizontal grid points (domain size)
- the size of the grid mesh (which strongly affects the time step)
- the number of vertical levels
- the frequency with which certain functions are iterated
- the duration of the simulation
- the complexity of the representation of cloud and precipitation processes
- the number of grid cells containing condensate
- the speed of the processors
- communication speed and bandwidth between processors

The computer system selected for the initial ERDAS was compliant with the various requirements. The ERDAS hardware components are listed in Table 1-2.

The workstation meets the basic performance requirements for the initial version of ERDAS. Based upon two years of testing and extensive use, ASTeR, Inc. selected the IBM RS/6000, Model 550 as the ERDAS platform. It is equipped with 64 megabyte RAM, two 400 megabyte internal disk drives, a 2.0 gigabyte external disk, a quarter-inch cartridge tape, operating under the IBM version of UNIX (AIX) and has a high-resolution (1280 x 1024) color monitor. It has been rated at slightly better than 25 megaflops performance. Benchmarks of RAMS against a single processor Cray X/MP show that the software can be executed on this platform at between one-forth and one-third the speed of the mainframe supercomputer.

The IBM RS/6000-550 system is comprised of a number of components listed in Table 1-2. The workstation CPU is compact and routinely situated as a desk side column. The ERDAS hardware is comprised entirely of standard, commercial off-the-shelf components. Routine maintenance can be provided under contract from the manufacturer after the end of the present contract.

Not included in the system is a high capacity external tape drive suitable for archiving large quantities of model output. The addition of a device, such as a 2.3 gigabyte capacity 8 mm Exabyte tape drive, is recommended.

The ERDAS computer requires no special facilities such as additional air or power conditioning. The RS/6000-550 draws about 1 kVA (110 V AC). The total heat output is estimated at 810 watts (2750 BTU/hour). The CPU size (24" x 26.6" x 14") allows it to be placed desk side. The display terminal and keyboard fits on a normal size work table or desk. The unit weighs approximately 117 pounds. There is no backup power source included other than that available for the RWO.

The RS/6000 has appropriate hardware and software to allow communications over Ethernet. The physical connection to the AMU Ethernet data line is via a standard connector from the Ethernet card.

Table 1-2. ERDAS Hardware Components

IBM Part	Description
7013-550	IBM RISC/6000-550 powerstation cpu
7013-2600	Internal CD-ROM drive
7013-2781	Hi performance 24 bit 3D color graphics
7013-2782	24 Bit Z Buffer Solid Rendering Option
7013-2980	Ethernet Hi Performance LAN adapter
7013-6010	Keyboard, USA 101 keys
7013-6041	Mouse, 3 button
7013-9220	SCSI I/O Controller
7013-9221	3.5" Diskette
7013-9235	32 MB HD3 Memory
7013-9245	800 MB SCSI Disk Drive
7013-9800	Line cord U.S./Canada
7207-001	150 MB Ext 1/4 inch Cartridge Tape Drive
7207-9119	SCSI Controller Cable
7207-9800	Line cord U.S./Canada
6091-019	Color Display

1.1.3.4. Visualization Requirements

The ERDAS system has a high resolution (1280 x 1024 pixel) display, with 8 bit color, double buffering capability to support relatively high speed playback and animation. The RS/6000 is capable of driving a standard Postscript black & white laser printer and a color hard copy device (for the latter, when using color Postscript output for NCAR Graphics, AVS and savi3D visualizations). The RS/6000 is capable of writing data files to standard 1/4-inch tape cartridges in UNIX tar format, as well as high density external tape device, for archival or other purposes.

1.2 Overview of AMU Evaluation

1.2.1 Goals and Focal Points of Evaluation

The evaluation of ERDAS by the AMU has followed the AMU Task Plan. The ERDAS tasks are described below:

System Configuration and Check-out

Perform a meteorological and performance evaluation of the ERDAS. As part of this effort, perform the following tasks:

- Install, in conjunction with Mission Research Corporation (MRC), the ERDAS hardware and software provided by MRC in the AMU laboratory.
- Connect the ERDAS hardware to the local area network (LAN) in the AMU laboratory.
- Develop/modify (in conjunction with MRC) software to transfer data on a scheduled basis from MIDDS to the ERDAS computer for mesoscale model initialization. This subtask may also require modification of ERDAS data ingestion software. Data to be extracted from MIDDS includes NGM model output and observations from local data sources.
- Perform (in conjunction with MRC) a system functional check-out of the ERDAS and develop a list of system deficiencies.
- Work (in conjunction with MRC) to resolve the items on the list of system deficiencies.
- Develop, install, and initiate a run-time configuration for the mesoscale model. The run-time configuration includes schedules for model initialization and forecast products.
- Archive forecast products and observed data. This information will be used to evaluate model results (e.g., case studies analyses and statistical analyses).

ERDAS Performance Evaluation

- Conduct a performance evaluation of ERDAS to include:
  - Evaluation of ERDAS graphics in terms of how well they facilitate user input and user understanding of the output.
  - Determination of the requirements that operation of ERDAS places upon the user.
  - Documentation of system response times based on actual system operation.

- Evaluation (in conjunction with range safety personnel) of the ability of ERDAS to meet range requirements for the display of toxic hazard corridor information.

- Evaluation of how successfully ERDAS can be integrated in an operational environment at CCAS.

Range User Training

- Provide user training for range personnel. The training will include information regarding operation of the system and interpretation of ERDAS output.

ERDAS Meteorological Evaluation

- Perform an evaluation of ERDAS meteorological predictions. Meteorological factors which will be included in the evaluation are wind speed, wind direction, wind turbulence, and the movement of sea breeze fronts. Part of the evaluation will focus on the examination of the relative accuracy of a forecast three-dimensional wind field as compared to the observed two-dimensional wind field in relation to use of the data for dispersion predictions.

- Document the results of the performance evaluation, meteorological evaluation, and recommendations for operational use in a report to be delivered within two weeks of the completion of the task.

ERDAS Dispersion Predictions

- Evaluate the ability of ERDAS to predict cloud rise and plume dispersion. Factors to be evaluated include cloud rise, bifurcation, trajectory, and horizontal/vertical dispersion. To perform this task, ENSCO will use available data to conduct the evaluation and will coordinate the evaluation with ongoing range evaluation efforts.

ERDAS Model Comparison

- Perform a comparison of Ocean Breeze Dry Gulch (OBDG) using the standard operational two dimensional Barnes windfield versus using OBDG with the three dimensional ERDAS windfield. Run OBDG for 30 selected cases and produce hard copy of the resultant dispersion patterns. Input data will be 5 minute averaged WINDS files. The cases will be selected for launch scenarios.

- Perform a comparison of OBDG using the standard operational two dimensional Barnes windfield versus the ERDAS HYPACT "particle-in-cell" dispersion algorithm with three dimensional windfield. Run OBDG for the same 30 cases using temperature lapse and standard deviation of the wind direction from the tower network and RAMS-produced wind field and produce hard copy of the resultant dispersion patterns.

- Compare the dispersion patterns from the two analyses and assess the validity of each. The objective of this analysis will be to determine if

launch availability would be increased and/or false alarms would be reduced by the use of the three dimensional RAMS windfield.

- Run RAMS/HYPACT on ERDAS for the same 30 cases and produce hard copy of the resultant dispersion patterns.

1.2.2 Accomplishments and Activities of Evaluation

The AMU completed the evaluation of ERDAS by accomplishing the tasks described in Section 1.2.1. Some of the primary activities which were conducted during the evaluation are listed below:

Documents produced during the ERDAS evaluation include the following:

- ERDAS System check-out Report - 26 April 1994
- Soil Moisture Sensitivity Analysis - 8 June 1994
- ERDAS System check-out Report (Addendum) - 8 July 1994
- ERDAS Model Evaluation Plan - 16 September 1994
- ERDAS Modeling of 20 August 94 N2O4 Release - 6 December 1994
- Sea Breeze Analysis Discussion - Quarterly Report - 30 April 1995
- Titan Launch Plume Comparison Study - Quarterly Report - 31 July 1995
- Comparison of OBDG and ERDAS models - In Review

Briefings presented during the ERDAS evaluation include the following:

- Toxic Release Assessment Group - June 94
- Mid Term Review Briefing - 12 Oct 94
- Toxic Release Assessment Group - Jan 95
- Briefing to Range Safety - Mar 95
- Briefing to JANNAF Safety and Environmental Protection Subcommittee - Dec 95

Other activities for ERDAS involvement

- Titan launches
  - K-10 3 May 94
  - K-9 24 Aug 94
  - K-14 22 Dec 94

- K-23 14 May 95
- K-19 10 Jul 95
- K-21 6 Nov 95

- Support for Model Validation Program
  - July 95 (limited involvement)
  - Nov 95

2. ERDAS System Performance Evaluation

The AMU Technical Directive 5-006 listed five criteria for evaluating the system performance of the ERDAS. In this section, we list each of the criteria for evaluating each of them. The performance evaluation criteria were:

- Evaluate ERDAS graphics in terms of how well they facilitate user input and user understanding of the output.
    - Compile a list of new and remaining deficiencies discovered since the initial check-out reports,
    - Compile and prioritize a list of recommended graphic improvements determined after 9 to 12 months of operating the system on a daily basis, running the RAMS model, and running and displaying meteorological and diffusion model output, and
    - Include comments and suggestions by Range Weather Operations and Range Safety personnel into the lists of graphic deficiencies and recommended improvements.
- Determine the requirements that operation of ERDAS places upon the user. After operating ERDAS on a daily basis and during launch operations for 9 to 12 months, compile a list of operator requirements. These requirements focus on operator interaction required to run the system and to display the various ERDAS products. Also address the training requirements.
- Document system response times based on actual operation. Document model runtimes and display response times.
- Evaluate (in conjunction with range safety personnel) the ability of ERDAS to meet range requirements for the display of toxic hazard corridor information. Compile a list of the general strengths and weaknesses observed during the operation of the diffusion models. Query Range Safety personnel to determine if the ERDAS outputs meet their requirements for diffusion data products. Range Safety requirements are based on their use of toxic hazard prediction models and displays to predict the launch exhaust plume and accidental releases.
- Evaluate how successfully ERDAS can be integrated in an operational environment at CCAS. Compile a list of items which must be completed to make ERDAS operational. This list is based on system deficiencies as well as requirements imposed by:
    - 45th Space Wing,
    - Eastern Range Program Office (SMC/CW-OLAK),
    - Range Weather Operations, and
    - Range Safety.

2.1 Requirements that Operation of ERDAS Places Upon User

The operation of ERDAS requires users to perform several tasks to maintain and operate ERDAS. Maintaining ERDAS requires daily, weekly, and periodic monitoring of the software, hardware, and the communication links of ERDAS. In addition, operating ERDAS to view the displays and run dispersion scenarios requires operation of the user interface and entering of certain data.

2.1.1 Maintenance requirements

During the AMU's evaluation of ERDAS over the past 20 months, maintenance of the system was necessary. This maintenance covered three areas: software, hardware, and communication links. Some of the maintenance required was:

Communication links

- Make sure Ethernet links to AMU's LAN were functioning properly. Input and output data are transmitted through this Ethernet. ERDAS obtains its input data from MIDDS through the AMU's Model 80. For output, ERDAS has access to the AMU's color and black and white printers and external hard disks through the network. The ERDAS operator must work with the LAN system operator to make sure all links are up and operating properly.

- Make sure ERDAS is receiving all of the expected input MIDDS data from the Model 80 in the AMU. The ERDAS operator must monitor the input data ERDAS receives and notify the Model 80 operator and/or the MIDDS operators of problems. Several times during the ERDAS evaluation, problems with input data from MIDDS/Model 80 were observed after ERDAS did not receive all of its input data. After notification, the MIDDS and Model 80 maintainers worked to fix these problems.

Software

- Document any software bugs detected. These bugs include problems detected with the user interface, the RAMS model, or with HYPACT/REEDM.

- Modify the software to fix bugs if possible. Some software problems can be fixed by making software changes and recompiling the code while other changes require consultation with the developers at MRC/ASTER.

Hardware

- The ERDAS hardware requires little maintenance by the operator. If the operator detects any hardware problems they must contact a hardware service provider for repairs.

2.1.2 Operating requirements

The operation of ERDAS is described in the ERDAS Users' Manual included in the ASTeR, Inc. Final Report (Lyons and Tremback 1994). While the Users' Manual does not contain all of the details on the operation of the system, it describes many of the procedures required to operate the ERDAS functions. The users should be trained to display and run the models within ERDAS. Training will be provided to potential users during the transition of ERDAS to operations in Room 148.

Table 2-1 presents a list of some of the operations different users of ERDAS must perform to operate the system. The table lists the group or groups most suited to perform each operation along with the time and frequency of each of the tasks. The data in the list are estimates determined by the AMU during the evaluation of the system over the past two years. Actual requirements may vary depending on the user and the situation. The checklist mentioned in the table is a checklist which a forecaster would use to check the validity of the RAMS model based on conditions that the model is known not to perform well e.g. cloudy conditions with precipitation.

Table 2-1. List of ERDAS operations along with requirements for personnel, time, and frequency of operation.

Operation	Who Performs?	Time Duration	How often, when?
Check RAMS Runs			
Check if RAMS is automatically running	Ops & Maint	2 min	1-2 times per day
Check on MIDDS data	Ops & Maint	2 min	1-2 times per day
Run data filter if data not there	Ops & Maint	10 min *	as needed
Start RAMS script if not running	Ops & Maint	10 min *	as needed
Check Model Validity			
Check current conditions w/checklist	Weather	5 min	1-2 times per day
Check forecast with checklist	Weather	10 min	1-2 times per day
Verify winds and sea breeze	Weather	10 min	1-2 times per day
Run HYPACT/REEDM			
Verify met data is there and valid	Safety/Wx	10 min	as needed
Run hybrid if desired	Safety/Wx	10 min *	as needed
Input spill/launch data	Safety/Wx	5 min	as needed
Verify run/output	Safety/Wx	5-15 min	as needed
Obtain hardcopy			
RAMS	Safety/Wx	5-15 min*	as needed
HYPACT	Safety/Wx	5-15 min*	as needed
Archive data			
Compress and backup RAMS data	Ops & Maint	10 min*	1 time per week
Save HYPACT/REEDM runs	Safety/Wx/ Ops & Maint	10 min*	1 time per week
Check software problems			
Document bugs or problems	Safety/Wx	15 min	as needed
Fix scripts	Ops & Maint	20 min	as needed
Fix Fortran code	Ops & Maint	10 min-? hrs	as needed
Discuss with vendor	Ops & Maint	15 min	as needed

* The times required for these operations would be reduced if ERDAS was hosted on faster computer.

The RAMS model is automatically initialized and run twice daily. The initialization data for RAMS originates from the mainframe data processing system serving the RWO (MIDDS). Data are transferred from MIDDS to the AMU's PS/2 (currently a Pentium) machine which allows the information to be received by the ERDAS RS/6000-550. The operator's role in the initialization will be primarily relegated to error checking the input, addressing the suitability of the model for use during the upcoming period's weather regimes, and possibly adjusting several parameters (such as soil moisture). The initializing of the dispersion models is accomplished within several minutes, with initial results available in between 1 and 5 minutes (some more complex calculations will take longer). The interpretation of the output of both the RAMS and dispersion models is aided by a variety of graphics and visualization products. The users interact with the system at all times through a Graphical User Interface (GUI). Most commands are by "point and click" operations. Typing is largely be limited to entering numeric quantities.

2.2 ERDAS Deficiencies and Enhancements

2.2.1 Deficiency List

One of the primary tasks of the AMU's ERDAS evaluation was to conduct a check-out of the system. A list of deficiencies was developed following this check-out and these were reported in the following documents submitted to SMC/CLN in 1994:

- ERDAS System Check-out Report (26 April 94)
- ERDAS System Check-out Report Addendum (8 July 94).

Following these reports many of the deficiencies were corrected by MRC/ASTER. These corrections were documented in the monthly reports. However, some of the deficiencies are still part of the system. In addition, during the course of the evaluation, new deficiencies were found. This section lists and briefly describes these deficiencies. At the conclusion of this final report, recommendations for future enhancements to ERDAS to correct many of the remaining deficiencies are presented.

ERDAS deficiencies found during the evaluation are listed in Table 2-2.

Table 2-2. List of defeciencies found within ERDAS along with suggested solutions to the deficiency.

Deficiency	Solution
1. The RAMS model produces erroneous initializations and incorrect results when bad observed data from the CCAS/KSC wind towers, surface observations, buoys, or rawinsondes are input to the model.	An automated quality control procedure is needed to check the data before it is ingested into the model.
2. Forecast Preparation function does not display meteorological data as designed.	The Forecast Preparation function was found to be minimally useful. Automated quality control of data is needed.

3. ERDAS lacks complete documentation.	Additional documentation will be developed during transition to operations.
4. The ERDAS user interfaces contain minor bugs.	
a. In HYPACT, the Release Rate must be entered manually and is not computed automatically from Release Amount and Release Size .	Modify HYPACT /User Interface software so program computes the Release Rate.
b. In Dispersion Control, there are no unit labels on the Release Rate.	Modify user interface software.
c. In HYPACT, the plots need date as well as time on them.	Modify software.
d. In HYPACT, users should be able to select their own concentration isopleths rather than have the model preselect them.	Modify software.
e. In HYPACT and RINGI, cross-sections (X-Z, Y-Z) need some indication of geographical features and/or latitude and longitude.	Modify software.
5. Some functions and operations in ERDAS are too slow and need to be faster for operational system.	
a. In its present configuration, ERDAS requires over 9 CPU hours to produce a 24-hr forecast.	Transport the ERDAS software to a more powerful computer. See discussion below.
b. In HYPACT, plot saves take 1 to 2 minutes to save one time period for later plotting.	Move ERDAS to faster machine.
c. In HYPACT and RINGI, producing and saving color and black and white prints is a slow process which takes over 20 steps to save and print 6 time periods of HYPACT plots.	Move ERDAS to faster machine. Modify print routines.
d. Maps of CCAS (MARSS map) takes 40 to 75 seconds to draw on screen.	Move ERDAS to faster machine.

Faster computer test

System should be moved to faster, more powerful computer to provide results in less time than current platform. During the ERDAS evaluation, a timing test was conducted to compare the length of run time needed for RAMS on an IBM RISC/6000 Model 390 workstation compared to its current platform, an IBM RISC/6000 Model 550. For the test, a 24-hour RAMS simulation was run on both machines and the run times were compared. The RAMS code was not recompiled on the Model 390. The results of the test were encouraging with regards to decreasing the

runtime of RAMS. The times for a 24-hr simulation from the start of model initialization to the finish of RAMS were:

- IBM 550 9:43 hours
- IBM 390 4:59 hours

The model ran almost twice as fast on the Model 390. Craig Tremback of MRC/ASTER believes that we can obtain further decreases in run time by actually recompiling the RAMS code on the Model 390 which was not done for this test.

2.2.1 Recommended Enhancement list

The following discussion provides a list of enhancements which are recommended as a result of the ERDAS evaluation. These enhancements will provide ERDAS with the capabilities to support operations and can be implemented in a phased approach.

1. Immediate implementation requirements to transition system to operations:

   - Documentation on software maintenance, hardware maintenance, certification testing, and training needed to transition system to operations.

2. Short term technical enhancements:

   - System should be moved to faster, more powerful computer to provide results in less time than current platform.
   - User interface needs minor revisions to provide users full capabilities of system.
   - The Observed Data/Forecast blending feature needs sufficient testing since it is important for diffusion predictions.
   - Current data interface to MIDDS should be modified for operations to provide smoother initialization data input.
   - ERDAS should be validated against tracer data.

3. Intermediate and long term technical enhancements which should be studied and possibly implemented include:

   - Activating the explicit cloud microphysics modules.
   - Reducing the finest RAMS grid resolutions from the currently-implemented 3-km resolution.
   - Adding near real-time input parameters for RAMS initialization such as soil moisture measurements and sea surface temperatures.
   - Automate quality control of input data used to initialize RAMS.
   - Implement four-dimensional data assimilation (nudging) in RAMS along with development of Local Analysis and Prediction System (LAPS). LAPS

is a system which ingests and displays near real-time 3-D meteorological data from a variety of sources including wind profilers, rawinsondes, surface observations, buoys, towers, WSR-88 Doppler radar, and GOES-8 visible and infrared radiance and sounding data. The LAPS data are used to initialize and update models such as RAMS and to provide dispersion models with observed 3-D data rather than predicted data.

- HYPACT should be modified to handle deposition of solid and liquid plume particulates as well as plume rise due to bouyant plumes.

- HYPACT should be modified to allow for calculation of cumulative dosages as well as instantaneous concentrations.

3. RAMS Soil Moisture Sensitivity

A study was conducted to test the sensitivity of RAMS to soil moisture by varying the soil moisture parameter in RAMS for one 24-hour simulation over the KSC/CCAS. The sensitivity analysis was performed to provide information regarding the importance of soil moisture measurements to mesoscale modeling efforts to those developing the meteorological support instrumentation siting and modernization input to the Spacelift Range System Specifications. Table 3-1 contains the test parameters used in the soil moisture sensitivity test.

Table 3-1. Soil Moisture Sensitivity Test Description

Test Parameter	Parameter Value
Simulation Start:	1200 UTC, 17 May 1994
Length of Simulation:	24 hours
Input Data:	Rawinsondes, surface data, buoy data, and tower data from 1200 UTC Nested Grid Model (NGM) forecast grids from 0000 UTC, 17 May 1994
RAMS Configuration:	See Lyons and Tremback 1994
Output Frequency:	Hourly
Experiment 1:	RAMS run with lower soil moisture (LSM), soil moisture parameter = 0.4
Experiment 2:	RAMS run with higher soil moisture (HSM), soil moisture parameter = 0.5 Note: Soil moisture is defined as the fraction of moisture present in a volume of soil relative to the total amount of moisture the soil can hold.

3.1 Description of Study

The RAMS model was run and hourly output of the predicted, surface (10 m) wind field was produced. RAMS runs were made using low soil moisture (LSM) values of 0.4 and high soil moisture (HSM) values of 0.5. Soil moisture is defined as the fraction of moisture present in a volume of soil relative to the total amount of moisture the soil can hold. The hourly predictions for the two different runs were then compared with each other and then also compared with the observed winds for the corresponding time periods for the CCAS area. Model predictions of upward vertical velocities at the 10-m level were also produced. The vertical velocities increase when surface convergence of the wind increases.

The observed wind data were obtained from the CCAS/KSC tower network for the 54-ft (16.5 m) level. These data were plotted on maps and are shown as wind barbs in the comparison figures. Hourly comparisons with RAMS predictions were made for the period 1400 UTC to 2000 UTC for the Cape Canaveral area.

The hourly surface predicted wind fields and observed tower winds for 1400 UTC, 1500 UTC, 1700 UTC, 1900 UTC, and 2000 UTC are presented in Figures 3-1 to 3-5. The observed tower data was not available for 1600 UTC and 1900 UTC so observed and modeled data for these hours are not shown. The forecast maps also show contours of upward vertical velocities (cm-sec^{-1}) at the 10-meter level.

At 1400 UTC (Figure 3-1), RAMS predicted westerly flow across the KSC/CCAS region. There was little difference between the LSM and HSM runs at this time. The observed wind barbs showed west and northwest flow at 1400 UTC.

At 1500 UTC (Figure 3-2), the two runs start to show a difference as the LSM began generating a sea breeze circulation while the HSM did not. The HSM produced weak southerly and southwesterly flow over the land and westerly and southwesterly flow over the ocean. The observed wind barbs showed west to northwest flow across the KSC/CCAS region.

At 1700 UTC (Figure 3-3), the LSM produced a well developed sea breeze with easterly winds and large upward vertical velocities across most of KSC/CCAS. The HSM produced the beginning of the sea breeze with easterly winds along the coast that did not penetrate very far inland. The observed wind barbs showed the onset of the sea breeze as the winds at the tip of the cape shifted around to easterly.

At 1800 UTC (Figure 3-4), the wind field produced by the LSM changed little from 1700 UTC. The HSM showed easterly winds and large vertical velocities along most of the coast as it predicted the sea breeze penetrating approximately 10 km inland at the areas to the north and south of the Cape. The observed wind barbs showed a pattern similar to the LSM with the easterly winds in the same areas to the north and south of the Cape.

At 2000 UTC (Figure 3-5), the LSM and HSM were similar but the LSM showed easterly winds further inland and the vertical velocities slightly larger than the HSM. The observed winds were easterly and northeasterly across all of the Cape and inland for approximately 30 km.

The observed and predicted wind speeds on this day were generally light with speeds of approximately 5 kts. Therefore, slight differences between the observed and predicted wind directions are not considered significant. However, wind shifts from westerly to easterly direction over time are an indicator of the passage of the sea breeze front as it moves inland during the day. This study compared the observed and predicted position and timing of the sea breeze front. This study did not analyze in detail the differences between the southwesterly predicted winds and northwesterly observed winds that existed in the light off-shore flow before sea breeze passage. The differences were due primarily to slight differences in observed and predicted pressure patterns in the central Florida and adjacent coastal region.

3.2 Soil Moisture Results

The results from this one case clearly show that the RAMS model is very sensitive to the soil moisture parameter for predicting the location and intensity of the sea breeze at KSC/CCAS. We recommended that soil moisture measurements be included in the meteorological support input to the Spacelift Range System Specifications for KSC/CCAS.

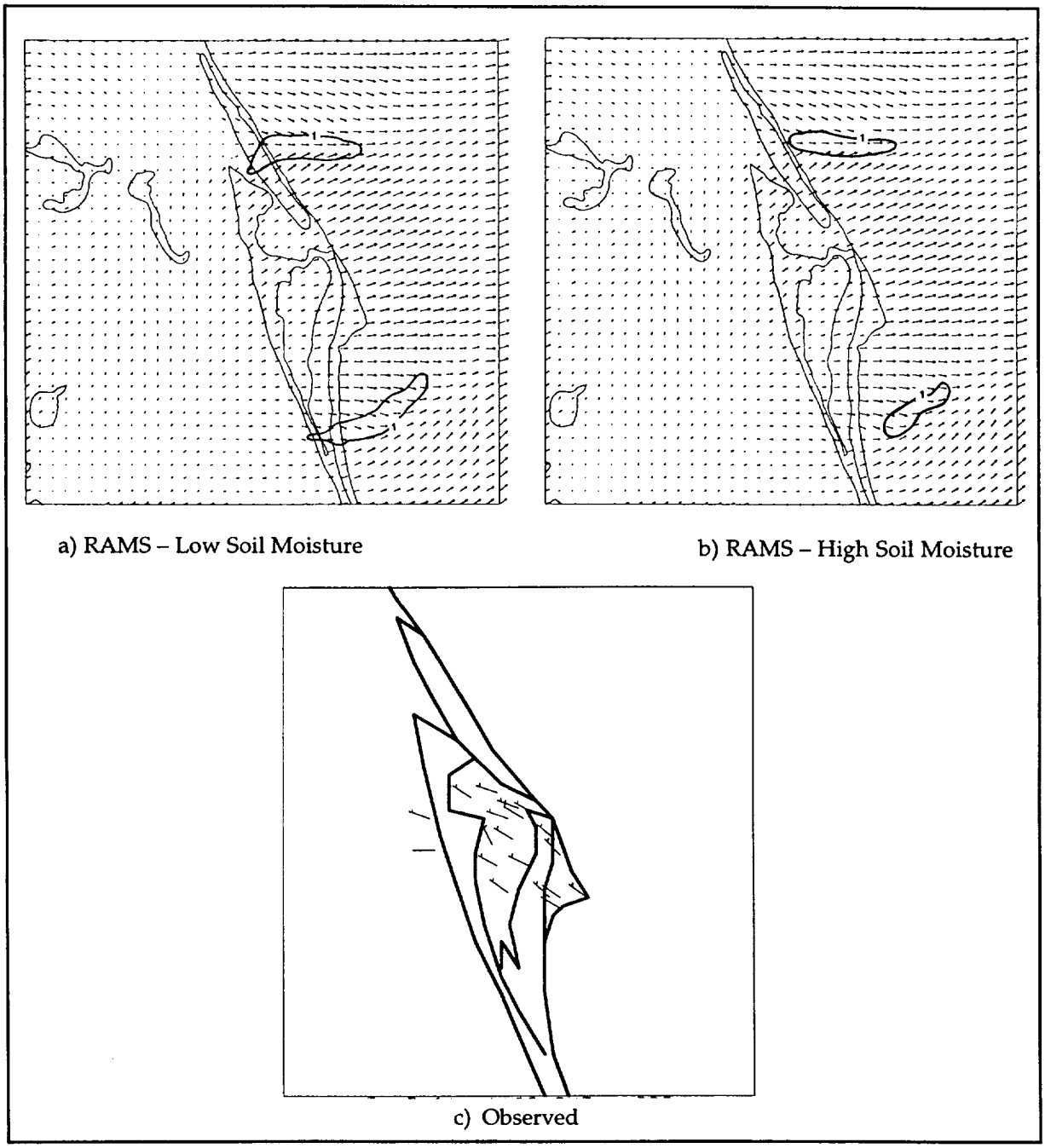

Figure 3-1. Illustrations of the hourly surface predicted wind fields and observed winds at 1400 UTC, 17 May 1994 for the Cape Canaveral area. Figure (a) shows the wind field for the low soil moisture (LSM) run with the overlaying contours showing vertical velocities (cm-sec^{-1}) at 10 meters. Figure (b) shows the wind field for the high soil moisture (HSM) run with the overlaying contours showing vertical velocities at 10 meters. Figure (c) shows the observed winds at CCAS/KSC at the 54-ft tower level.

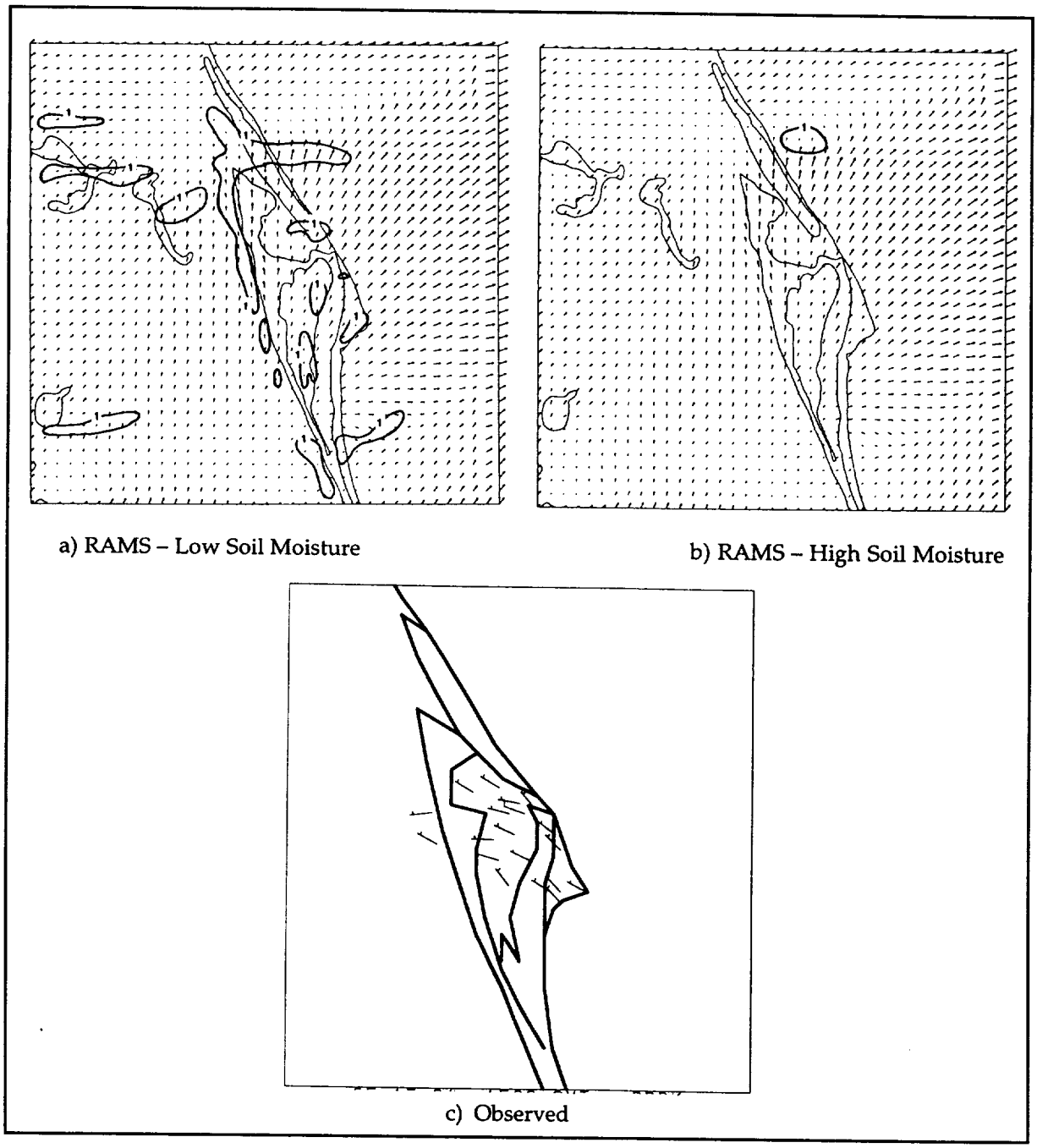

Figure 3-2. Illustrations of the hourly surface predicted wind fields and observed winds at 1500 UTC, 17 May 1994 for the Cape Canaveral area. Figure (a) shows the wind field for the low soil moisture (LSM) run with the overlaying contours showing vertical velocities (cm-sec^{-1}) at 10 meters. Figure (b) shows the wind field for the high soil moisture (HSM) run with the overlaying contours showing vertical velocities at 10 meters. Figure (c) shows the observed winds at CCAS/KSC at the 54-ft tower level.

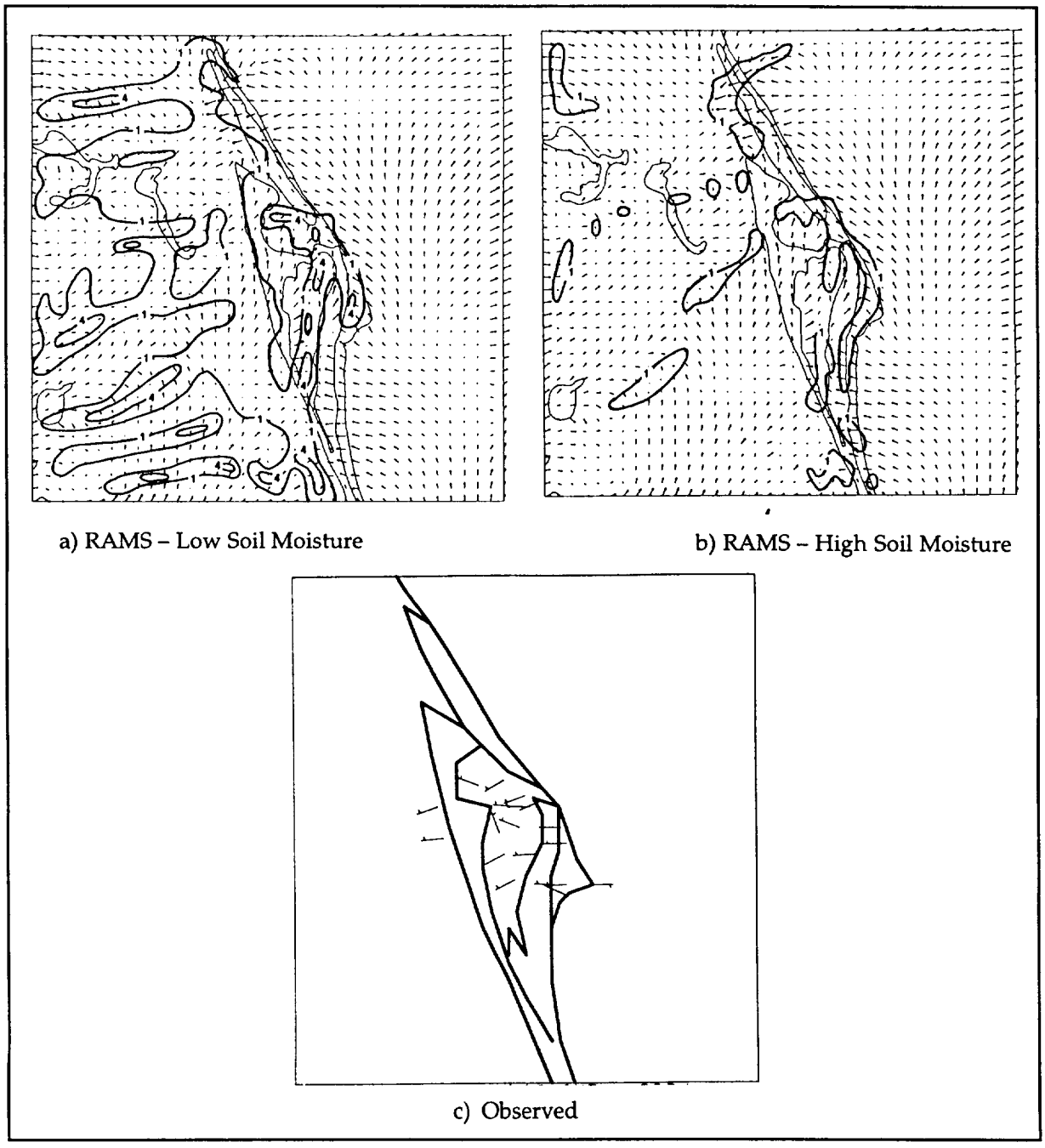

Figure 3-3. Illustrations of the hourly surface predicted wind fields and observed winds at 1700 UTC, 17 May 1994 for the Cape Canaveral area. Figure (a) shows the wind field for the low soil moisture (LSM) run with the overlaying contours showing vertical velocities (cm-sec^{-1}) at 10 meters. Figure (b) shows the wind field for the high soil moisture (HSM) run with the overlaying contours showing vertical velocities at 10 meters. Figure (c) shows the observed winds at CCAS/KSC at the 54-ft tower level.

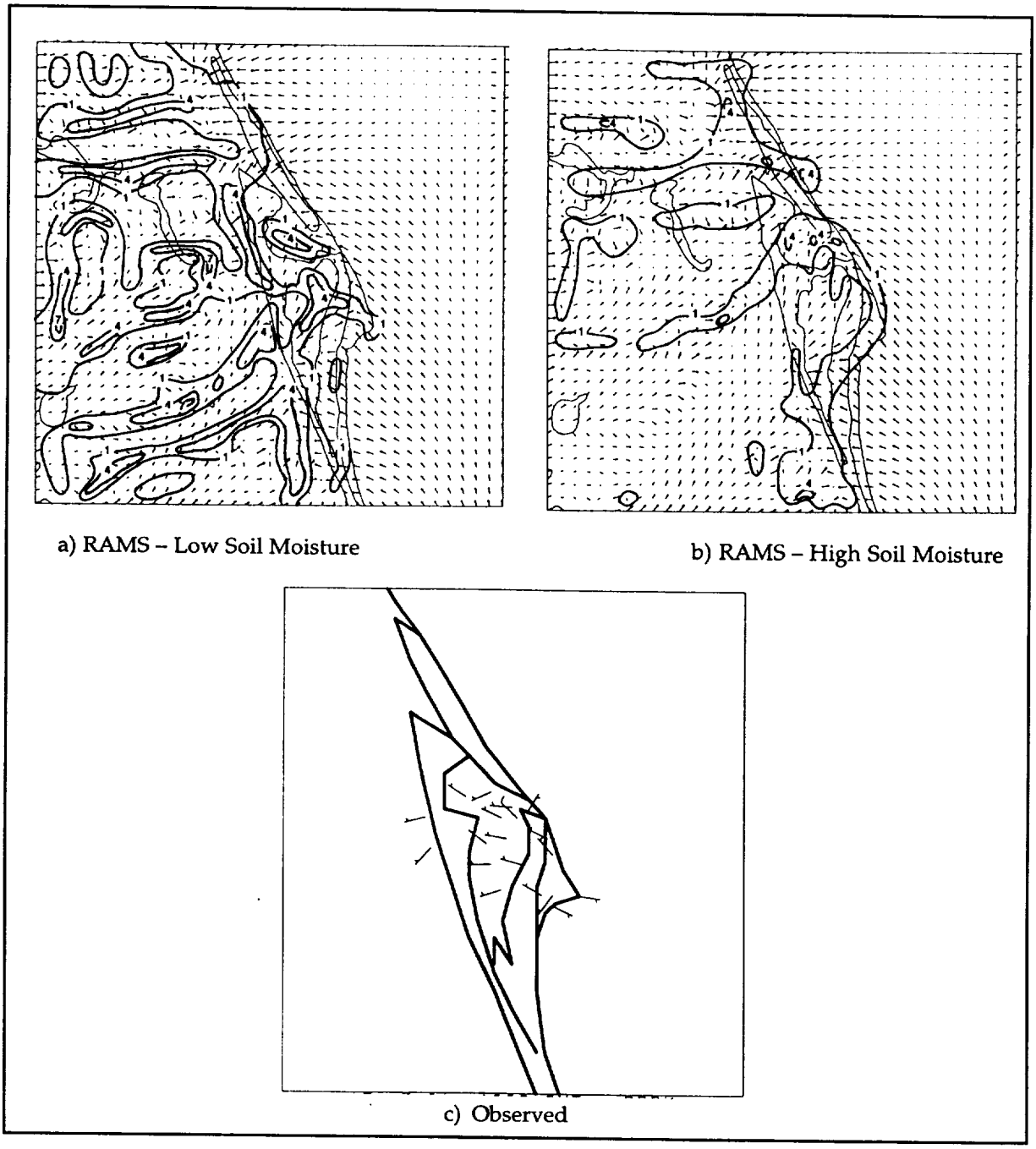

Figure 3-4. Illustrations of the hourly surface predicted wind fields and observed winds at 1800 UTC, 17 May 1994 for the Cape Canaveral area. Figure (a) shows the wind field for the low soil moisture (LSM) run with the overlaying contours showing vertical velocities (cm-sec^{-1}) at 10 meters. Figure (b) shows the wind field for the high soil moisture (HSM) run with the overlaying contours showing vertical velocities at 10 meters. Figure (c) shows the observed winds at CCAS/KSC at the 54-ft tower level.

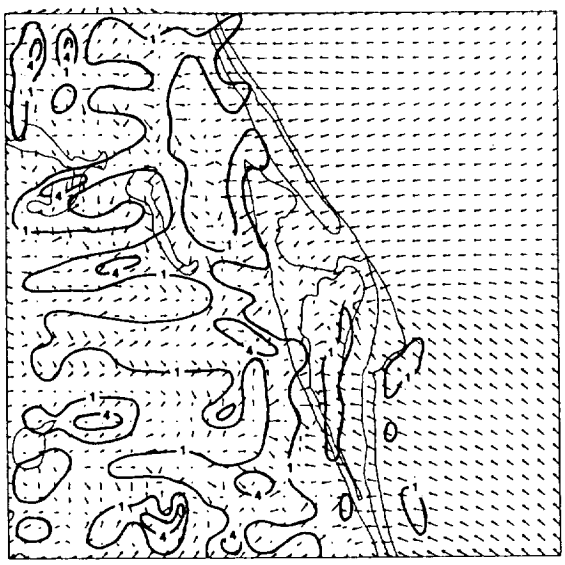

a) RAMS – Low Soil Moisture

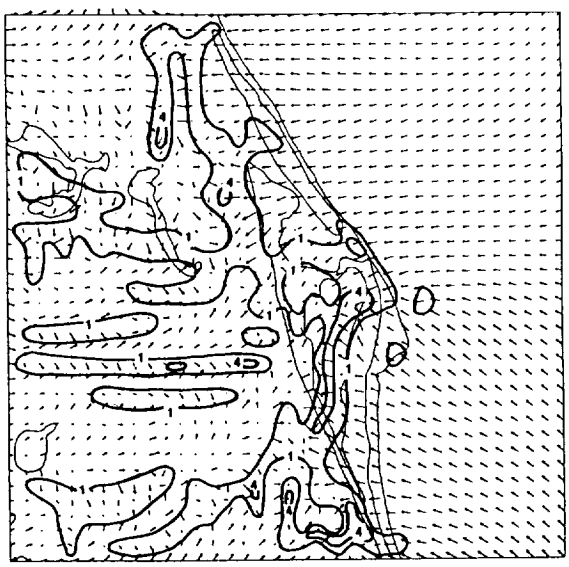

b) RAMS – High Soil Moisture

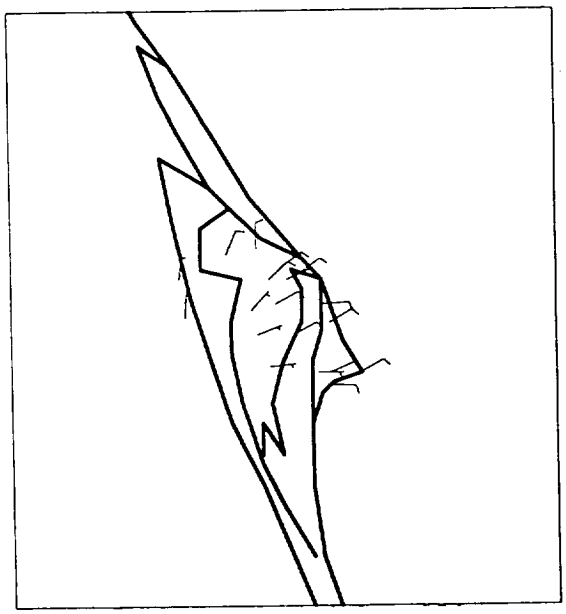

c) Observed

Figure 3-5. Illustrations of the hourly surface predicted wind fields and observed winds at 2000 UTC, 17 May 1994 for the Cape Canaveral area. Figure (a) shows the wind field for the low soil moisture (LSM) run with the overlaying contours showing vertical velocities (cm-sec^{-1}) at 10 meters. Figure (b) shows the wind field for the high soil moisture (HSM) run with the overlaying contours showing vertical velocities at 10 meters. Figure (c) shows the observed winds at CCAS/KSC at the 54-ft tower level.

4. Sea Breeze Predictions

RAMS' predictions of the occurrence and movement of the sea breeze was evaluated for the months of July and August 1994. The following paragraphs describe the results of the evaluation and RAMS' performance for a representative week.

The RAMS model configuration for ERDAS has been documented in several reports and papers written by Lyons and Tremback. The ERDAS Final Report (Lyons and Tremback 1994) presents details of the configuration (Section 2.1: Meteorological Modeling). Important features of the model configuration are:

- The horizontal grid spacing of the three nested grids are 60 km (38 x 36 points), 15 km (34 x 38 points), and 3 km (37 x 37 points).
- In the vertical, there are 22 telescoping layers extending to a height of 13.5 km for the large and medium size domain grids and to a height of 3 km for the small domain size grid.
- The model runs twice daily producing hourly forecasts for a total of 24 hours beginning at 0000 UTC and 1200 UTC.
- The model physics selected for ERDAS do not include clouds, condensation, or precipitation.

Dispersion models require accurate wind data to produce accurate concentration predictions. Therefore, the evaluation focused on RAMS' predictions of wind speed and wind direction. The RAMS predictions were compared to the observed hourly wind speeds and directions from several towers and surface observation sites in the Cape Canaveral area. Figure 4-1 presents graphs showing observed and predicted wind speed and wind direction for a representative seven-day period.

4.1 Case Study of One-Week: 15-21 July 1994

The analysis presented in this report compares the wind data collected at the 4-meter level of Tower 110 with the RAMS wind data from the lowest grid height of 11 meters interpolated to the Tower 110 location. Tower 110 is located between Launch Complexes 40 and 41, approximately 1 km west of the coastline. The example analysis period presented in this report is the seven-day period 15-21 July 1994.

To determine the effect of clouds and precipitation on the RAMS predictions, graphs were produced of hourly observed total sky cover and observed weather (thunder, rain, rain shower, and/or thunderstorm) from the Shuttle Landing Facility. Graphs with this data are included in Figure 4-1.

The graphs comparing observed and predicted winds are presented in Figure 4-1. The primary goals of comparing the observed and predicted winds were to determine:

- How well RAMS predicted the sea breeze with regard to its timing and location,
- What effect did cloudy skies and thunderstorms have on RAMS predictions, and

- How well did RAMS predict the diurnal variability of wind speed.

The typical sea breeze regime on Florida's east coast is characterized by an early morning, westerly, off-shore component wind (1200 UTC to approximately 1800 UTC) that switches to an easterly, on-shore component wind during late morning or early afternoon (approximately 1600 UTC to 2000 UTC). Of the seven days shown in Figure 4-1, RAMS predicted a morning westerly component wind that switched to an east wind on six of the days. Of these six days, Tower 110 observed a westerly wind that switched to an east wind on five of the days. On 15 July 1994, the observed wind was easterly through the morning hours. RAMS consistently predicted a morning westerly wind for only one hour before switching the winds to easterly as shown on the wind direction graphs as gray spikes at 1300 or 1400 UTC on 15-19 July. On these days, the pressure gradient was relatively weak, and the model was most likely detecting the early morning land breeze sometimes referred to as a drainage flow.

Even though RAMS did a good job predicting the occurrence of the sea breeze for these seven days, it predicted the switch from westerly to easterly flow earlier than it occurred on all but one of the five days that it correctly predicted the sea breeze occurrence. Table 4-1 presents the times of the predicted and observed sea breeze passage at Tower 110.

Table 4-1. Time of sea breeze passage at Tower 110 for 15-21 July 1994.

Date	RAMS	Observed	Difference of Predicted–Observed
15 July 94	1500 UTC	Continuous easterly winds	-
16 July 94	1400 UTC	1600 UTC	-2 hours
17 July 94	1400 UTC	1600 UTC	-2 hours
18 July 94	1400 UTC	1500 UTC	-1 hours
19 July 94	1400 UTC	1700 UTC	-3 hours
20 July 94	No sea breeze predicted	No sea breeze observed	-
21 July 94	1500 UTC	1500 UTC	0 hours

In general, the graph comparing wind directions for the seven day period indicated that the wind directions from RAMS agree reasonably well with the observed wind directions except on 19 and 20 July. The graph of the sky cover and weather events at the bottom of Figure 4-1 shows that on 19 and 20 July there was significant cloud cover through the morning hours. The other five days in the analysis period had minimal sky cover during the morning hours.

RAMS accurately predicted the wind direction on days that were not cloudy during the morning hours but was unable to predict wind direction during the cloudy conditions of 19 and 20 July. This result is not surprising since the model is configured to run in the "dry mode"

meaning the microphysics module in RAMS that generates clouds and precipitation is turned off to reduce the model runtime. Therefore, the model was not expected to perform well during these cloudy conditions and the results of this analysis confirm this.

Comparing the modeled and observed wind speeds (middle graph, Figure 4-1) indicates that RAMS predicted the diurnal increase and decrease of the wind speed. However, the predicted wind speeds were greater than the observed wind speeds during the afternoon hours. One explanation for the over estimates of predicted wind speed is that the RAMS winds at 11 meters are being compared with the observed winds at 4 meters. Wind speeds typically increase with height near the surface due to less friction. Therefore, wind speeds at 4 meters would tend to be less than those at 11 meters.

Figure 4-1. Graphs comparing the winds observed at Tower 110 (black) and predicted by RAMS (gray) for 15-21 July 1994. The top graph shows wind direction (deg.), the middle graph shows wind speed (ms^{-1}), and the bottom graph shows observed sky cover in tenths (gray diamonds) and observed weather (black asterisks) at the SLF. RAMS data were produced by daily RAMS runs which were initialized at 1200 UTC and which ran for 24 hours.

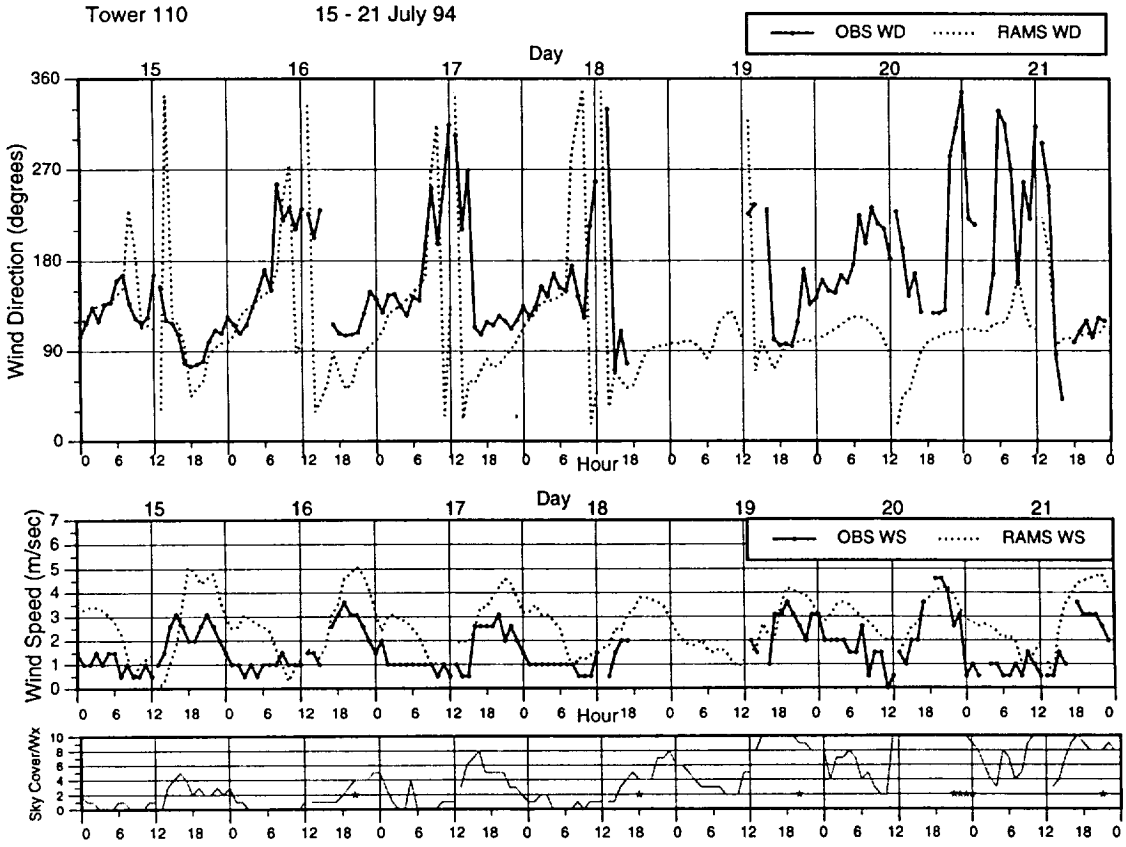

4.2 Analysis of July and August 1994

Tables summarizing the analysis of the observed and predicted wind speed and directions at Towers 303, 805, and 110 (Tables 4-2 to 4-7) are presented in this section. The Siler diffusion classifications for each day are also included in each table (Siler 1980). The Siler diffusion classes are the nine basic weather patterns associated with the different transport and diffusion patterns typically observed at CCAS/KSC. These classifications were determined by Siler using climatological data collected during 1968 through 1974.

The notations used in Tables 4-2 to 4-7 are as follows:

- A dash "-" indicates that the predicted and/or observed data were not complete enough to determine the sea breeze movement. Therfore, a comparison analysis was not conducted for these days.

- A blank corresponds to a "no" answer to the question: "Sea breeze predicted?" or "Sea breeze observed?" A comparison analysis was not conducted for these days.

- A "no(east)" with a time of 12 UTC indicates the winds were easterly at the start of the simulation at 12 UTC and that there was no wind shift from westerly to easterly. Sea breeze passage was determined by the wind direction shifting from westerly to easterly.

Graphs similar to Figure 4-1 above are presented in Appendix A.

Table 4-2. RAMS-predicted versus observed sea breeze data for Tower 110, July 1994. RAMS runs began at 1200 UTC.

Day	Sea breeze predicted?	Time (UTC)	Sea breeze observed?	Time (UTC)	Pred.– Obs time (hours)	Siler diffusion class
1	yes	15	yes	16	-1	A1
2	-		-			A2
3	-		-			E
4	-		-			A2
5	-		-			A2
6	no		no			A2
7	no		no			A1
8	no		no			A1
9	no		no			A1
10	no		no			A1
11	no		no			A1
12	yes	16	-			A2
13	yes	16	yes	17	-1	A1
14	no		no			A1
15	yes	16	no(east)	12	+4	A1
16	yes	15	yes	18	-3	A3
17	yes	15	yes	17	-2	A3,LV
18	yes	15	yes	16	-1	A3,LV
19	yes	15	yes	18	-3	A3
20	no(east)	12	yes	16	-4	A3
21	yes	16	yes	16	0	A3
22	yes	16	yes	16	0	A1
23	yes	16	yes	18	-2	A2
24	no(east)	12	yes	19	-7	A3
25	yes	18	yes	18	0	A2
26	no(east)	12	yes	17	-5	A3
27	yes	14	yes	18	-4	A2
28	no		yes	17		A2
29	-		-			A2
30	no		no			A1
31	yes	16	no			A1

Table 4-3. RAMS-predicted versus observed sea breeze data for Tower 110, August 1994. RAMS runs began at 1200 UTC.

Day	Sea breeze predicted?	Time (UTC)	Sea breeze observed?	Time (UTC)	Pred.– Obs time (hours)	Siler diffusion class
1	no		no			A1
2	no		no			A1
3	no		no			A1
4	-		-			A1
5	yes	17	yes	17	0	A3
6	-		-			D1
7	yes	14	yes	17	-3	D1
8	yes	16	yes	16	0	D1
9	yes	16	yes	17	-1	B
10	no		no			B
11	no		no			A1
12	no		no			A1
13	no		no			A1
14	no		no			A2
15	no		no			E
16	no		no			E
17	yes	15	yes	18	-3	A2
18	yes	16	yes	17	-1	A2
19	no(east)	12	yes	16	-4	LV,A1
20	yes	16	yes	15	+1	A1
21	yes	16	yes	17	-1	A2
22	no		no			A1,A3
23	yes	16	yes	17	-1	D1
24	yes	16	no(east)	12	+4	D1,B
25	no		no			B
26	-		-			B
27	yes	15	no(east)	12	+3	A1
28	-		-			A1
29	yes	16	-			A1
30	yes	16	-			LV
31	-		-			A2

Table 4-4. RAMS-predicted versus observed sea breeze data for Tower 303, July 1994. RAMS runs began at 1200 UTC.

Day	Sea breeze predicted?	Time (UTC)	Sea breeze observed?	Time (UTC)	Pred.– Obs time (hours)	Siler diffusion class
1	yes	15	yes	16	-1	A1
2	-			-		A2
3	-			-		E
4	-			-		A2
5	-			-		A2
6	yes	17	yes	16		A2
7	no		no			A1
8	no		no			A1
9	no		no			A1
10	no(east)	12	yes	20	-8	A1
11	no(east)	12	yes	19	-7	A1
12	yes	16	-			A2
13	yes	16	yes	16	0	A1
14	no(east)	12	yes	16	-4	A1
15	no(east)	12	yes	14	-2	A1
16	yes	15	yes	18	-3	A3
17	yes	15	yes	15	0	A3,LV
18	no		yes	16		A3,LV
19	yes	15	yes	18	-3	A3
20	no(east)	12	yes	15	-3	A3
21	no(east)	12	yes	16	-4	A3
22	yes	15	yes	17	-2	A1
23	yes	16	yes	17	-1	A2
24	no(east)	12	yes	17	-5	A3
25	yes	17	yes	18	-1	A2
26	yes	15	yes	17	-2	A3
27	yes	14	yes	18	-4	A2
28	no(east)	12	yes	18	-6	A2
29	-		-			A2
30	no(east)	12	yes	17	-5	A1
31	no		no			A1

Table 4-5. RAMS-predicted versus observed sea breeze data for Tower 303, August 1994. RAMS runs began at 1200 UTC.

Day	Sea breeze predicted?	Time (UTC)	Sea breeze observed?	Time (UTC)	Pred.– Obs time (hours)	Siler diffusion class
1	no		no			A1
2	no		no			A1
3	no		no			A1
4	-		-			A1
5	yes	19	yes	17	+2	A3
6	-		-			D1
7	yes	14	yes	18	-4	D1
8	no		no			D1
9	yes	16	yes	16	0	B
10	no		no			B
11	no		yes	17		A1
12	no		no			A1
13	no		no			A1
14	no		yes	15		A2
15	yes	14	yes	16	-2	E
16	no		no			E
17	yes	15	yes	19	-4	A2
18	yes	16	-			A2
19	no(east)	12	yes	17	-5	LV,A1
20	yes	15	yes	15	0	A1
21	yes	16	yes	16	0	A2
22	no(east)	12	yes	19	-7	A1,A3
23	yes	16	yes	15	+1	D1
24	yes	16	no			D1,B
25	yes	15	yes	16	-1	B
26	-		-			B
27	yes	15	no			A1
28	-		-			A1
29	yes	16	yes	17	-1	A1
30	yes	16	-			LV
31	-		-			A2

Table 4-6. RAMS-predicted versus observed sea breeze data for Tower 805, July 1994. RAMS runs began at 1200 UTC.

Day	Sea breeze predicted?	Time (UTC)	Sea breeze observed?	Time (UTC)	Pred.– Obs time (hours)	Siler diffusion class
1	yes	15	no			A1
2	-		-			A2
3	-		-			E
4	-		-			A2
5	-		-			A2
6	no		no			A2
7	no		no			A1
8	no		no			A1
9	no		-			A1
10	no		no			A1
11	no		no			A1
12	yes	18	-			A2
13	yes	18	yes	18	0	A1
14	no		no			A1
15	yes	18	yes	18	0	A1
16	yes	15	yes	20	-5	A3
17	yes	15	yes	16	-1	A3,LV
18	no		yes	17		A3,LV
19	yes	15	yes	19	-4	A3
20	no(east)	12	yes	15	-3	A3
21	yes	17	yes	16	+1	A3
22	yes	16	yes	15	+1	A1
23	yes	16	yes	18	-2	A2
24	yes	20	yes	20	0	A3
25	yes	18	yes	17	+1	A2
26	yes	16	yes	20	-4	A3
27	yes	16	yes	18	-2	A2
28	no		yes	20		A2
29	-		-			A2
30	no		no			A1
31	no		no			A1

Table 4-7. RAMS-predicted versus observed sea breeze data for Tower 805, August 1994. RAMS runs began at 1200 UTC.

Day	Sea breeze predicted?	Time (UTC)	Sea breeze observed?	Time (UTC)	Pred.– Obs time (hours)	Siler diffusion class
1	no		no			A1
2	no		no			A1
3	no		no			A1
4	-		-			A1
5	no		no			A3
6	no		no			D1
7	yes	16	-			D1
8	yes	16	yes	19	-3	D1
9	yes	18	yes	16	+2	B
10	no		no			B
11	no		no			A1
12	no		no			A1
13	no		no			A1
14	no(east)	12	yes	15	-3	A2
15	yes	14	-			E
16	no		no			E
17	yes	15	yes	20	-5	A2
18	yes	17	-			A2
19	no		no			LV,A1
20	yes	16	yes	18	-2	A1
21	yes	19	yes	18	+1	A2
22	yes	17	no			A1,A3
23	yes	20	yes	19	+1	D1
24	yes	16	no(east)	12	+4	D1,B
25	yes	15	no(east)	12	+3	B
26	-		-			B
27	yes	15	-			A1
28	-		-			A1
29	yes	18	yes	18	0	A1
30	yes	18	-			LV
31	-		-			A2

5. Titan Launch Plume Analysis - 3 May 94

Part of the ERDAS model evaluation included evaluation of the REEDM and HYPACT diffusion models. The evaluation consisted of comparing model data with launch plume data collected since March 1994 for Space Shuttle and Titan IV launches. The following paragraphs describe the AMU's evaluation of the ERDAS diffusion models for the Titan IV Launch on 03 May 1994.

The Titan IV rocket was launched from Launch Complex 41 (LC-41) at Cape Canaveral Air Station (CCAS) at 1555 UTC on 03 May 1994. The ERDAS meteorological model RAMS and diffusion models REEDM and HYPACT were used to model the transport and diffusion of the exhaust plume and to compare the modeled plume data with observed data collected by Aerospace Corporation's plume imaging cameras. The following is a discussion of the modeling analyses of this launch.

5.1 Meteorology

On the morning of 03 May, high pressure was located in the Middle Atlantic States with a weak cold front extending westward from southern Georgia into the northern Gulf of Mexico. Temperatures at the Shuttle Landing Facility (SLF) on 03 May ranged from a low of 66°F to high of 85°F. The winds were from the east and southeast across Florida. Weather observers at the SLF reported scattered clouds during the morning before the launch and thunder and thunderstorms three hours after the launch beginning at 1855 UTC.

5.2 RAMS Analyses

ERDAS runs the RAMS model twice daily beginning at 0000 UTC and 1200 UTC. Each simulation runs for 24 hours and produces hourly output of meteorological data. The RAMS simulation starting at 1200 UTC on 03 May was used for this analyses. At 1600 UTC, near the time of the launch, RAMS predicted the surface winds at a height of 10.6 m to be from approximately 110° and the winds aloft at a height of 1212 m to be from approximately 150°. The RAMS wind field for these levels at 1600 UTC are shown in Figures 5-1 and 5-2.

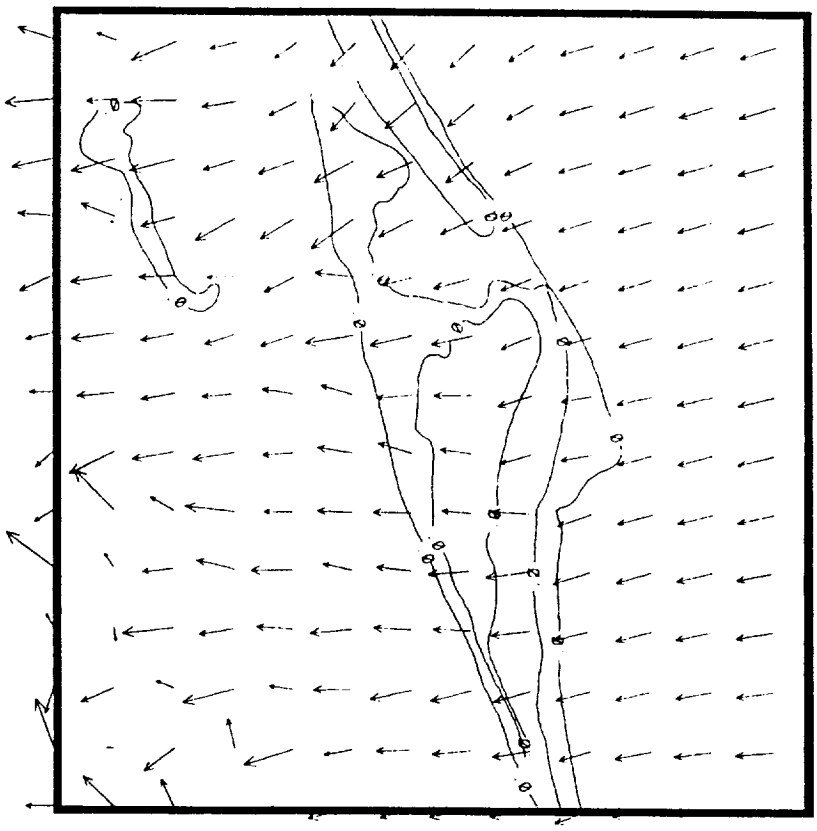

Figure 5-1. RAMS wind field at the surface (10.6 m)at 1600 UTC on 03 May 1994.

To assess the accuracy of the RAMS wind predictions on the morning of 03 May, RAMS data were compared with data measured at Tower 110, located less than 2 km from LC-41. The winds at the lowest two tower levels (3.6 m and 16.4 m) and the winds in the lowest RAMS layer (10.6 m) for 1500 UTC, 1600 UTC, 1700 UTC are compared in Table 5-1. For these three times, the data show that the RAMS wind directions at 10.6 m were more easterly than the observed southeasterly winds at 3.6 m and 16.4 m at Tower 110. The RAMS average wind direction was 87° while the average observed wind directions were 122° at 3.6 m and 132° at 16.4 m. The RAMS wind speeds were slightly stronger than the observed wind speeds at both tower levels. RAMS average wind speeds were 5.3 m s^{-1} while the observed wind speeds averaged 3.6 m s^{-1} at 3.6 m and 4.4 m s^{-1} at 16.4 m.

5.3 ERDAS Diffusion Analyses

5.3.1 REEDM launch plume source term predictions

ERDAS uses REEDM to predict the initial source term for the Titan IV launch plume. The source term is defined as the release rate (mass per unit time) of emitted material. REEDM generates the source term by taking data stored for each launch vehicle and for each material emitted during a launch and computing the total amount of material released. REEDM then distributes the material into different vertical layers. For the launch analysis presented here, hydrogen chloride (HCl) was selected because it is a chemical routinely modeled by Range Safety during pre-launch operations.

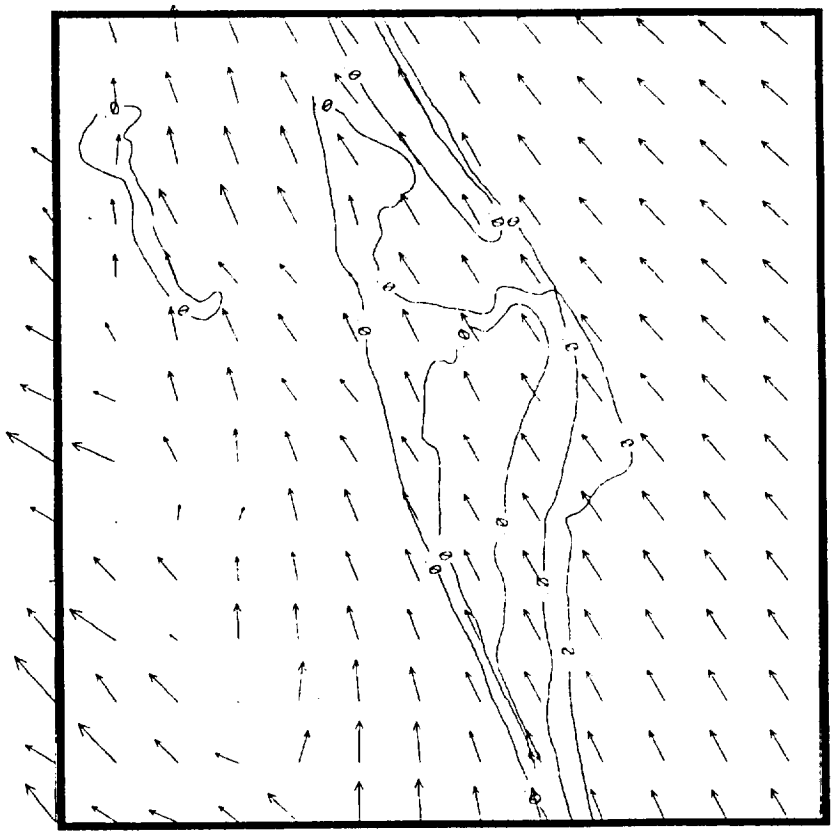

Figure 5-2. RAMS wind field aloft (1212 m) at 1600 UTC on 03 May 1994.

Table 5-1. Observed wind data at Tower 110 during the period 1500 UTC to 1700 UTC.

	Observed 3.6 m		Observed 16.4 m		RAMS 10.6 m	
Time	Wind direction	Wind speed	Wind direction	Wind speed	Wind direction	Wind speed
(GMT)	(degrees)	(m s^{-1})	(degrees)	(m s^{-1})	(degrees)	(m s^{-1})
1500	134	3.6	142	4.6	106	4.3
1600	111	3.6	127	4.1	79	5.7
1700	121	3.6	128	4.6	77	5.9

For this case, REEDM generated 29 layers from the surface up to 3000 m and put material in 17 of the highest layers beginning at 400 m (Table 5-2). The layers with the most material were layers 19 to 22 located at 1000 m to 1400 m. REEDM calculated the cloud stabilization height at 930 meters. The cloud stabilization height is defined as the height of the center of the cloud at the point the cloud temperature approaches the ambient temperature or the cloud buoyancy approaches zero (Bjorklund 1990).

Table 5-2. REEDM exhaust cloud calculations for Titan IV launch on 03 May 1994. Meteorological data were provided by RAMS predictions from 1200 UTC run.

		-----EXHAUST CLOUD-----				
MET. LAYER NO.	TOP OF LAYER	LAYER SOURCE STRENGTH	CLOUD UPDRAFT VELOCITY	CLOUD RADIUS	STD. DEVIATION MATERIAL DIST.	
					ALONG WIND	CROSSWIND
	(m)	(grams)	($m\ s^{-1}$)	(m)	(m)	(m)
1	10.1	0.00000E+00	7.6	.0	.0	.0
2	20.1	0.00000E+00	9.3	.0	.0	.0
3	35.1	0.00000E+00	9.9	.0	.0	.0
4	50.0	0.00000E+00	9.7	.0	.0	.0
5	66.6	0.00000E+00	9.3	.0	.0	.0
6	83.3	0.00000E+00	8.7	.0	.0	.0
7	100.0	0.00000E+00	8.1	.0	.0	.0
8	133.3	0.00000E+00	7.2	.0	.0	.0
9	166.6	0.00000E+00	6.4	.0	.0	.0
10	199.9	0.00000E+00	5.7	.0	.0	.0
11	249.9	0.00000E+00	5.0	.0	.0	.0
12	299.9	0.00000E+00	4.5	.0	.0	.0
13	399.9	4.49427E+05	3.8	328.0	152.8	152.8
14	499.9	3.44982E+06	3.3	462.3	215.4	215.4
15	600.2	5.90615E+06	2.8	547.7	255.2	255.2
16	700.1	7.76001E+06	2.3	605.1	282.0	282.0
17	800.1	9.06326E+06	1.7	642.1	299.2	299.2
18	900.1	9.80135E+06	0.8	662.1	308.5	308.5
19	1000.0	1.25856E+07	.0	666.7	310.7	310.7
20	1100.0	1.31756E+07	.0	656.2	305.8	305.8
21	1200.0	1.20427E+07	.0	629.9	293.5	293.5
22	1399.9	1.85109E+07	.0	555.4	258.8	258.8
23	1600.2	7.48185E+06	.0	347.4	161.9	161.9
24	1800.1	5.51435E+06	.0	199.9	93.2	93.2
25	2000.1	5.18670E+06	.0	199.9	93.2	93.2
26	2250.0	6.09702E+06	.0	199.9	93.2	93.2
27	2500.0	5.73472E+06	.0	199.9	93.2	93.2
28	2750.1	5.43047E+06	.0	199.9	93.2	93.2
29	3000.1	5.16506E+06	.0	199.9	93.2	93.2

5.3.2 HYPACT plume predictions

HYPACT is the advanced Lagrangian particle dispersion model in ERDAS. Dispersion in the Lagrangian mode of HYPACT is simulated by tracking a large set of particles. Subsequent positions of each particle are computed from the relation:

$$X[t+\Delta t] = X[t] + [u + u'] \Delta t$$

$$Y[t+\Delta t] = Y[t] + [v + v'] \Delta t$$

$$Z[t+\Delta t] = Z[t] + [w + w' + w_p] \Delta t$$

where u, v and w are the resolvable scale wind components which are derived from RAMS or the hybrid (RAMS/tower observations) wind field, and u', v', and w' are the subgrid turbulent wind components deduced from RAMS. The w_p term is the terminal velocity resulting from external forces such as gravitational settling.

For modeling launch scenarios, the HYPACT model obtains the source term data (release rate) from the REEDM launch plume data. HYPACT then diffuses the plume using the RAMS-predicted wind fields and potential temperature fields to advect and disperse the particles vertically and horizontally downwind from the source.

5.3.3 Comparison with observations

To determine how well ERDAS modeled the launch plume, Mr. Evans compared the REEDM/HYPACT predictions with observations made by Aerospace Corporation's plume imaging cameras (Aerospace 1995). Aerospace Corporation is collecting measurements of Titan IV launch clouds using visible and infrared cameras as part of a project to validate models such as REEDM. A description of the imaging project is provided in Aerospace (1995). Data from the 03 May 1994 Titan IV launch were obtained from Heidner (1994).

Heidner (1994) provided a graph showing a plane view of the horizontal movement of the plume as it moved away from LC-41. Figure 5 shows this plume centerline on a map of CCAS. Heidner (1994) also showed a time-height cross section of the plume from the time of the launch to 45 minutes after launch. This cross section is presented in Figure 5-3. For the first 5 minutes after launch, the exhaust plume was very buoyant and rose until it stabilized in the layer between 900 m (2950 ft) and 1300 m (4270 ft). The plume was observed to stay close to this level for the remaining 20 minutes of measurements. Data were missing for the period from 5 to 25 minutes after launch. The top of the plume reached a peak of 1500 m (4920 ft) at 33 minutes and the bottom dropped to a minimum height of 700 m (2300 ft) at 25 minutes. The centerline of the plume was also mapped to show the movement of the plume away from the source. Figure 5-2 shows how the observed plume moved initially to the west with the low-level easterly winds and then moved north as it rose upward reaching the level of the southerly winds at approximately 1200 m.

For this Titan IV launch, HYPACT moved the lowest part of the plume (at a height of approximately 400 m) to the west in response to the low-level easterly flow. HYPACT moved the upper part of the plume (at a height of approximately 1300 m) to the north-northwest with the south-southeasterly flow aloft.

To compare the REEDM/HYPACT modeled plume location to the observed location, HYPACT's plume for the layer 1000 to 1500 meters was used for the comparison since this layer matched the height of the observed plume. Figure 5-3 shows the paths of the observed and REEDM/HYPACT modeled plumes. The HYPACT-predicted plume followed a very similar trajectory to the observed plume but HYPACT moved it more to the west than observed. HYPACT predicted the northward

movement beginning at 15 minutes after launch as it moved the plume in a north-northwesterly direction. The observed plume began moving north after approximately 5 minutes.

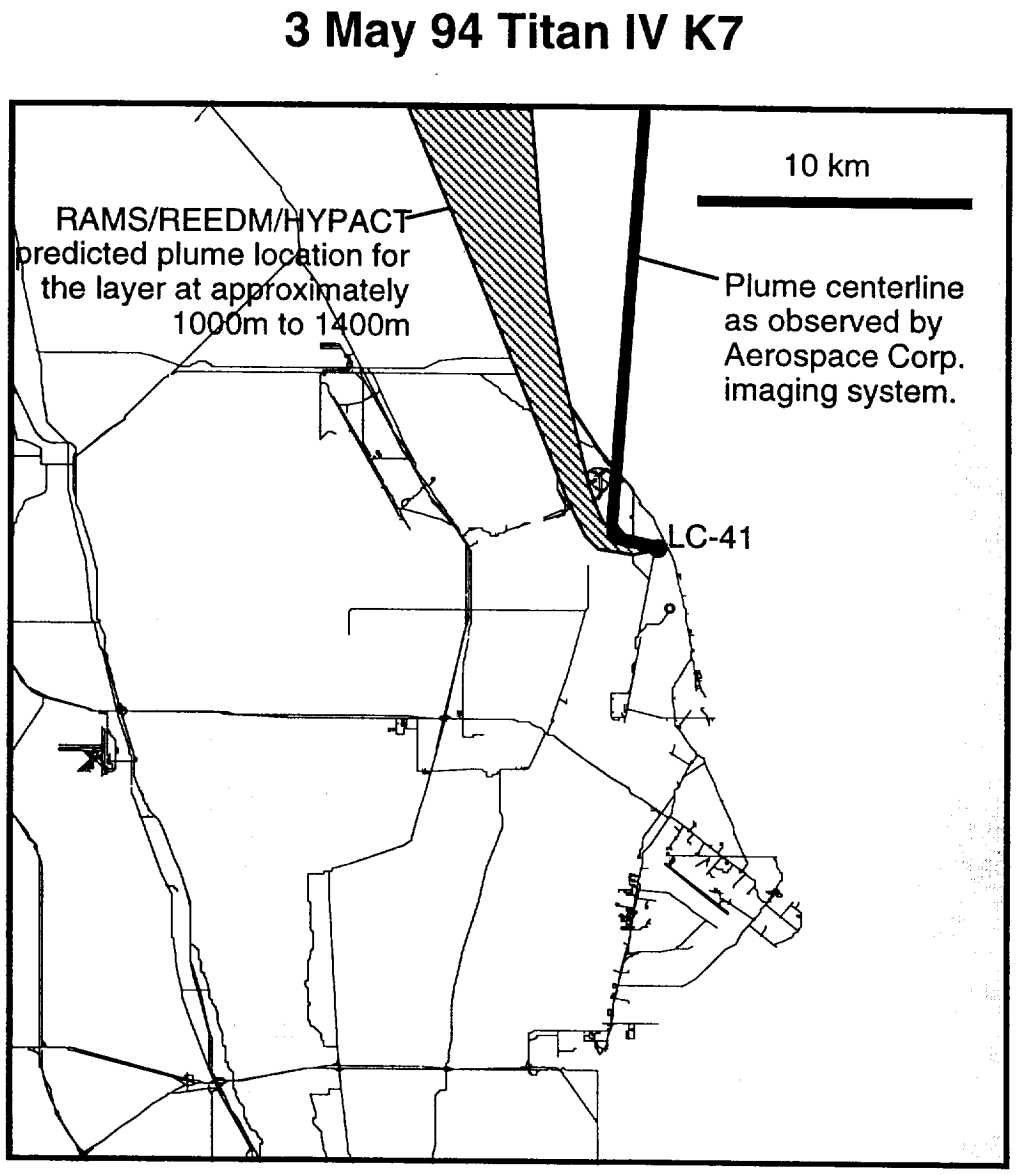

Figure 5-3. Centerline trajectories of observed plume and REEDM/HYPACT modeled plume for Titan IV K7 launch on 03 May 1994.

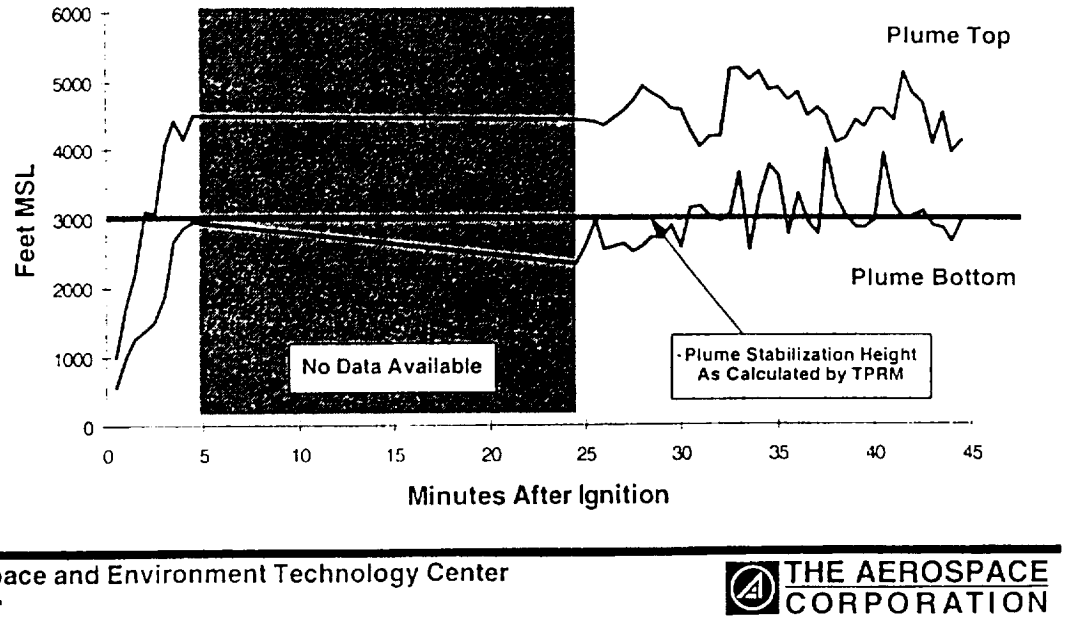

Figure 5-4. Titan IV plume height versus time for launch on 03 May 1995 as measured by Aerospace Corporation plume imaging cameras (Aerospace 1995).

5.4 Results and Conclusions

The analyses of this Titan IV launch case study indicate that the RAMS/REEDM/HYPACT modeling system has promising potential for modeling launch exhaust plumes. However, the case study also showed ERDAS needs improvements in some areas.

The promising results were:

- RAMS correctly predicted the 3-dimensional structure of the wind field, although the directions differed by approximately 35° and RAMS slightly overpredicted the wind speeds. The prevailing surface winds on 03 May were southeasterly and the winds at approximately 1200 m were southerly. During the period from the RAMS initialization at 1200 UTC to 1700 UTC, RAMS predictions of the easterly surface winds followed the tower observations but showed a trend of more easterly than southeasterly winds. RAMS overpredicted the wind speeds by 1 to 2 m s^{-1}. RAMS predicted the winds at 1212 m to be from the southeast. However, the plume observations indicated that the winds at the 1000 m to 1500 m level were more southerly than southeasterly.

- HYPACT-predicted plume trajectory closely followed the observed trajectory with some variation over time. Figure 5.3 shows the comparison of the predicted versus observed plume trajectories. The predicted trajectory followed closely the observed trajectory but went a little further west before rising into the southeasterly flow aloft. The stronger wind speeds predicted by RAMS may account for the initial movement further west than observed. Once reaching the

southeasterly flow aloft the RAMS winds moved the plume more to the northwest than north because of the slight difference in the wind direction discussed in the previous paragraph.

The improvements needed are:

- HYPACT should be modified to handle buoyant plumes rather than treating the plumes as passive tracers. The actual Titan IV rocket exhaust plumes are heated and are quite buoyant initially after launch. Although REEDM considers buoyancy effects in computing its source term properties, these are not all taken into consideration by HYPACT. For example, REEDM computes buoyancy-driven updraft velocities ranging from 0.8 to 3.8 m s^{-1} for the layers between 400 and 900 m (Table 5-2). However, HYPACT does not use these REEDM-predicted vertical velocities to move material vertically out of these layers. HYPACT does not change the plume due to its own buoyant properties but moves and disperses it due to environmental winds and turbulence.

- HYPACT should be modified to handle deposition of solid and liquid plume particulates since deposition from launch plumes is an important factor in the diffusion. Also, because of the solid rocket motor exhaust, there is considerable deposition of HCl particulates and other materials from a Titan IV launch. The version of HYPACT in ERDAS does not model dry deposition effects but only models passive tracer material.

6. Space Shuttle Plume

The AMU conducted a study to compare the ERDAS launch plume preditions with the ground footprint resulting from the hydrogen chloride (HCl) deposition of 5 Space Shuttle plumes. The launches chosen for the study were those that occurred during the initial 18-month ERDAS evaluation period (March 1994 to September 1995) for which complete ERDAS model data were available. The locations of the observed and predicted and launch plumes for the 5 launches are presented in Figures 6-1 through 6-5.

6.1 Observed Launch Plume Data

Dynamac Corporation (Bionetics Corp.) collects HCl deposition data after each Space Shuttle launch to determine the environmental effects on vegetation, fish, wildlife, and water quality. The plume generated by a Shuttle launch contains HCl which falls to the ground at distances up to 23 km downwind of the launch pad (Duncan and Schmalzer 1994). The depostion pattern on the ground is determined by a field survey of vegetation after each launch. Following this survey maps are produced and included in reports issued by Dynamac (Bionetics). These maps showed plume location only and did not provide plume concentration data. These maps were compared with the maps generated by ERDAS.

6.2 ERDAS-Predicted Launch Plumes

The ERDAS diffusion models REEDM and HYPACT were run for each of the Space Shuttle launches during the the ERDAS evaluation period in which meteorological data from RAMS were availble. Data were available for 5 launches. Maps were generated by ERDAS which showed the REEDM/HYPACT-predicted plume location. ERDAS uses REEDM to generate the source term (release rate) to initialize HYPACT. HYPACT then diffuses the plume downwind. Because observed concentration data were not available, only plume locations were compared.

6.3 Comparison Results

The data on the results of the comparison of the 5 plumes is presented in Table 6-1. Maps comparing the model-predicted plumes with the observed plume are presented in Figures 1 to 5. Some results of this comparison are:

- HYPACT/REEDM plume was wider than the observed plume because the modeled plume stretched over 1000 meters vertically and therefore encountered significant directional wind shear. The observed plume tended to concentrate near the plume stabilization height.

- Plumes closely overlapped for part of their trajectories in 4 of 5 cases.

- RAMS surface wind direction was within 40° in 4 of 5 cases. For other levels not shown in Table, RAMS did fairly well at predicting wind direction.

- ERDAS did fairly well at predicting plume path. However, depth of plume initialization and depostion of launch plume particles in HYPACT needs some adjustment.

Table 6-1. Data comparing Space Shuttle launch plumes predicted by ERDAS with ground deposition footprints observed from Dynamac Corp.'s (Bionetics Corp.) vegetation survey.

Launch	Date	Time	Launch Complex (	Plume direction	Ob-served plume distance (km)	Model time to reach plume distance (min)	HYPACT/ REEDM plume spread	Observed Plume spread	Twr 110 speed/ direction (dir/kts)	RAMS sf winds at launch complex (dir/kts)
STS-65	8Jul94	1243L	39A	NW	14	37	290°-325°	300°-320°	120°/6	47°/8.7
STS-64	9Sep94	1823L	39B	NW	11	32	292°-020°	297°-320°	118°/5	71°/5.6
STS-66	3Nov94	1200L	39B	WSW	5	10	240°-305°	230°-270°	68° /7	21°/15.5
STS-63	3Feb95	0022L	39B	NE	1+	~2	70°-100°	40°-60°	251°/4	227°/10.
STS-67	2Mar95	0138L	39A	ESE	1+	-	70°-160°	90°-110°	280°/5	307°/9.0

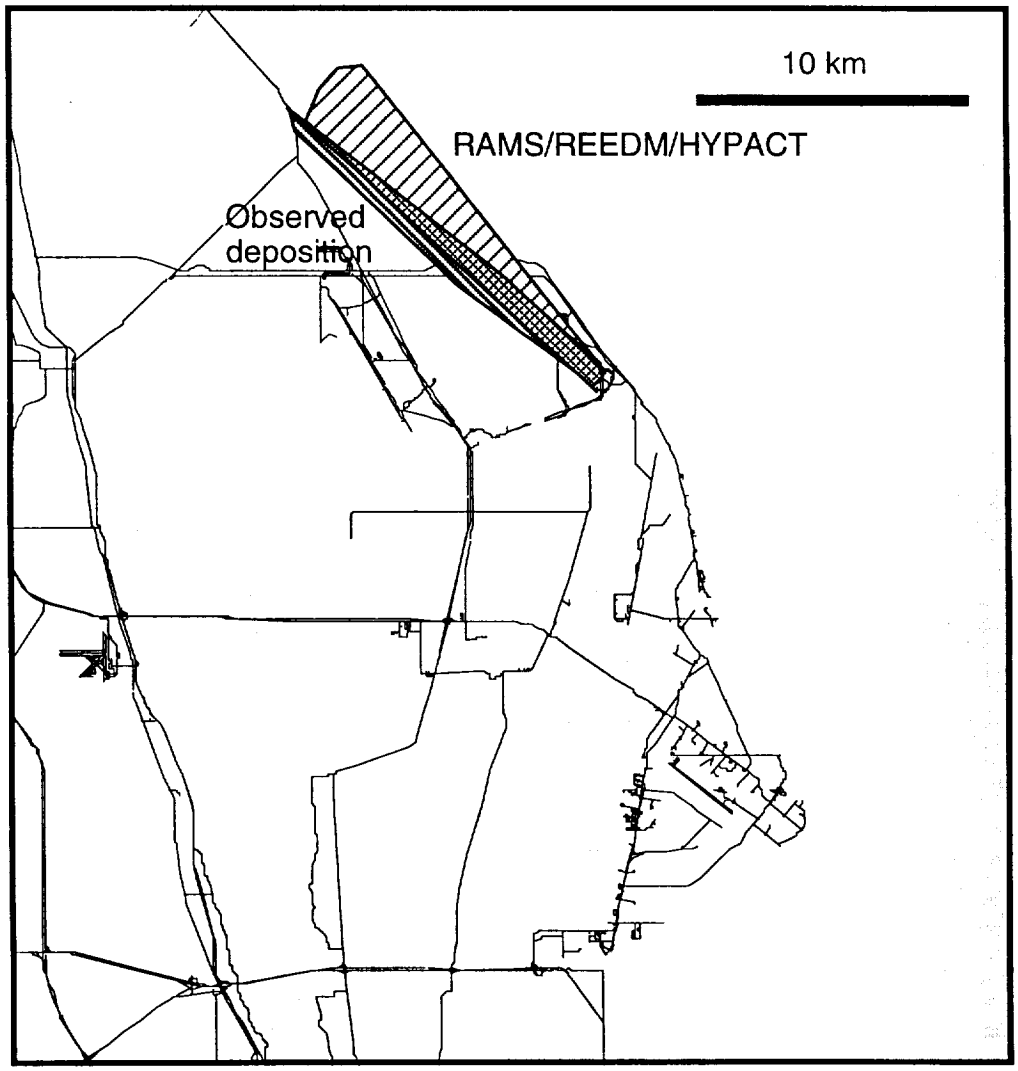

Figure 6-1. Comparison of observed and predicted launch plumes from STS-65 on 8 July 1994. The location of the observed plumes was determined by a ground survey of HCl deposition on vegetation (Bionetics 1994). The location of the predicted plumes was determined by the ERDAS models: RAMS, REEDM, and HYPACT.

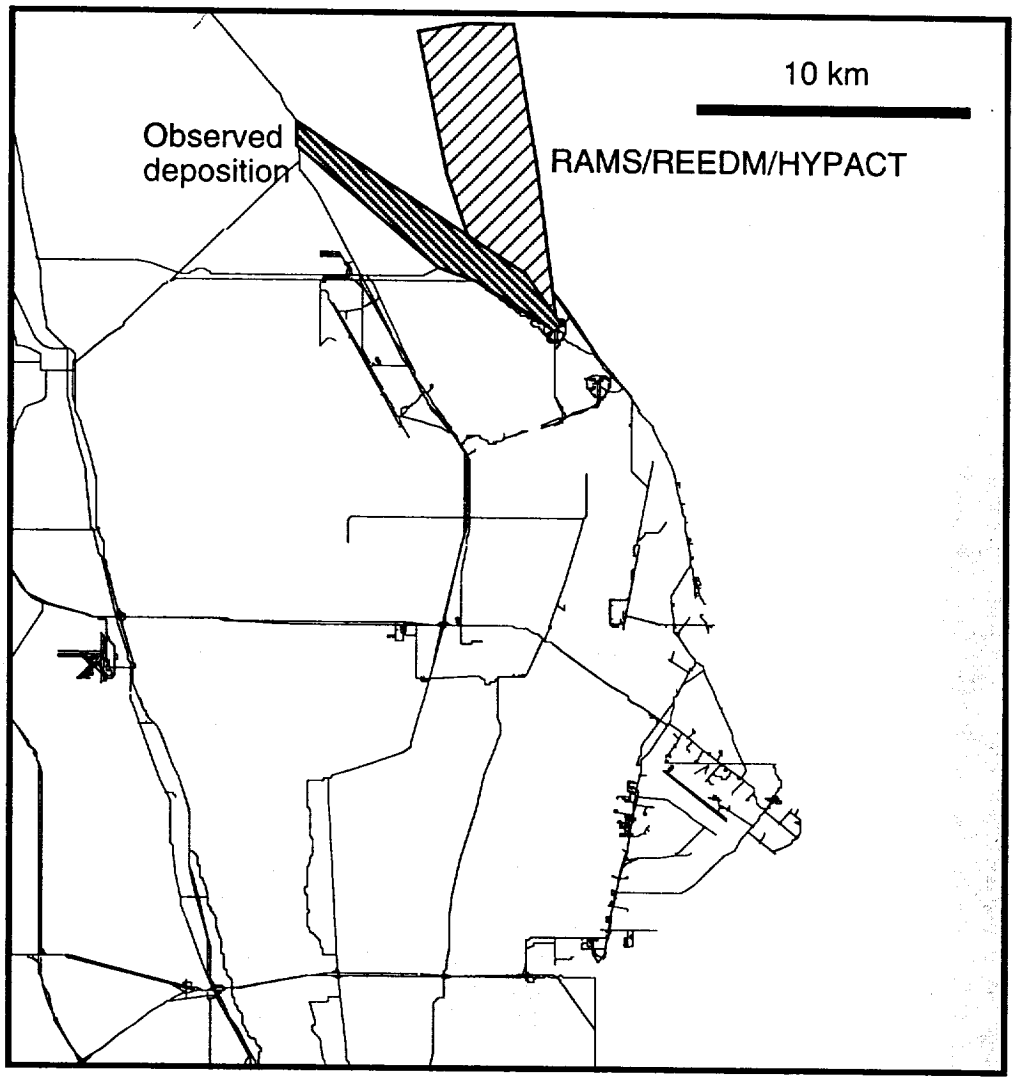

Figure 6-2. Comparison of observed and predicted launch plumes from STS-64 on 9 September 1994. The location of the observed plumes was determined by a ground survey of HCl deposition on vegetation (Bionetics 1994). The location of the predicted plumes was determined by the ERDAS models: RAMS, REEDM, and HYPACT.

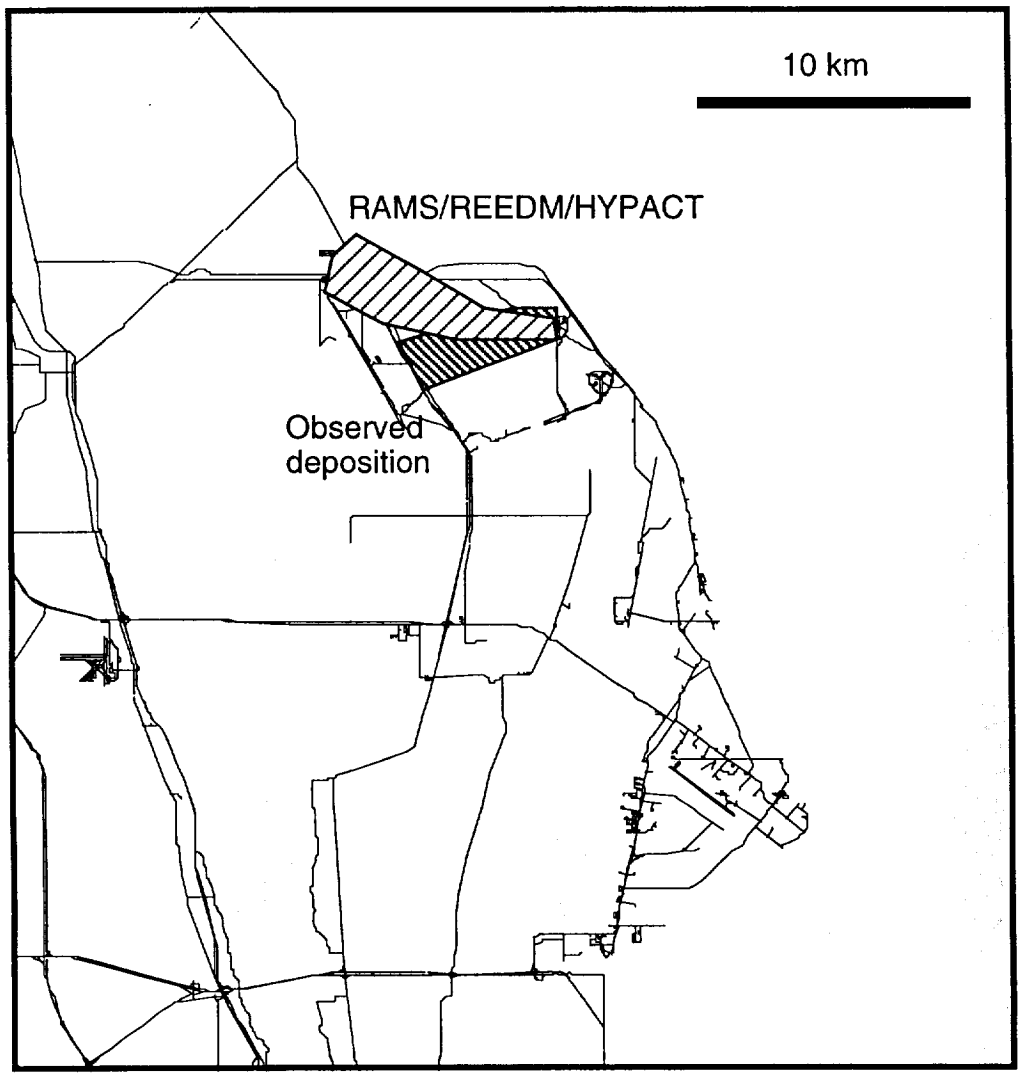

Figure 6-3. Comparison of observed and predicted launch plumes from STS-66 on 3 November 1994. The location of the observed plumes was determined by a ground survey of HCl deposition on vegetation (Bionetics 1994). The location of the predicted plumes was determined by the ERDAS models: RAMS, REEDM, and HYPACT.

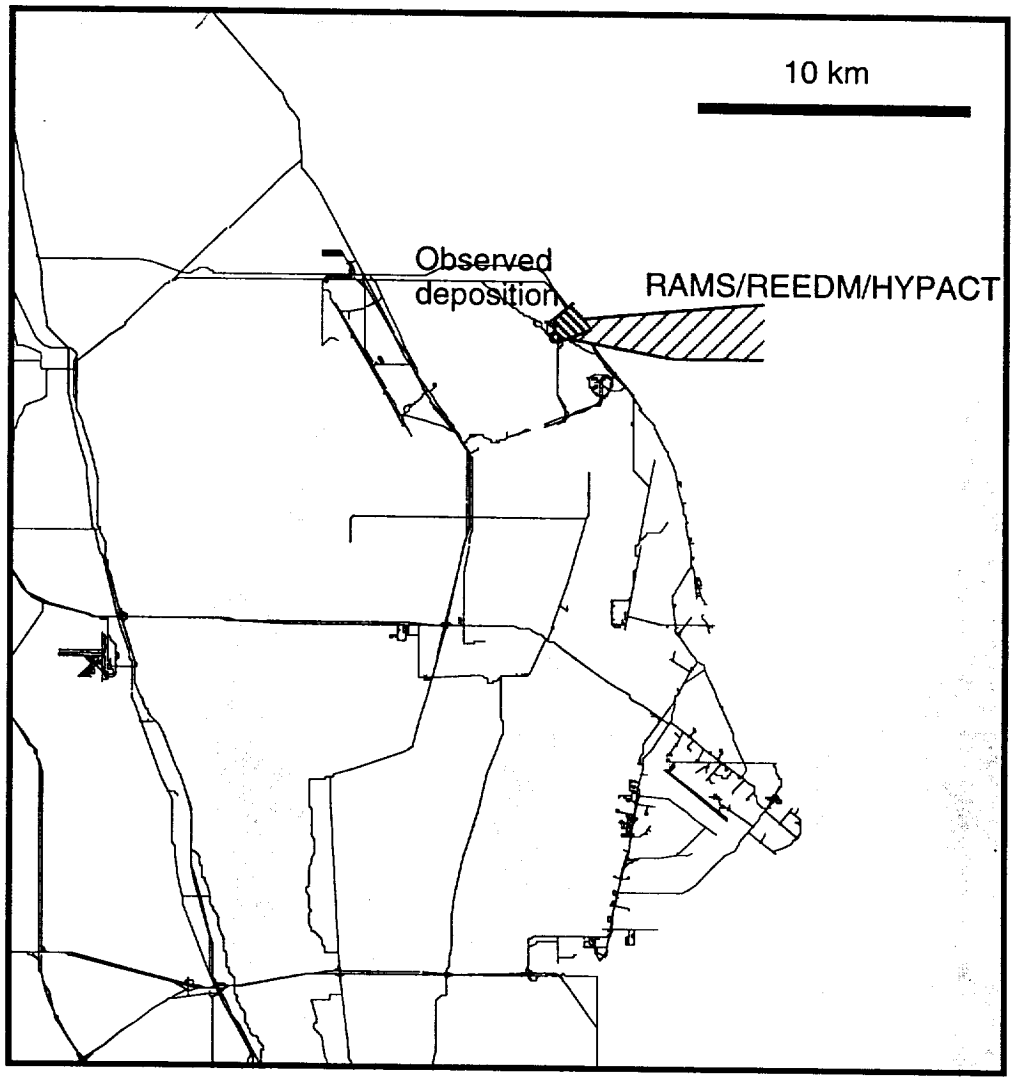

Figure 6-4. Comparison of observed and predicted launch plumes from STS-63 on 3 February 1995. The location of the observed plumes was determined by a ground survey of HCl deposition on vegetation (Dynamac 1995). The observed plume does not extend over the water because no ground survey of the plume was conducted when it moved offshore. The location of the predicted plumes was determined by the ERDAS models: RAMS, REEDM, and HYPACT.

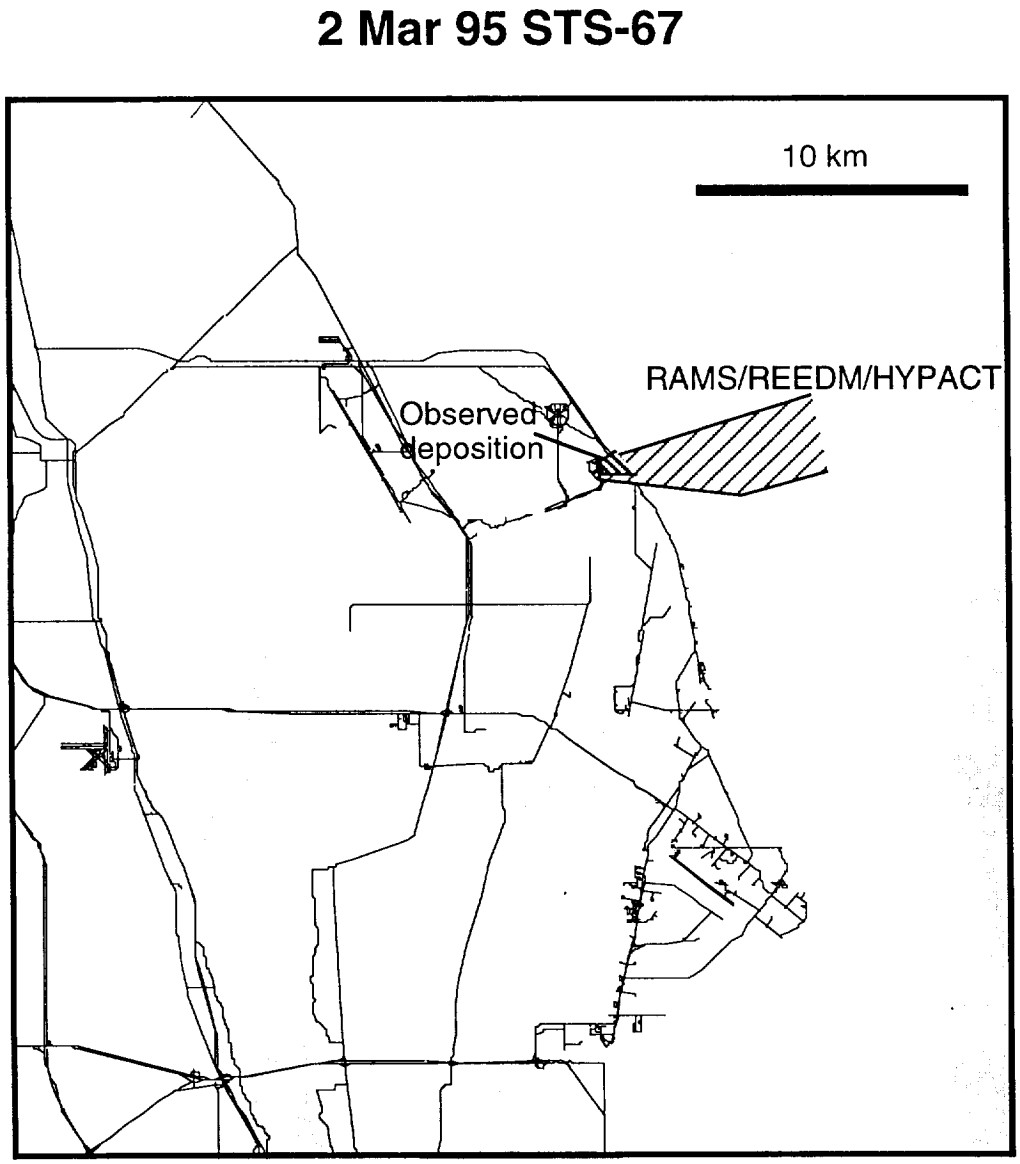

Figure 6-5. Comparison of observed and predicted launch plumes from STS-67 on 2 March 1995. The location of the observed plumes was determined by a ground survey of HCl deposition on vegetation (Dynamac 1995). The observed plume does not extend over the water because no ground survey of the plume was conducted when it moved offshore. The location of the predicted plumes was determined by the ERDAS models: RAMS, REEDM, and HYPACT.

7. N2O4 Release Case Study

At 1426 UTC on 20 August 1994, a nitrogen tetroxide (N_2O_4) pipeline at Titan Complex 41 on Cape Canaveral Air Station (CCAS) ruptured and released 200 to 400 gallons of N_2O_4 vapor into the atmosphere. The AMU used the accident as a case study for evaluating ERDAS' ability to model the release and accurately predict the location and concentration of the plume. We evaluated output from both of the major models within ERDAS–the meteorological model, RAMS (Regional Atmospheric Modeling System), and the diffusion model, HYPACT (Hybrid Particle and Concentration Transport).

Although no measurements were taken of the concentrations within the plume, witnesses observed the brownish-orange plume drift west, rise, and then drift northward offshore during the one to two hour period after the release.

7.1 Model Configuration

The RAMS model configuration for ERDAS was discussed in Section 3.2 of this report. Land use classification of the RAMS 3-km grid cells were derived from high resolution U. S. Geological Survey digital data bases (Figure 7-1). Classes include water and 18 land classifications along with percentage of land coverage.

7.2 Meteorology on 20 August 1994

On the morning of 20 August 1994, a large high pressure area stretched from the South Carolina area eastward into the Atlantic (Figure 7-2). The pressure gradient over Florida was very weak as was indicated by the light and variable surface winds which prevailed at most Florida stations. At 1200 UTC, the WINDS system was reporting wind speeds less than 1.5 ms^{-1} at all towers. Table 7-1 presents the tower data from three towers located near Complex 41 (Figure 7-3). The analyzed surface wind field from RAMS for 1200 UTC showed light northeasterly flow over CCAS and light north and northwesterly flow over Merritt Island (Figure 7-4a). Data from Tower 313 at 1200 UTC (Table 7-2) and from the rawinsonde at 0900 UTC (Table 7-3) showed that the winds above 150 meters were generally from the south at speeds less than 4 ms^{-1}.

During the morning, there was sufficient warming of the surface with the clear skies to produce a sea breeze. Surface winds at Tower 110, located south of Complex 41, were westerly at 1 ms^{-1} at 1300 UTC and then switched to south-southeast at 0.5 ms^{-1} at 1400 UTC. At tower 311, located northwest of Complex 41, the winds went from calm at 1300 UTC to northeasterly at 1 ms^{-1} at 1400 UTC. At tower 509, located southwest of Complex 41, the winds went from southerly at 0.5 ms^{-1} at 1300 UTC to southwesterly at 4 knots at 1425 UTC to south-southeasterly at 1 ms^{-1} at 1505 UTC.

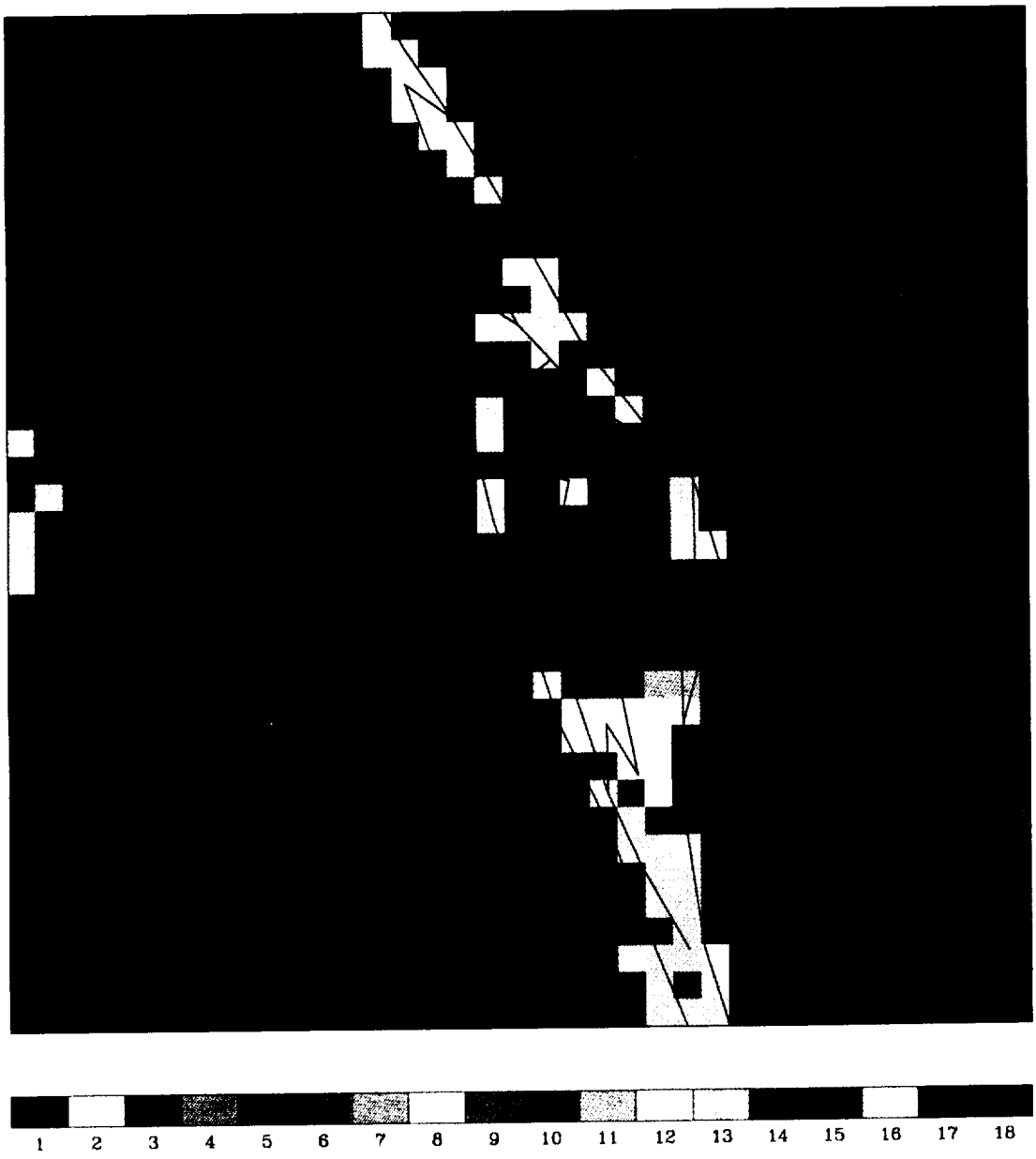

Figure 7-1. Land use classifications for the 3-km grid in ERDAS. Key to map above:

1	Crop/mixed farming	10	Irrigated crop
2	Short grass	11	Semi-desert
3	Evergreen needleleaf tree	12	Ice cap/glacier
4	Deciduous needleleaf tree	13	Bog or marsh
5	Deciduous broadleaf tree	14	Inland water
6	Evergreen broadleaf tree	15	Ocean
7	Tall grass	16	Evergreen shrub
8	Desert	17	Deciduous shrub
9	Tundra	18	Mixed woodland

Table 7-1. Data from selected towers from the morning of 20 August 1994. Data presented are wind direction (degrees), wind speed (knots), temperature (°F), and dew point (°F). Locations of towers are shown on map in Figure 7-3.

		1200	1300	1400	1405	1410	1415	1420	1425	1430	1435	1440	1445	1450	1455	1500	1505	1510	1515	1520	1525	1530	1535	1540	1545	1550	1555	1600	1700
Twr 110	WD	80	267	162	159	135	118	169	168	164	185	171	161	161	163	165	134	142	253	138	143	252	117	104	114	98	120	106	81
	WS	0	2	1	2	2	2	2	2	2	3	2	2	3	2	2	3	3	3	2	4	4	6	5	6	6	6	5	4
	T	79	83	85	85	86	86	86	86	86	86	85	85	86	85	86	85	85	86	86	86	87	87	86	86	87	86	86	86
	Td	78	78	77	78	78	79	78	78	78	77	77	77	77	77	77	77	77	77	77	77	78	78	78	78	79	78	79	78
Twr 311	WD	0	340	47	55	110	80	74	134	166	142	105	75	140	38	9	195	195	231	279	52	231	102	104	85	94	111	80	76
	WS	0	0	2	2	1	1	2	2	2	3	2	3	2	1	0	2	2	4	0	2	4	3	3	3	3	4	2	4
	T	77	81	83	83	82	82	82	82	83	84	84	85	85	85	85	85	85	85	84	84	86	83	83	82	82	82	81	80
Twr 509	WD	171	173	188	203	194	172	227	230	239	237	214	214	173	199	169	167	214	246	258	279	247	313	335	329	310	217	195	59
	WS	1	1	3	2	2	3	4	4	3	2	3	2	3	2	3	2	2	5	3	2	4	2	4	3	2	5	3	4
	T	77	82	85	84	84	84	84	84	84	84	85	86	86	86	86	86	87	85	85	85	86	84	84	85	85	87	87	84

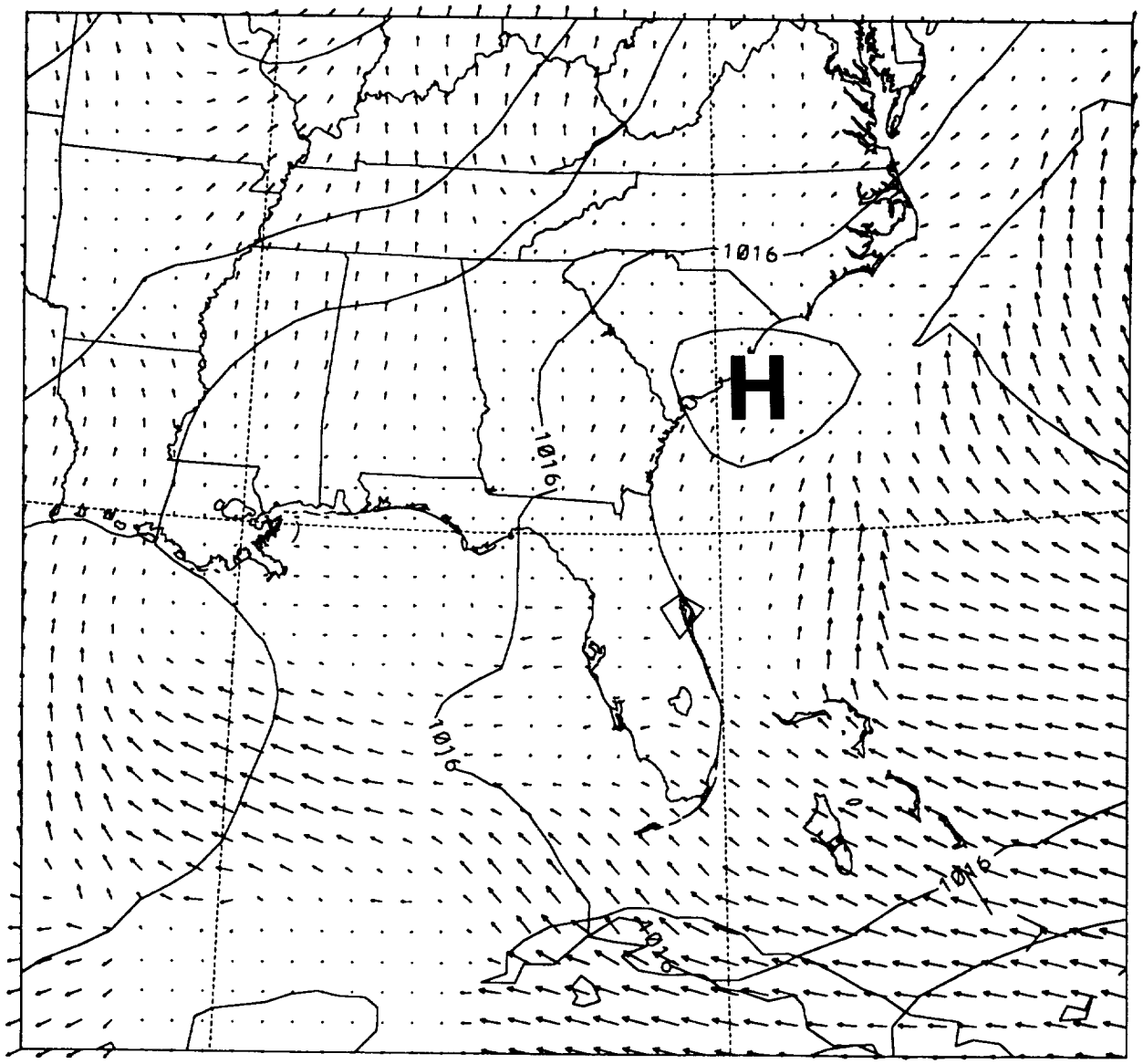

Figure 7-2. Surface map of southeast United States showing pressure (mb) and RAMS-initialized wind vectors at 1200 UTC on 20 August 1994.

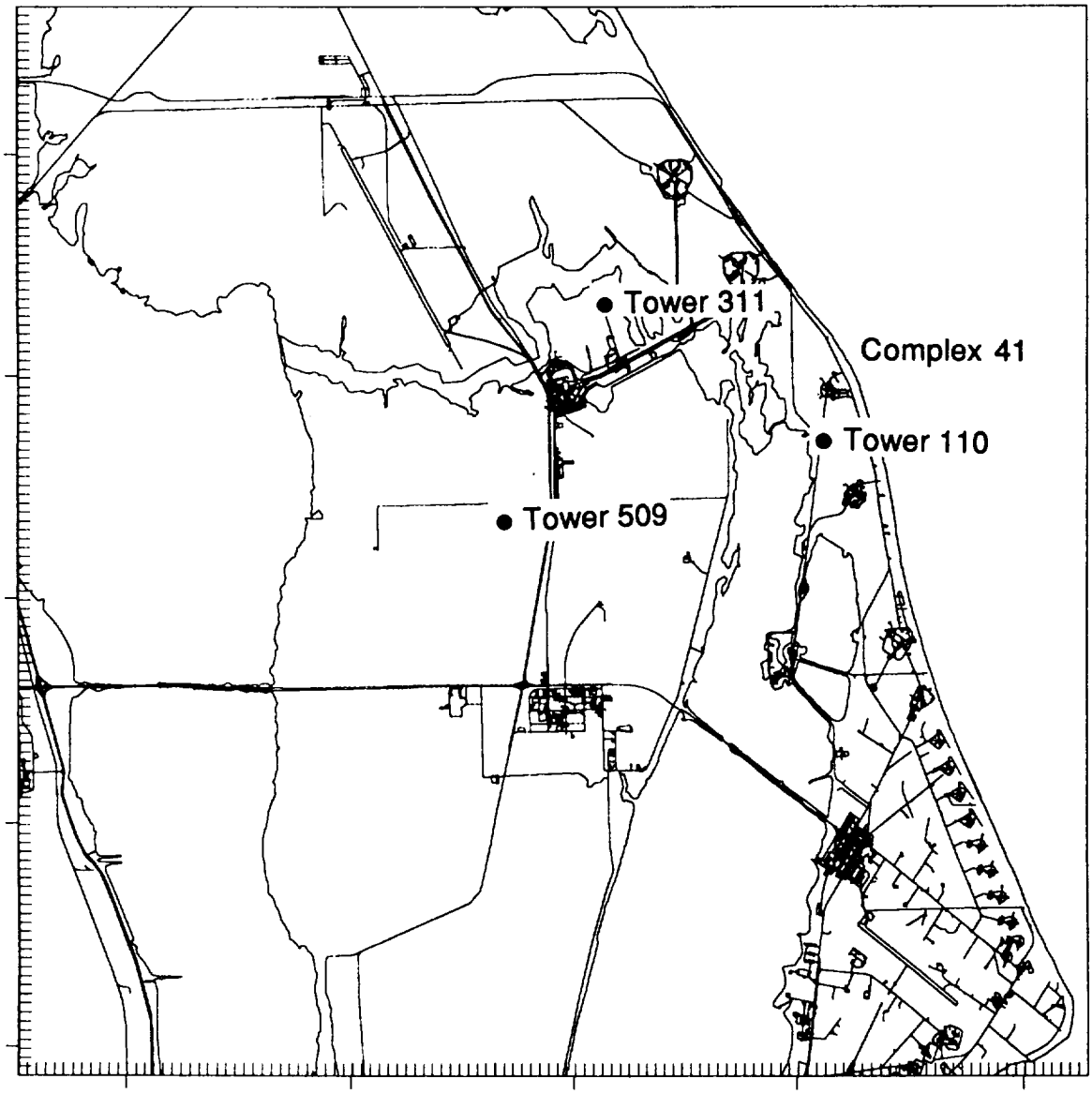

Figure 7-3. Cape Canaveral map showing location of towers listed in Table 7-1.

Table 7-2. Tower 313 winds at 1200 UTC.

Height (m)	Wind direction (degrees)	Wind speed (m/sec)
3.7	-	0
16.5	178	1.0
49.4	190	0.5
62.2	175	1.0
90.0	217	0.5
120.1	173	1.5
150.0	169	1.5

Table 7-3. Cape Canaveral rawinsonde data at 900 UTC.

DAY	TIME (UTC)	IDN	Z (m)	P (mb)	T (°K)	TD (°K)	DIR (deg)	SPD (m/sec)
94232	900	74794	3	1016.0	296.56	295.36	170	1.0
94232	900	74794	153	1000.0	299.36	297.86	170	4.1
94232	900	74794	1572	850.0	291.36	285.36	175	2.5
94232	900	74794		796.0	287.36	283.86		
94232	900	74794	3204	700.0	279.96	275.56	80	3.6
94232	900	74794	5900	500.0	264.86	251.86	275	6.6
94232	900	74794	7590	400.0	254.26	238.26	255	9.2
94232	900	74794	9670	300.0	239.06	227.06	260	7.7
94232	900	74794	10920	250.0	229.26		260	9.2
94232	900	74794	12390	200.0	218.46		255	6.1
94232	900	74794	14180	150.0	209.46		320	7.7
94232	900	74794		109.0	203.06		115	1.5
94232	900	74794	16630	100.0	203.86		105	4.6

Table 7-4. Cape Canaveral rawinsonde data at 1500 UTC.

DAY	TIME (UTC)	IDN	Z (m)	P (mb)	T (°K)	TD (°K)	DIR (deg)	SPD (m/sec)
94232	1500	74794	3	1018.0	303.16	296.16	180	3.6
94232	1500	74794	164	1000.0	301.36	295.36	170	3.6
94232	1500	74794	1585	850.0	290.56	287.06	185	2.0
94232	1500	74794	3218	700.0	280.96	274.96	185	3.0
94232	1500	74794		536.0	267.86	256.86		
94232	1500	74794	5910	500.0	264.26	253.26	240	6.6
94232	1500	74794	7610	400.0	254.86	241.86	240	7.2
94232	1500	74794	9690	300.0	238.06	229.06	255	8.2
94232	1500	74794	10930	250.0	229.26		345	3.6
94232	1500	74794	12390	200.0	217.86		25	5.1
94232	1500	74794		164.0	209.86		355	7.2
94232	1500	74794	14190	150.0	210.46		335	4.1
94232	1500	74794	16650	100.0	206.86		150	2.0

The tower data in Table 7-1 and the analyzed surface wind field presented in Figures 7-4a to 7-4f were used to follow the progression of the sea breeze inland during the morning. The analyzed surface wind field was obtained by performing a gridded Barnes analysis on the tower, buoy and surface data. At 1300 UTC the sea breeze had not moved inland as indicated by the westerly wind at Tower 110. Figure 7-4b shows th southerly and westerly winds which prevailed over most of CCAS and Merritt Island. At 1410 UTC, the winds at Tower 110 switched to southeasterly as the sea breeze moved inland. The analyzed wind field at 1400 UTC (Figure 7-4c) shows weak easterly winds across most of CCAS but not over Merritt Island where winds were from the west. The data from Tower 311 indicates that the sea breeze passed this tower at 1535 UTC as the wind direction shifted from southwesterly to easterly and the temperature dropped from 86°F to 83°F between 1530 and 1535 UTC. The analyzed wind field at 1500 UTC (Figure 7-4d) showed little difference from the 1400 UTC wind field, but by 1600 UTC (Figure 7-4e) the winds were easterly over CCAS and most of Merritt Island. By 1600 and 1700 UTC the sea breeze had moved past Merritt Island to the Indian River as weak easterly flow prevailed over all of KSC/CCAS through 1700 UTC (Figure 7-4f).

7.3 RAMS Results

We compared the observed data with the modeled data to determine the reliability of RAMS for the day of the N_2O_4 release. The results from the RAMS model were obtained from the run which began at 1200 UTC on 20 August. Figures 7-5a to 7-5f show the RAMS-predicted wind field for 10.6 meters (surface) and 254.1 meters for the hours 1200 to 1700 UTC. We compared RAMS' three-dimensional meteorological fields with observed data from the various tower levels, surface observation sites, and the 1500 UTC CCAS rawinsonde (Table 7-4). The observed wind fields for the hours 1200 to 1700 UTC are presented in Figures 7-4a to 7-4f.

At 1300 UTC, RAMS predicted weak westerly and northwesterly flow over the CCAS area at the surface and aloft as shown in the wind fields at 10.6 and 254.1 meters (Figure 7-5b). There was no significant upward vertical motion over Merritt Island or CCAS except for a small east-west oriented line of convergence located near the southern end of Merritt Island. The direction of the observed wind vectors (Figure 7-4b) did not agree very well with the direction of the RAMS-predicted surface wind vectors over most of the grid because the winds were very light over most of the area. However, when winds are light, the directions tend to vary considerably because of the lack of dominant prevailing wind. The wind vectors from the observed and predicted wind fields did agree in the area of northern Merritt Island. Observed winds in the north Merritt Island area were west-northwest at approximately 1 ms^{-1} while the RAMS-predicted winds were northwest at approximately 2 ms^{-1}.

At 1400 UTC, RAMS did not show signs of a sea breeze circulation but decreased the westerly flow over the CCAS land area and Merritt Island as the land surfaces warmed (Figure 7-5c). RAMS predicted light northerly winds at the surface over CCAS while the winds at the grid points on Merritt Island became almost calm. RAMS predicted easterly winds at the height of 254.1 m over CCAS and Merritt Island. The light, near-calm winds predicted by RAMS over CCAS and Merritt Island agreed with the observed winds shown in Figure 7-4c.

At 1500 UTC, RAMS predicted weak easterly flow over Merritt Island and northern CCAS as it began to generate a sea breeze circulation (Figure 7-5d). Upward vertical motion increased over CCAS and Merritt Island from 1400 UTC. The observed (Figure 7-4d) and predicted wind fields showed good agreement over CCAS and Merritt Island where the winds were very light.

By 1600 UTC, RAMS predicted the winds to increase from the northeast at the 10.6-meter level over northern Merritt Island and CCAS. RAMS did not strengthen the sea breeze

circulation which was evident in the 1500 UTC RAMS output. The strength of the updrafts as indicated by the vertical motion fields increased but remained centered over CCAS and Merritt Island (Figure 7-5e). The observed wind field (Figure 7-4e)at this time showed that the sea breeze had moved inland to near the Indian River.

At 1700 UTC, RAMS continued the northeasterly winds over the northern CCAS land area and northern Merritt Island. The strength of the updrafts increased from the previous hour but remained located over the center of the CCAS land area and over the center of Merritt Island. The model did not predict any upward motions over the Complex 41 area. RAMS continued to under predict the strength of the surface wind flow compared to the observed wind field. The observed wind field showed an increase in the easterly flow over CCAS.

The 3-km resolution of the land use in the ERDAS configuration significantly affected the RAMS predicted wind fields at Complex 41. The narrow strip of land where Complex 41 is located is approximately 1 ½ to 4 km wide, bounded on the west by the Banana River and on the east by the Atlantic Ocean. The land use in the area is very complex due to the oceans, estuaries, swamps and vegetated land. RAMS attempts to apply a single land use class and percent land area to each 3 km x 3 km grid square. RAMS classified the grid square where Complex 41 is located as inland water or ocean (Classes 14 and 15) with a percent land fraction of less than 40%. The grid squares surrounding the Complex 41 grid square were classified as bog and marsh (Class 13), evergreen shrub (Class 16), and short grass (Class 2). This inaccurate classification can lead to inaccurate modeling of horizontal and vertical velocities and turbulence.

The narrow strip of land where Complex 41 is located showed no significant upward motion because of the inaccurate land use classification due to the coarse resolution in this area. The coarse resolution resulted in the model's attempting to apply a single land use class (water) and percent land area to the 3 km x 3 km grid area surrounding Complex 41.

7.4 HYPACT Results

We ran HYPACT for two different scenarios. The two scenarios were identical except for the release point of each. The basic data input to HYPACT were the following:

Spill Amount:	400 gallons
Chemical:	Nitrogen Tetroxide (N_2O_4)
Pool Size:	500 square feet
Release Rate:	50.0 lbs/min
Release Time:	1426 UTC
Release Duration:	14 minutes
Dispersion Simulation End:	1700 UTC

HYPACT produces predictions of the three-dimensional plume every 10 minutes as it disperses over time. HYPACT models the plume by tracking a large set of particles released from a designated point or area. HYPACT transports and disperses the particles using the RAMS-predicted wind fields and displays the plume locations by overlaying the particles on maps and vertical cross-sections. HYPACT calculates pollutant concentrations based on the particle dispersion. The concentration calculation function, however, does not currently work in ERDAS and is being corrected by ASTER/MRC.

For this release, the simulated plume behaved like a single puff rather than a continuous plume because of the short 14-minute release time.

7.4.1 Complex 41 Release Point

For the first HYPACT simulation, we modeled the release from its actual release location at Complex 41. The actual land use in the area is very complex due to the oceans, estuaries, swamps and vegetated land in the area. However, the ERDAS configuration of RAMS sets the finest grid spacing at 3 km and classifies the land use at the Complex 41 grid square as water and surrounding grid squares as bog and marsh, evergreen shrub, and short grass. RAMS sets the percent land fraction at Complex 41 to less than 40%. As mentioned earlier, this inaccurate classification significantly affects the RAMS wind field predictions and thus the HYPACT results.

Figures 7-6a to 7-6f show a series of maps and vertical cross-sections at 30 minute intervals that track the HYPACT-predicted plume from just after its release at 1426 UTC to 1700 UTC. The map and cross section at approximately 1.5 hours after the release are shown in Figure 7-6d. Arrows on the map indicate the plume track from Complex 41.

For the first hour after the 1426 UTC release, HYPACT, guided by the light northerly surface winds, moved the plume 3 km south of Complex 41 to a location just southwest of Complex 40 (Figures 7-6a to 7-6c. Vertically, HYPACT kept the plume near the surface and in the layer below 100 meters since RAMS had predicted very little upward motion in this area.

From 1530 to 1630 UTC, HYPACT moved the plume southwest to an area in the western Banana River (Figure 7-6d and 7-6e). HYPACT predicted the plume would begin to rise but stay below 400 meters through 1630 UTC. From 1630 to 1700, HYPACT moved the plume west to the eastern part of Merritt Island where it encountered stronger convection and rose vertically reaching a height of 500 meters (Figures 7-6f).

Comparing the modeled plume trajectory to the actual plume trajectory (based on observations of witnesses), HYPACT performed poorly when Complex 41 was input as the release point. It predicted that the plume would remain close to the ground and move south and west from Complex 41. Witnesses observed the actual plume drift slightly west, rise and then move northward offshore during the one to two hour period after the release. Due to the coarse grid resolution and the resulting inaccurate land use classification in this area, RAMS did not predict significant upward motion thus causing poor HYPACT results.

7.4.2 10 km South of Complex 41 Release Point

For the second HYPACT simulation, we moved the release point 10 kilometers south of Complex 41 to the Cape Canaveral Industrial Area. We picked this point to see how HYPACT would model a release from a grid square where RAMS had not classified the land use as water. The land use classification for the 3 km x 3 km grid square containing the Industrial Area is crop/mixed farming with a percent land fraction of 100%. RAMS predicted strong upward motion in this area.

For the first 30 minutes after the release, HYPACT moved the plume slightly to the northwest to less than 1 km from its source (Figures 7-7a and 7-7b). It remained close to the ground and was lifted to a height of 200 meters. At 1530 UTC, HYPACT began lifting the plume vertically, extending it to a height of over 600 meters by 1600 UTC (Figures 7-7c and 7-7d). Because of the predicted weak sea breeze in the area, HYPACT moved the plume to the north and northwest. HYPACT split the plume as it moved the upper part of the plume faster and more to the north than the lower part of the plume. From 1630 to 1700 HYPACT continued to lift the plume lofting it up to over 700 meters (Figures 7-7e and 7-7f). The upper and lower parts of the plume moved in different directions; the lower part of the plume drifted north-northwest

and the upper part moved to the north as the stronger southerly winds aloft began affecting the plume.

Comparing the modeled plume trajectory to the actual plume trajectory (based on observations of witnesses), HYPACT produced a more accurate trajectory when the release location was moved to 10 km south of Complex 41 than it did with the release location at Complex 41. The HYPACT trajectory from the Cape Canaveral Industrial Area was correct in its northward movement and upward lofting. If the modeled plume were transposed to the actual release point at Complex 41 its trajectory would look accurate.

7.5 Summary

When HYPACT was run with the release point at Complex 41, it modeled the plume by moving it southwest and never lifted it higher than 400 meters above the surface for the first 2 hours after release. However, when the release point was moved south 10 km, HYPACT handled the plume very differently. HYPACT predicted the plume to move initially to the northwest, but then because of the strong upward vertical motion over the CCAS land area, it lifted the plume to over 700 m above the surface during the 2 hours after the release. Once the plume became elevated, the model's light southerly winds aloft carried the plume to the north. If the path of the plume in this second scenario could be transposed to the actual location of the release at Complex 41, it would closely resemble the actual path of the plume as observed by witnesses at the time of the release.

The difference between the two vastly different HYPACT runs was due to the difference between the way the model characterizes the land use at the release points. Because of the 3 km grid resolution, the model classifies the narrow strip of land where Complex 41 is located primarily as water with a percent land fraction of less than 40%. The model classifies the CCAS land area to the south as crop land with a percent land fraction of 100%. This different land use classification significantly affects RAMS' predictions of surface convergence and vertical motion and turbulence. Based on the results of our analysis, we believe that the model showed promise in modeling the N_2O_4 release and would have produced good results if a smaller grid spacing were used. The smaller grid spacing would better enable RAMS to resolve the complex land use characteristics surrounding Complex 41.

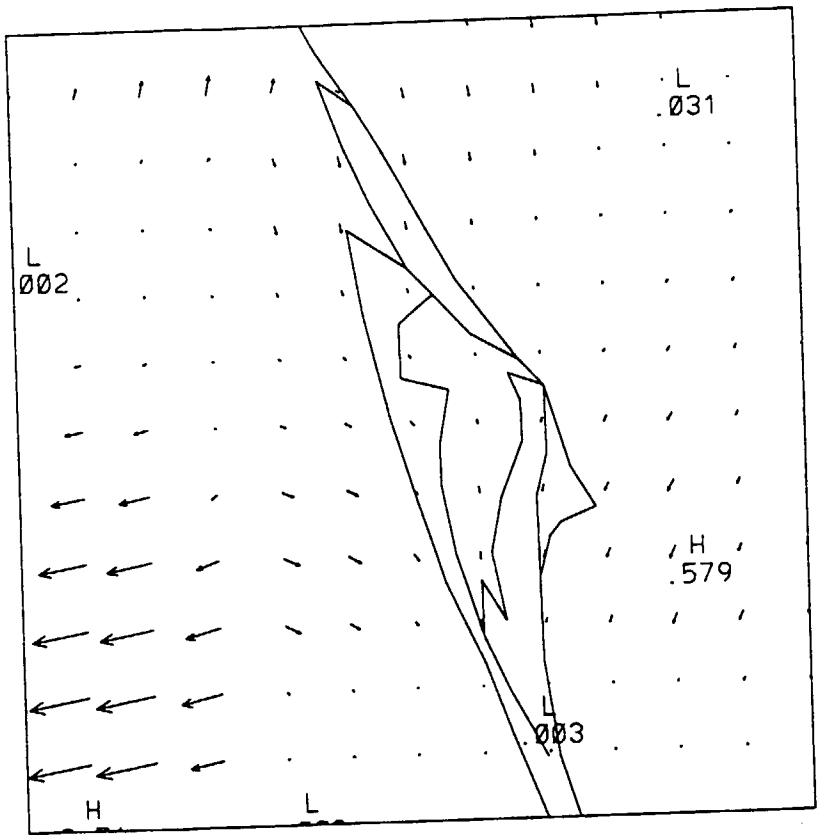

Figure 7-4a. Observed analyzed wind field for 1200 UTC on 20 August 1994. Data used for the analysis included surface observations, buoys, and surface tower observations. Figure shows wind vectors at every third grid point on the 3-km spaced grid and displays maximum and minimum wind speed (m/sec) values.

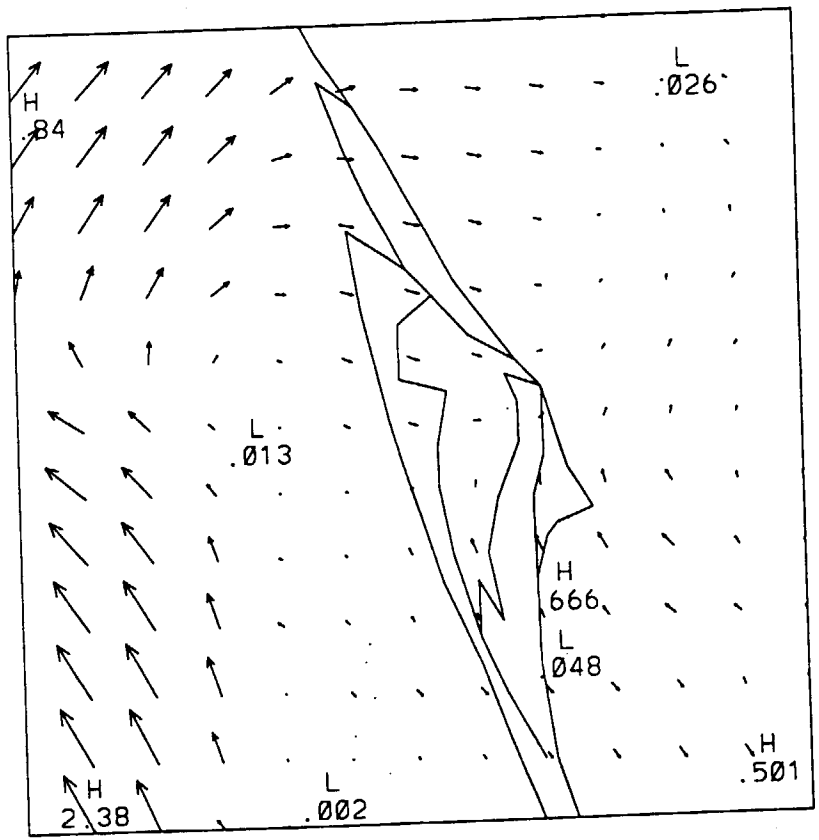

Figure 7-4b. Observed analyzed wind field for 1300 UTC on 20 August 1994. Data used for the analysis included surface observations, buoys, and surface tower observations. Figure shows wind vectors at every third grid point on the 3-km spaced grid and displays maximum and minimum wind speed (m/sec) values.

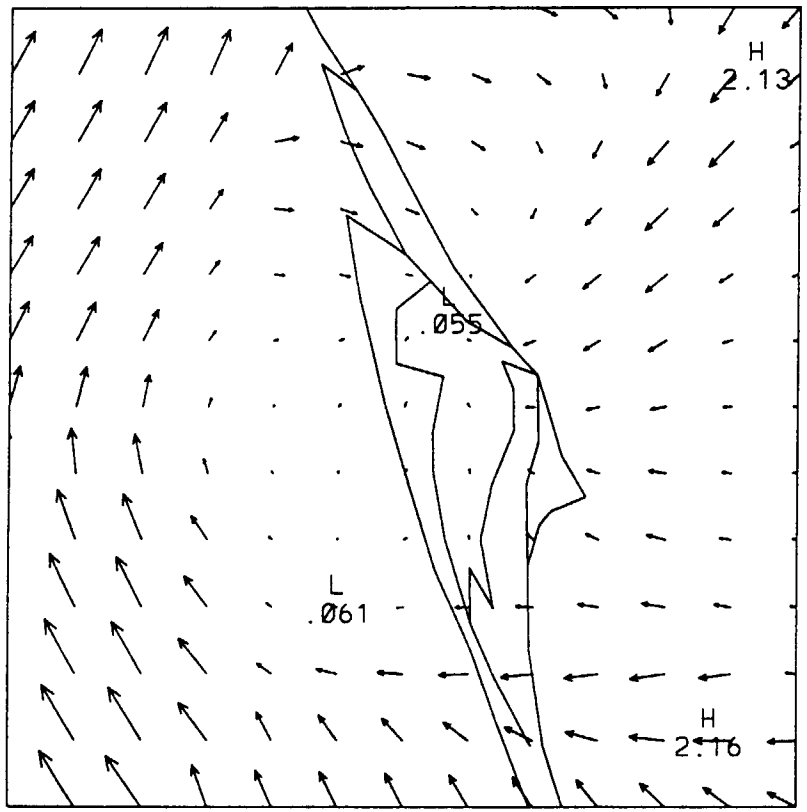

Figure 7-4c. Observed analyzed wind field for 1400 UTC on 20 August 1994. Data used for the analysis included surface observations, buoys, and surface tower observations. Figure shows wind vectors at every third grid point on the 3-km spaced grid and displays maximum and minimum wind speed (m/sec) values.

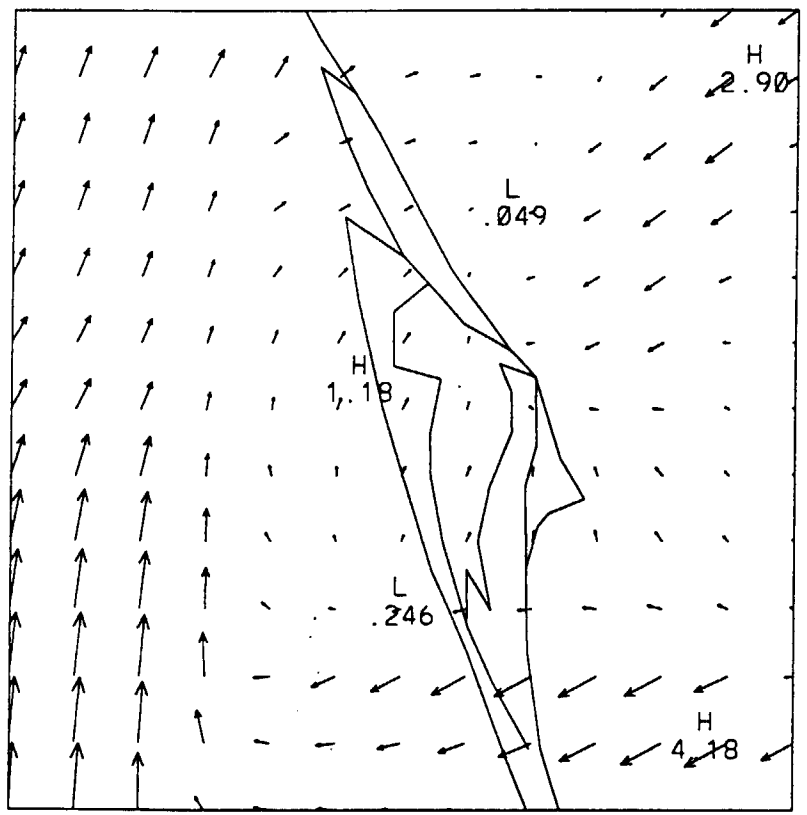

Figure 7-4d. Observed analyzed wind field for 1500 UTC on 20 August 1994. Data used for the analysis included surface observations, buoys, and surface tower observations. Figure shows wind vectors at every third grid point on the 3-km spaced grid and displays maximum and minimum wind speed (m/sec) values.

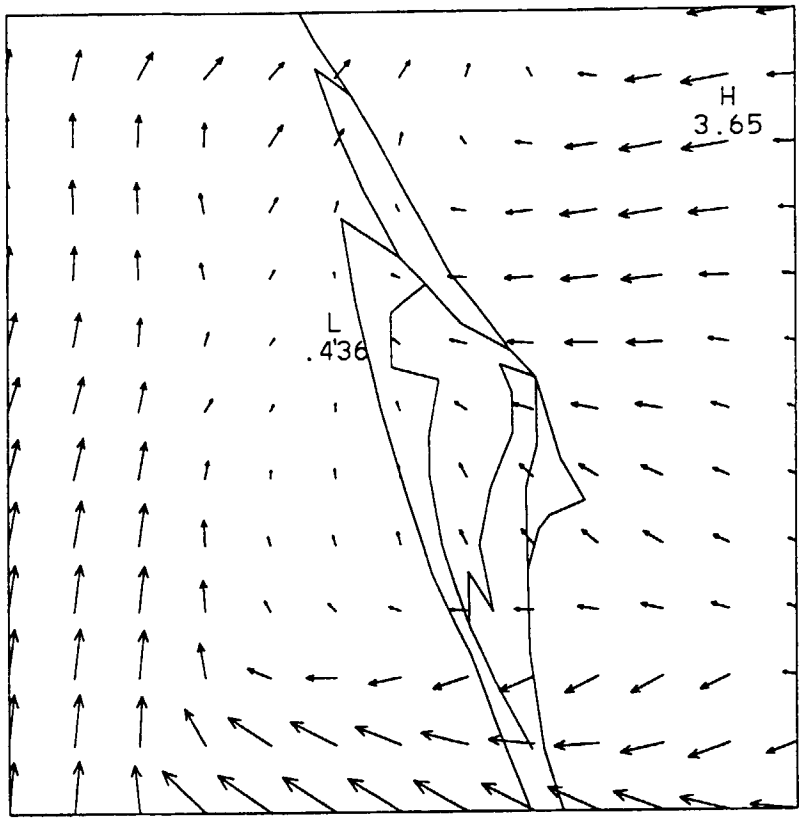

Figure 7-4e. Observed analyzed wind field for 1600 UTC on 20 August 1994. Data used for the analysis included surface observations, buoys, and surface tower observations. Figure shows wind vectors at every third grid point on the 3-km spaced grid and displays maximum and minimum wind speed (m/sec) values.

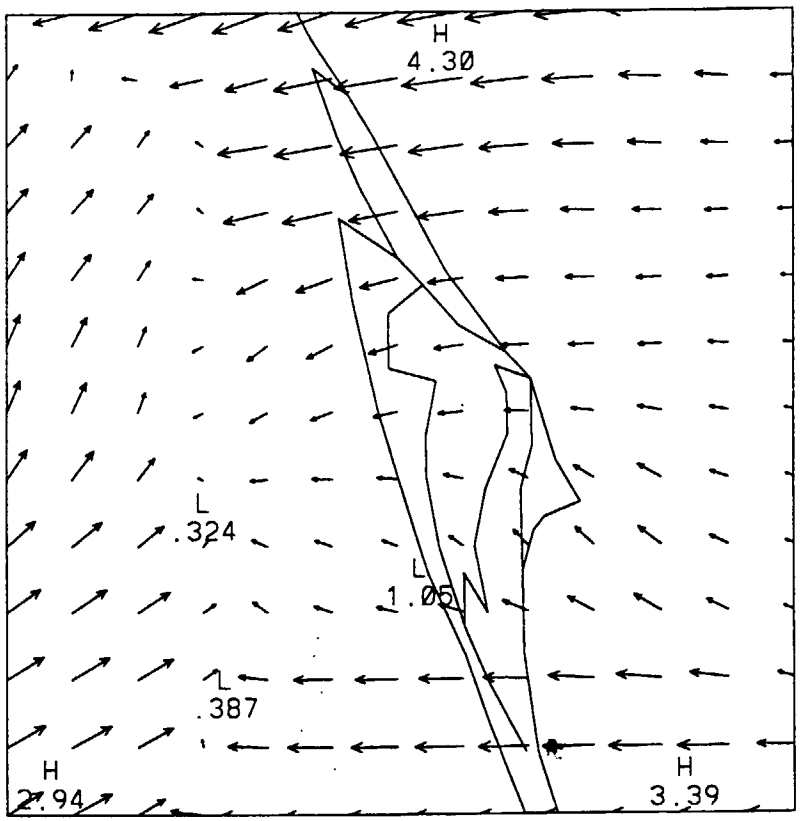

Figure 7-4f. Observed analyzed wind field for 1700 UTC on 20 August 1994. Data used for the analysis included surface observations, buoys, and surface tower observations. Figure shows wind vectors at every third grid point on the 3-km spaced grid and displays maximum and minimum wind speed (m/sec) values.

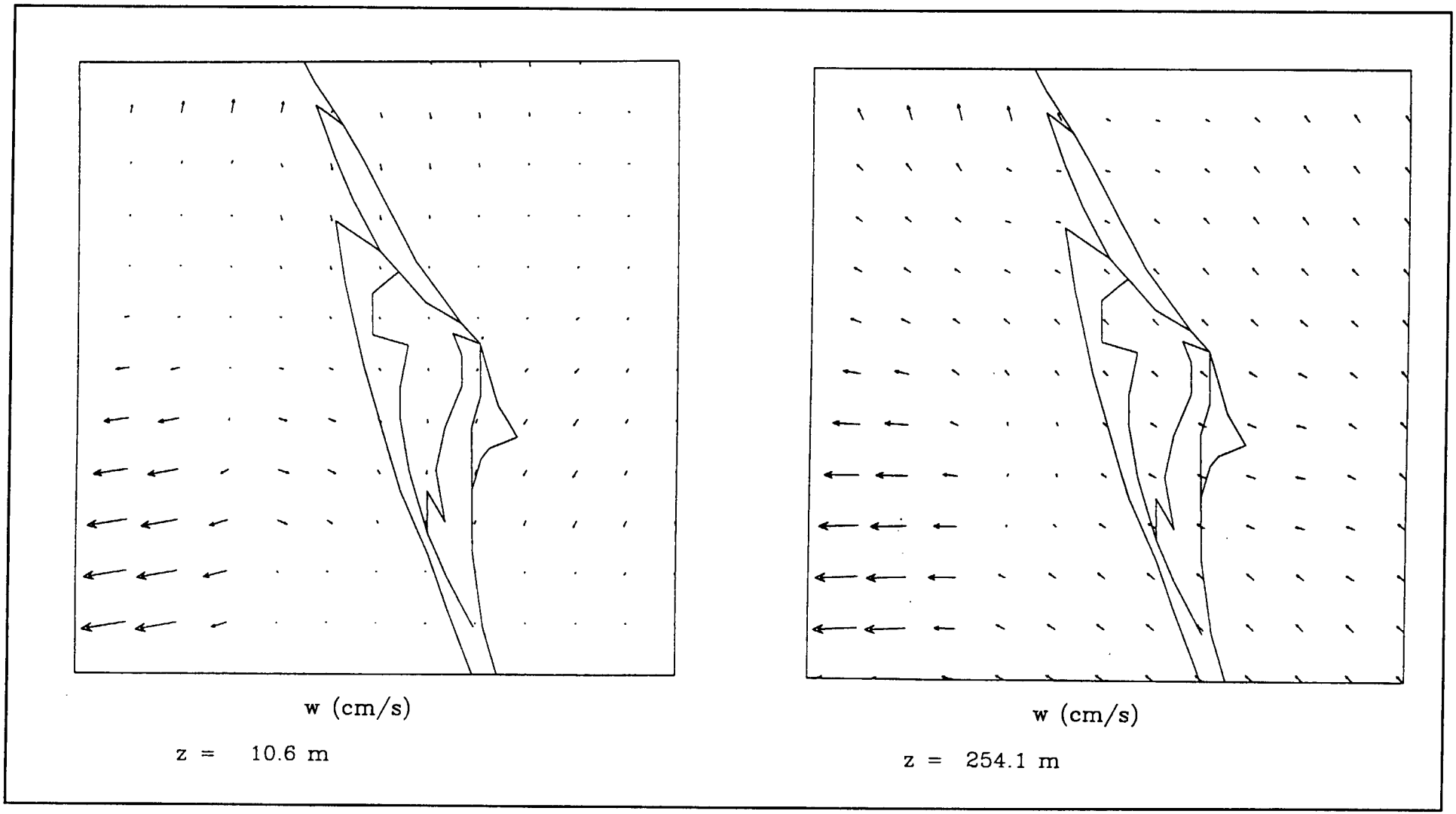

Figure 7-5a. RAMS-predicted wind fields for 1200 UTC on 20 August 1994 for the 10-meter (left) and 250-meter (right) layers. The maps show contours of positive vertical velocity (areas of upward motion) along with the wind vectors at every third grid point on the 3-km spaced grid. The maximum wind vector for the map on the left represents a speed of 2.7 m/sec and for the map on the right represents a speed of 2.5 m/sec.

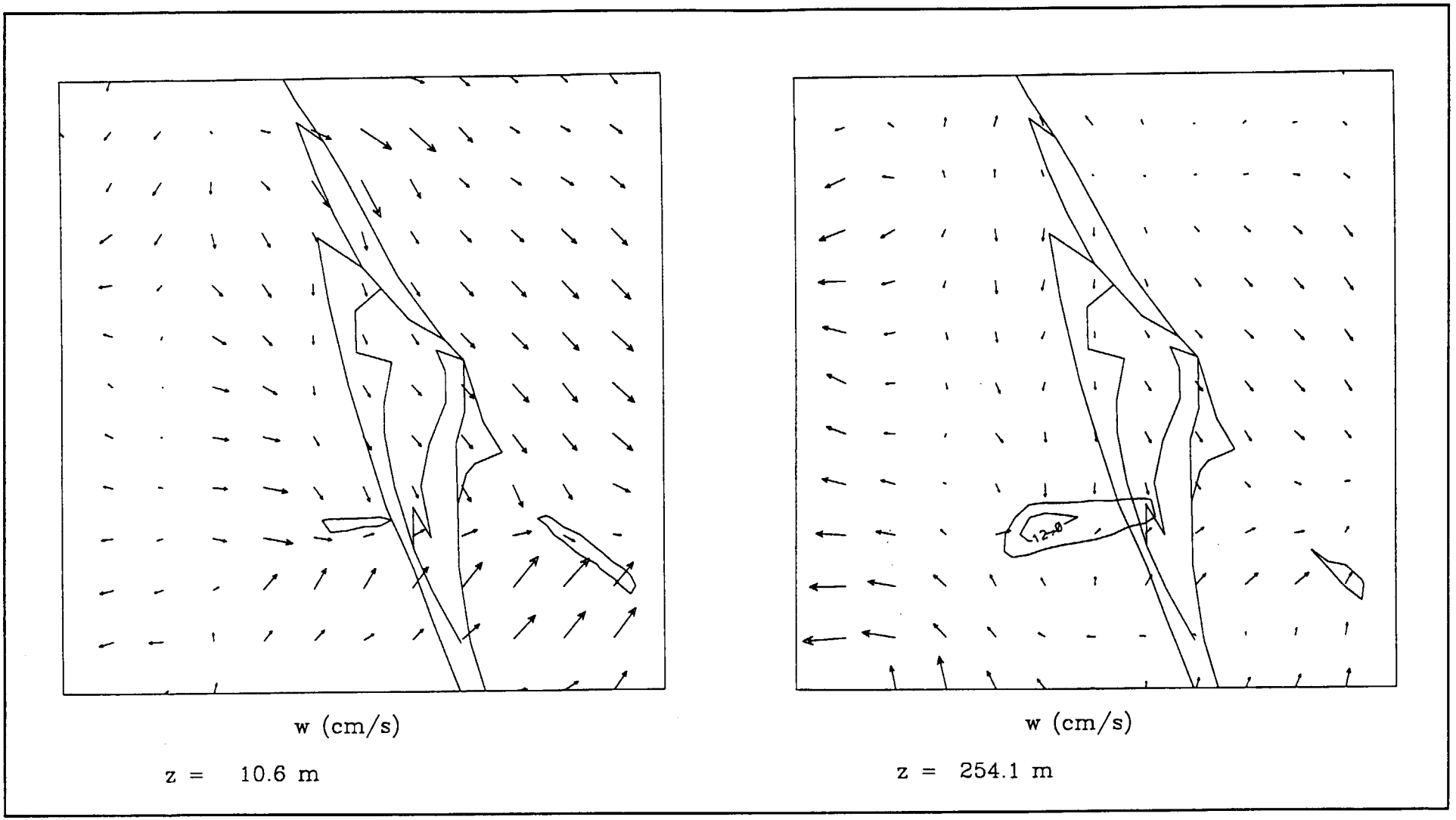

Figure 7-5b. RAMS-predicted wind fields for 1300 UTC on 20 August 1994 for the 10-meter (left) and 250-meter (right) layers. The maps show contours of positive vertical velocity (areas of upward motion) along with the wind vectors at every third grid point on the 3-km spaced grid. The maximum wind vector for the map on the left represents a speed of 2.9 m/sec and for the map on the right represents a speed of 2.3 m/sec.

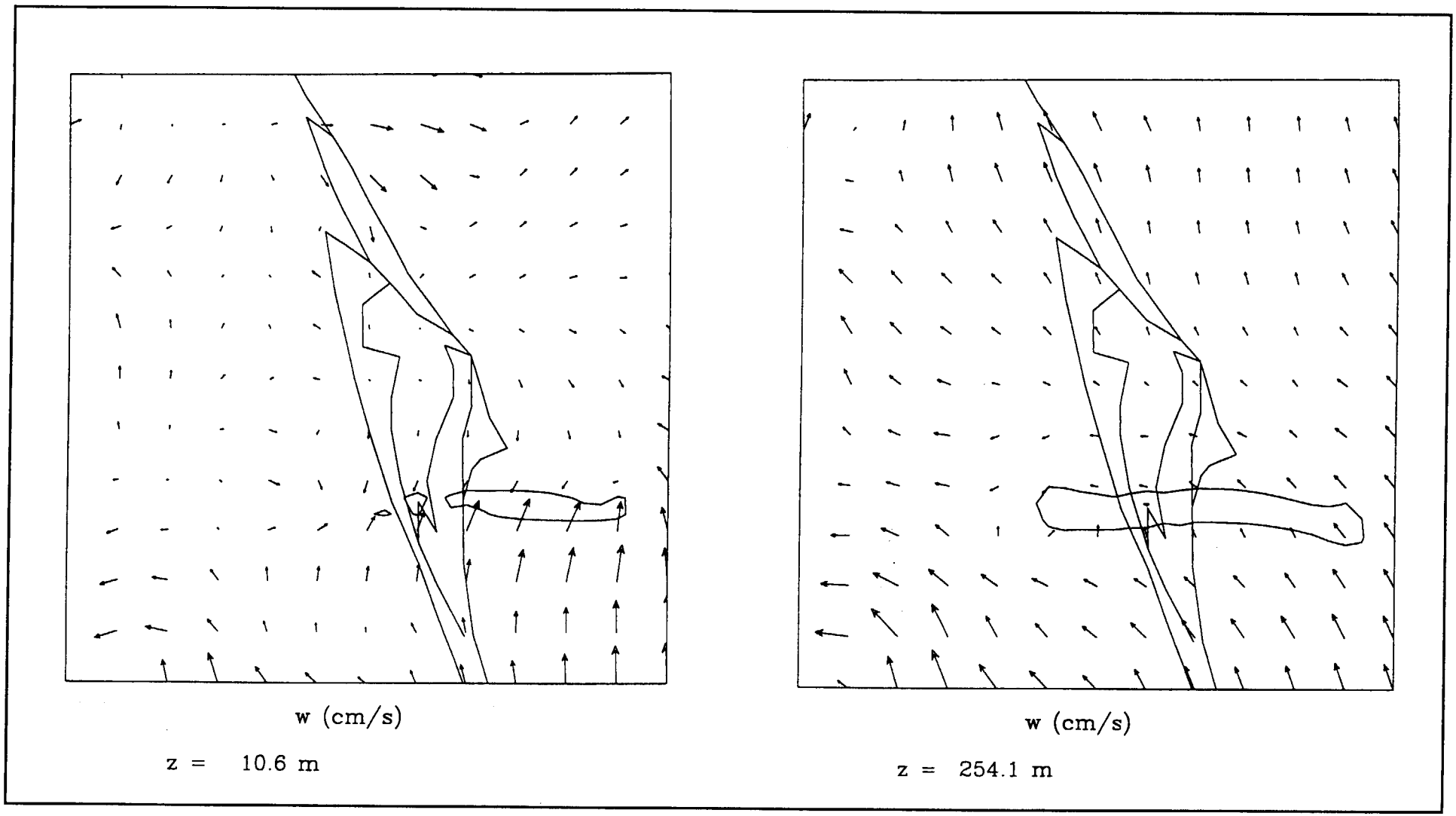

Figure 7-5c. RAMS-predicted wind fields for 1400 UTC on 20 August 1994 for the 10-meter (left) and 250-meter (right) layers. The maps show contours of positive vertical velocity (areas of upward motion) along with the wind vectors at every third grid point on the 3-km spaced grid. The maximum wind vector for the map on the left represents a speed of 3.8 m/sec and for the map on the right represents a speed of 4.2 m/sec.

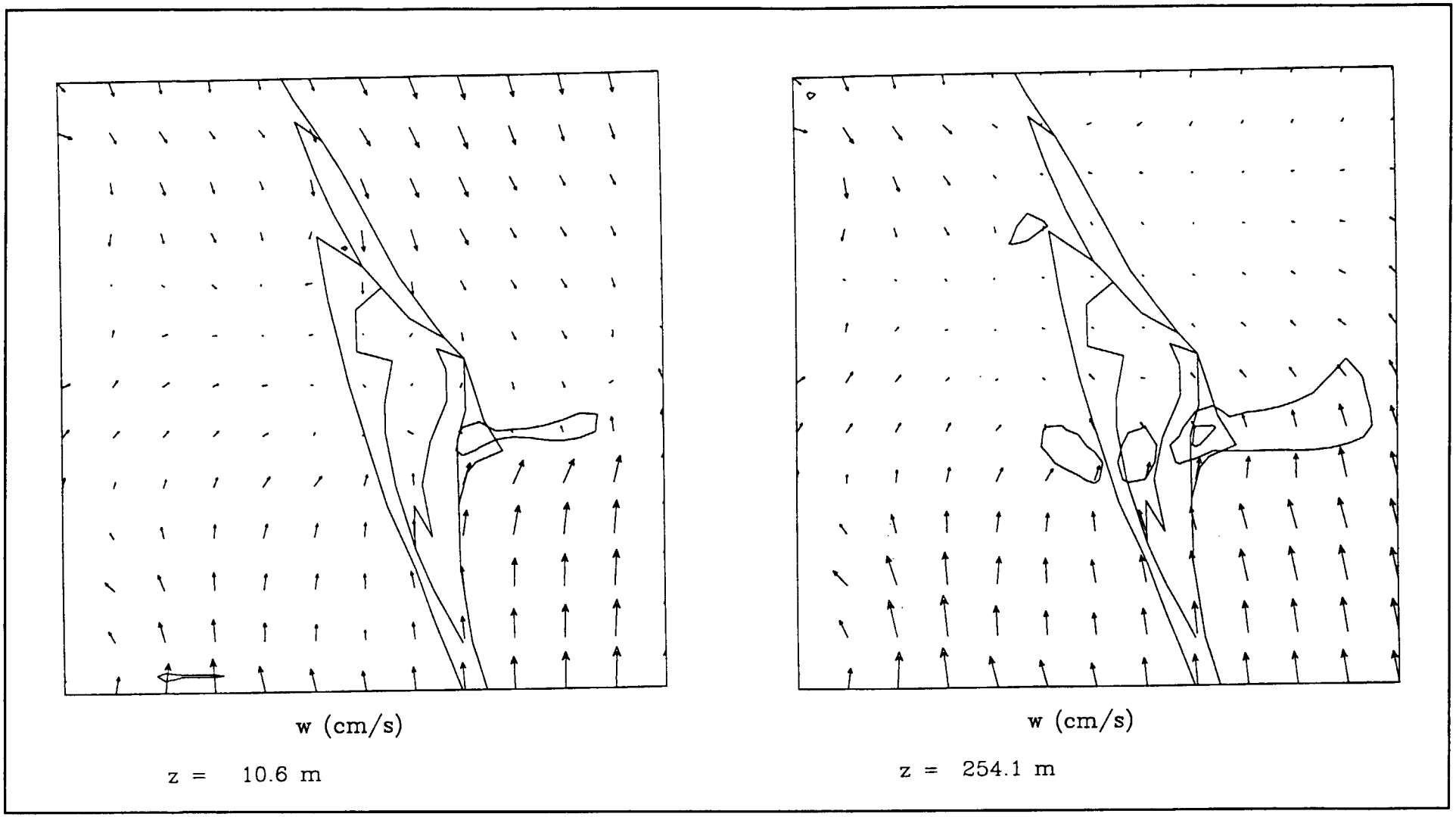

Figure 7-5d. RAMS-predicted wind fields for 1500 UTC on 20 August 1994 for the 10-meter (left) and 250-meter (right) layers. The maps show contours of positive vertical velocity (areas of upward motion) along with the wind vectors at every third grid point on the 3-km spaced grid. The maximum wind vector for the map on the left represents a speed of 6.0 m/sec and for the map on the right represents a speed of 5.8 m/sec.

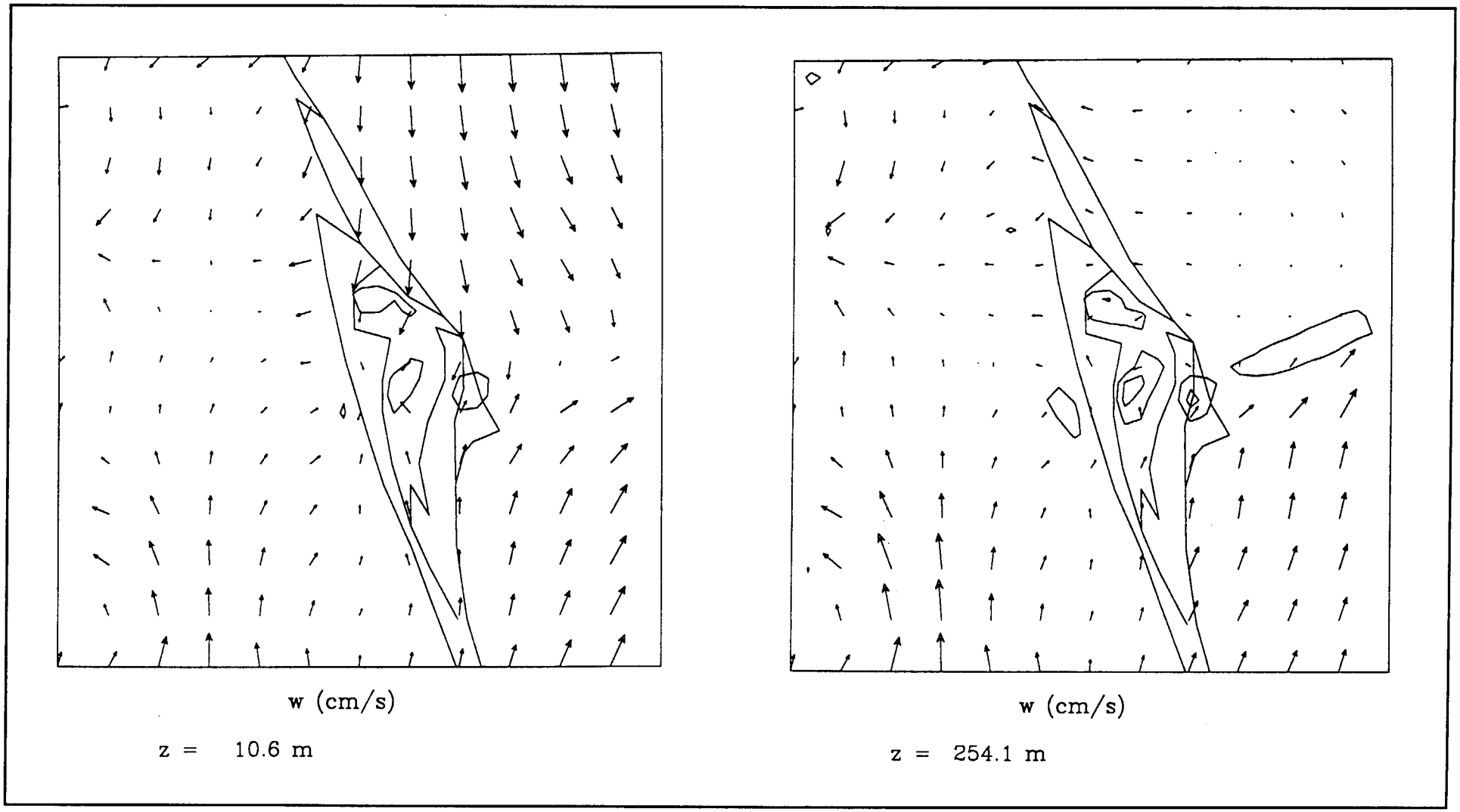

Figure 7-5e. RAMS-predicted wind fields for 1600 UTC on 20 August 1994 for the 10-meter (left) and 250-meter (right) layers. The maps show contours of positive vertical velocity (areas of upward motion) along with the wind vectors at every third grid point on the 3-km spaced grid. The maximum wind vector for the map on the left represents a speed of 4.0 m/sec and for the map on the right represents a speed of 3.5 m/sec.

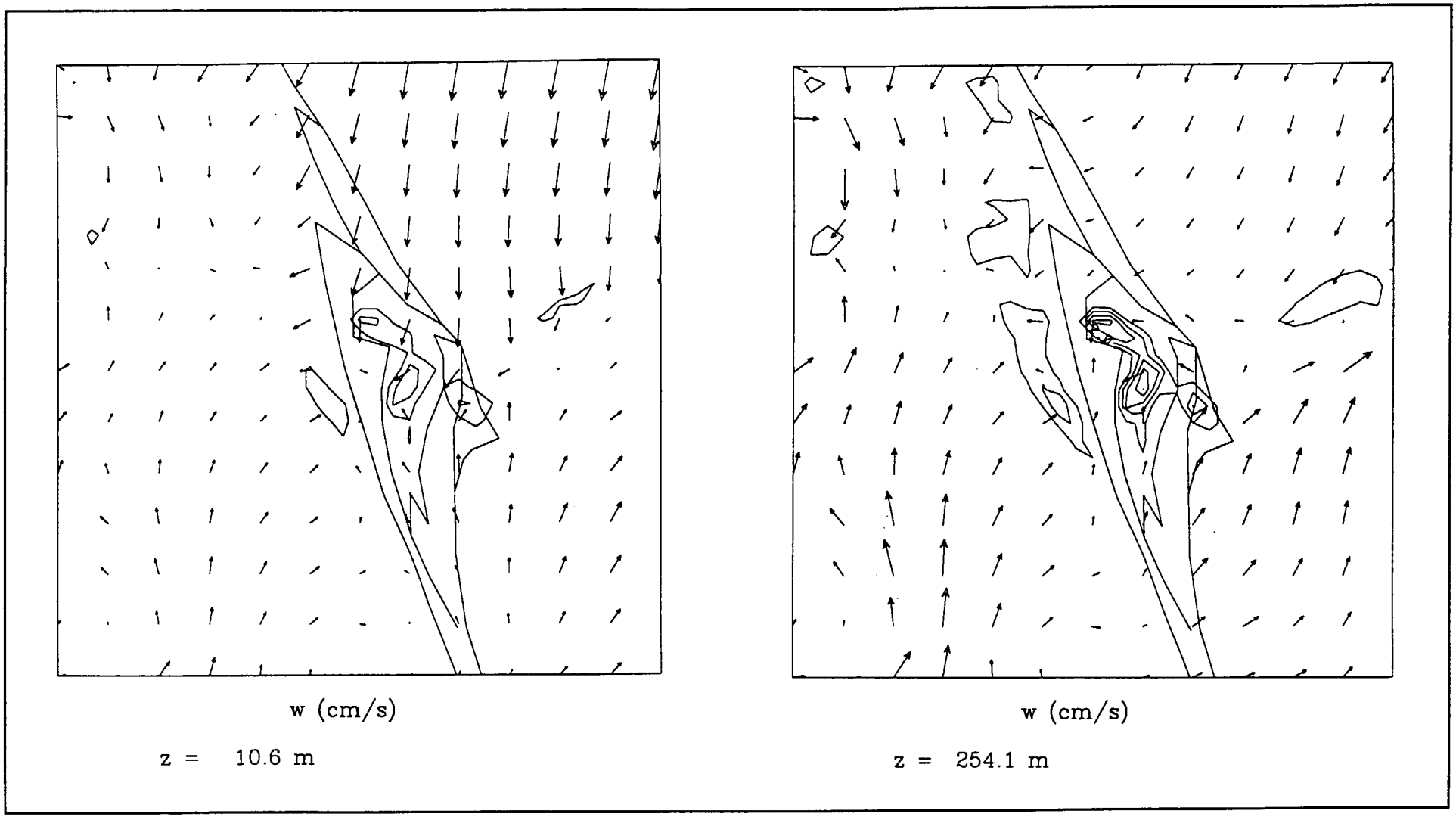

Figure 7-5f. RAMS-predicted wind fields for 1700 UTC on 20 August 1994 for the 10-meter (left) and 250-meter (right) layers. The maps show contours of positive vertical velocity (areas of upward motion) along with tthe wind vectors at every third grid point on the 3-km spaced grid. The maximum wind vector for the map on the left represents a speed of 4.9 m/sec and for the map on the right represents a speed of 2.9 m/sec.

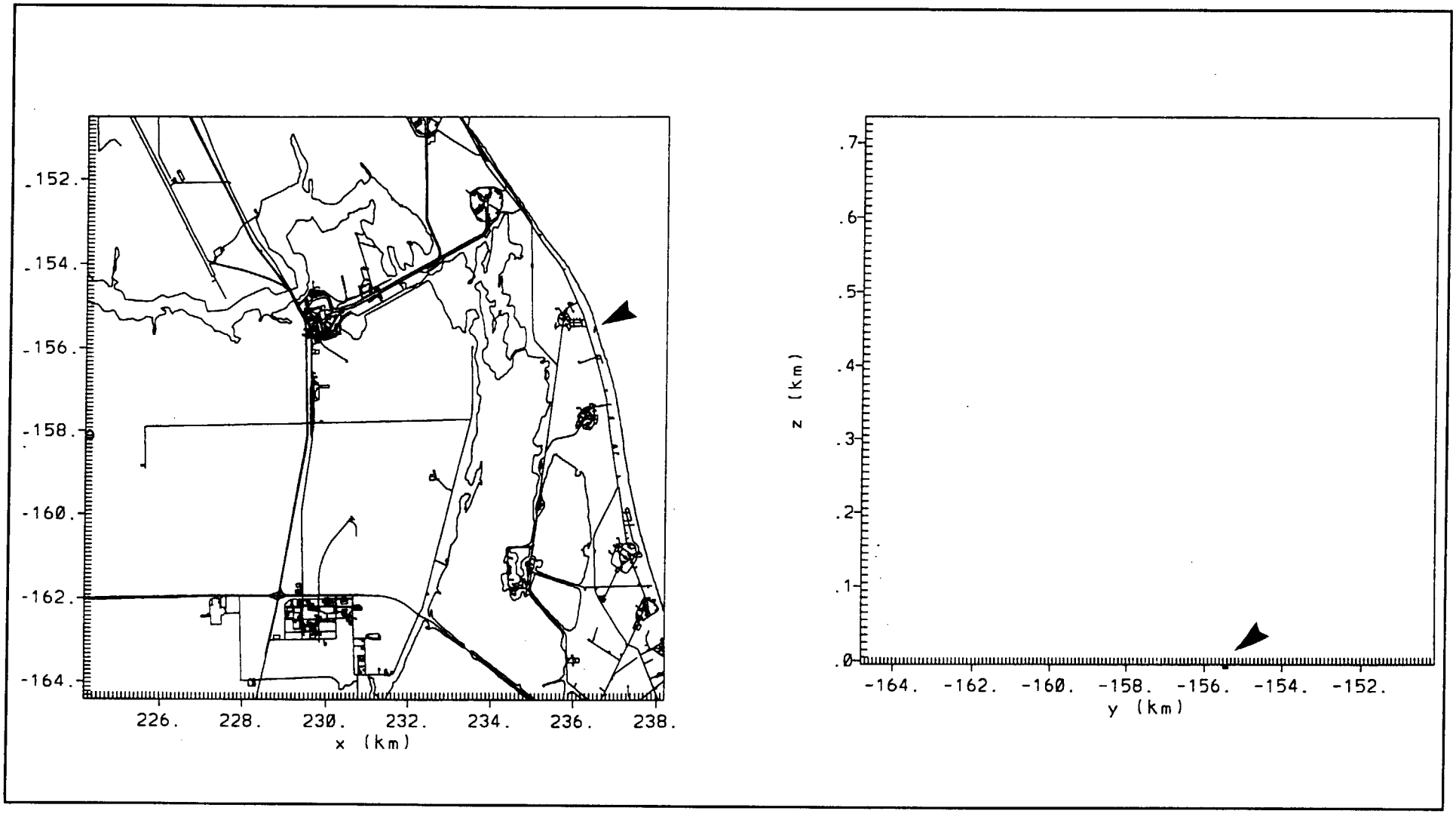

Figure 7-6a. HYPACT results at 1430 UTC of N_2O_4 released from Complex 41 at 1426 UTC on 20 August 1994. Figure shows plan view (left) and west-facing cross-section (right) of plume particles . Arrows point to plume particles.

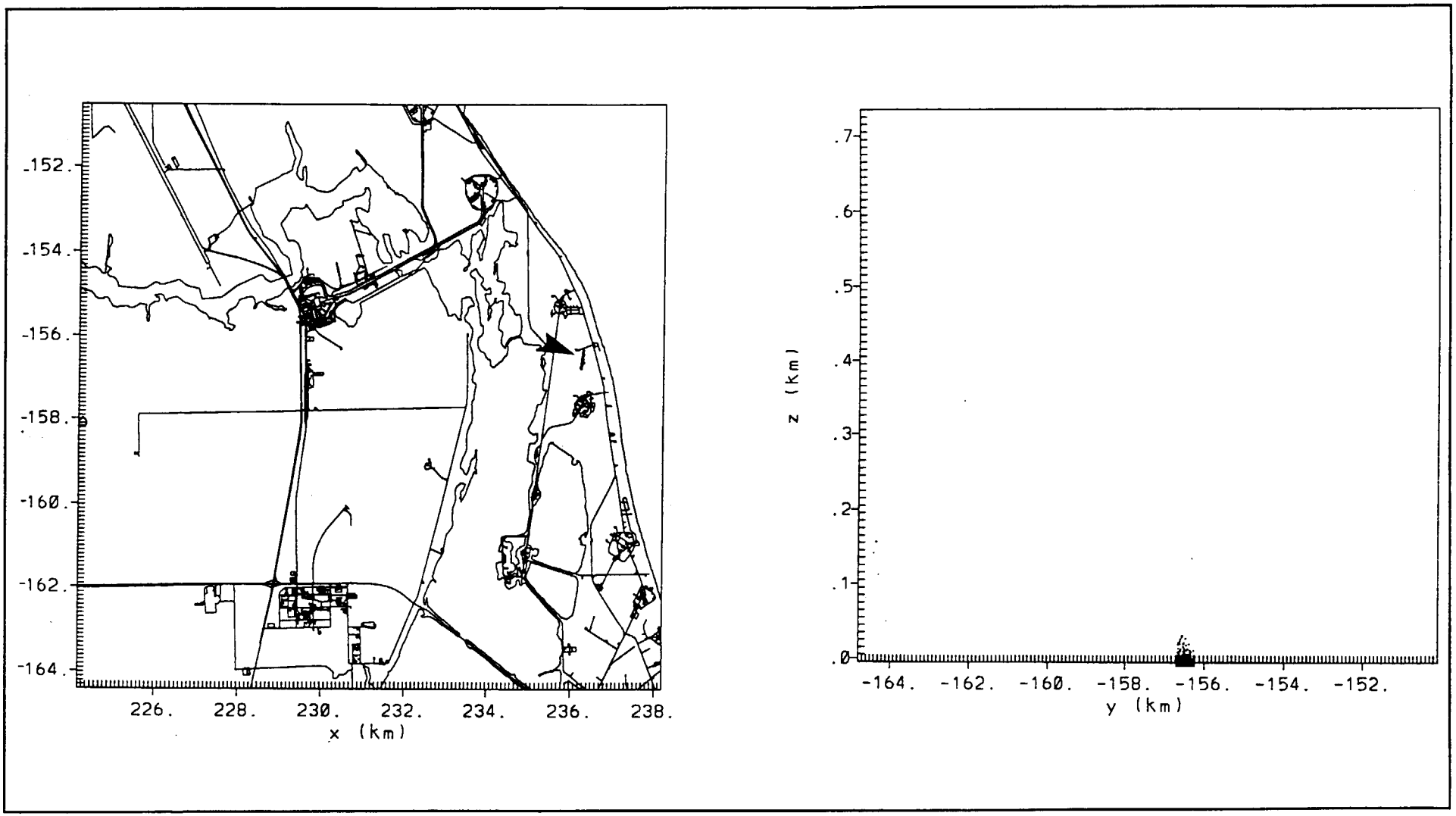

Figure 7-6b. HYPACT results at 1500 UTC of N_2O_4 released from Complex 41 at 1426 UTC on 20 August 1994. Figure shows plan view (left) and west-facing cross-section (right) of plume particles . Arrows point to plume particles.

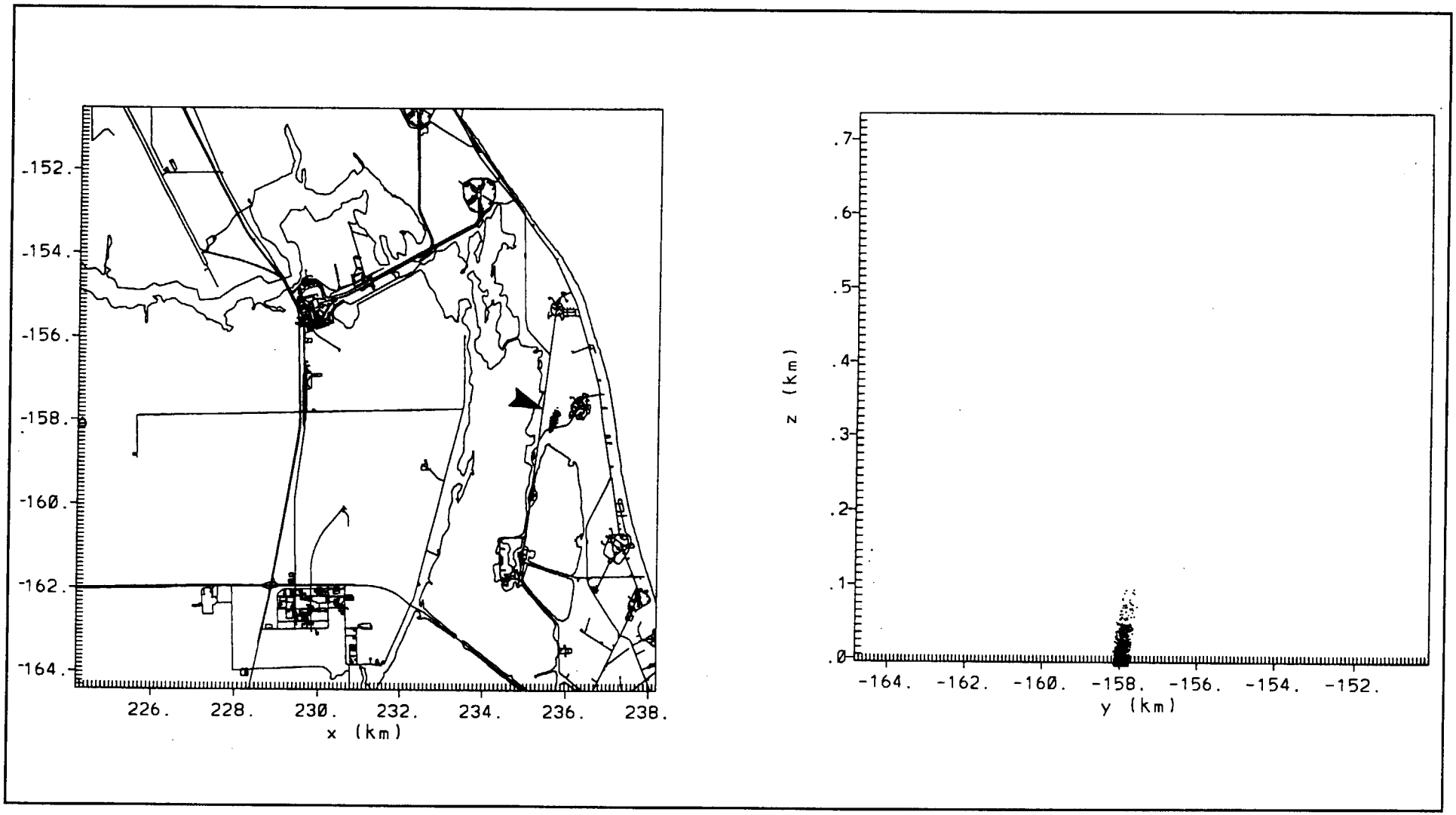

Figure 7-6c. HYPACT results at 1530 UTC of N_2O_4 released from Complex 41 at 1426 UTC on 20 August 1994. Figure shows plan view (left) and west-facing cross-section (right) of plume particles .

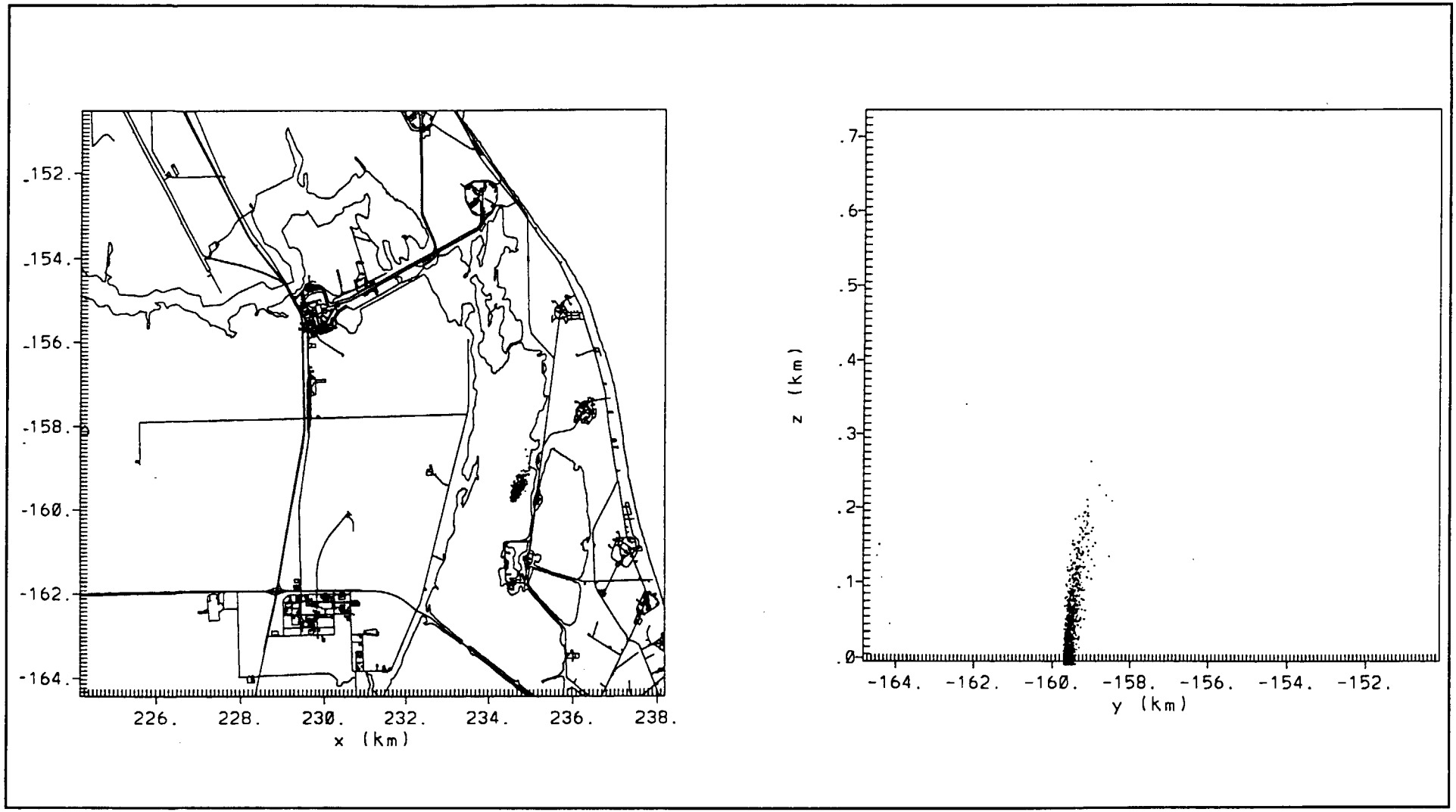

Figure 7-6d. HYPACT results at 1600 UTC of N_2O_4 released from Complex 41 at 1426 UTC on 20 August 1994. Figure shows plan view (left) and west-facing cross-section (right) of plume particles .

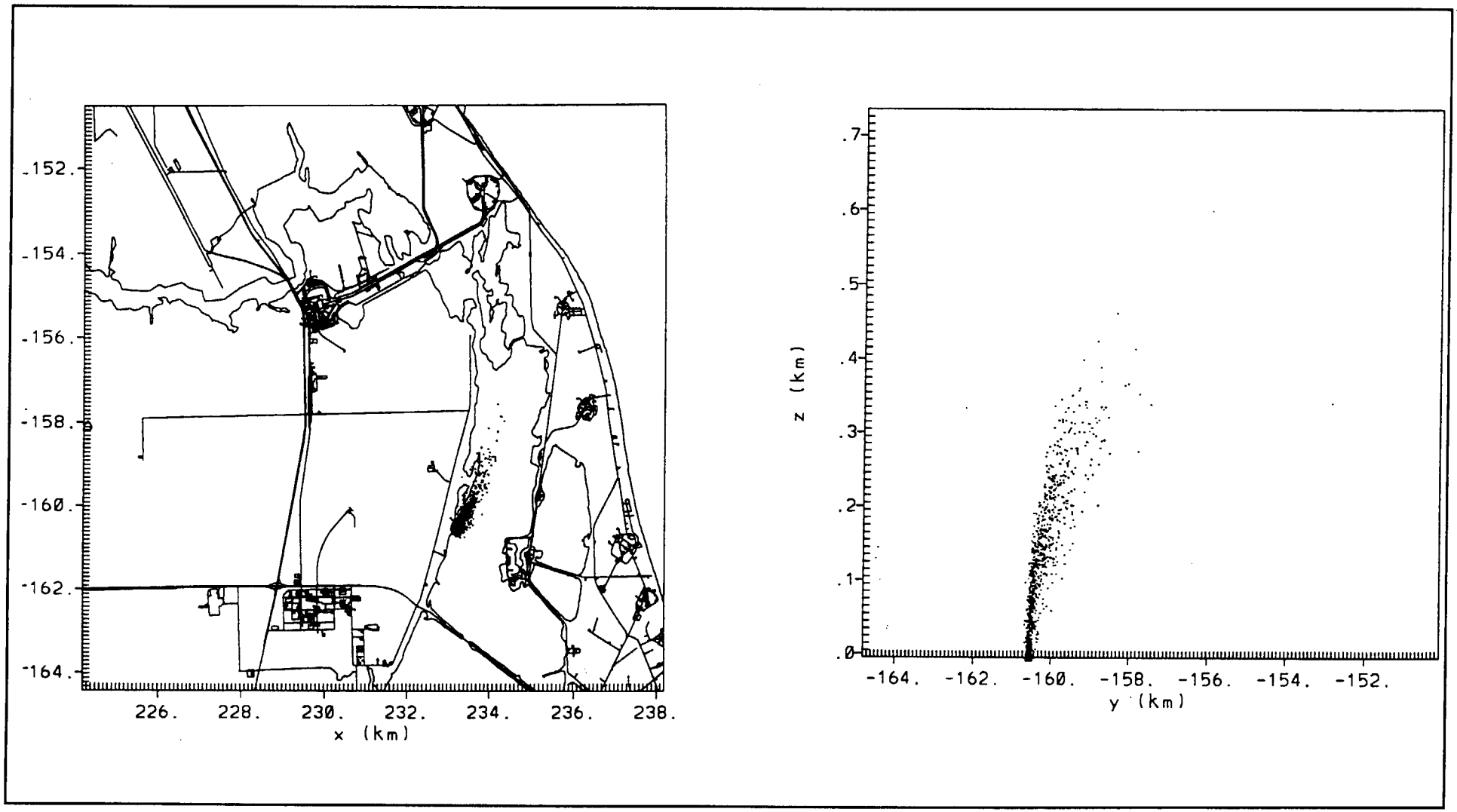

Figure 7-6e. HYPACT results at 1630 UTC of N_2O_4 released from Complex 41 at 1426 UTC on 20 August 1994. Figure shows plan view (left) and west-facing cross-section (right) of plume particles .

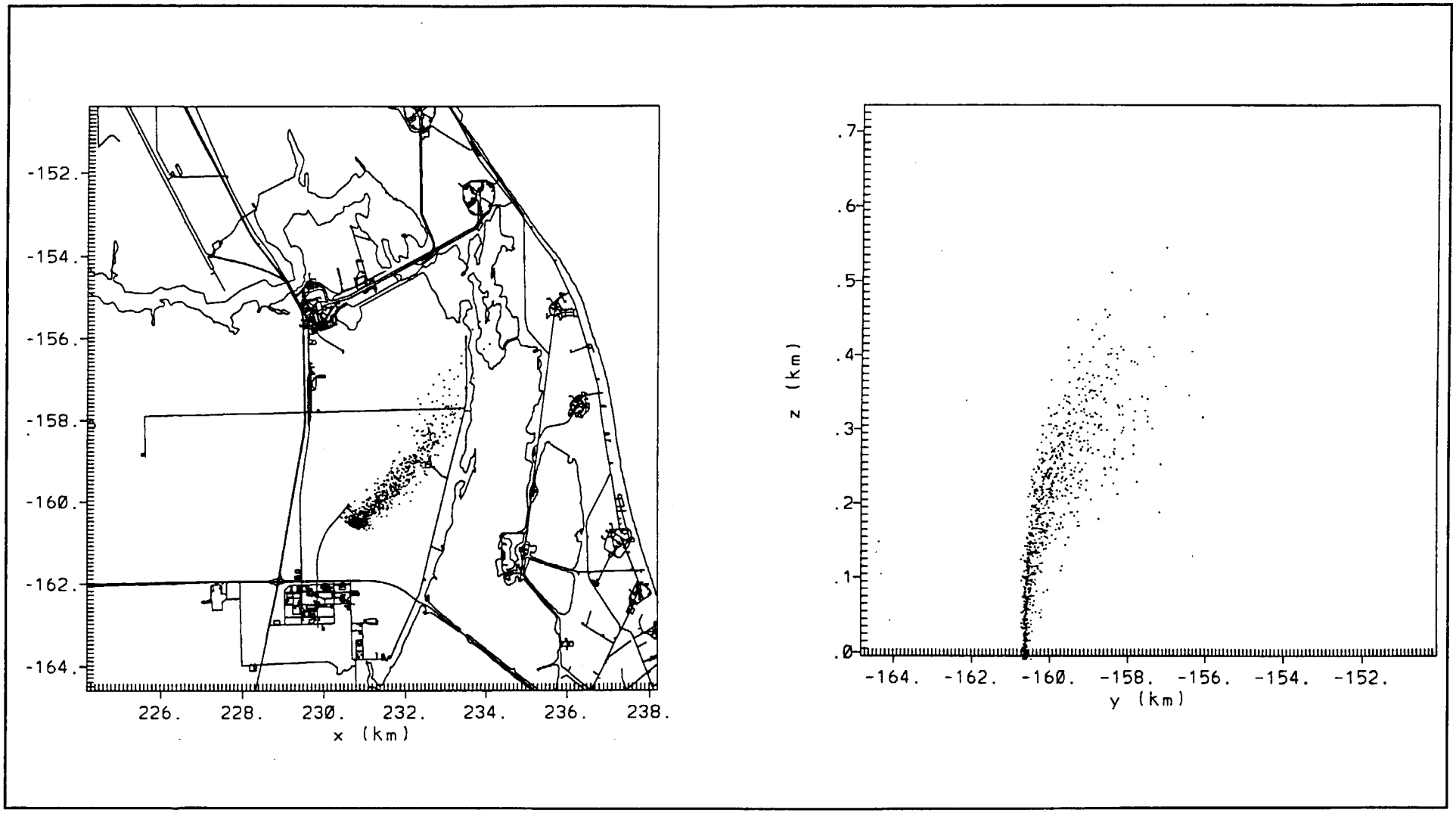

Figure 7-6f. HYPACT results at 1700 UTC of N_2O_4 released from Complex 41 at 1426 UTC on 20 August 1994. Figure shows plan view (left) and west-facing cross-section (right) of plume particles .

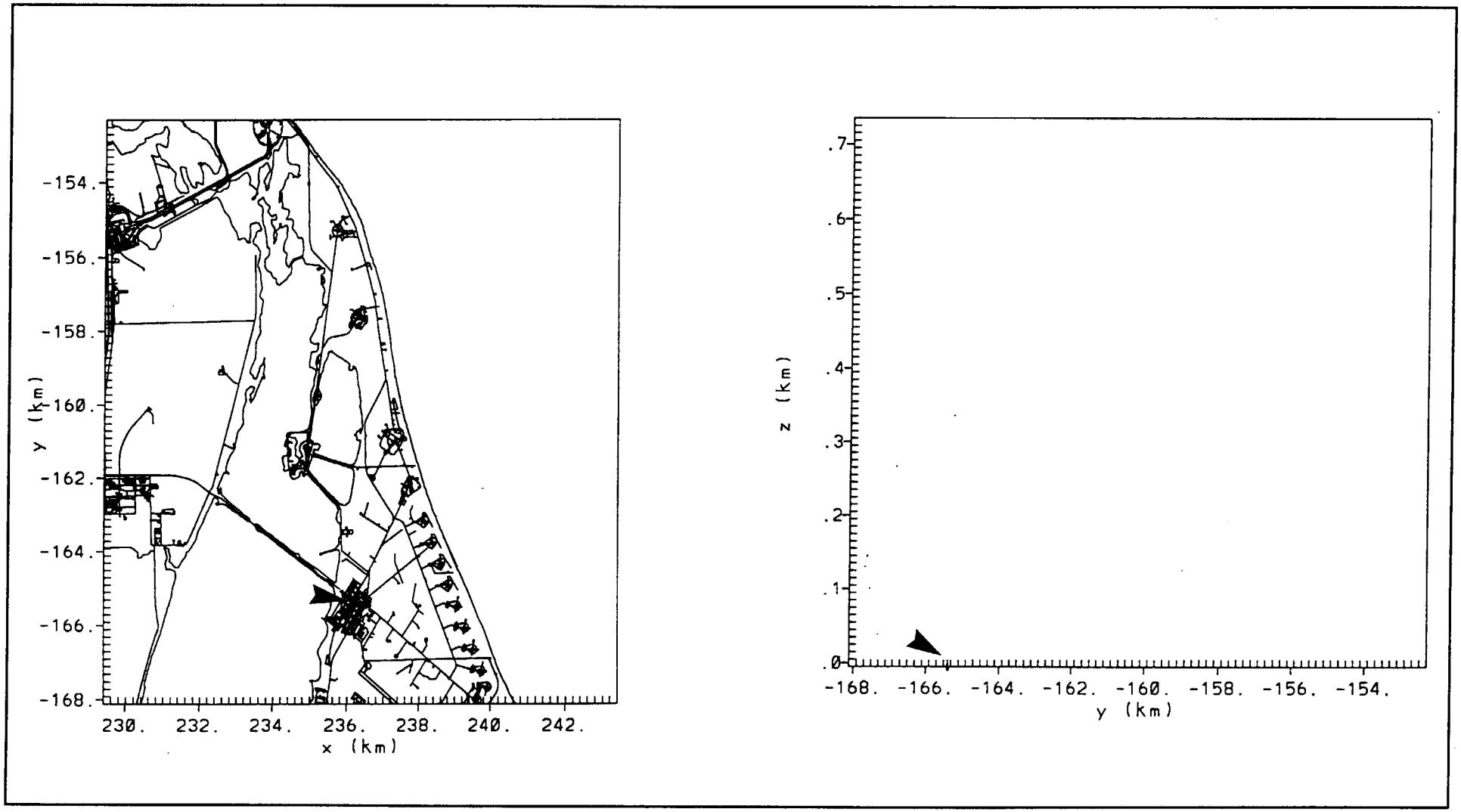

Figure 7-7a. HYPACT results at 1430 UTC of N_2O_4 released from 10 km south of Complex 41 (CCAS Industrial Area) at 1426 UTC on 20 August 1994. Figure shows plan view (left) and west-facing cross-section (right) of plume particles. Arrows point to plume particles.

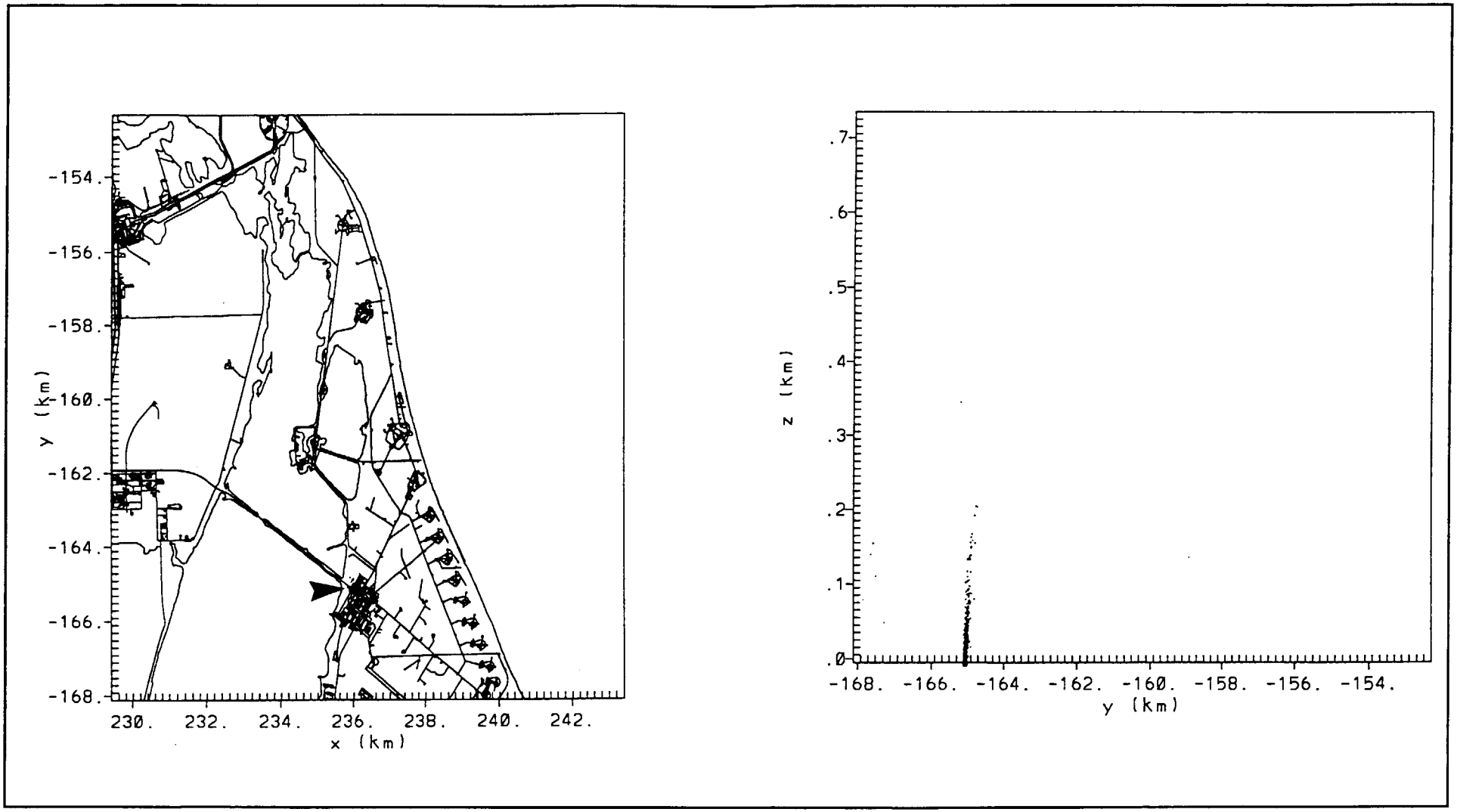

Figure 7-7b. HYPACT results at 1500 UTC of N_2O_4 released from 10 km south of Complex 41 (CCAS Industrial Area) at 1426 UTC on 20 August 1994. Figure shows plan view (left) and west-facing cross-section (right) of plume particles. Arrows point to plume particles.

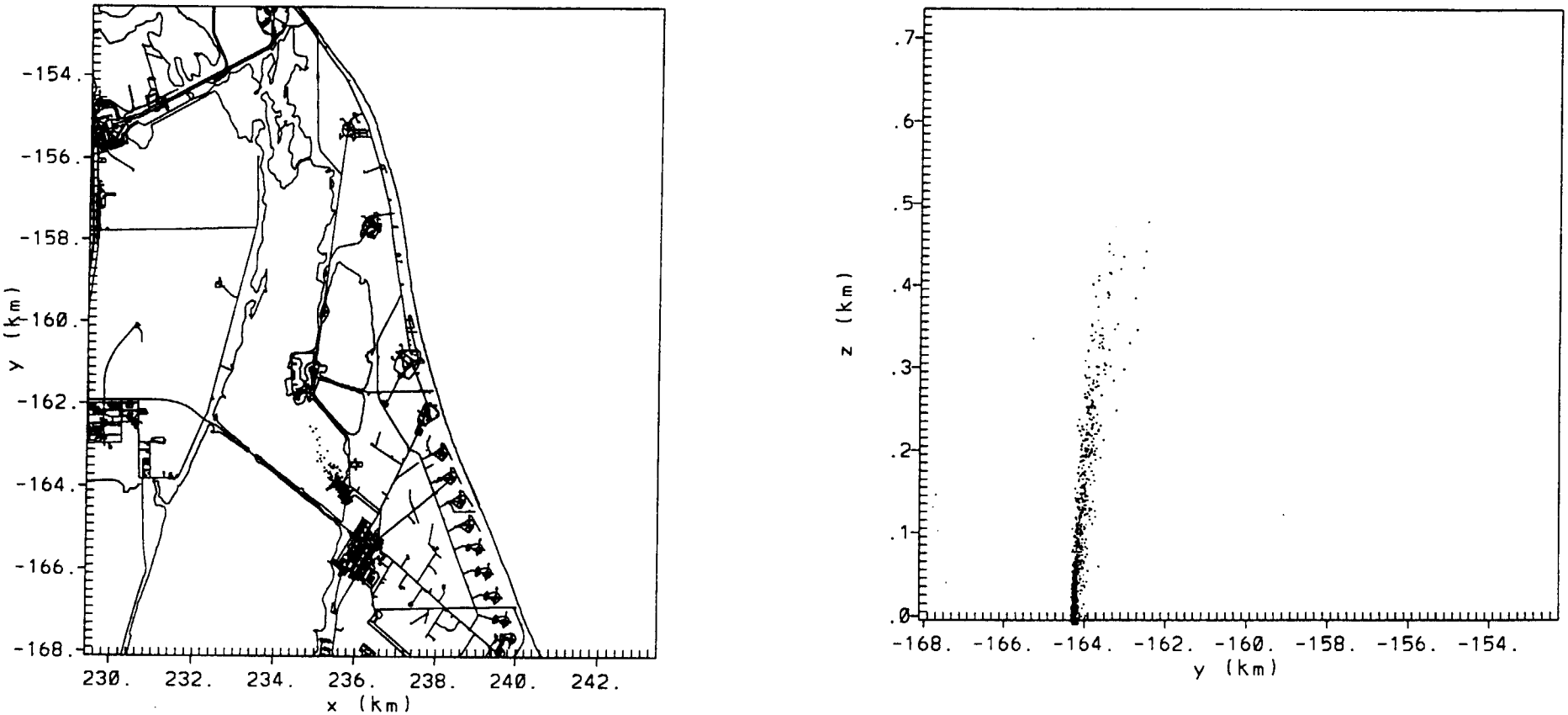

Figure 7-7c. HYPACT results at 1530 UTC of N_2O_4 released from 10 km south of Complex 41 (CCAS Industrial Area) at 1426 UTC on 20 August 1994. Figure shows plan view (left) and west-facing cross-section (right) of plume particles.

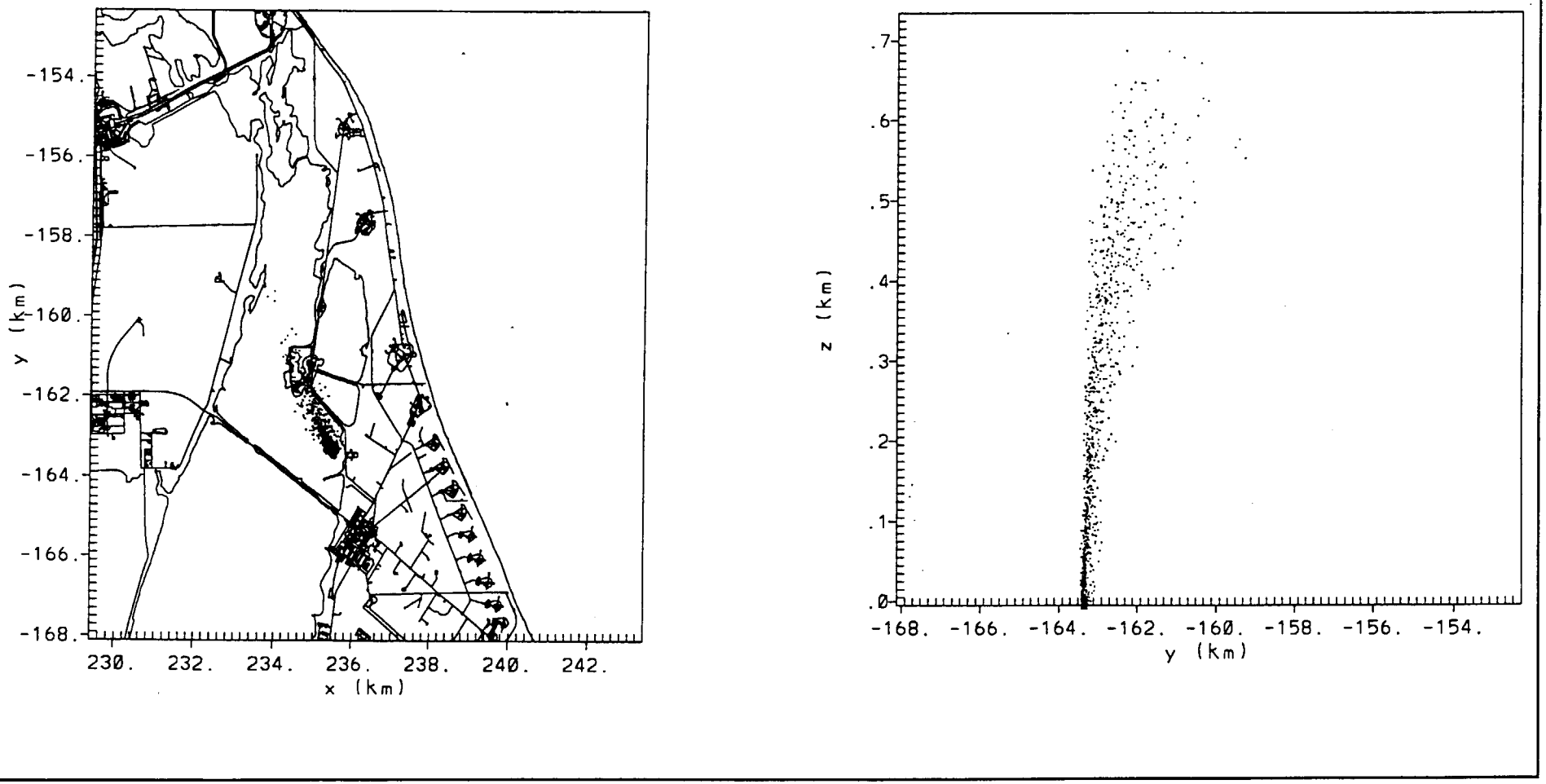

Figure 7-7d. HYPACT results at 1600 UTC of N_2O_4 released from 10 km south of Complex 41 (CCAS Industrial Area) at 1426 UTC on 20 August 1994. Figure shows plan view (left) and west-facing cross-section (right) of plume particles.

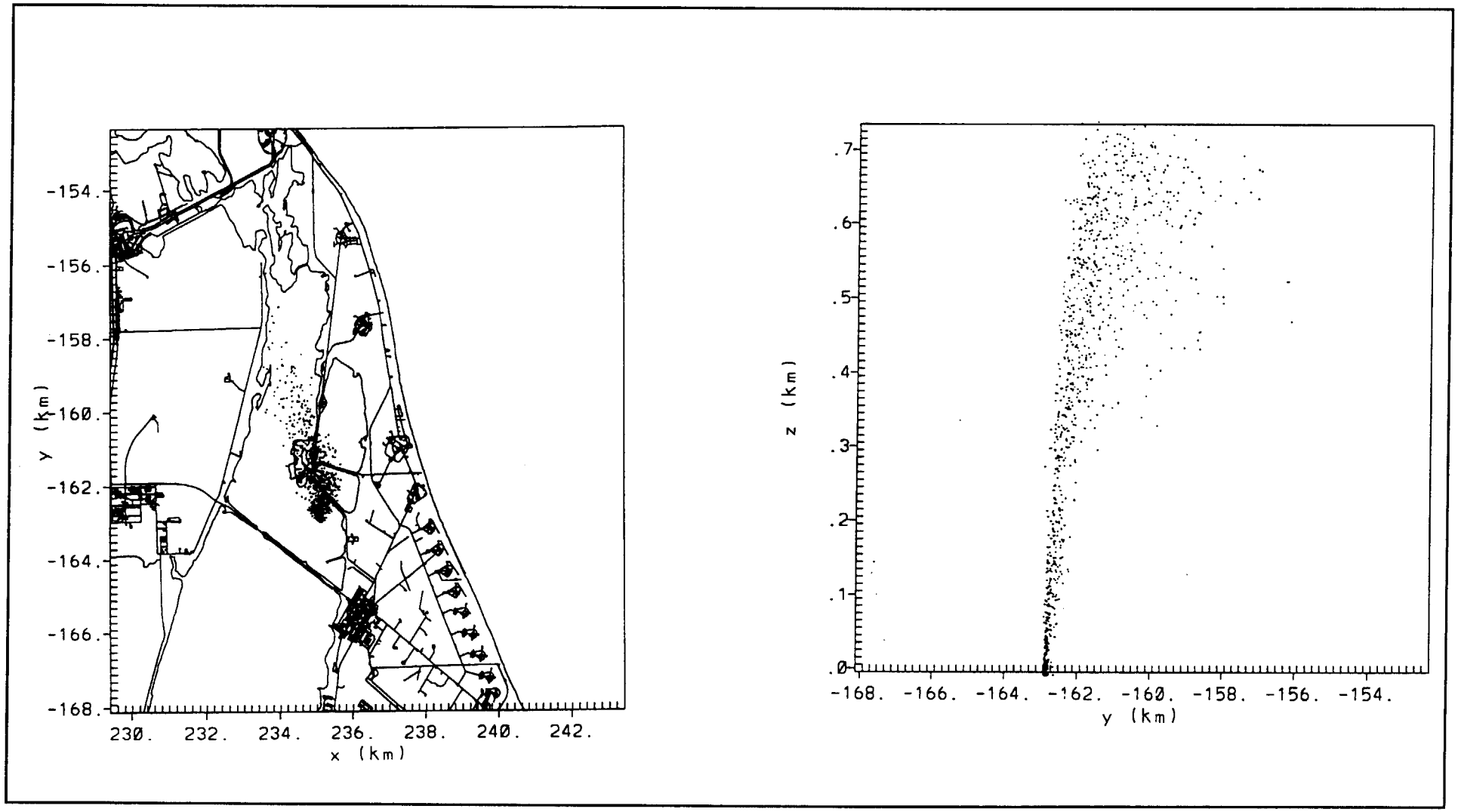

Figure 7-7e. HYPACT results at 1630 UTC of N_2O_4 released from 10 km south of Complex 41 (CCAS Industrial Area) at 1426 UTC on 20 August 1994. Figure shows plan view (left) and west-facing cross-section (right) of plume particles.

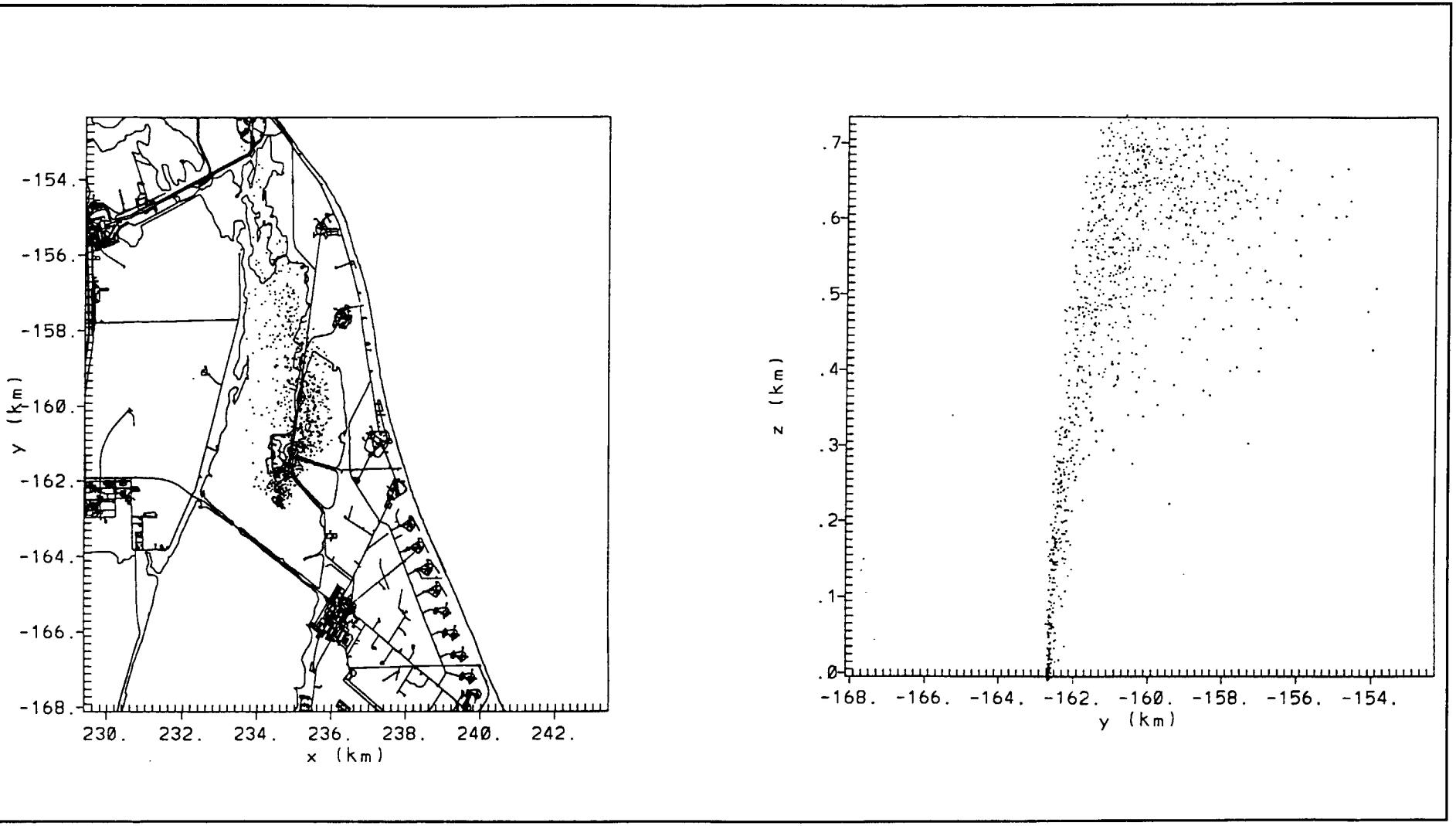

Figure 7-7f. HYPACT results at 1700 UTC of N_2O_4 released from 10 km south of Complex 41 (CCAS Industrial Area) at 1426 UTC on 20 August 1994. Figure shows plan view (left) and west-facing cross-section (right) of plume particles.

8. Comparison of Dispersion from the Ocean Breeze Dry Gulch Model and the RAMS/HYPACT model

8.1 Introduction

8.1.1 Background

The Ocean Breeze Dry Gulch (OBDG) model is the model currently certified by the Air Force for predicting downwind toxic corridors resulting from accidental spills of hazardous materials at Cape Canaveral Air Station/Kennedy Space Center (CCAS/KSC). Range Safety personnel run the OBDG model using the Meteorological and Range Safety Support (MARSS) system.

Recent studies have determined that the OBDG model is deficient for use as the primary model for modeling accidental hazardous releases. Hosker et al. (1993) determined:

- "The review team believes that the OBDG model is both limited in applicability and outdated, and recommends that it be replaced with a more capable model."

- "Given recent advances in dispersion modeling and computer technology, the NOAA review team considers the empirical/statistical OB/DG model to be obsolete. The model has only a rudimentary ability to take advantage of the extensive meteorological data available at KSC, and no ability to account for vertical variations in the wind. Moreover, its applicability is limited to daytime periods of unstable onshore flow. Also, OBDG is unable to deal with elevated releases of effluents, for operational uses such as launch vehicle fueling.

- "The OBDG equation does quite well for those situations which fall within the range of atmospheric conditions covered by the measurement program."

- "The OB tracer data were collected under on-shore flow situations, which are a common occurrence at KSC."

- "Dispersion was measured only for near-surface releases; elevated releases may behave differently, especially at night."

- "The influences of convection and sea breeze convergence on vertical plume displacements and recirculations were not determined [during the Ocean Breeze experiment]."

- "The Regional Atmospheric Modeling System (RAMS) model should be made operational, and used to help understand KSC conditions."

In an evaluation of the OBDG model, Kunkel (1984) found:

- "The major disadvantage of the OBDG model is in its limited application. It is limited to ground level, point source, continuous spills of neutral density gases, or if used in combination with a evaporative source strength model, instantaneous liquid spills. It is not suitable for buoyant, heavy, or

liquefied gases, and does not take into account the height of the inversion layer. The presence of such an inversion could greatly increase the hazard distance of a large spill. The model is also designed specifically for spills over surfaces with a roughness length of about 10 cm."

In a review of the OBDG equations, Ohmstede et al (1983) found:

- "The most serious shortcoming of the OBDG model appears to be its unconservative estimates of the downwind hazard distance in smooth, very stable conditions."

8.1.2 Purpose

The Applied Meteorology Unit (AMU) has been evaluating the Emergency Response Dose Assessment System (ERDAS) since it was installed in the AMU in March 1994. The evaluation has focused on the assessment of:

- The meteorological predictions made by the RAMS mesoscale model.

- The diffusion predictions made by the Hybrid Particle and Concentration Model (HYPACT) and Rocket Exhaust Effluent Dispersion Model (REEDM) dispersion models.

- The overall ERDAS system performance.

As part of the evaluation of the diffusion models, the AMU was tasked to compare the diffusion predictions made by the ERDAS models with those made by the OBDG model. While the OBDG model and the HYPACT model both produce maps with concentration isopleths, they are extremely different in the methodology they each employ to compute them. The primary differences are summarized in Table 8-1.

To compare the predictions made by OBDG and HYPACT, the AMU designed a study for comparing OBDG model predictions with HYPACT model predictions. Ideally, the models' predictions should be compared with actual concentration data collected during a field program. However, no tracer data for the KSC/CCAS was available at this time. Tracer experiments conducted in July and November 1995 as part of the Model Validation Program (Lundblad 1995) will provide an extremely valuable data set for model evaluation.

This OBDG/HYPACT comparison study consisted of selecting ten case days to compare and then producing maps of ground level concentrations. These maps were analyzed and the different runs were compared. The following model configurations were used in this study:

- OBDG-Observed. The OBDG model was run in its normal configuration. Meteorological input data was provided by Weather Information Network Display System (WINDS) 5-minute average tower data.

- OBDG-RAMS. The OBDG model was run with RAMS wind speed and direction data and WINDS tower data. Varying-level wind data obtained from RAMS was substituted for the observed winds in the tower data files. Wind levels were chosen based on model-predicted vertical motion.

Table 8-1. Comparison of OBDG and HYPACT models.

	OBDG	HYPACT
Diffusion Technique		
Basis	Empirically based, Eulerian	Lagrangian scheme
Derivation method	Least squares fit of tracer data	Turbulence parameter derived from first-order Markov scheme
Plume representation	Distance to peak downwind concentration	Aggregate of particles
Plume distribution	Gaussian	Plume scatter determined by wind, turbulence
Source data		
Release type	Continuous	Continuous, Instantaneous
Vertical plume description	Passive, no buoyancy	Passive, no buoyancy
Meteorological Input Data		
Data Source	WINDS towers	RAMS model
Input variables	wind direction, temperature lapse rate (54 – 6 ft.), wind direction standard deviation	wind velocity components (u, v, w), potential temperature profiles, turbulent kinetic energy
Horizontal data distribution	tower locations, grid	Grid: 37 x 37 points at 3 km spacing
Vertical data distribution	single level winds: 54 ft.	21 sigma layers (11-2824 m)
Output		
Concentrations	Normal distribution of centerline concentration	Gridded, interpolated isopleths
Display	2-dimensional	3-dimensional

- HYPACT-RAMS. The HYPACT model was run in its normal ERDAS configuration. RAMS provided HYPACT with the required meteorological input data. HYPACT produced maps showing 3-dimensional plume locations and predicted surface concentrations.

Another goal of this study was to determine if launch processing availability would be increased or decreased if the OBDG-RAMS model or the HYPACT-RAMS model were used instead of the currently certified OBDG-Observed model. If launch processing availability was different, under what meteorological conditions would it change and how would it change? Also, if safety personnel used the HYPACT-RAMS model, would they have more information to make safety decisions than with the currently certified OBDG-Observed model.

In this report, Section 8.2 describes the procedures used to conduct the comparison of the three different model configurations. The description includes the criteria and selection of the ten cases along with the procedures used to prepare the meteorological data base and the diffusion analysis. The results of the comparison along with case study descriptions are presented in Section 8.3. Conclusions and recommendations are presented in Section 8.4.

8.2. Procedures

The Applied Meteorology Unit conducted this comparison study by following several steps to select, process and analyze the meteorological and diffusion data. A description of these steps is provided in this section.

8.2.1 Data and Selection of Case Studies

Ten case study days for the comparison were chosen using the Shuttle Landing Facility observations. For ERDAS, the RAMS model is run with the precipitation and cloud formation microphysics inactive. Therefore, for this study, days were chosen which had no occurrence of precipitation and very little cloud cover. At least one day from each month between January and July 1995 was chosen. A sea breeze occurred on six of the ten days (Table 8-2). Each 'day'

Table 8-2. Classification of the 10 days analyzed in this study.

Sea Breeze Days	Non-sea Breeze Days
April 13-14	January 31- February 1
May 29-30	February 6-7
June 9-10	March 26-27
June 19-20	May 7-8
July 5-6	
July 15-16	

covers the 24-hour period from 1200 UTC to 1200 UTC. In order to analyze how the models perform during certain times of the day, three 2-hour periods were chosen for each day: 0500 - 0700 UTC (early morning), 1500 - 1700 UTC (midday), and 2100 - 2300 UTC (late afternoon).

8.2.2 Diffusion analyses

Three different diffusion analyses were conducted for this study and each one is described in the following sections. Figure 8-1 presents a block diagram of the configuration of the three different diffusion runs and their input and output.

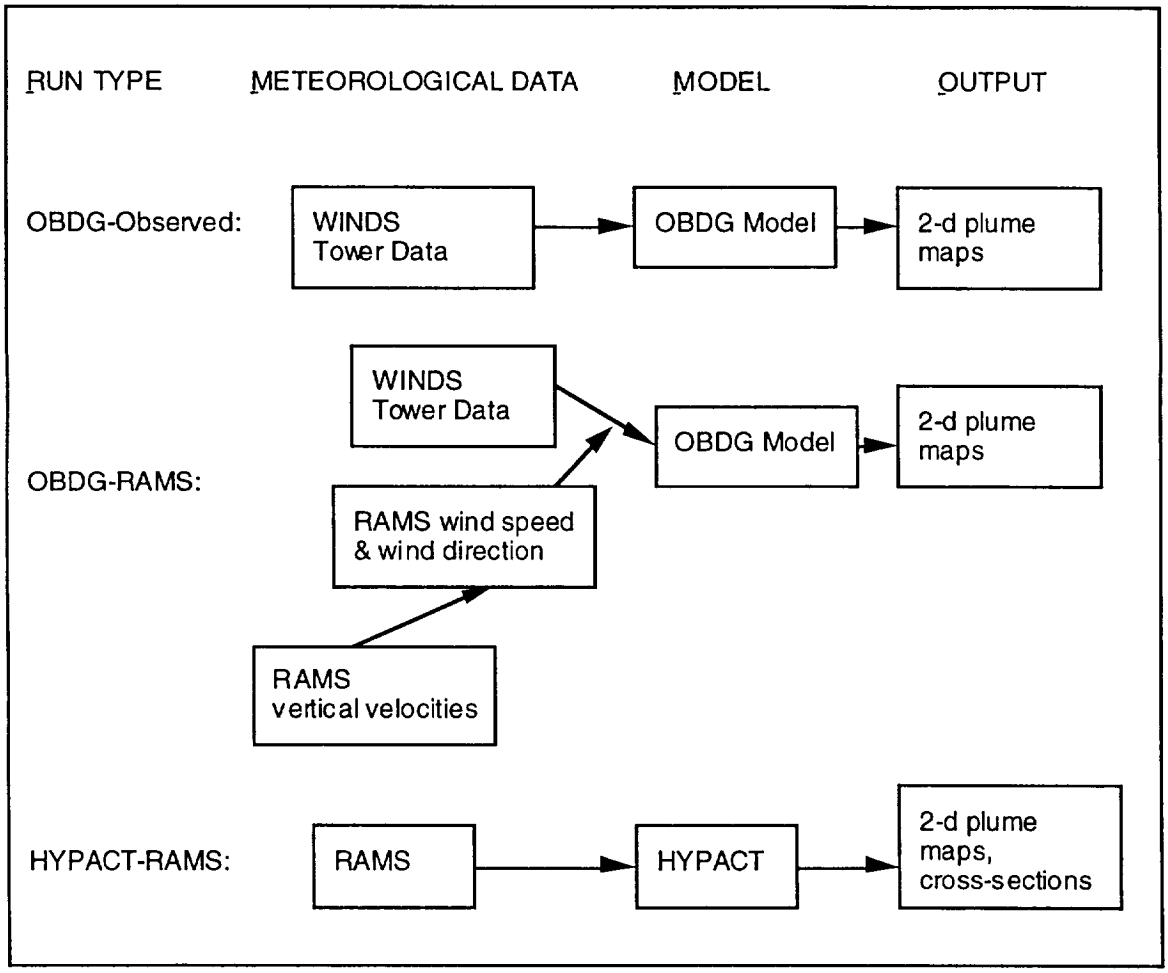

Figure 8-1. Configuration of the three different runs in this study.

8.2.2.1 OBDG with WINDS tower observations (OBDG-Observed)

The AMU generated the OBDG analyses using the standard Meteorological and Range Safety Support (MARSS) configuration. The OBDG model depends on the OBDG diffusion prediction equation, a purely empirical statistical best fit (least-squares multiple linear regression) to tracer data collected in the Ocean Breeze, Dry Gulch and Prairie Grass experiments. The equation as implemented in MARSS is:

$$X = SN(Cp/Q)^{-0.51}(\Delta T + 10)^{2.21}\sigma_\theta^{-0.258}$$

where

SN is a pollutant specific constant

Cp = concentration of pollutant (g m^{-3})

Q = source strength (g sec^{-1})

X = downwind distance (m)

ΔT = 54 – 6 ft temperature difference (°F)

σ_θ = standard deviation of wind (degrees)

Users must input basic spill information such as type of material, amount of material released, location point of release, and desired concentration isopleths. For input data, the OBDG model in MARSS requires ΔT and σ_θ data obtained from WINDS. These data are interpolated to the release point using the Barnes interpolation scheme. The OBDG equation computes the downwind distance of a particular concentration. MARSS produces maps showing the plume location. The plume location and shape are determined by the wind direction and the wind direction standard deviation measured at the 54-ft level on towers surrounding the plume.

To conduct the analyses for this study, the AMU used the OBDG function of the Meteorological Monitoring System (MMS) at ENSCO's Melbourne office. Five-minute data obtained from the WINDS system for the periods of interest were input into the MMS and plots were produced. These plots showed the predicted plume with two levels of isopleths and two levels of toxic corridor sectors. The plots were used for comparison with the other diffusion analyses.

The data in Table 8-3 were input into the OBDG model for the OBDG-observed simulations made with the observed tower data.

Table 8-3. Input data for OBDG-observed model run

Spill Amount	4100 gallons
Chemical	Nitrogen Tetroxide
Pool Size	66042 square feet
Release Rate	6604.2 pounds/minute
Release Time	Continuous: 1500-1700 UTC, 2100-2300 UTC, 0500-0700 UTC
Plume Update Interval	5 minutes
Release Location	Launch Complex 40 (lat.: 28.55864; lon.: 80.58012)
Release Height	0.0 feet
Concentration Isopleths	5 ppm, 1 ppm

The meteorological data obtained from the WINDS towers at 5-minute intervals was input into OBDG. These data had been stored in MIDDS format and were converted back to WINDS

format using AMU conversion software. Only tower data used by OBDG were converted back to the WINDS format. These data include the following parameters:

- Wind speed
- Wind direction
- Wind direction standard deviation (σ_θ)
- Temperature difference between 54 feet and 6 feet (ΔT)

Launch Complex 40 was chosen as the source of the release because it is a Titan IV launch complex and represents a location where toxic material are stored and could therefore be a potential source of a release.

OBDG with RAMS wind predictions (OBDG-RAMS)

The AMU generated OBDG analyses using winds extracted from RAMS forecasts. The RAMS winds replaced the wind speeds and directions at the 54-ft level of the WINDS tower files. The RAMS winds which were inserted in place of the observed winds were obtained from different levels of the RAMS model.

This new data set provided the OBDG model with a two-dimensional wind field that contained some characteristics of the three dimensional wind structure. For cases where the wind direction varied with height and there was upward vertical motion above the release point, this new data set would cause OBDG plume directions to follow the the RAMS-predicted upper level winds. The plume width and length would not change however since the OBDG model with RAMS winds was still run with the same observed σ_θ and ΔT as in the OBDG-obs runs.

Plots showing the OBDG predicted plume were produced for the same times as the OBDG-obs times. These plots were compared with the OBDG-Observed plots and with the plume predictions of HYPACT.

The RAMS meteorological model was run for all 10 days and produced 3-km gridded data every 5 minutes. These data were used in both the HYPACT and OBDG model runs. OBDG requires tower site wind speeds and directions in its calculations but RAMS only produces the horizontal wind components, u and v, at grid point locations. Therefore, post-processing of the RAMS data was necessary to format it for input into OBDG. Vertical velocity calculations from RAMS were also used.

In addition, the 3-D RAMS calculations allow for a plume to rise or sink based on the vertical velocity, w. A review of several HYPACT runs shows that plumes rarely rise above 1 km in the 2 hour period following a release. This height corresponds closely to model level 15 (1053 m) in the finest grid. In order to save computer time and memory with minimal degradation of the scientific results, the horizontal winds in the first 15 model levels were processed for input to OBDG. The vertical velocities at the grid points closest to the three chosen release sites were also output during each run. These were used to determine which model level winds would be input to OBDG.

RAMS horizontal wind data were converted from the u and v components (m s^{-1}) at the grid points to wind speed (kt) and direction (degrees) at the 61 tower locations for use in OBDG. The interpolated horizontal wind components were then used to calculate the wind speed and

direction at each tower location for model levels 1-15, and the wind speeds were converted from meters per second to knots.

8.2.2.3 HYPACT with RAMS predictions (HYPACT-RAMS)

The primary model used for computing dispersion estimates is HYPACT. HYPACT is the advanced Lagrangian particle dispersion model in ERDAS. Dispersion in the Lagrangian mode of HYPACT is simulated by tracking a large set of particles. Subsequent positions of each particle are computed from the relation:

$$X[t+Dt] = X[t] + [u + u'] Dt$$

$$Y[t+Dt] = Y[t] + [v + v'] Dt$$

$$Z[t+Dt] = Z[t] + [w + w' + w_p] Dt$$

where u, v and w are the resolvable scale wind components which are derived from RAMS or the hybrid (RAMS/tower observations) wind field, and u', v', and w' are the random subgrid turbulent wind components deduced from RAMS. The w_p term is the terminal velocity resulting from external forces such as gravitational settling. Dt is the model time step. HYPACT uses the RAMS-predicted wind fields and potential temperature fields to advect and disperse the plume particles vertically and horizontally downwind from the source.

HYPACT can model any number of sources which are specified anywhere in the domain and configured as point, line, area, or volume sources. The emissions from these sources can be instantaneous, intermittent, or continuous and the pollutants can be treated as gases or aerosols. A primary release scenario which ERDAS will model is a cold spill of toxic chemicals at launch pads and storage facilities, in which evaporation takes place from pools. Using both small or large numbers of particles, HYPACT produces plumes which are viewed on a map background and then calculates detailed concentrations and dosage estimates.

For this study, HYPACT was run to simulate a cold spill at a Titan launch complex resulting from the release of nitrogen tetroxide (N_2O_4) from a fueled Titan IV rocket. This scenario was chosen because an accidental release of N_2O_4 from the Titan IV is potentially one of the most dangerous due to the amount N_2O_4 and the concentration levels which are of concern to safety personnel.

The release data entered into HYPACT is listed in Table 8-4.

Table 8-4. Input data for HYPACT runs.

Spill Amount	4100 gallons
Chemical	Nitrogen Tetroxide (N_2O_4)
Pool Size	66042 square feet
Release Rate	6604.2 pounds/minute
Release Time	1500 UTC, 2100 UTC, 0500 UTC
Dispersion Simulation End	1700 UTC, 2300 UTC, 0700 UTC
Release Duration	90 minutes
Release Location	Launch Complex 40 (lat.: 28.55864; lon.: 80.58012)
Release Height	0.0 feet
Concentration Isopleths	5 ppm, 1 ppm

8.3. Results

The results of the analysis and comparison of the diffusion model runs – the OBDG-observed, the OBDG-RAMS and HYPACT-RAMS – for the 10 selected days are presented in this section. Tables summarizing each models' performance for each time period are presented in Tables 8-7 to 8-16. A detailed discussion of the models' performance during two case study days is presented in Section 8.3.2. Maps and cross-sections showing the results of the models' runs are presented in Figures 8-2 to 8-32.

8.3.1 Comparison Summaries

Summary tables were compiled for each of the three different model runs for the three different time periods of the ten case days selected (Tables 8-7 to 8-16). These summaries provide information on the model results for the OBDG-Obs, the OBDG-RAMS, and the HYPACT-RAMS runs. Information on plume direction during the two-hour period was compiled at 15-minute intervals for the OBDG runs and at 20 minute intervals for the HYPACT runs. The release point for all of the model runs was LC-40. A one-page table showing the key data from each of the 30 cases is presented in Table 8-5.

For the OBDG-RAMS runs, data on the height of the RAMS sigma-level are provided. The sigma levels are the vertical grid points in RAMS where winds are computed. The sigma levels were selected for the OBDG-RAMS runs based on the vertical velocities as described in 8.2.2. For the OBDG-RAMS runs, the RAMS winds replaced the observed winds.

The direction of the plume predicted by the OBDG models was assessed by determining the direction from the LC-40 source. OBDG computes a new plume location every five minutes as new meteorological data are received. The location of each plume is independent of the plumes produced five-minute before or after. Therefore, if the wind direction at the source location shifted from one five-minute period to the next, then the plume location would also shift. During conditions of light and variable winds, shifts of wind directions and resulting plume directions may be frequent.

In contrast to the OBDG models, the direction of the plume predicted by the HYPACT model is dependent on the wind field from one time to another. HYPACT plumes are emitted and are then advected with the RAMS-predicted wind field which can change with time and space. Therefore, sudden changes in wind direction do not make a dramatic difference in the location of the HYPACT plume from one time period to the next. HYPACT plumes can stretch and diffuse in horizontal and vertical directions.

The plume directions listed in Tables 8-7 to 8-16 for the OBDG models were determined by analyzing the maps of the OBDG output for a given five-minute period at 15-minute intervals. The plume directions listed for the HYPACT model were determined by analyzing maps produced at 20-minute intervals.

8.3.1.1 OBDG-Observed / OBDG-RAMS Comparison

The comparison of the OBDG-Observed plume directions with the OBDG-RAMS plume directions indicates that for the 252 comparison times, the directions agree 34% of the time. The plume directions were within 90° of each other for all of the 252 comparison times. These results indicate the wind directions predicted by RAMS agreed fairly well with the observed wind directions. RAMS did fairly well at predicting wind direction shifts from one two-hour period to the next. For example, on 13 April 1995 (Table 8-10) the OBDG-RAMS plume direction was modeled to move offshore during the midday runs, onshore during the late afternoon runs.

Table 8-5. Summary of the Comparison Summaries which were compiled for each of the 30 time periods analyzed in this study. The Plume Direction columns show the observed versus predicted plume direction determined at each 15-minute interval during one of the indicated time periods. The column showing degrees converts the cardinal directions to degrees. For example, during the midday period of 31 Jan, a period of 2 hours, the largest difference at any one 15-minute period occured when the plume direction from the OBDG-Observed was ESE and from the OBDG-RAMS was SE, leading to a difference in degrees of 22.5°.

Date	Time period	Plume Direction				Wind spd. av. obs (knots)	Wind spd. av RAMS (knots)	Maximum height of RAMS winds (m)	HYPACT plume direction	Maximum height of HYPACT plume (m)
		OBDG-Observed vs. OBDG-RAMS								
		Largest Difference		Smallest Difference						
		Direction	De-grees	Direction	De-grees					
31 Jan 95	midday	ESE-SE	22.5	SE-SE	0	7.2	9.7	11	SE	200
	late afternoon	E-S	90	E-E	0	8.0	11.0	910	S->E	500
	nighttime	E-ESE	22.5	ESE-ESE	0	6.3	10.0	11	ESE	100
6 Feb 95	midday	SE-ESE	22.5	SE-SE	0	8.3	10.0	11	SE->SSE	200
	late afternoon	S-SW	45	SSW-SSW	0	5.1	10.6	320	SW->S	600
	nighttime	ESE-NE	67.5	ENE-NE	22.5	6.9	7.0	11	NE	100
26 Mar 95	midday	W-SSW	67.5	W-W	0	7.2	10.8	910	SW->W	1000
	late afternoon	W-WNW	22.5	WNW-WNW	0	6.3	15.8	142	WNW	300
	nighttime	-	-	-	--	-	-	-	-	-
13 Apr 95	midday	ENE-ENE	0	ENE-ENE	0	6.4	7.0	1053	E	600
	late afternoon	WNW-WSW	45	NW-WNW	22.5	7.0	14.1	94	W	200
	nighttime	ESE-SE	22.5	SE-SE	0	7.9	8.3	11	SE	200
7 May 95	midday	WSW-SW	22.5	SW-SW	0	7.7	8.1	94	SW->W	150
	late afternoon	WSW-W	22.5	WSW-WSW	0	8.8	16.8	94	W	300
	nighttime	WSW-NW	67.5	W-NW	45	5.6	9.9	60	NW	100
29 May 95	midday	NW-SW	90	WNW-WSW	45	8.1	10.3	142	SW->W	900
	late afternoon	WNW-W	22.5	WNW-WNW	0	8.	16.2	142	W	200
	nighttime	NNW-NW	22.5	NNW-NNW	0	5.	9.1	34	NW	200
9 Jun 95	midday	SSW-W	67.5	SW-SW	0	5.8	8.2	60	W->SW	1300
	late afternoon	W-WSW	22.5	WSW-WSW	0	4.8	17.7	196	WSW	400
	nighttime	ENE-NNE	45	NNE-NNE	0	5.0	4.7	11	NNE	100
19 Jun 95	midday	SSE-SW	67.5	SSW-SW	22.5	6.1	9.4	142	SW	1500
	late afternoon	SW-W	45	SW-SW	0	6.3	12.9	142	WSW	400
	nighttime	ENE-NNE	45	NNE-NNE	0	5.1	8.3	11	NW	100
5 Jul 95	midday	W-WSW	22.5	W-W	0	4.3	6.3	34	WSW	900
	late afternoon	WNW-W	22.5	W-W	0	6.7	16.0	142	W	300
	nighttime	NW-NNE	67.5	NNW-N	22.5	3.2	5.0	11	N	100
15 Jul 95	midday	W-SW	45	WSW-SW	22.5	5.6	9.4	60	SW	1100
	late afternoon	WNW-W	22.5	W-W	0	8.2	14.7	142	W	300
	nighttime	N-NE	45	NNW-NW	22.5	5.1	5.9	11	N->NE	200

with the sea breeze, and then offshore again during the nighttime runs. The OBDG-RAMS plume directions followed the same pattern as the OBDG-Observed runs which showed offshore flow during the midday, onshore flow with the sea breeze during the late afternoon, and then back to offshore flow during the nighttime.

The vertical velocity algorithm which was used to select the height of the RAMS winds used in the OBDG-RAMS runs was not a significant factor in determining plume direction in most of the runs. Table 8-6 shows the RAMS layers where winds were computed which were available for selection by the algorithm. This vertical velocity algorithm caused the RAMS winds in layers above 300 meters to be used in only four of the 29 different periods. During these four periods, RAMS predicted enough heating over the land to produce upward vertical motions in the vicinity of LC-40. In these four cases, the upper level winds did not differ significantly from the low level winds. Therefore, as vertical velocities increased, the upper level winds caused OBDG-RAMS to move the plume in the same direction as OBDG-Observed.

Table 8-6. Sigma levels in RAMS available for OBDG-RAMS wind selection.

Sigma level	1	2	3	4	5	6	7	8	9	10	11	12	13	14	15
Height (m)	11	34	60	94	142	196	254	320	393	474	566	668	782	910	1053

8.3.1.2 OBDG / HYPACT-RAMS Comparison

The direction of the HYPACT plumes were analyzed to see how they compared with the OBDG plumes and to determine if launch processing availability would be increased or decreased if the HYPACT model was used instead of the OBDG model. Of the 26 cases analyzed launch processing availability would have increased for 2 of the cases, decreased for 1 of the cases, and stayed the same on the rest. A change in launch processing availability was determined by comparing the length and location of the ground level plume as indicated by the 5 and 25 ppm isopleths. If there was a significant change in the length or location (in relation to populated areas), then it was inferred that there was a change in the launch processing availability.

Even though most of the cases showed no change in launch processing availability, the HYPACT analyses provided valuable information on the 3-dimensional structure of the plume for 15 of the 26 cases. For these 15 cases, which were all from the midday and late afternoon runs, the plumes were lofted up above 300 meters at some point along its trajectory causing material to be transported upward. This material could eventually mix downward to the surface under the right conditions although the two-hour simulations run for this study did not show downward plume mixing. Of the 15 cases in which plumes were lofted upward, 13 of them occurred with on-shore easterly flow. RAMS accounts for the heating over the land and generates the strongest upward motions over the inland areas.

8.3.2 Case studies

Two case studies were selected for detailed analysis and are discussed in this section. These two cases were selected because of the complex dynamic meteorological conditions which occurred locally on these days. On 13 April 95, a typical sea breeze developed and moved

westward across CCAS/KSC. RAMS predicted the formation and passage of the sea breeze. On 9 June 1995, the diffusion was significantly affected by the convection and vertical motion which occurred over the CCAS/KSC land areas. The 3-dimensional meteorological structure of the lower atmosphere played an important role in modeling the plume diffusion.

8.3.2.1 13 April 95

The modeling analyses of the midday runs on 13 April 95 provided a case study of the onset of the sea breeze during the late morning and early afternoon. During the two-hour period from 1500 to 1700 UTC, the OBDG-Observed and OBDG-RAMS runs agreed closely with each other (Figures 8-2 through 8-9). The observed winds during this entire period were generally light and from the west at all the tower locations across CCAS/KSC and the RAMS-predicted winds agreed. Therefore, the plumes predicted by both OBDG runs extend eastward into the Atlantic Ocean and showed no threat to any populated areas resulting from a potential toxic spill of N_2O_4 at Launch Complex 40.

The HYPACT-predicted plume was very similar to the OBDG plumes for this period since HYPACT moved the plume eastward over the ocean and did not indicate that it would affect any populated areas during the two-hour period (Figures 8-10 through 8-15). However, the HYPACT runs clearly showed the start of the sea breeze that moved onshore after 1700 UTC. The start of the sea breeze is shown in the 1610 UTC (Figure 8-13), 1630 UTC (Figure 8-14), and 1650 UTC (Figure 8-15) horizontal maps and vertical cross-sections of the HYPACT plume. HYPACT moved the plume approximately 6 km offshore until 1610 UTC when the plume encountered low level flow from the east. The opposing flow produced a line of convergence which produced upward vertical motion and forced the plume upward. By 1650 UTC, HYPACT lifted the plume upward to 600 meters. HYPACT also began moving the plume westward back toward the coastline after it had originally moved the plume eastward at the beginning of the simulation.

The value the HYPACT analyses provides to safety personnel is the forecast of the wind shift. HYPACT correctly predicted that the plume shown by OBDG to be located offshore would move back onshore and that the offshore flow present during the morning would change. Figure 8-16 shows the OBDG-observed and OBDG-RAMS plumes at 2145 UTC and Figure 8-17 shows the HYPACT plume at 2150 UTC. The sea breeze moved westward across the Cape prior to the time of these maps resulting in easterly flow which moved the plumes to the west.

Figure 8-18 shows the OBDG-observed and OBDG-RAMS plumes at 0530 UTC and Figure 8-19 shows the HYPACT plume at 0530 UTC. During the nighttime hours the offshore flow re-established itself and the plumes were predicted to move to the southeast. The plume direction is the same for all three models.

8.3.2.2 9 June 1995

The modeling analyses of the midday runs on 9 June provided a case where the HYPACT model provided information on the 3-dimensional nature of the plume that was not available from the 2-dimensional output produced by the OBDG models. The HYPACT plume extended upward to 1300 meters during a period that the OBDG model only shows a surface-based 2-dimensional plume.

At 1515 UTC, near the beginning of the midday run, RAMS predicted easterly winds and moved the OBDG plume to the west while the observed winds were from the northeast and the OBDG-Observed runs moved the plume to the southwest (Figures 8-20 and 8-21). During the midday period RAMS gradually shifted the easterly winds around to northeasterly (Figures 8-

22, 8-23, and 8-24) and at 1630 UTC, the RAMS-predicted northeasterly winds agreed with the observed northeasterly winds (Figure 8-25). The OBDG plumes were located southwest of the source over Merritt Island (Figure 8-26).

During the early part of the midday period, HYPACT predicted a plume that was similar to the OBDG models (8- 27 through 8-32). Using the RAMS winds which were easterly during the early part of the period, HYPACT moved the plume westward and kept it contained below 100 meters (Figures 8-27 through 8-28). However, beginning at 1550 UTC (Figure 8-29), the leading edge of the plume was over the center of Merritt Island where RAMS predicted strong upward convective motion. This strong upward vertical motion continued through the midday period and caused HYPACT to lift the plume upward (Figure 8-30). From 1550 to 1650 UTC, HYPACT lifted the top of the plume from 500 to 1300 meters (Figures 8-31 and 8-32) where the cross sections show the pronounced vertical plume development predicted by HYPACT.

8.4 Conclusions

A special study was conducted to compare the currently certified OBDG model with the ERDAS models to determine if the ERDAS models changed launch availability. The study was limited in that it looked at dispersion during 30 two-hour periods over a 6-month period. These periods included late afternoon periods similar to the original OBDG study but it also included a higher percentage of late morning cases than the original OBDG study and included nighttime cases which were not included in the original OBDG study. The results of the study were:

- Cases where the winds shifted over time and space were the ones where major differences existed between the OBDG model and the ERDAS model. Currently certified OBDG model did not adequately handle wind shifting situations while the ERDAS models provided a more realistic picture of dispersion when wind shifts occurred.

- The ERDAS models could provide safety personnel with a better understanding of the three-dimensional wind field causing plume dispersion resulting from a potential toxic spill. Information on vertical plume development is not available from the OBDG model. This information can help safety personnel in making evacuation decisions and answer questions such as:

    - Will potential toxic plumes which have lofted upward eventually mix back down to surface? Are concentrations aloft large enough to pose a threat to populated areas if they reach the surface?

    - Will potential toxic plumes which have moved offshore eventually move back onshore?

- Comparing diffusion model predictions made by the OBDG model and the ERDAS models in this limited comparison study produced results which showed that using the ERDAS models for non-continuous spill scenarios improves launch processing availability in 19 of 29 cases. For continuous spill scenarios, ERDAS improves launch processing availability in 2 out of 29 cases. A non-continuous spill is one that has a limited release duration (less than approximately one hour). The OBDG model assumes a continuous release.

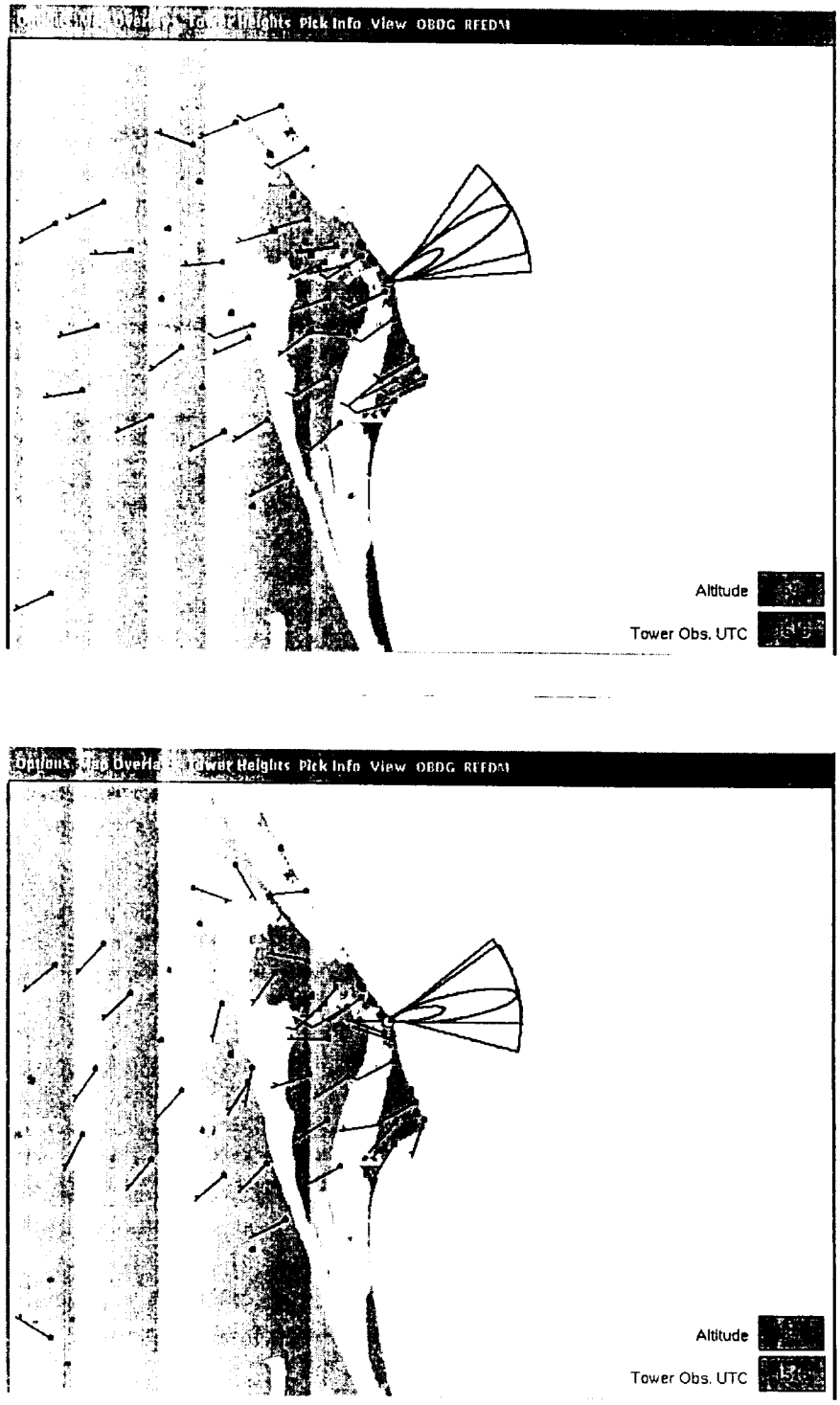

Figure 8-2. OBDG plumes computed using observed data (top) and RAMS wind speed and direction data (bottom) for 13 April 1995 at 1515 UTC.

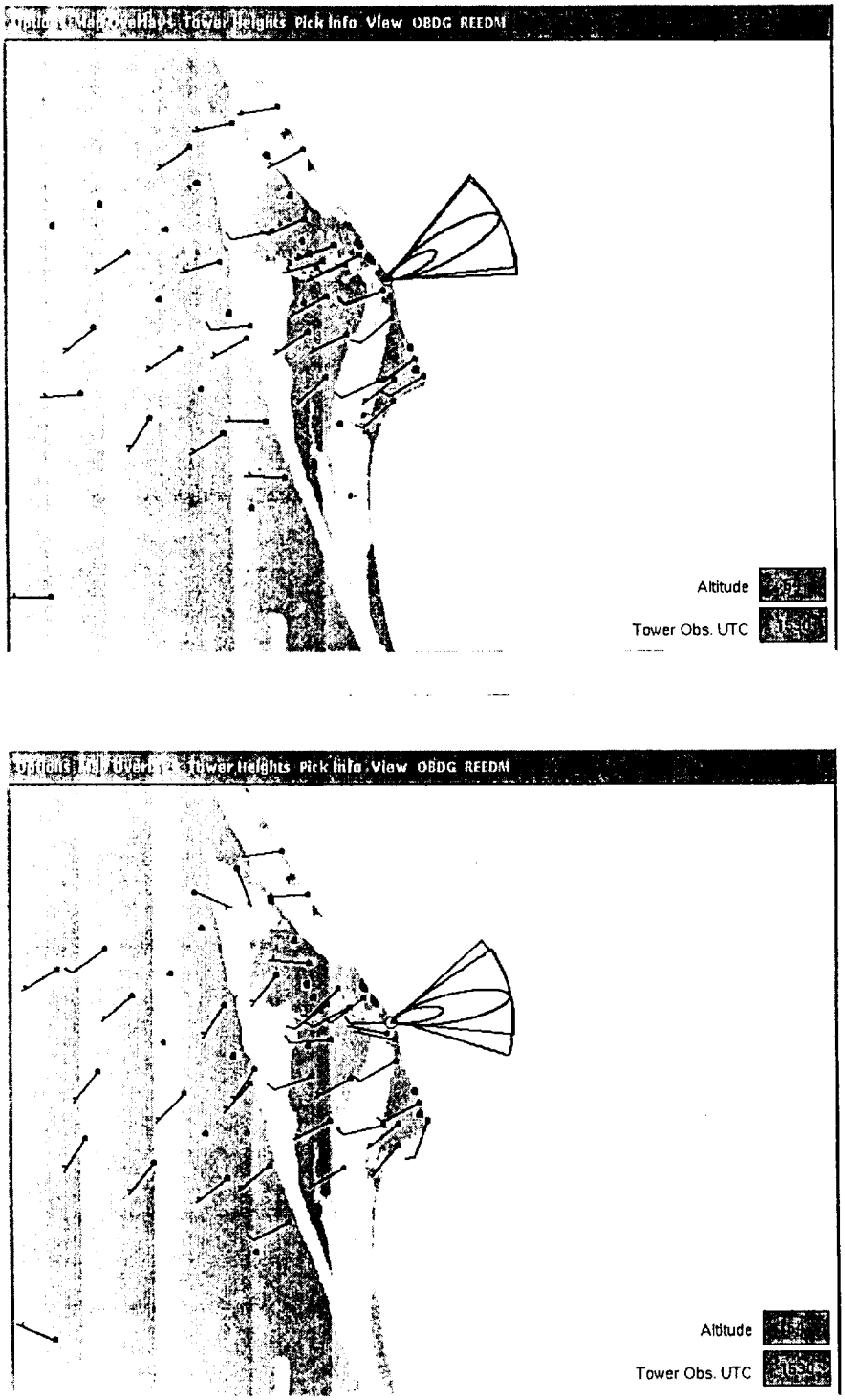

Figure 8-3. OBDG plumes computed using observed data (top) and RAMS wind speed and direction data (bottom) for 13 April 1995 at 1530 UTC.

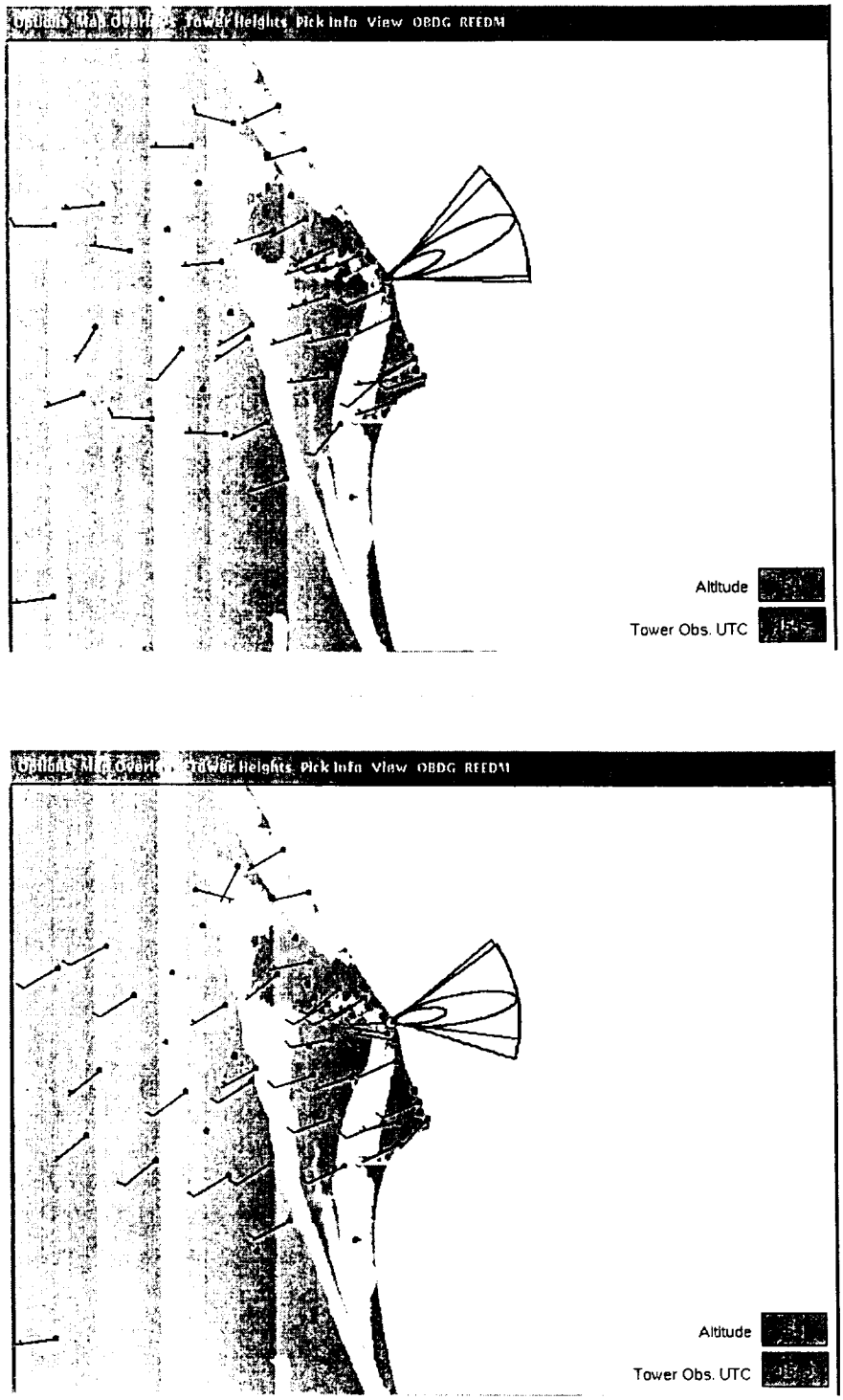

Figure 8-4. OBDG plumes computed using observed data (top) and RAMS wind speed and direction data (bottom) for 13 April 1995 at 1545 UTC.

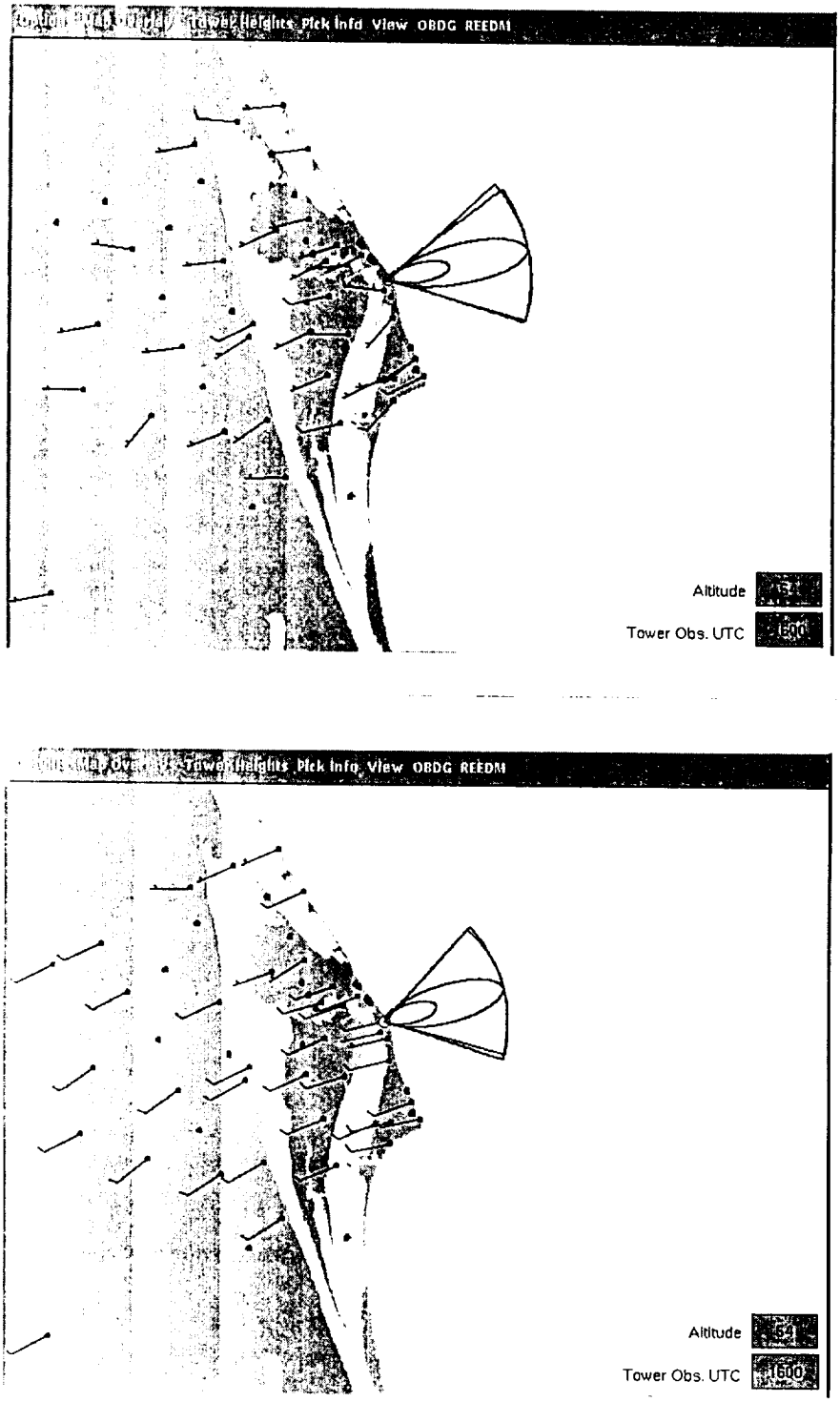

Figure 8-5. OBDG plumes computed using observed data (top) and RAMS wind speed and direction data (bottom) for 13 April 1995 at 1600 UTC.

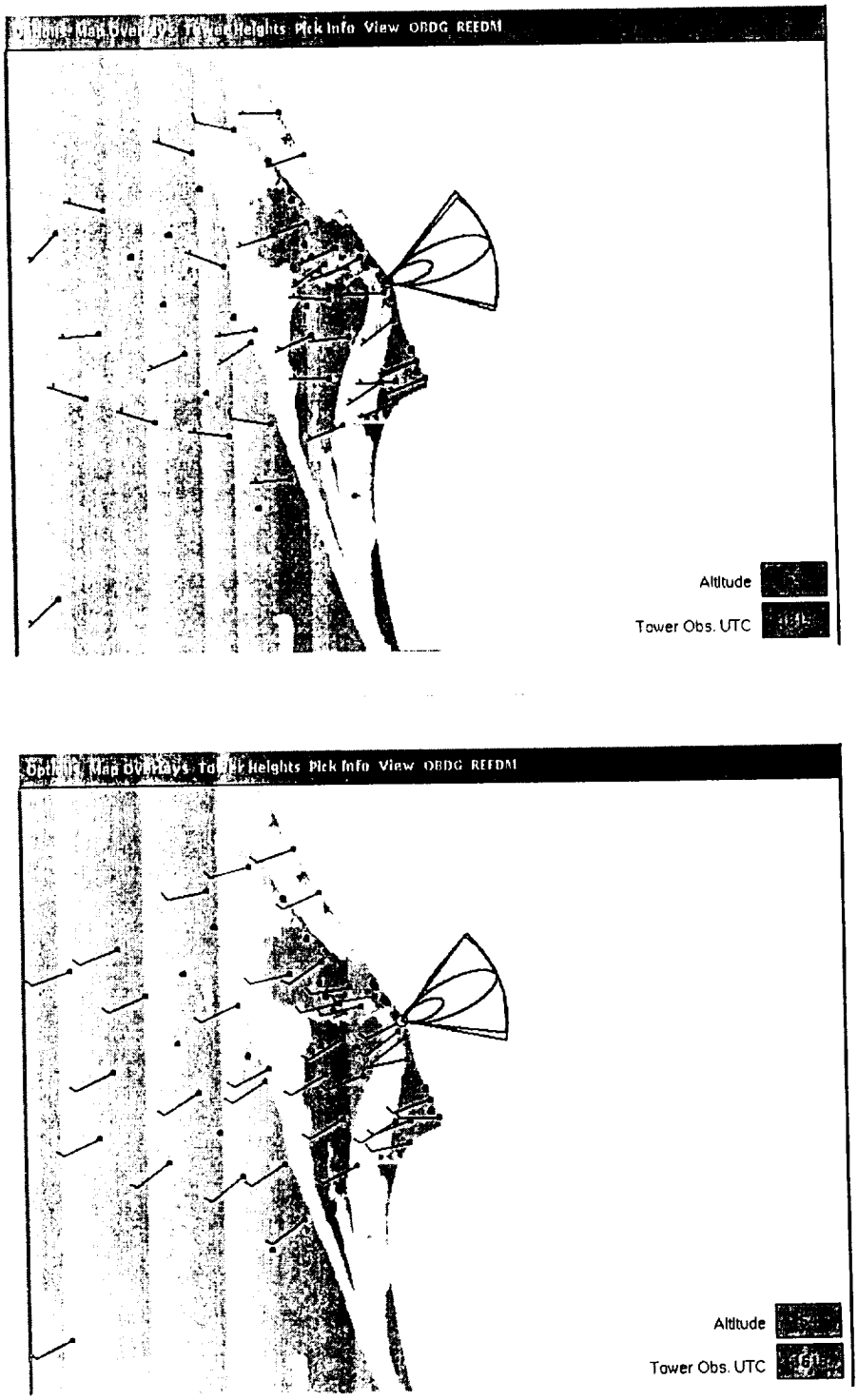

Figure 8-6. OBDG plumes computed using observed data (top) and RAMS wind speed and direction data (bottom) for 13 April 1995 at 1615 UTC.

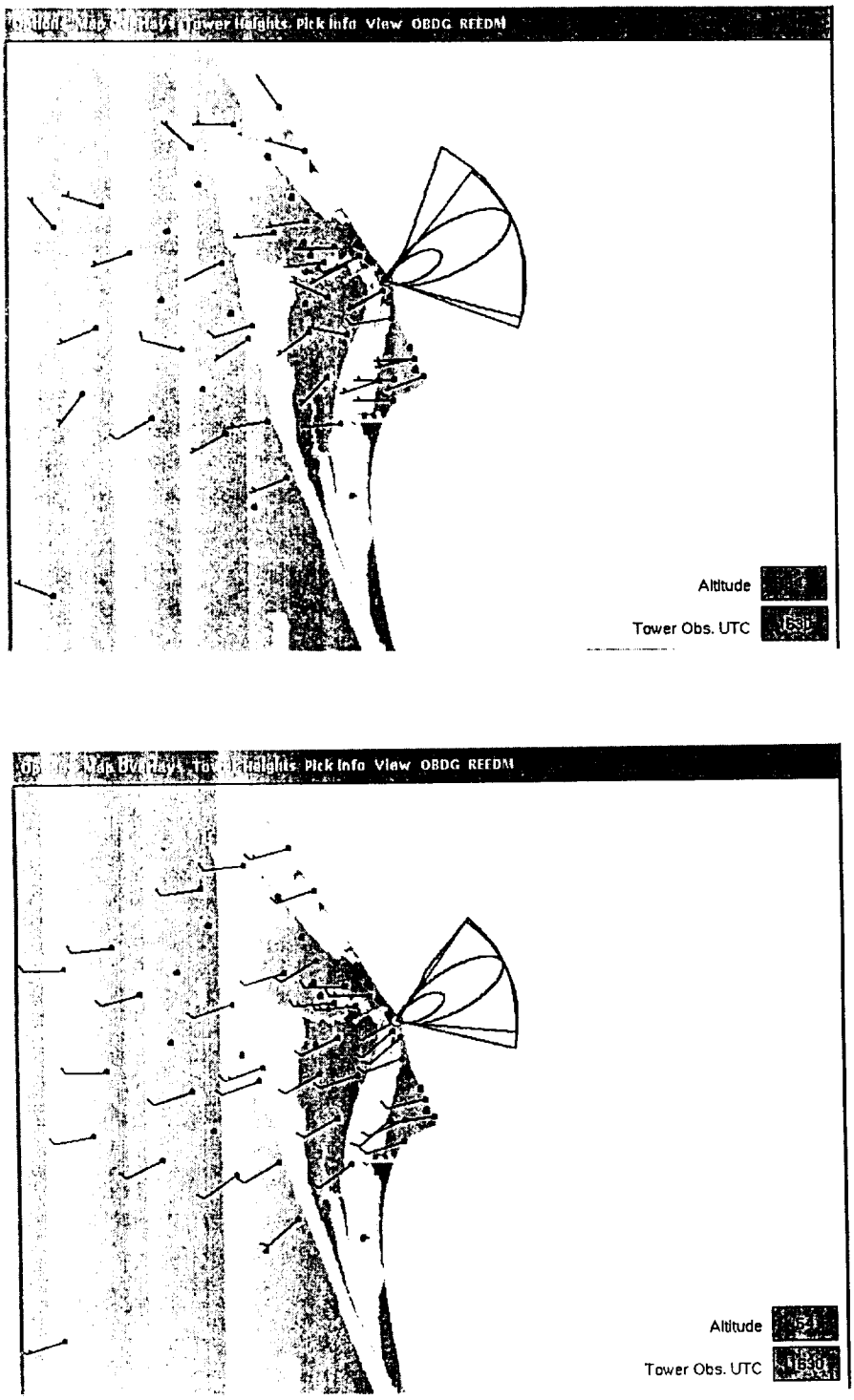

Figure 8-7. OBDG plumes computed using observed data (top) and RAMS wind speed and direction data (bottom) for 13 April 1995 at 1630 UTC.

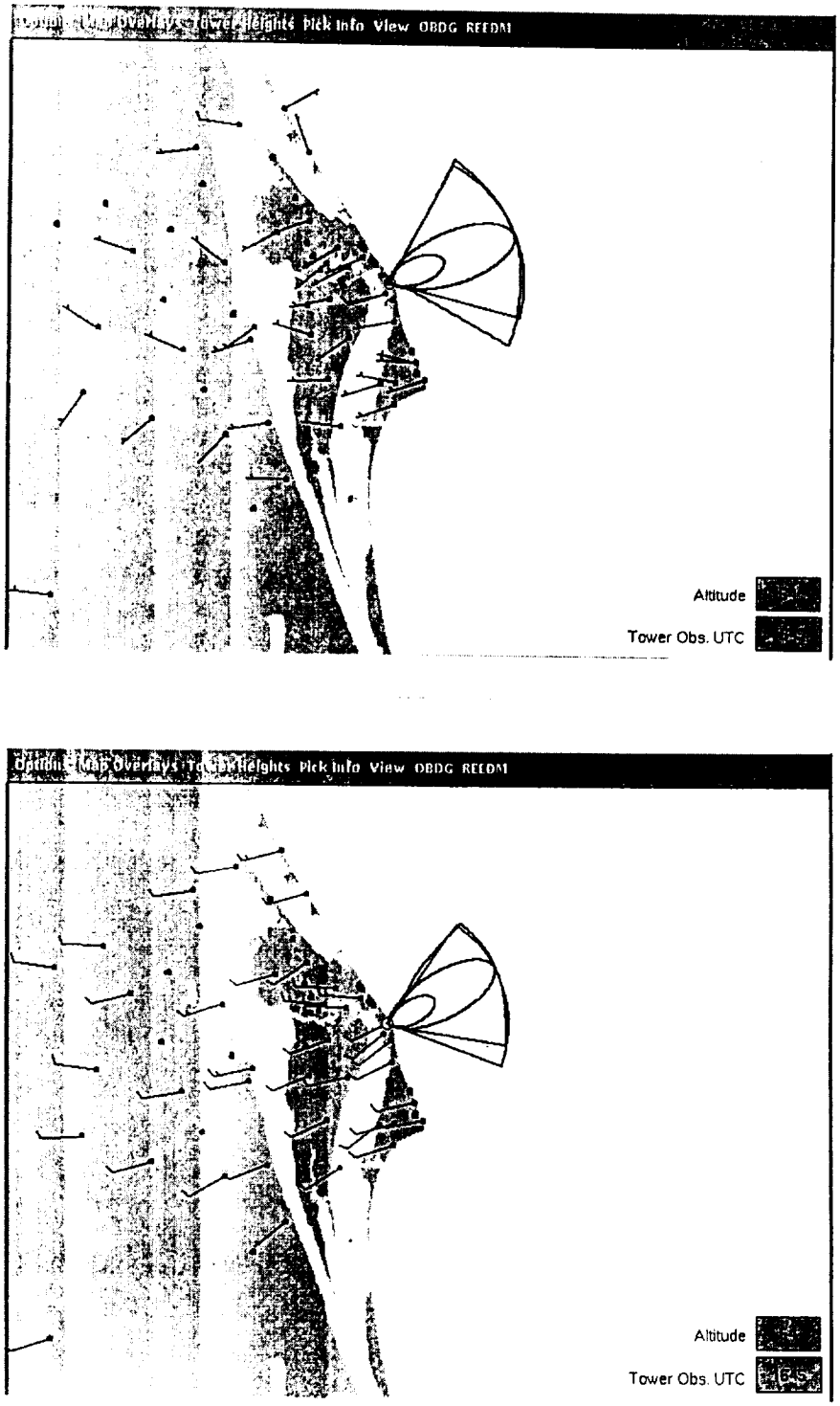

Figure 8-8. OBDG plumes computed using observed data (top) and RAMS wind speed and direction data (bottom) for 13 April 1995 at 1645 UTC.

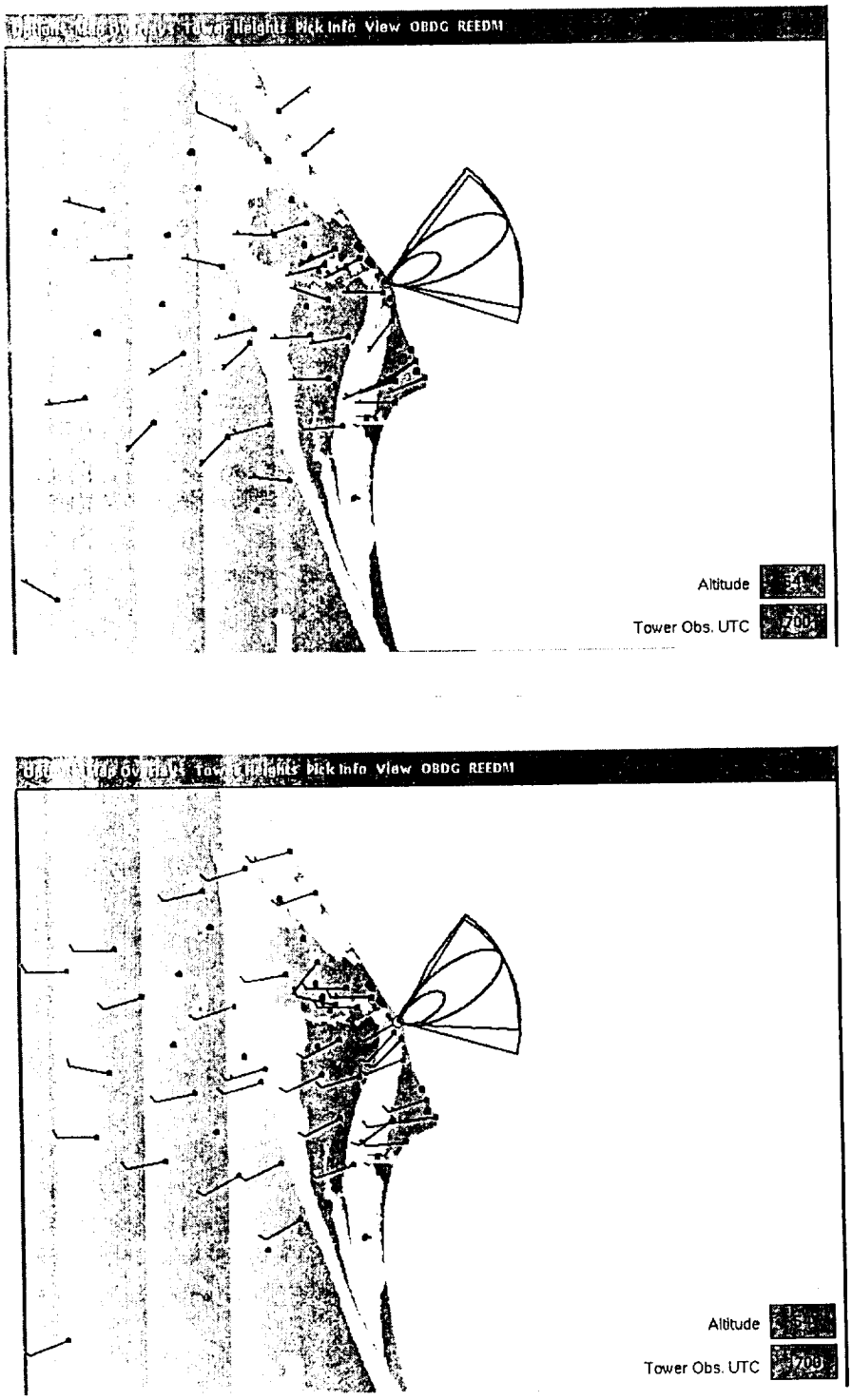

Figure 8-9. OBDG plumes computed using observed data (top) and RAMS wind speed and direction data (bottom) for 13 April 1995 at 1700 UTC.

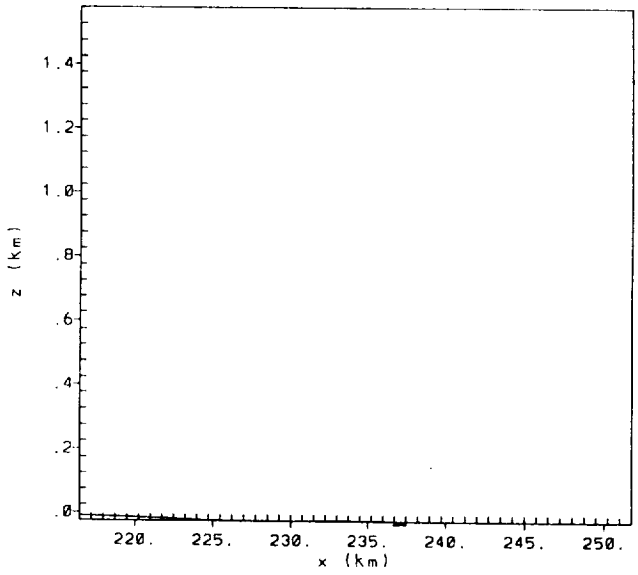

y = −190.47 km 1510 UTC

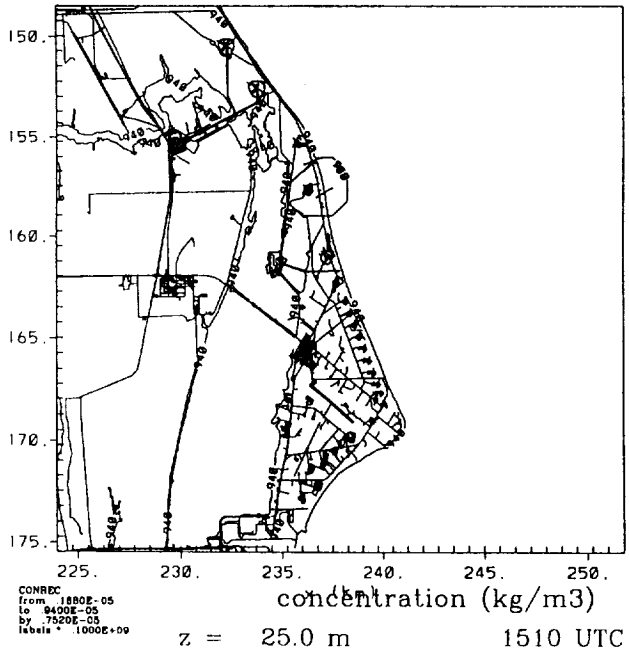

z = 25.0 m 1510 UTC

Figure 8-10. Cross-section (top) and map (bottom) of HYPACT plume computed using RAMS data for 13 April 1995 at 1510 UTC.

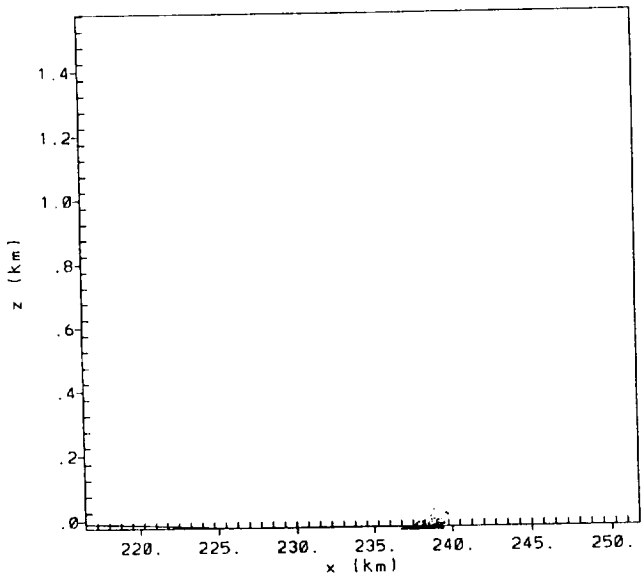

y =-190.47 km 1530 UTC

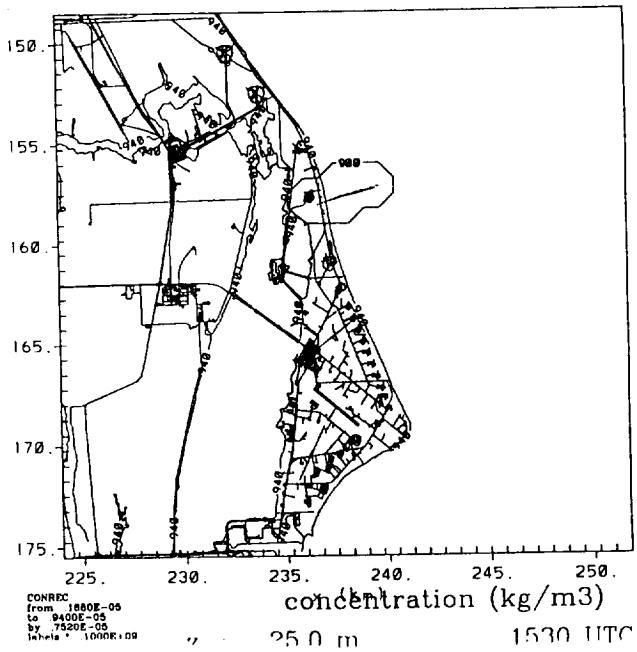

Figure 8-11. Cross-section (top) and map (bottom) of HYPACT plume computed using RAMS data for 13 April 1995 at 1530 UTC.

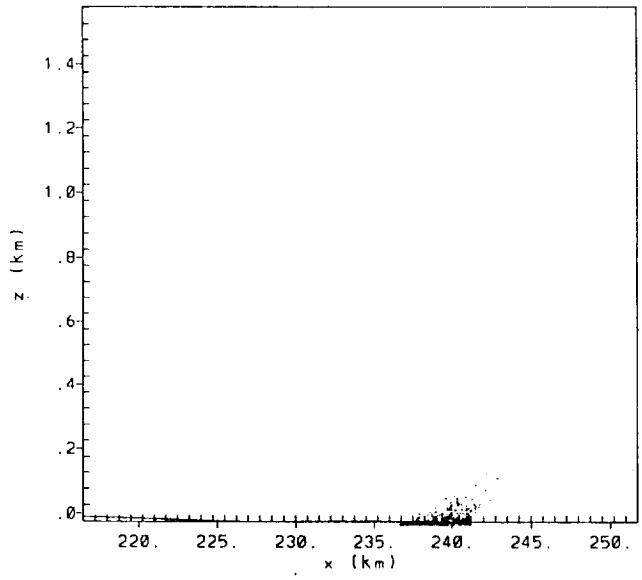

y = −190.47 km 1550 UTC

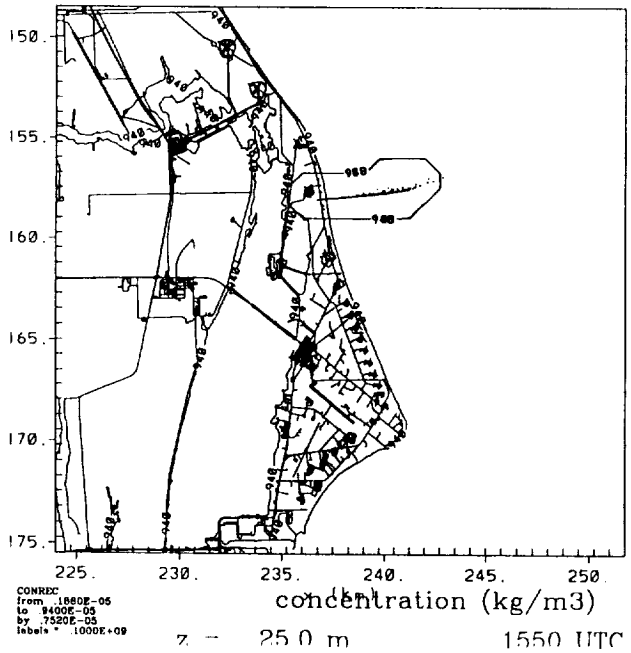

Figure 8-12. Cross-section (top) and map (bottom) of HYPACT plume computed using RAMS data for 13 April 1995 at 1550 UTC.

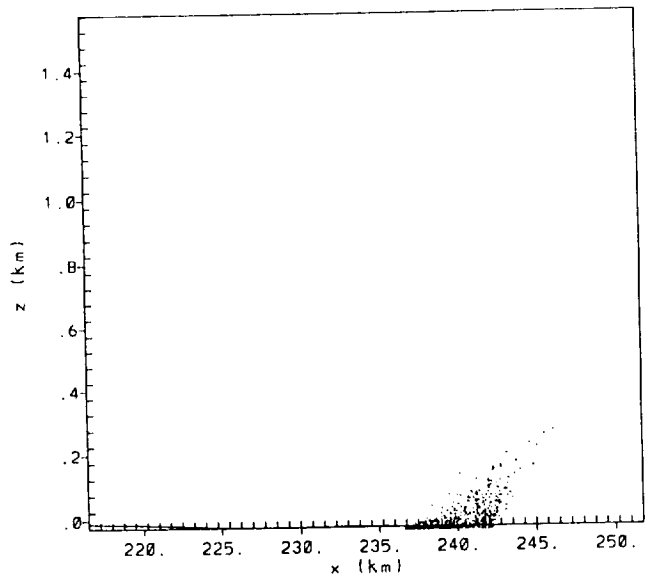

y =−190.47 km 1610 UTC

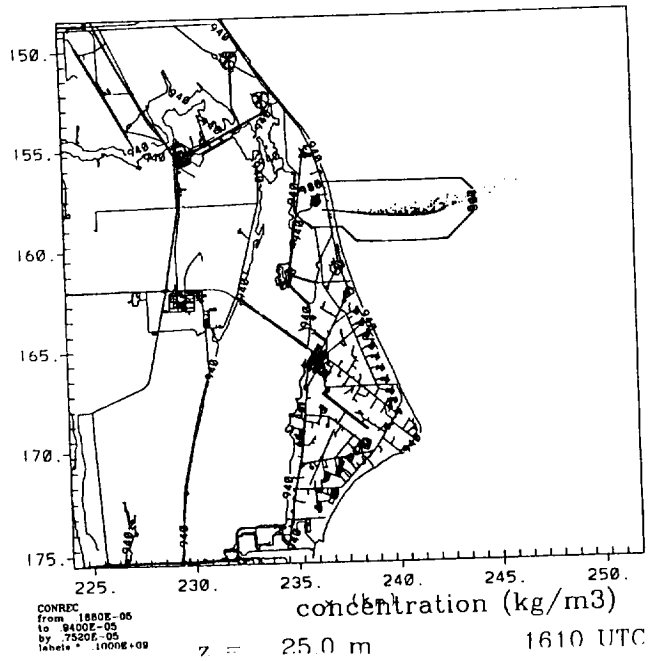

Figure 8-13. Cross-section (top) and map (bottom) of HYPACT plume computed using RAMS data for 13 April 1995 at 1610 UTC.

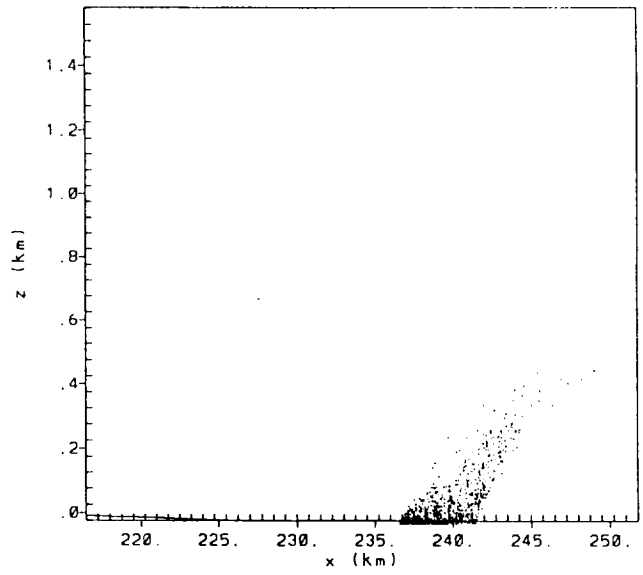

y =−190.47 km 1630 UTC

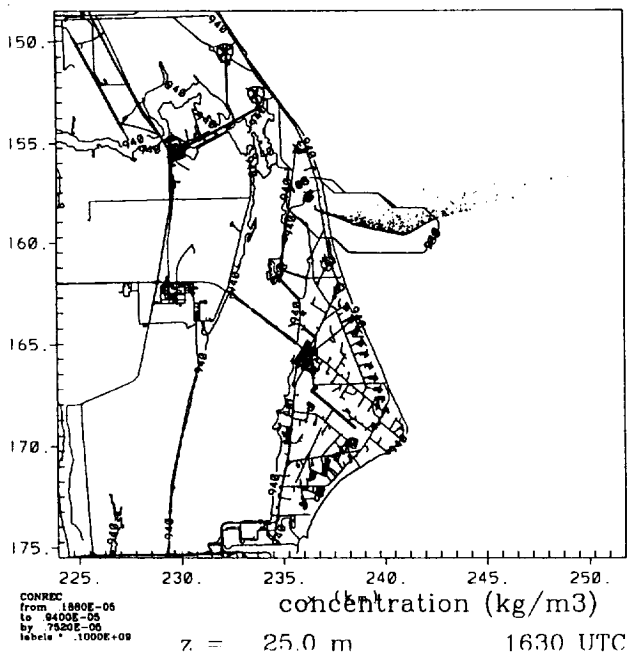

Figure 8-14. Cross-section (top) and map (bottom) of HYPACT plume computed using RAMS data for 13 April 1995 at 1630 UTC.

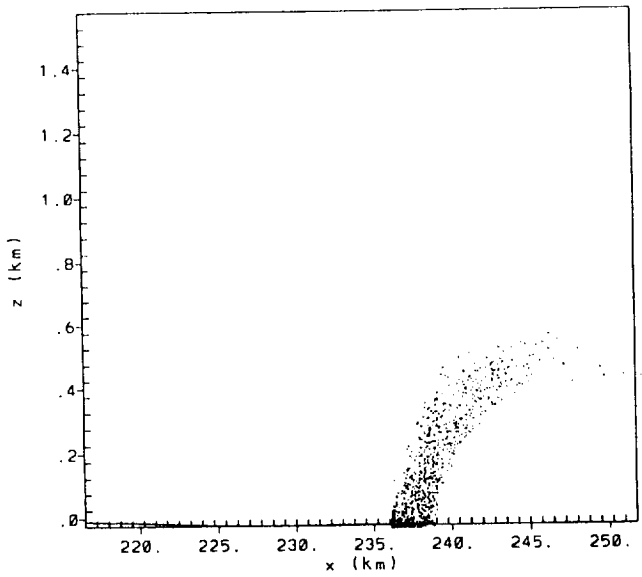

y =−190.47 km 1650 UTC

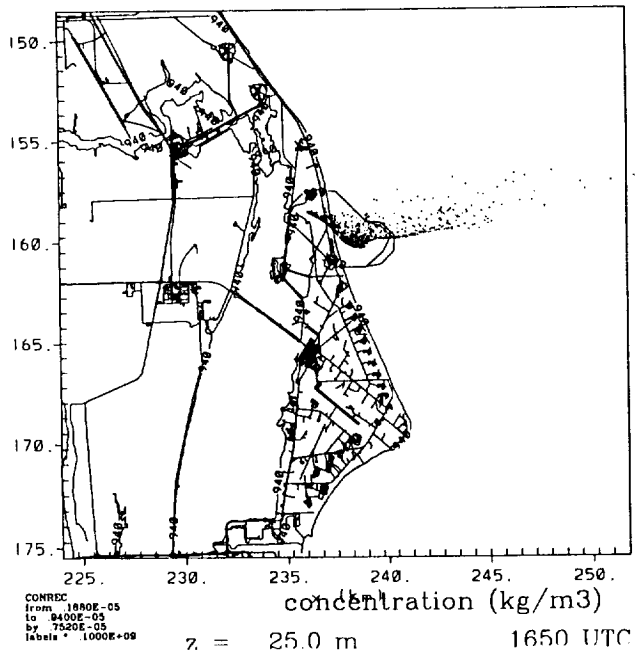

Figure 8-15. Cross-section (top) and map (bottom) of HYPACT plume computed using RAMS data for 13 April 1995 at 1650 UTC.

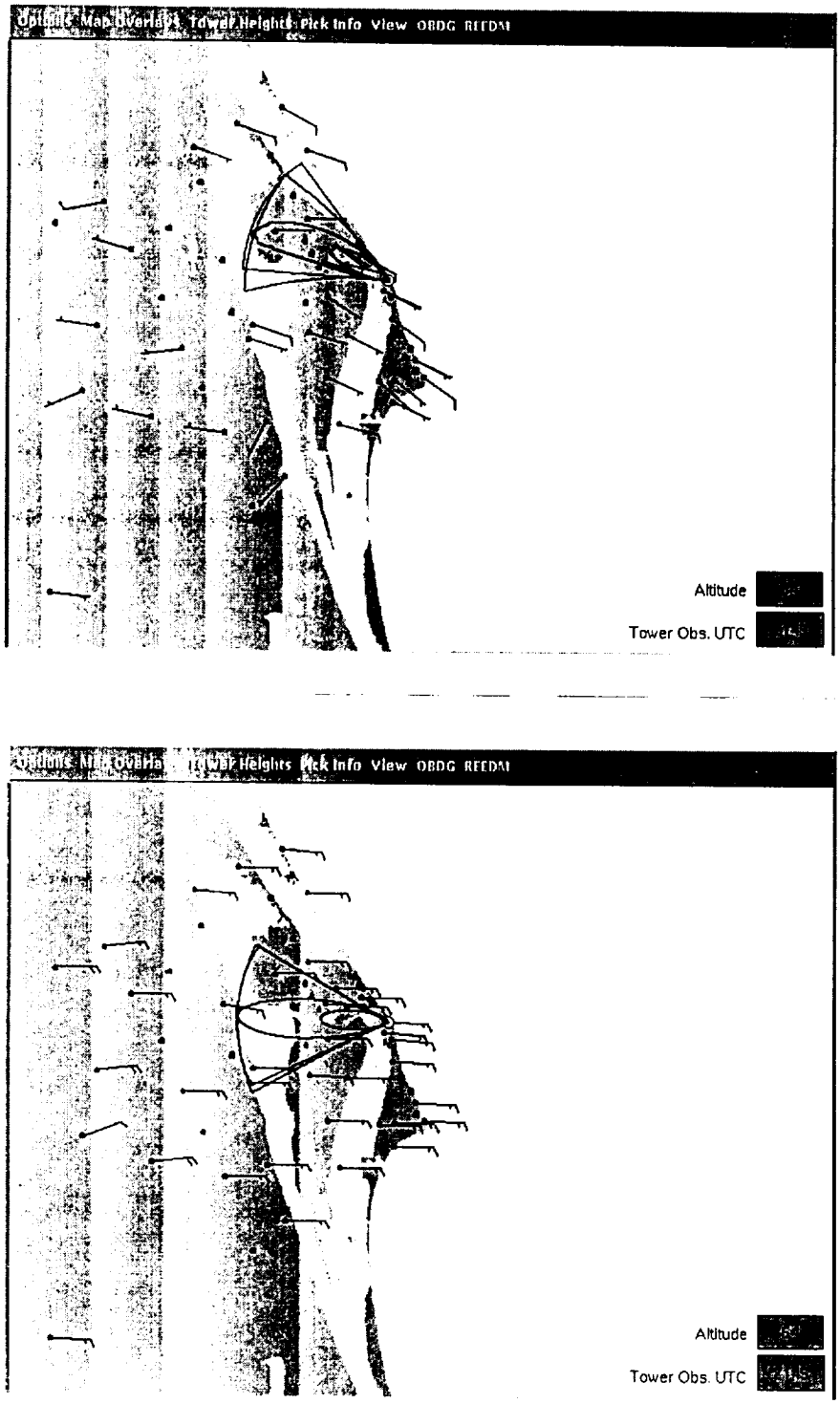

Figure 8-16. OBDG plumes computed using observed data (top) and RAMS wind speed and direction data (bottom) for 13 April 1995 at 2145 UTC. Sea breeze has moved inland producing easterly flow at Cape Canaveral for this time.

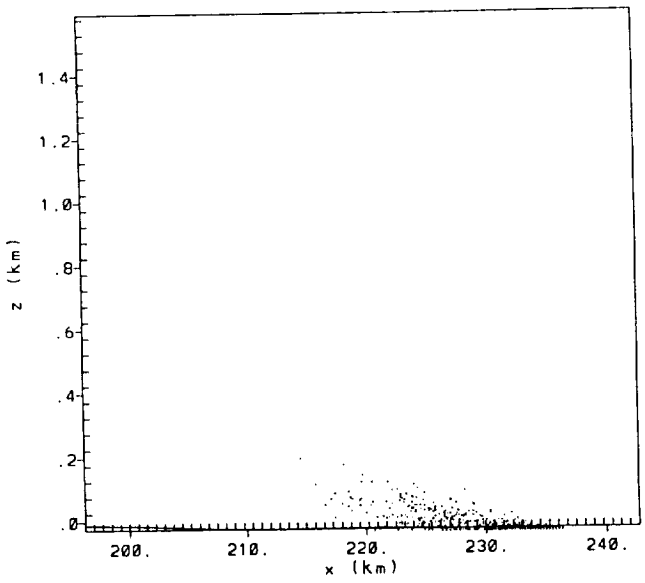

y =-190.47 km 2150 UTC

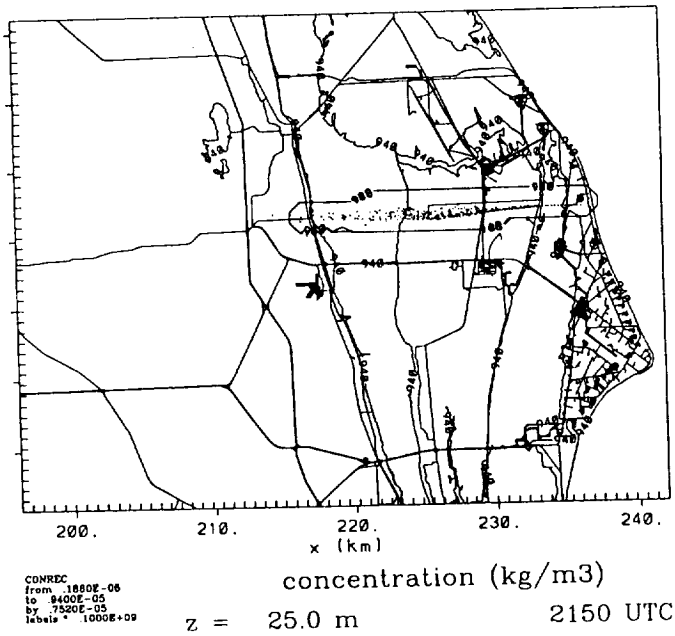

z = 25.0 m 2150 UTC

Figure 8-17. Cross-section (top) and map (bottom) of HYPACT plume computed using RAMS data for 13 April 1995 at 2150 UTC.

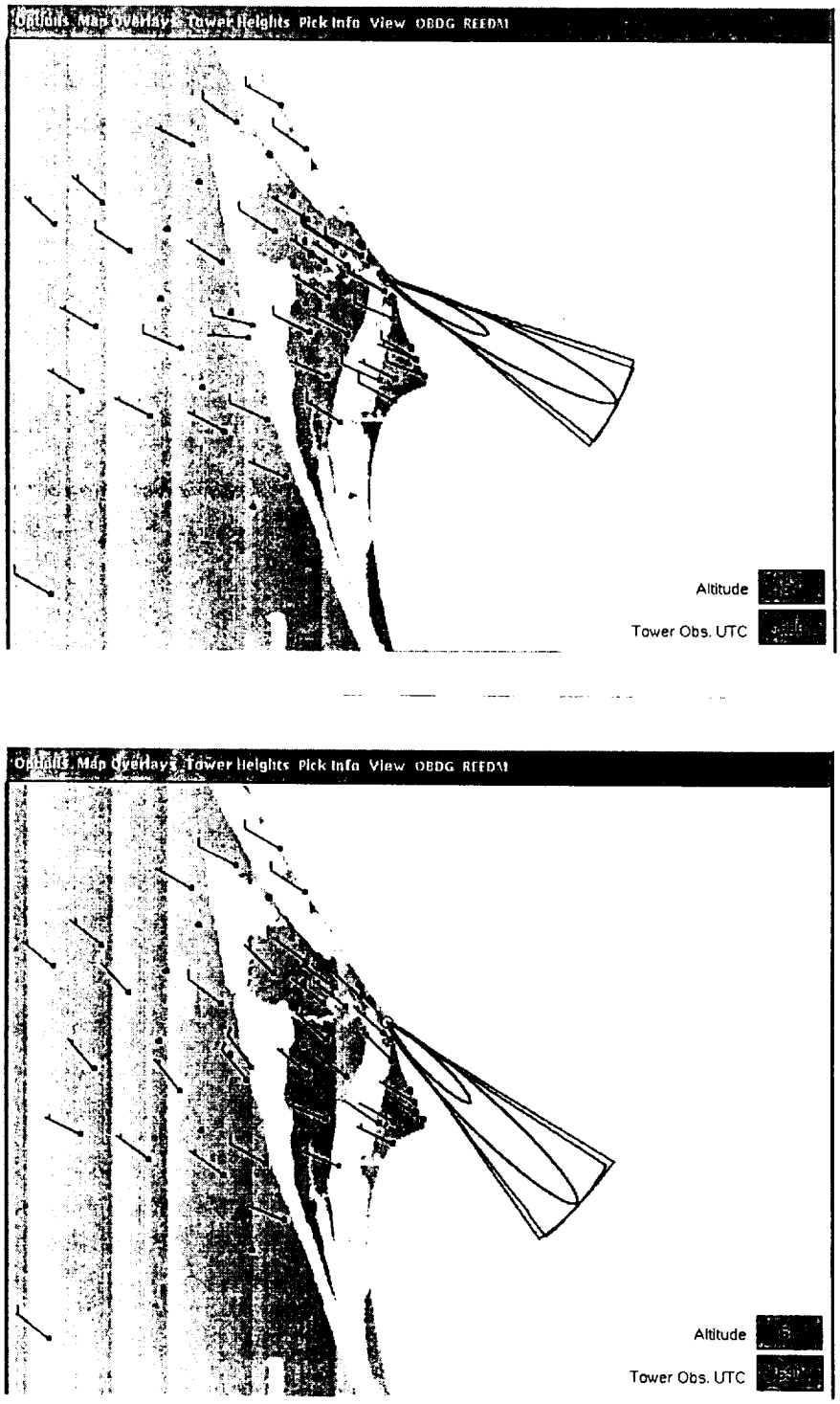

Figure 8-18. OBDG plumes computed using observed data (top) and RAMS wind speed and direction data (bottom) for 14 April 1995 at 0530 UTC. Winds returned to off-shore flow during nighttime.

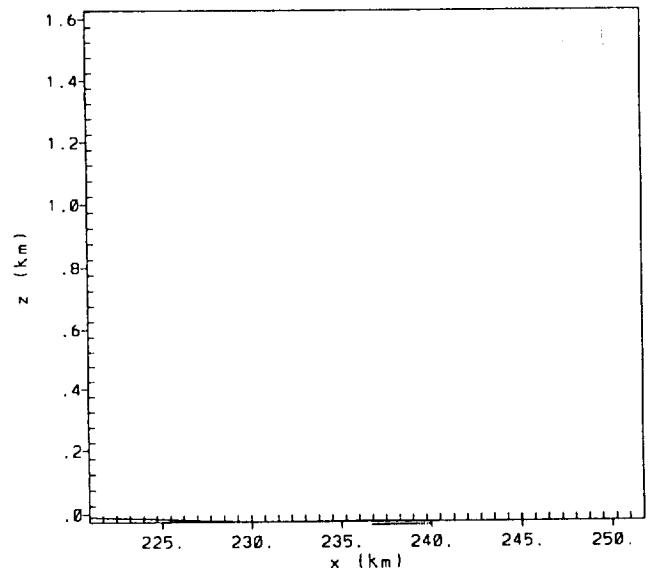

y =−190.47 km 0530 UTC

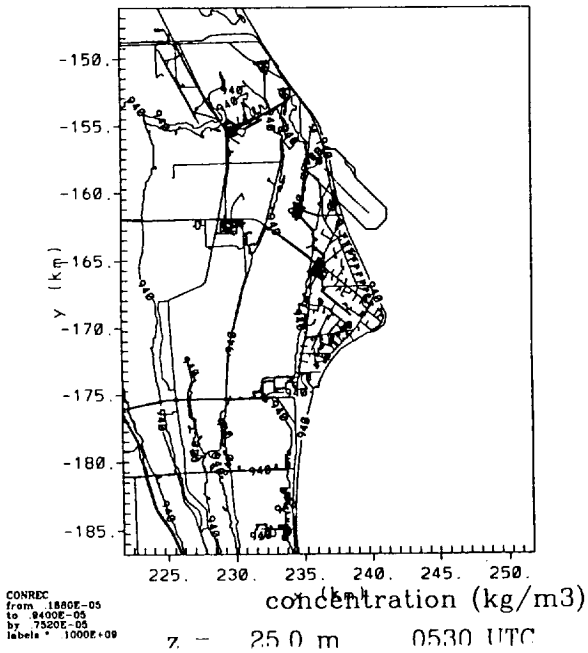

Figure 8-19. Cross-section (top) and map (bottom) of HYPACT plume computed using RAMS data for 14 April 1995 at 0530 UTC.

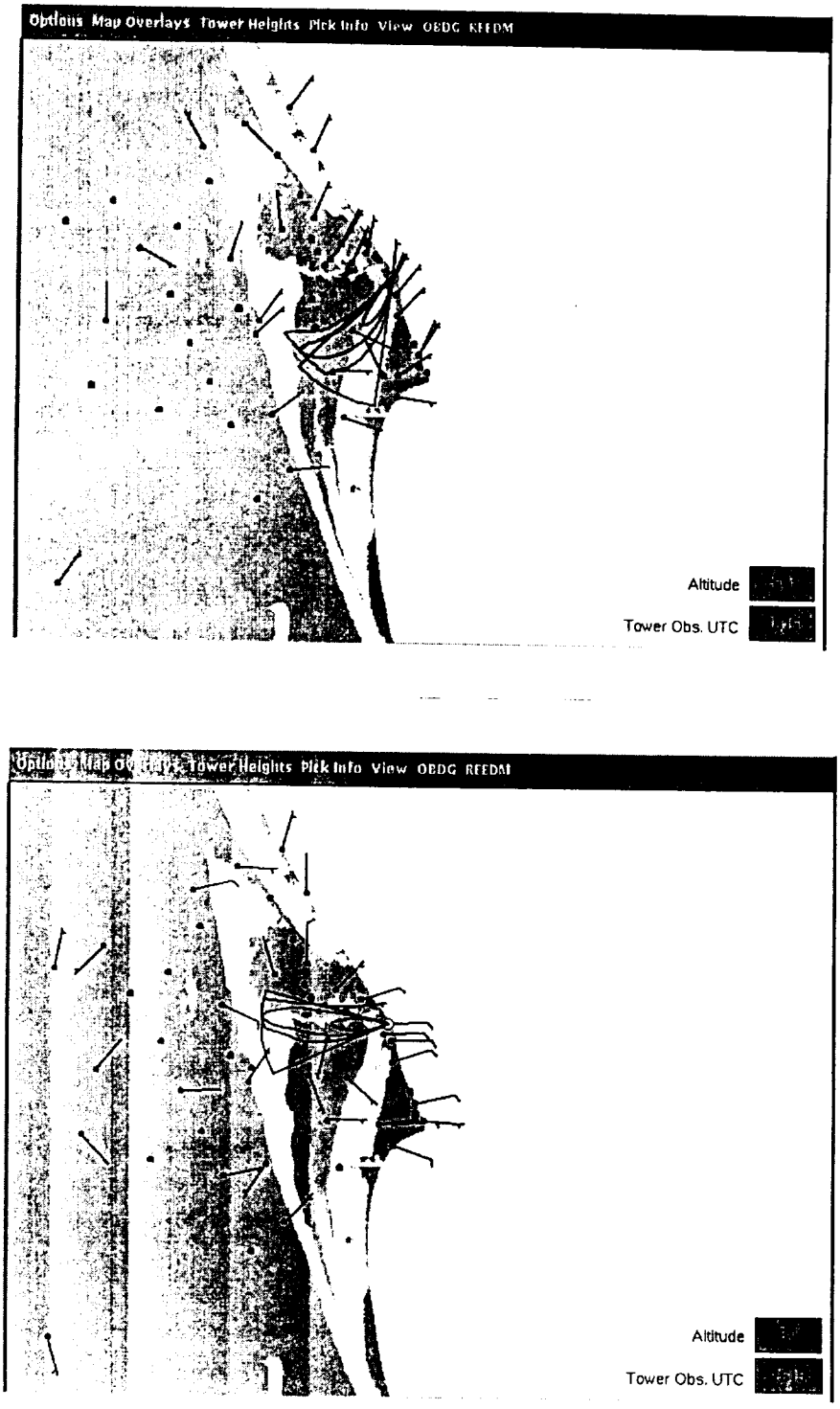

Figure 8-20. OBDG plumes computed using observed data (top) and RAMS wind speed and direction data (bottom) for 9 June 1995 at 1515 UTC.

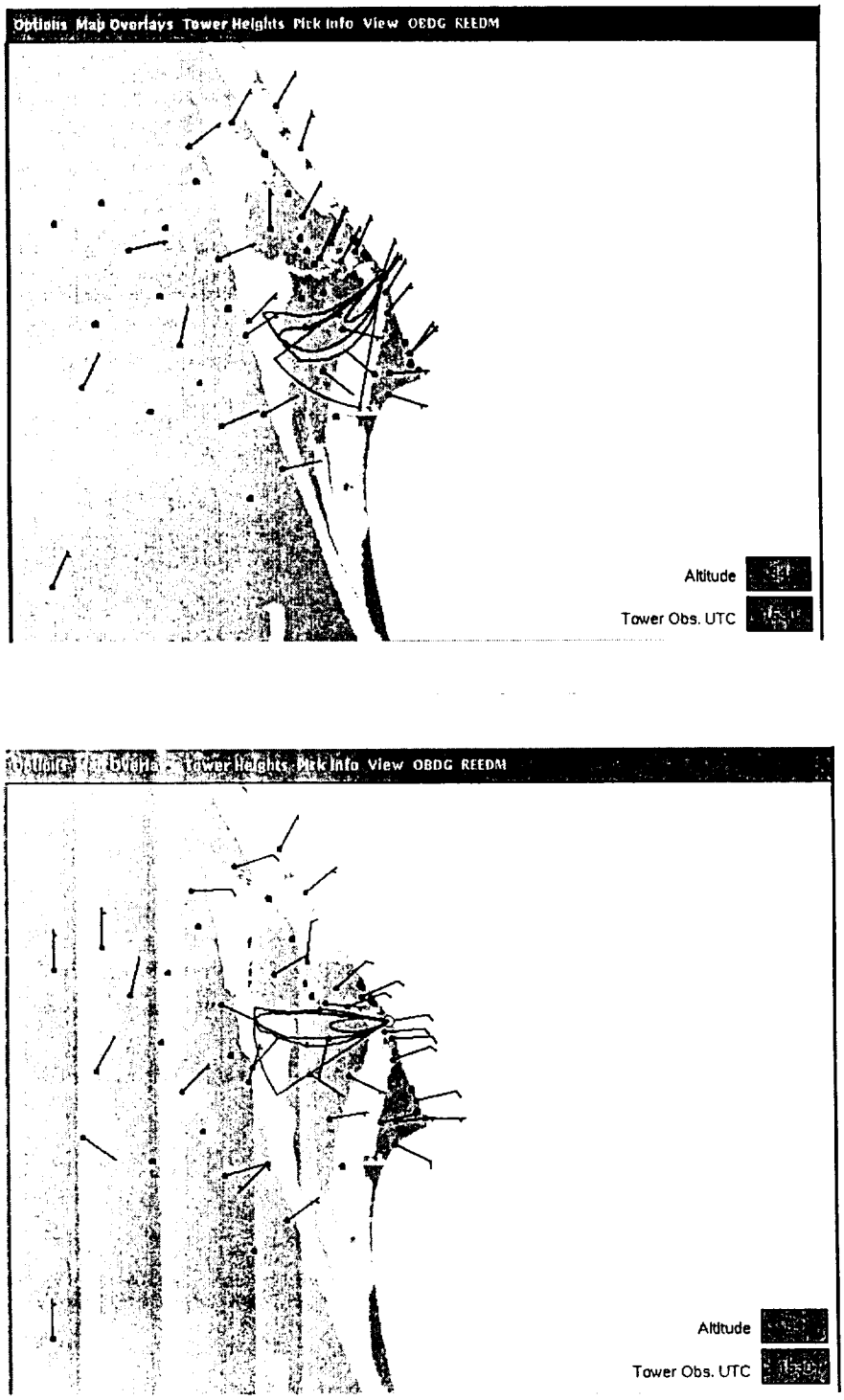

Figure 8-21. OBDG plumes computed using observed data (top) and RAMS wind speed and direction data (bottom) for 9 June 1995 at 1530 UTC.

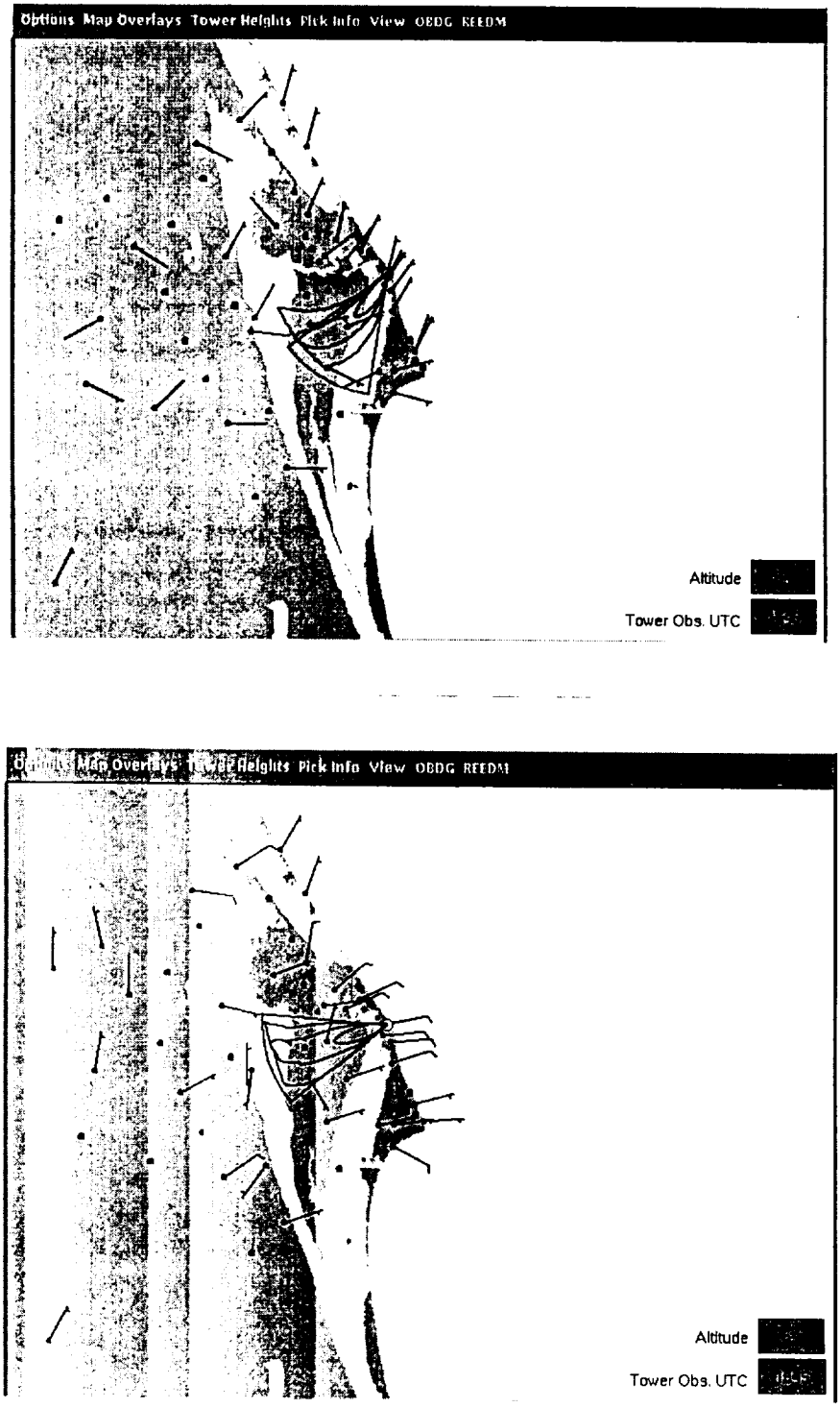

Figure 8-22. OBDG plumes computed using observed data (top) and RAMS wind speed and direction data (bottom) for 9 June 1995 at 1545 UTC.

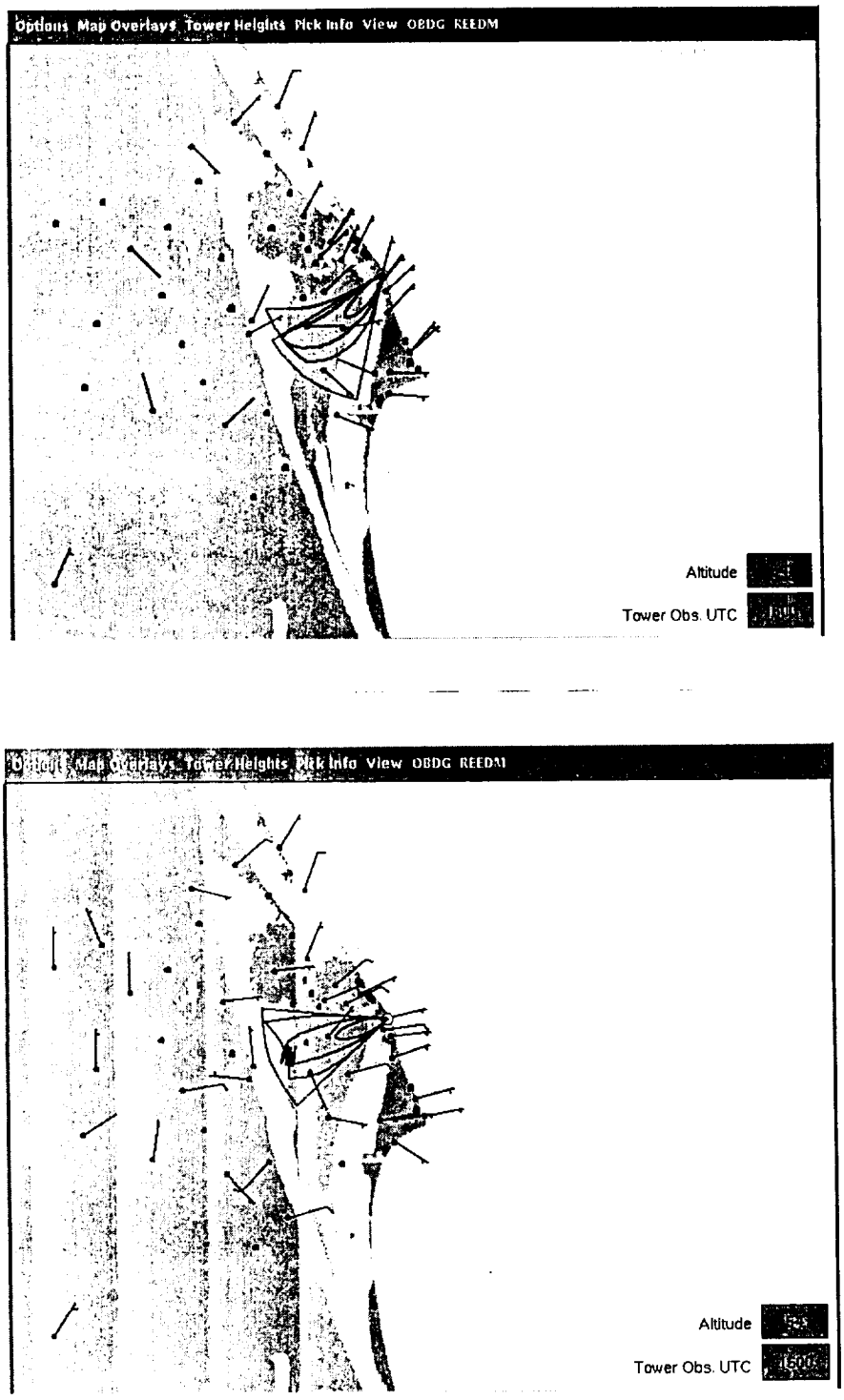

Figure 8-23. OBDG plumes computed using observed data (top) and RAMS wind speed and direction data (bottom) for 9 June 1995 at 1600 UTC.

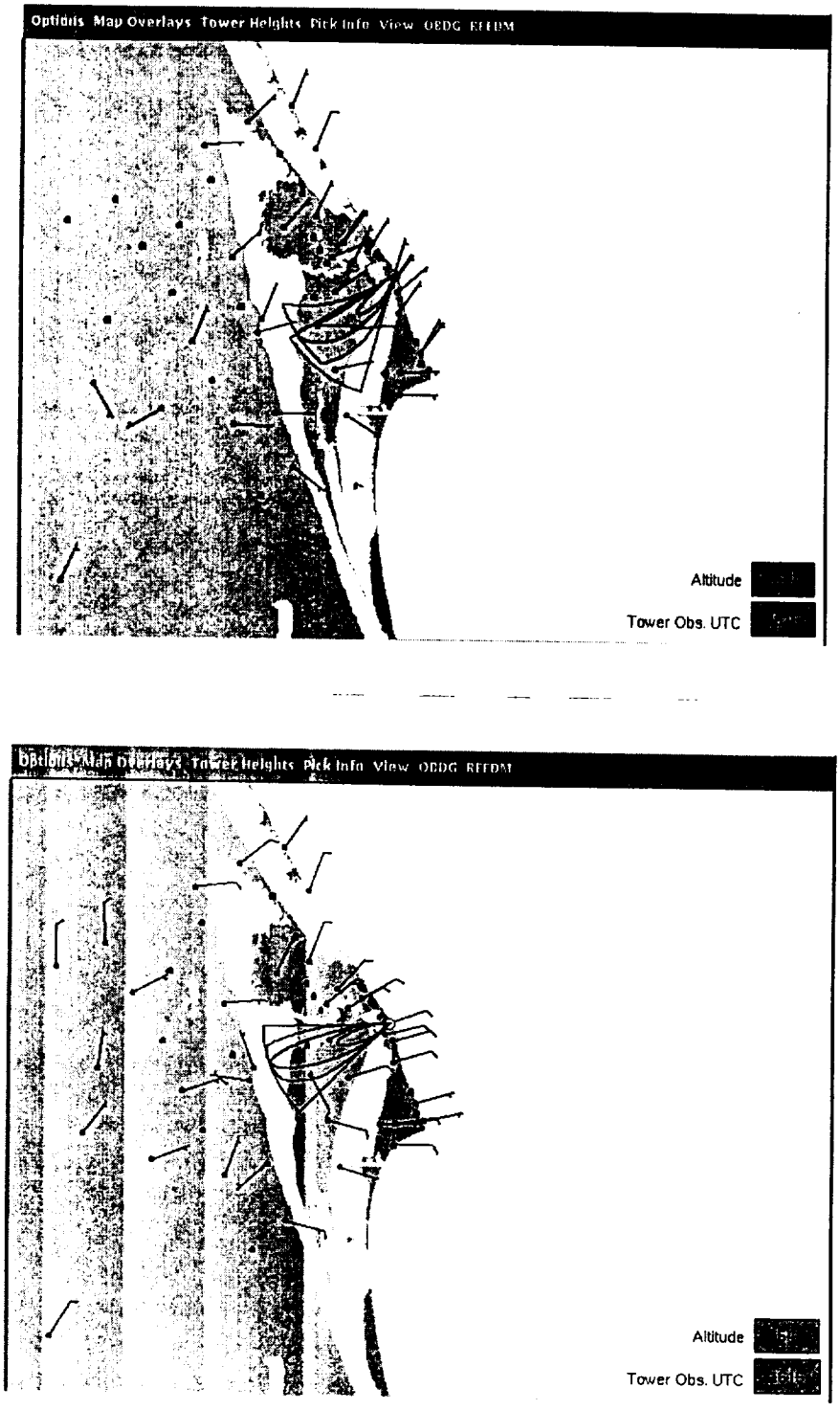

Figure 8-24. OBDG plumes computed using observed data (top) and RAMS wind speed and direction data (bottom) for 9 June 1995 at 1615 UTC.

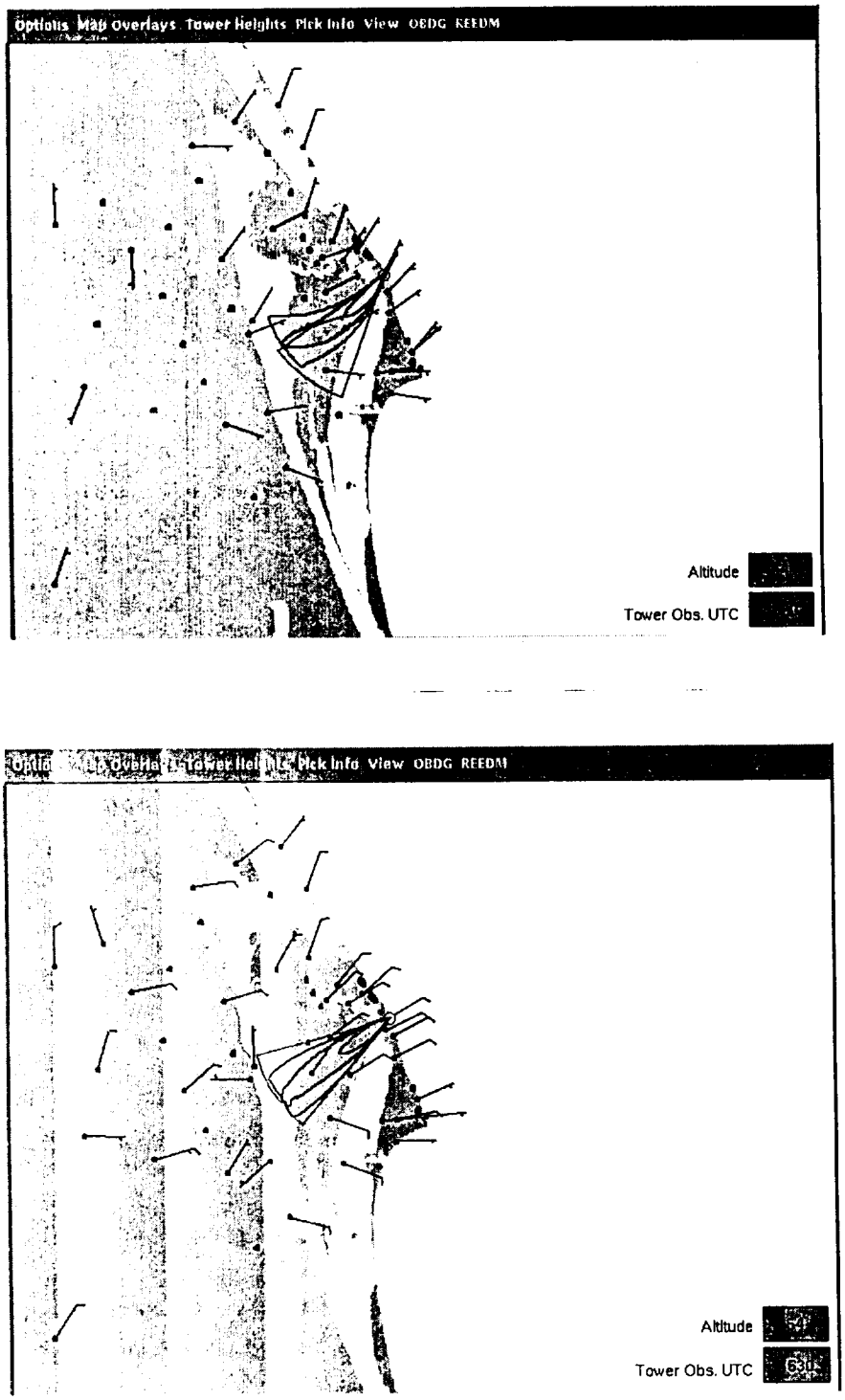

Figure 8-25. OBDG plumes computed using observed data (top) and RAMS wind speed and direction data (bottom) for 9 June 1995 at 1630 UTC.

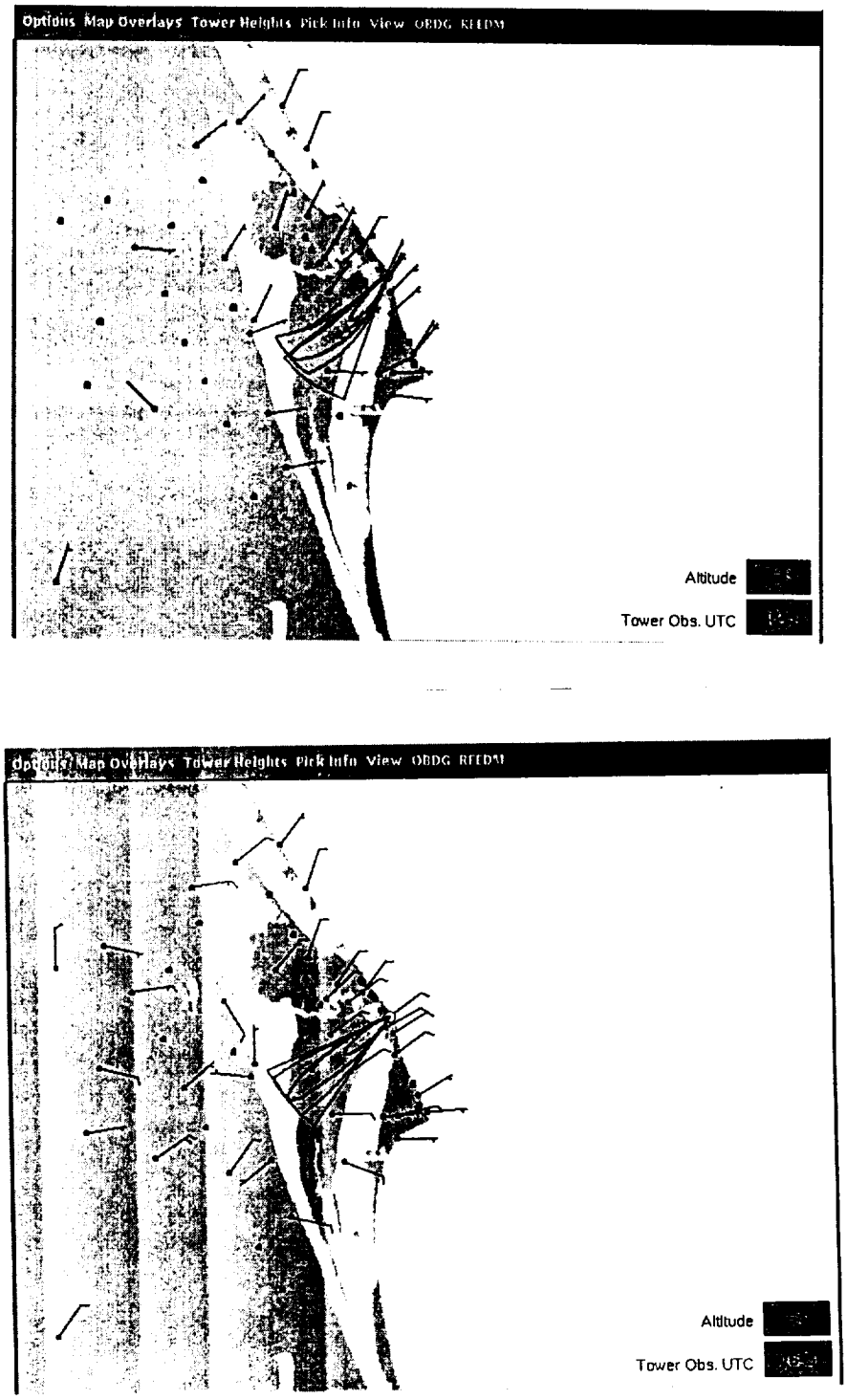

Figure 8-26. OBDG plumes computed using observed data (top) and RAMS wind speed and direction data (bottom) for 9 June 1995 at 1645 UTC.

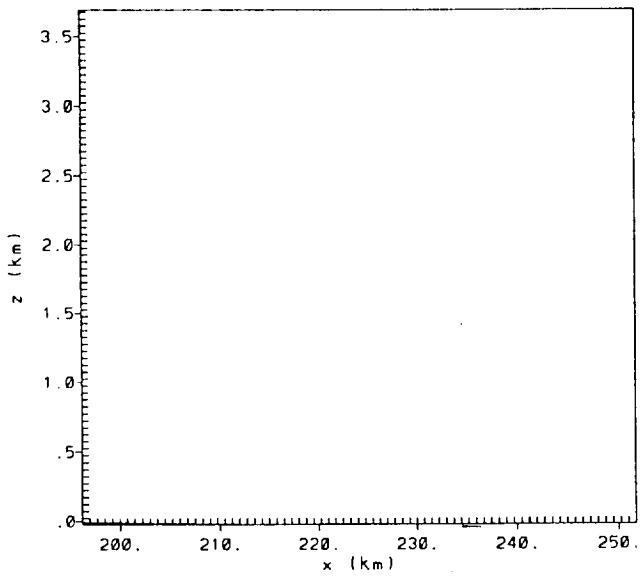

y =−190.47 km 1510 UTC

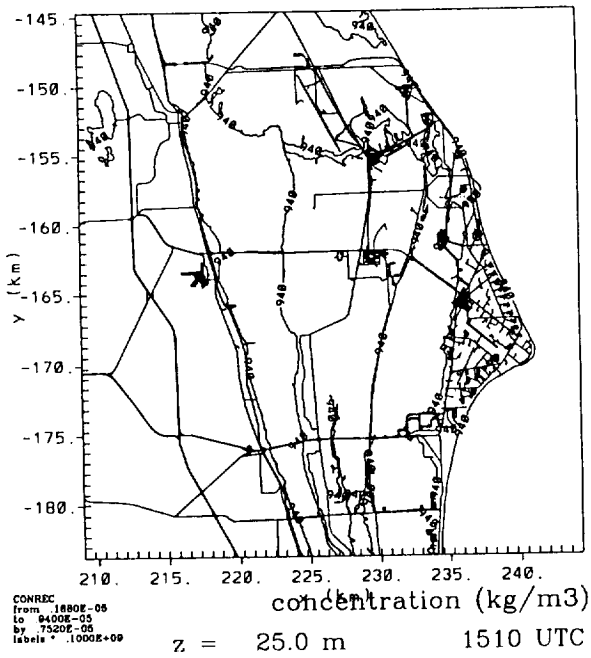

z = 25.0 m 1510 UTC

Figure 8-27. Cross-section (top) and map (bottom) of HYPACT plume computed using RAMS data for 9 June 1995 at 1510 UTC.

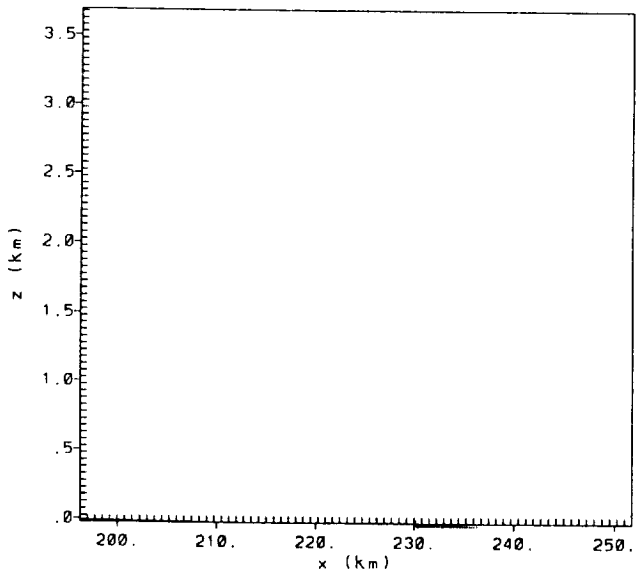

y =-190.47 km 1530 UTC

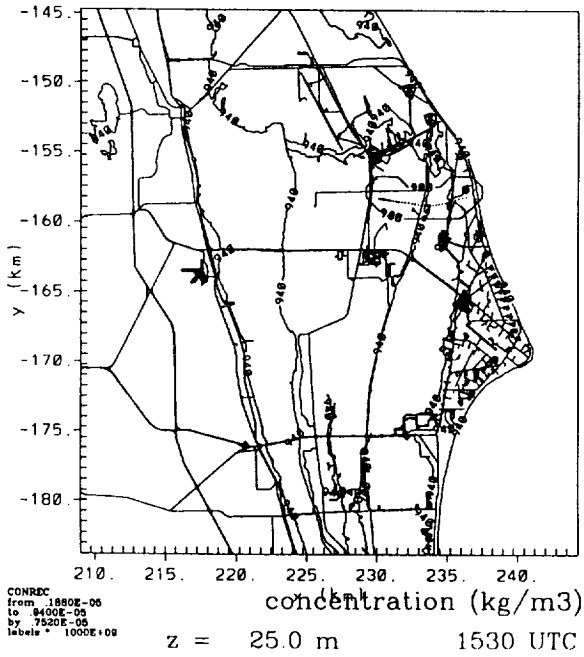

z = 25.0 m 1530 UTC

Figure 8-28. Cross-section (top) and map (bottom) of HYPACT plume computed using RAMS data for 9 June 1995 at 1530 UTC.

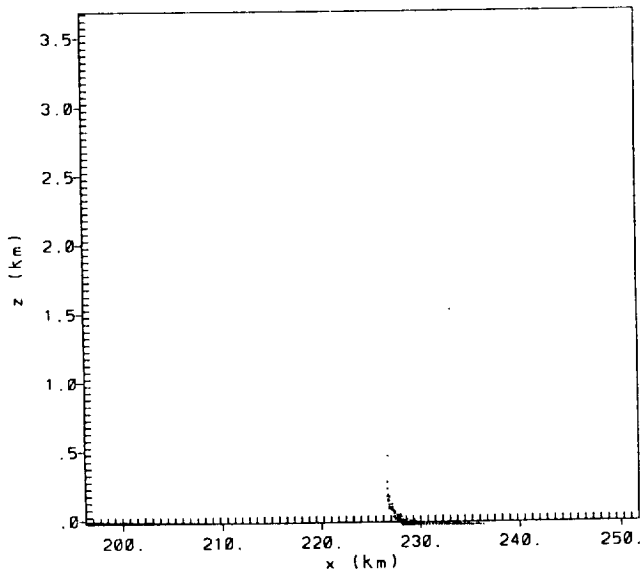

y =−190.47 km 1550 UTC

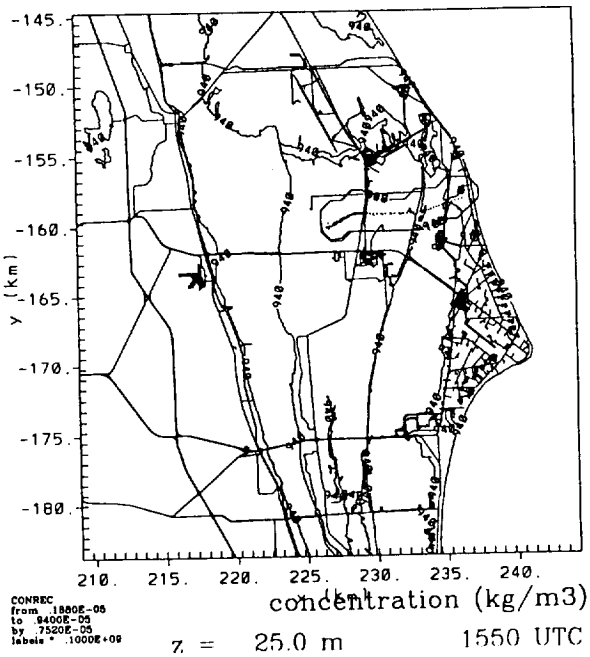

Figure 8-29. Cross-section (top) and map (bottom) of HYPACT plume computed using RAMS data for 9 June 1995 at 1550 UTC.

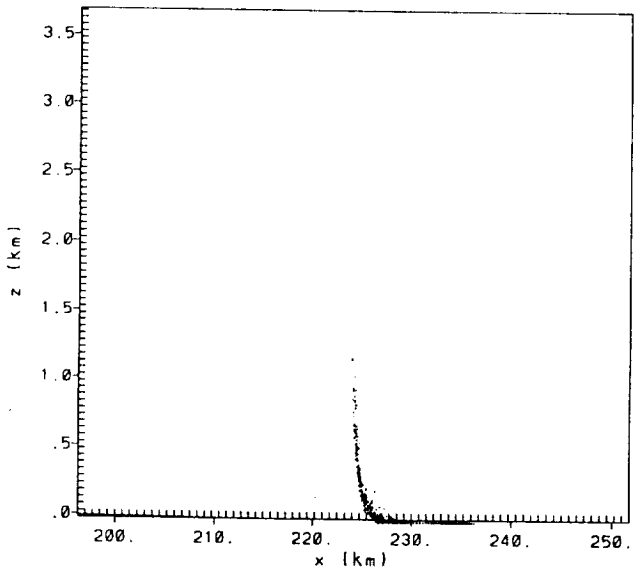

y =-190.47 km 1610 UTC

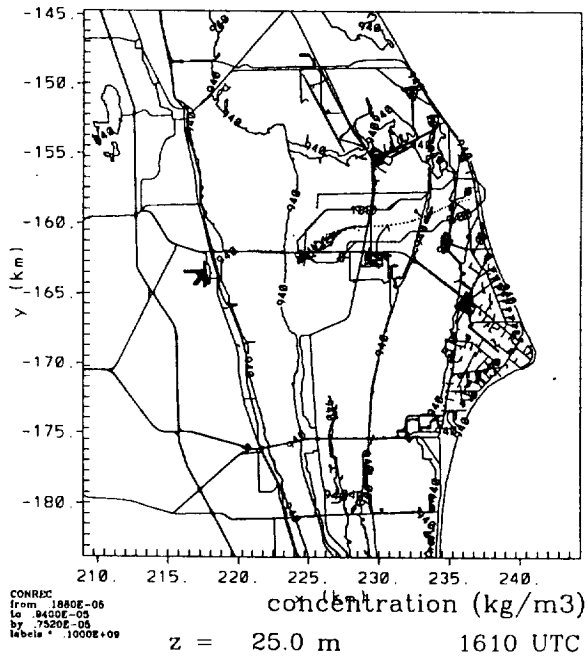

z = 25.0 m 1610 UTC

Figure 8-30. Cross-section (top) and map (bottom) of HYPACT plume computed using RAMS data for 9 June 1995 at 1610 UTC.

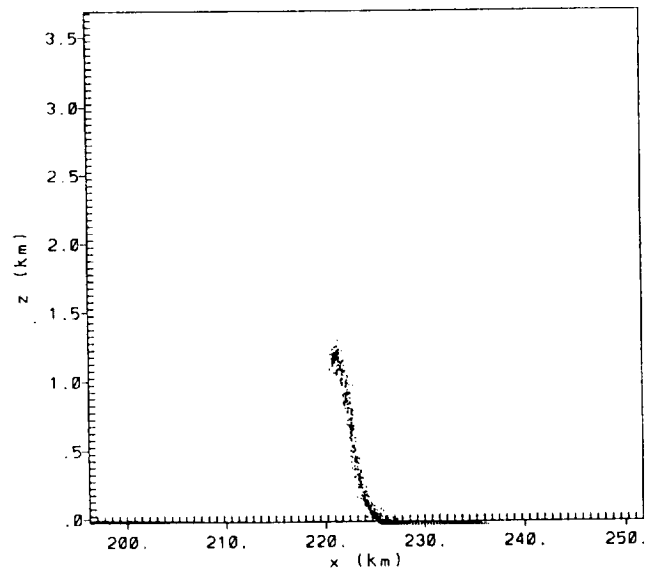

y = −190.47 km 1630 UTC

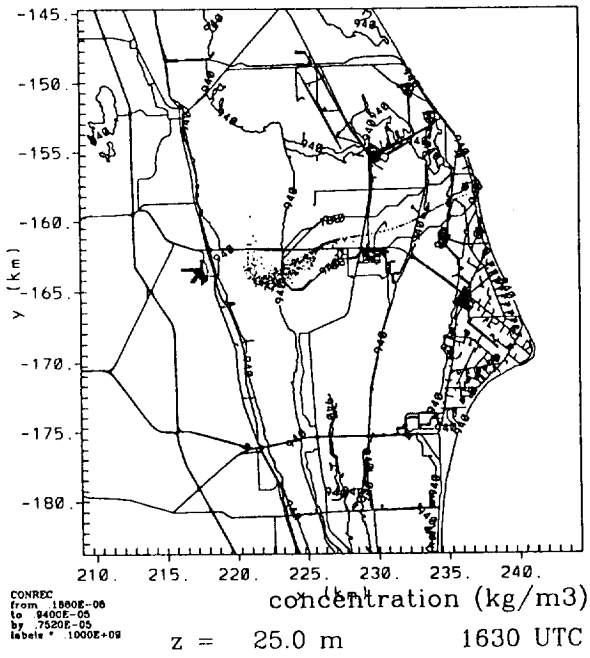

z = 25.0 m 1630 UTC

Figure 8-31. Cross-section (top) and map (bottom) of HYPACT plume computed using RAMS data for 9 June 1995 at 1630 UTC.

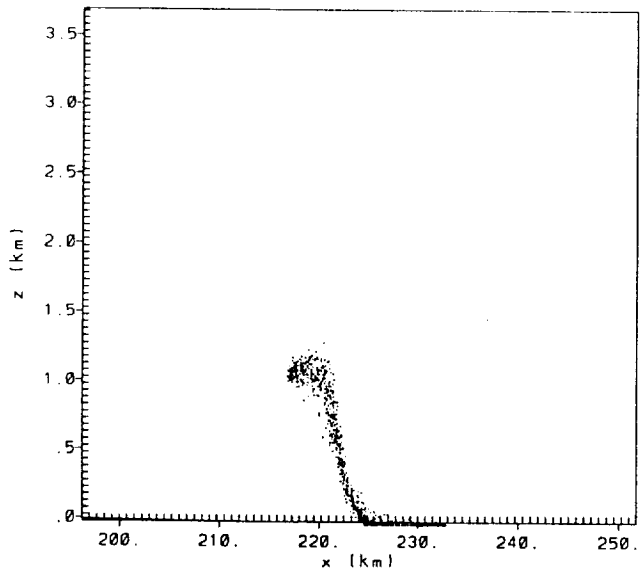

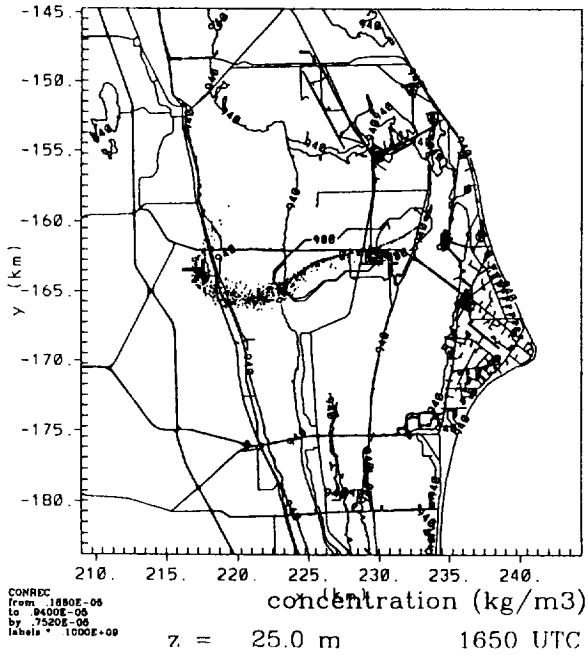

Figure 8-32. Cross-section (top) and map (bottom) of HYPACT plume computed using RAMS data for 9 June 1995 at 1650 UTC.

	OBDG-Obs	OBDG-RAMS		HYPACT-RAMS		
Time (UTC)	Plume direc-tion	Plume direc-tion	Sigma Level (m)	Time (UTC)	Plume direc-tion	Maxi-mum plume height (m)
1500	SE	SE	11			
1515	SE	SE	11	1510	SE	0
1530	SE	SE	11	1530		0
1545	SE	SE	11	1550		100
1600	SE	SE	11			
1615	SE	SE	11	1610		150
1630	SE	SE	11	1630		150
1645	SE	SE	11	1650		200
1700	ESE	SE	11			
2100	E	S	11			
2115	E	S	34	2110	S	0
2130	E	S-SSE	60	2130		100
2145	E	SSE	142	2150		200
2200	ESE	SSE	320			
2215	E	ESE	668	2210	E	400
2230	E	ESE	782	2230		400
2245	E	E	910	2250		500
2300	E	E	910			
0500	ESE	ESE	11			
0515	E	ESE	11	0510	ESE	0
0530	E	ESE	11	0530		50
0545	E	ESE	11	0550		50
0600	E	ESE	11			
0615	E	ESE	11	0610		50
0630	ESE	ESE	11	0630		50
0645	E	ESE	11	1650		100
0700	E	ESE	11			

31 Jan 95

OBDG-Obs. Consistent NW winds.

OBDG-RAMS. Consistent NW flow matches obs.
HYPACT. Stable flow as the plume pushes offshore.

The three models are similar with stable conditions and persistent wind flow.

No change in launch availability.

OBDG-Obs. Fairly persistent W'ly offshore flow.
OBDG-RAMS. RAMS uses N'ly lower winds while upper winds late in period agree w/ W obs winds.
HYPACT. Plume moved south initially then east over water.
Model differs from observations because of wind direction difference in first hour. OBDG-RAMS and HYPACT predicted plume to south producing less launch availability. However, model shows the area of concern to the south.

OBDG-Obs. Persistent W'ly offshore flow.
OBDG-RAMS. Persistent WNW flow.
HYPACT. Persistent offshore flow

No difference between all models with stable , persistent flow. No change in launch availability.

Table 8-7. Comparison summary of three different model runs for January 31-February 1.

	OBDG-Obs	OBDG-RAMS		HYPACT-RAMS		
Time (UTC)	Plume direc-tion	Plume direc-tion	Sigma Level (m)	Time (UTC)	Plume direc-tion	Maxi-mum plume height (m)
1500	SE	ESE	11			
1515	SE	SE	11	1510	SE &	0
1530	SE	SE	11	1530	SSE	100
1545	SSE	SE	11	1550	.	200
1600	SSE	SE	11		.	
1615	SSE	SE	11	1610	.	200
1630	SSE	SE	11	1630	.	200
1645	SSE	SSE	11	1650	.	200
1700	SSE	SSE	11			

6 Feb 95

OBDG-Obs, plume stays SSE-SE, centerlining the coastline.
OBDG-RAMS. RAMS produces light NW winds,shifting NNW.
HYPACT. plume over water, stable conditions.
All models agree fairly well . No change in launch availability.

2100	S	SW	11			
2115	S	SW	11	2110	SW	0
2130	S	SW	34	2130	S	50
2145	S	SW	34	2150	.	200
2200	S	SW	60		.	
2215	S	SW	94	2210	.	400
2230	S	SW	142	2230	.	500
2245	S-SSW	SW	196	2250	.	600
2300	SSW	SSW	320			

OBDG-Obs. Sea breeze pushed inland ~9 km and stopped. Flow from N and NE pushed plume S and slightly W.
OBDG-RAMS. RAMS moved sea breeze a little more than observed.
HYPACT. With sea breeze, plume moved SW then S. Lift to 600 over land not too strong with minimum Feb. heating.
All models agree relatively well. RAMS models show plume further west with stronger sea breeze.
No change in launch availability.

0500	ENE	NE	11			
0515	ENE	NE	11	0510	NE	0
0530	ENE	NE	11	0530	.	0
0545	E	NE	11	0550	.	0
0600	E	NE	11		.	
0615	E	NE	11	0610	.	50
0630	ESE	NE	11	0630	.	50
0645	ESE	NE	11	1650	.	100
0700	ESE	NE	11			

OBDG-Obs. OBDG-RAMS. Persistent , light winds, stable flow plume offshore.
OBDG-Obs. Persistent light winds, w/ stable conditions moves plume offshore.
HYPACT. Plume to NE.

RAMS predicted SW winds when WSW, W, and WNW observed. However, plume offshore and no change in launch availability.

Table 8-8. Comparison summary of three different model runs for February 6-7.

	OBDG-Obs	OBDG-RAMS		HYPACT-RAMS		
Time (UTC)	Plume direc-tion	Plume direc-tion	Sigma Level (m)	Time (UTC)	Plume direc-tion	Maxi-mum plume height (m)
1500	W	SSW	11			
1515	W	SW	34	1510	SW	0
1530	W	SW	60	1530		50
1545	W	SW	196	1550	.	200
1600	W	W	474		.	
1615	W	W	782	1610	W	800
1630	W	W	910	1630	WSW	900
1645	W		910	1650	.	1000
1700	W	W	910			

26 Mar 95

OBDG-Obs. Plume extends 30 km then down to 7 km with easterly flow.
OBDG-RAMS. Low-level winds from NE. Upper-level winds from E.
HYPACT. plume moved SW w/ low level flow. Strong uplift at 1610 UTC as plume lifted. Plume extend 15 km downwind to W and WSW.
OBDG-Obs at 1500 UTC extends too far. HYPACT would increase launch availability. At 1630, plume to W, launch availability decreased. However, HYPACT shows vertical extent of plume.

2100	W	WNW	11			
2115	W	WNW	11	2110	WNW	0
2130	W	WNW	34	2130		100
2145	W	WNW	34	2150	.	150
2200	WNW	WNW	60		.	
2215	WNW	WNW	60	2210	.	200
2230	WNW	WNW	94	2230	.	300
2245	WNW	WNW	94	2250	.	300
2300	NW	WNW	142			

OBDG-Obs. Persistent E flow w/reinforced sea breeze pushed plume11 km inland.

OBDG-RAMS. Good match of observed with ESE flow.
HYPACT. Plume exends 40 km to WNW.
RAMS and observed show good agreement. HYPACT plume extends much further inland.

0500						
0515				0510		
0530				0530	.	
0545				0550	.	
0600					.	
0615				0610	.	
0630				0630	.	
0645				1650	.	
0700						

No obs data.

Table 8-9. Comparison summary of three different model runs for March 26-27.

	OBDG-Obs	OBDG-RAMS		HYPACT-RAMS		
Time (UTC)	Plume direc-tion	Plume direc-tion	Sigma Level (m)	Time (UTC)	Plume direc-tion	Maxi-mum plume height (m)
1500	ENE	ENE	11			
1515	ENE	ENE	34	1510	E	0
1530	ENE	ENE	60	1530	.	50
1545	ENE	ENE	142	1550	.	100
1600	ENE	ENE	320		.	
1615	ENE	ENE	566	1610	.	300
1630	ENE	ENE	910	1630	.	400
1645	ENE	ENE	1053	1650	.	600
1700	ENE	ENE	1053			

13 Apr 95

OBDG-Obs. The WSW fow was persistent as sea breeze had not formed yet.
RAMS. RAMS matched observed winds with strong W upper level winds.
HYPACT. Plume moved E w/ W flow. However, the beginning of the sea breez was just offshore and plume went up there and stopped moving east.
Hypact picked up beginning of sea breeze which would start soon after 1700 UTC. Good sea breeze prediction.
No change in launch availability since plume was offshore.

2100	WNW	WSW	11			
2115	WNW	WSW	11	2110	W	0
2130	WNW	W	11	2130		50
2145	WNW	W	34	2150	.	200
2200	WNW	W	34		.	
2215	NW	W	34	2210	.	200
2230	NW	W	60	2230	.	200
2245	NW	W	60	2250	.	200
2300	NW	WNW	94			

OBDG-Obs. Sea breeze in w/ESE winds shifting to SE.

OBDG-RAMS. Sea breeze in w/ E winds stronger than observed.
HYPACT. With sea breeze in, conditions are somewhat stable. Plume travels over 30 km west and rises a little.
Launch availability is about the same with sea breeze already established. Model adds value during sea breeze onset.

0500	ESE	SE	11			
0515	ESE	SE	11	0510	SE	0
0530	ESE	SE	11	0530	.	0
0545	ESE	SE	11	0550	.	0
0600	ESE	SE	11		.	
0615	ESE	SE	11	0610	.	50
0630	SE	SE	11	0630	.	100
0645	SE	SE	11	1650	.	200
0700	SE	-	11			

OBDG-Obs. WNW flow with stable persistent condition pushed plume offshore.
OBDG-RAMS. Similar to obs with winds shifted slightly more NW'ly.
HYPACT. Plume offshore in stable conditions.
No change in launch availability with offshore flow.

Table 8-10. Comparison summary of three different model runs for April 13-14.

	OBDG-Obs	OBDG-RAMS		HYPACT-RAMS		
Time (UTC)	Plume direc-tion	Plume direc-tion	Sigma Level (m)	Time (UTC)	Plume direc-tion	Maxi-mum plume height (m)
1500	WSW	WSW	11			
1515	WSW	SW	11	1510	SW	0
1530	WSW	SW	11	1530	W	0
1545	SW	SW	34	1550	.	0
1600	SW	SW	34		.	
1615	SW	SW	34	1610	.	50
1630	SW	SW	60	1630	.	100
1645	SW	SW	60	1650	.	150
1700	SW	SW	94			

7 May 95

OBDG-Obs. NE flow pushced plume SW/ Persistent E flow; no sea breeze this day.
RAMS. Close match to obs , with consistent NE winds.
HYPACT. Plume distance nearly same as OBDG.

No change in launch availability with stable conditions.

2100	WSW	WSW	11			
2115	WSW	WSW	34	2110	W	0
2130	WSW	WSW	60	2130	.	50
2145	WSW	WSW	60	2150	.	200
2200	WSW	WSW	60		.	
2215	WSW	W	60	2210	.	300
2230	WSW	W	94	2230	.	300
2245	WSW	W	94	2250	.	300
2300	WSW	W	94			

OBDG-Obs. Persistent ENE flow.

OBDG-RAMS. Very strong (>25 kts) E winds by end of period.
HYPACT. Strong E winds, stable conditions, plume stays narrow and stretches to W 40 km.
Launch availability is unchanged with stable conditions.

0500	W	NW	11			
0515	W	NW	11	0510	NW	0
0530	W	NW	34	0530	.	0
0545	W	NW	34	0550	.	100
0600	W	NW	34		.	
0615	W	NW	34	0610	.	100
0630	W	NW	34	0630	.	100
0645	WSW	NW	60	1650	.	100
0700	WSW	NW	60			

OBDG-Obs. Persistent E flow. Very long wide plume extends ~40 km.
OBDG-RAMS. SE flow instead of E as observed.
HYPACT. Long narrow plume to NW with stable conditions .

No change in launch availability.

Table 8-11. Comparison summary of three different model runs for May 7-8.

	OBDG-Obs	OBDG-RAMS		HYPACT-RAMS		
Time (UTC)	Plume direc-tion	Plume direc-tion	Sigma Level (m)	Time (UTC)	Plume direc-tion	Maxi-mum plume height (m)
1500	WNW	SW	11			
1515	NW	SW	11	1510	SW	0
1530	NW	SW	34	1530	W	0
1545	NW	SW	34	1550	.	300
1600	WNW	SW	60		.	
1615	WNW	WSW	94	1610	.	600
1630	WNW	W	142	1630	.	700
1645	WNW	WSW	94	1650	.	900
1700	WNW	WSW	94			

29 May 95

OBDG-Obs. Sea breeze in early this day. SE flow prevailed.
RAMS. RAMS had sea breeze in to Indian R. w/ NE flow. By 1615 UTC all winds E'ly. Approx. 45° difference with obs.
HYPACTPlume moved SW and W, hit sea breeze front , lifted to 600 at 1610 UTC then to 900 m at 1650 UTC.

Hypact plume extends further than OBDg plumes but HYPACT plume is narrower. No change in launch availability.

2100	WNW	W	11			
2115	WNW	W	34	2110	W	0
2130	WNW	W	34	2130	.	50
2145	WNW	WNW	34	2150	.	100
2200	WNW	WNW	60		.	
2215	WNW	WNW	60	2210	.	150
2230	NW	WNW	94	2230	.	200
2245	WNW	WNW	94	2250	.	200
2300	WNW	WNW	142			

OBDG-Obs. Persistent ESE flow.

OBDG-RAMS. Strong, persistent (~20 kts) E and ESE winds. Good agreement with obs
HYPACT. Stable conditions , persistent winds. Narrow plume.

Launch availability is unchanged. RAMS forecasts good.

0500	NNW	NW	11			
0515	NNW	NW	11	0510	NW	0
0530	NNW	NW	34	0530	.	50
0545	NNW	NNW	34	0550	.	100
0600	NNW	NNW	34		.	
0615	NNW	NNW	34	0610	.	200
0630	NNW	N-NNW	34	0630	.	200
0645	NNW	N-NNW	34	1650	.	200
0700	N	-	34			

OBDG-Obs. Persistent stable flow from SSE flow.
OBDG-RAMS. RAMS winds are good match with obs.
HYPACT. All plumes very similar.

No change in launch availability.

Table 8-12. Comparison summary of three different model runs for May 29-30.

	OBDG-Obs	OBDG-RAMS		HYPACT-RAMS		
Time (UTC)	Plume direc-tion	Plume direc-tion	Sigma Level (m)	Time (UTC)	Plume direc-tion	Maxi-mum plume height (m)
1500	SSW	W	11			
1515	SW	W	11	1510	W	0
1530	SW	W	11	1530	SW	0
1545	SW	WSW	11	1550	.	500
1600	SW	WSW	11		.	
1615	SW	WSW	34	1610	.	1100
1630	SW	SW	34	1630	.	1300
1645	SW	SW	34	1650	.	1300
1700	SW		60			

9 Jun 95

OBDG-Obs. NE flow fairly persistent thru period

RAMS. RAMS had persistent E & NE flow over area. There is a hint that sea breeze extends to west of Indian R.

HYPACTPlume moved W and then SW, hit sea breeze front at Indian R, lifted to 1200 m at 1630 UTC.

Good model agreement. OBDG models do not detect sea breeze and significant lifting Plume extent is the same and there is no change in launch availability. However, lifting information is missing from OBDG runs.

2100	WSW	WSW	11			
2115	WSW	WSW	34	2110	WSW	0
2130	WSW	WSW	34	2130	.	100
2145	WSW	WSW	60	2150	.	200
2200	WSW	WSW	94		.	
2215	W	WSW	94	2210	.	300
2230	WSW	WSW	142	2230	.	400
2245	WSW	WSW	142	2250	.	400
2300	WSW	W	196			

OBDG-Obs. Persistent ENE flow.

OBDG-RAMS. Strong, E flow. Good agreement with obs

HYPACT. Narrow plume to WSW extending 40 km.

Launch availability is unchanged. All models agree.

0500	N	NNE	11			
0515	NNE	NNE	11	0510	NNE	0
0530	NNE	NNE	11	0530	.	0
0545	NE	NNE	11	0550	.	0
0600	ENE	NNE	11		.	
0615	ENE	NNE	11	0610	.	50
0630	ENE-NE	NE	11	0630	.	100
0645		NE	11	1650	.	100
0700	ENE	-	11			

OBDG-Obs. Wind shifted from S to SW during period with light offshore flow.

OBDG-RAMS. RAMS showed shift from SSW to SW flow and closely matched obs .

HYPACT. Stable flow offshore from SSW.

All model agree. No change in launch availability.

Table 8-13. Comparison summary of three different model runs for June 9-10.

	OBDG-Obs	OBDG-RAMS		HYPACT-RAMS		
Time (UTC)	Plume direc-tion	Plume direc-tion	Sigma Level (m)	Time (UTC)	Plume direc-tion	Maxi-mum plume height (m)
1500	SSE	SW	11			
1515	SSE	SW	34	1510	SW	0
1530	S	SW	34	1530	.	0
1545	S	SW	34	1550	.	250
1600	SSE	SW	34		.	
1615	S	SW	60	1610	.	1200
1630	S	SW	94	1630	.	1500
1645	S	SW	142	1650	.	1500
1700	SSW	SW	142			

19 Jun 95

OBDG-Obs. A sea breeze but not a strong one pushes plume to S and eventually to SSW. Line of convergence at Indian R.
RAMS. RAMS predicts sea breeze and NE flow stronger than observed. Convergence line over Merritt Island at 1530.
HYPACTPlume moved SW and then W, hits convergence line at 1550 and rises to 1200 m at 1610 and 1500 m at 1630. Return flow starts then and upper part of plume moves E.

Good example of 3-d situation with return flow and upward vertical motion at sea breeze front. Model shows value since sea breeze convergence line was really there.
No change in launch availability.

2100	SW	SW	11			
2115	SW	WSW	34	2110	WSW	0
2130	SW	WSW	34	2130	.	50
2145	SW	WSW	60	2150	.	200
2200	SW	WSW	60		.	
2215	SW	WSW	94	2210	.	300
2230	SW	W	94	2230	.	300
2245	SW	W	142	2250	.	400
2300	SW	W	142			

OBDG-Obs. Sea breeze E flow established earlier persisted w/ NE flo.

OBDG-RAMS. Like obs, the E flow continued and upper level winds more from E than NE. Wind direct. off ~ 30°.
HYPACT. Plume moves WSW and extends 40 km and stays narrow.

All models in pretty good agreement w/ wind direction off slightly . Using upper winds w/ OBDG makes more sense. No change in launch availability

0500	N	NNE	11			
0515	NNE	NNE	11	0510	NW	0
0530	NNE	NNE	11	0530	.	0
0545	NE	NNE	11	0550	.	100
0600	ENE	NNE	11		.	
0615	ENE	NNE	11	0610	.	100
0630	ENE-NE	NE	11	0630	.	100
0645		NE	11	1650	.	100
0700	ENE	-	11			

OBDG-Obs. Weak SW flow, stable conditions, plume extends 32 km.
OBDG-RAMS. RAMS predicted SE flow which differed by 45° .
HYPACT. Stable conditions, plume moves NW and stays below 100m

Table 8-14. Comparison summary of three different model runs for June 19-20.

	OBDG-Obs	OBDG-RAMS		HYPACT-RAMS		
Time (UTC)	Plume direc-tion	Plume direc-tion	Sigma Level (m)	Time (UTC)	Plume direc-tion	Maxi-mum plume height (m)
1500	W	WSW	11			
1515	W	WSW	34	1510	WSW	0
1530	W	WSW	34	1530	.	0
1545	W	WSW	34	1550	.	50
1600	W	WSW	34		.	
1615	W	W	34	1610	.	600
1630	W	W	34	1630	.	800
1645	WSW	W	34	1650	.	900
1700	W	W	34			

5 Jul 95

OBDG-Obs. E flow with sea breeze. Plume extends 16 km as E winds prevail over Cape.
RAMS. RAMS winds matched obs w/ shift from ESE to E. Sea breeze already in.
HYPACTPlume moved WSW and then W, hits sea breeze at 1610 at Indian R. and lifts to 1000 m. No return flow.

Pretty good model agreement. Hypact shows the lifting that occurs.

2100	W	W	11			
2115	W	W	34	2110	W	0
2130	W	W	34	2130	.	50
2145	W	W	34	2150	.	200
2200	W	W	60		.	
2215	W	W	60	2210	.	300
2230	WNW	W	94	2230	.	300
2245	WNW	W	94	2250	.	300
2300	WNW	W	142			

OBDG-Obs. Steady E flow , plume extends 18 km.

OBDG-RAMS. Very steady, strong E winds.
HYPACT. Strong E winds produce straight lijne plume w/ some diffusion vetically and horizontally. Plume extends 40 km.

Good model agreement . No change in launch availability Hypact plume extends farther.

0500	NNW	N	11			
0515	NNW	N-NNW	11	0510	N	0
0530		N	11	0530	.	0
0545	NW	N	11	0550	.	0
0600	NW	N	11		.	
0615	NW	N	11	0610	.	50
0630	NW	N	11	0630	.	100
0645	NNW	N	11	1650	.	100
0700	NW	NNE	11			

OBDG-Obs. Steady flow from SE w/winds getting very light. Plume extends over 50 km.
OBDG-RAMS. RAMS wind direction off by -30° but winds light .
HYPACT. Hypact plume extends 25-30 km to N , stays narrow w/ little diffusion.
Launch availability increased as model shows plume offshore and not as far as obs.

Table 8-15. Comparison summary of three different model runs for July 5-6.

	OBDG-Obs	OBDG-RAMS		HYPACT-RAMS		
Time (UTC)	Plume direc-tion	Plume direc-tion	Sigma Level (m)	Time (UTC)	Plume direc-tion	Maxi-mum plume height (m)
1500	WSW	SW	11			
1515	WSW	SW	11	1510	SW	0
1530	WSW	SW	34	1530	.	0
1545	WSW	SW	34	1550	.	50
1600	WSW	SW	60		.	
1615	W	SW	60	1610	.	500
1630	WSW	SW	34	1630	.	1000
1645	WSW	SW	34	1650	.	1100
1700	WSW	SW	34			

15 Jul 95

OBDG-Obs. ENE flow persists. Plume extends 18.
RAMS. RAMS predicts river breezes which bend plume. Strong NE flow along coast.
HYPACTPlume moved SW, hits sea breeze and is forced up. No further horizontal push, only vertical.

Good 3-d effects are seen by RAMS/HYPACT. No change in launch availability

2100	WSW	WSW	11			
2115	WSW	WSW	11	2110	W	0
2130	W	W	34	2130	.	50
2145	W	W	34	2150	.	200
2200	W	W	60		.	
2215	W	W	60	2210	.	300
2230	WNW	W	94	2230	.	300
2245	WNW	W	94	2250	.	300
2300	WNW	W	142			

OBDG-Obs. Steady E and ESE flow , plume extends 19 km.

OBDG-RAMS. RAMS matches closely to obs wind direction. Speeds higher with upper level winds.
HYPACT. Typical 21Z plume which spreads little,rises to 300 m and moves W. Plume extends 40 km.

Good example of RAMS model verifying since it picked up subtle wind shifts . No change in launch availability.

0500	NNW	NNW	11			
0515	NNW	N	11	0510	N	0
0530	NNW	N	11	0530	NE	50
0545	NNW	N	11	0550	.	100
0600	NNW	N	11		.	
0615	NNW	NNE	11	0610	.	100
0630	N	NNE	11	0630	.	200
0645	N	NE	11	1650	.	200
0700	N	NE	11			

OBDG-Obs. Typical nighttime, stable conditions with plume offshore. Plume extends over 50 km.
OBDG-RAMS. RAMS predicts offshore, steady, light, winds.
HYPACT. String plume to N then NE. Launch availability increased as model shows plume offshore.

Table 8-16. Comparison summary of three different model runs for July 15-16.

9.0 References

Aerospace, Corp., 1995: Ground cloud dispersion measurements during the Titan IV Mission #K14 (22 December 1994) at Cape Canaveral Air Station. Aerospace Report No. TR-95(5448)-2, 15 June 1995.

Bionetics Corp., 1994: STS-64 Launch Effects Summary Report. NASA Contract NAS10-11624, Doc. No. BIO-ENV-115, 22 Sep 1994.

Bionetics Corp., 1994: STS-65 Launch Effects Summary Report. NASA Contract NAS10-11624, Doc. No. BIO-ENV-112, 22 Jul 1994.

Bionetics Corp., 1994: STS-66 Launch Effects Summary Report. NASA Contract NAS10-11624, Doc. No. BIO-ENV-120, 16 Nov 1994.

Bjorklund, J.R., 1990: User's manual for the REEDM Version 7 (Rocket Effluent Diffusion Model) Computer Program. TR-90-157-01, April 1990.

Duncan, B.W. and P.A. Schmalzer, 1994: Using a Geographical Information System for monitoring Space Shuttle launches: Determining cumulative distribution of deposition and an empirical test of a spatial model. *Environmental Management*, **18**, pp. 465-474.

Dynamac Corp., 1995: STS-63 Launch Effects Summary Report. NASA Contract NAS10-12180, 8 Feb 1995.

Dynamac Corp., 1995: STS-67 Launch Effects Summary Report. NASA Contract NAS10-12180, Mar, 1995.

Ernst, J.A. and F.J. Merceret, 1995: The Applied Meteorology Unit: a tri-agency applications development facility supporting the Space Shuttle. *Preprints, 6th Conf. on Aviation Weather Systems*, Dallas, TX, Amer. Meteor. Soc., Boston, p. 266-268.

Evans, R.J., C.J. Tremback, W.A. Lyons, 1996: Mesoscale modeling of the sea breeze and its sensitivity to land use classification and soil moisture parameterization at CCAS/KSC. *Preprints, Conf. on Coastal Oceanic and Atmospheric Prediction*, Atlanta, GA, Amer. Meteor. Soc., Boston, 6 pp.

Garratt, J.R., 1990: The Internal Boundary Layer - A Review. *Boundary Layer Meteorology*, **50**, 171-185.

Heidner, R.F., B.P. Kaspar, and D.R. Schulthess, 1994: Imagery of the Titan IV ground cloud. Presented at the Toxic Release Assessment Group (TRAG), Los Angeles, CA, 28 June, 1994.

Hosker, Jr., R.P., K.S. Rao, R.M. Eckman, J.T. McQueen, and G.E. Start, 1993: An assessment of the dispersion Models in the MARSS system used at the Kennedy Space Center. NOAA Tech Memo ERL ARL-205, 91pp.

Kunkel, B.A., 1984: An evaluation of the Ocean Breeze/Dry Gulch model. Air Force Geophysics Laboratory technical report AFGL-TR-84-0313, 18 pp.

Lundblad, B., 1985: MVP Test Plan (Draft), June 1995, 16 pp.

Lyons, W. A. and C. J. Tremback, 1994: Final Scientific and Technical Report: Predicting 3-D wind flows at Cape Canaveral Air Force Station using a mesoscale model. Contract No. F04701-91-C-0058. Prepared by ASTER/MRC for US Air Force Space and Missile Systems Center, SMC/CLNE, 30 June 1994.

Lyons, W.A., and R.G. Fisher, 1988: Climatographic analyses for the southeast coastline of Florida in support of emergency response studies. *Preprints, 4th Conf. on the Meteorology and Oceanography of the Coastal Zone,* AMS, Anaheim, 101-106.

Lyons, W.A., E.R. Sawdey, J.A. Schuh, R.H. Calby and S.S. Keen, 1981: An updated and expanded coastal fumigation model. *Presented, 74th Annual Meeting of the Air Pollution Control Association,* 81-31.4, Philadelphia, PA, 16pp.

Lyons, W.A., R.A. Pielke, R.L. Walko and M.E. Nicholls, 1991: Feasibility of numerical thunderstorm forecasts for specific KSC work complexes. Final Report, ASTeR, Inc. NASA SBIR Phase I, Contract NAS10-11759, 326 pp.

Lyons, W.A., R.A. Pielke, W.R. Cotton, C.S. Keen and D.A. Moon, 1992: Final results of an experiment in operational forecasting of sea breeze thunderstorms using a mesoscale numerical. *Preprints, Symposium on Weather Forecasting,* AMS, Atlanta, 6 pp.

Lyons, W.A., R.A. Pielke, W.R. cotton, M. Uliasz, C.J. Tremback, R.L. Walko and J.L. Eastman, 1993: The application of new technologies to modeling mesoscale dispersion in coastal zones and complex terrain. *Air Pollution,* Eds. P. Zannetti, C.A. Brebbia, J.E. Garcia Gardea and G. Ayala Milian, Elsevier Applied Science, Computational Mechanics Publications, London, 3-8.

Ohmstede, W.D., R.K. Dumbauld, and G.G. Worley, 1983: Ocean Breeze/Dry Gulch equation review. USAF Engineering and Services Laboratory technical report ESL-TR-83-05 (ADB-080677; avail. Defense Tech. Info. Ctr., Alexandria, VA), 178 pp.

Pielke, R.A., W.R. Cotton, R.L. Walko, C.J. Tremback, W.A. Lyons, L. Grasso, M.E. Nicholls, M.D. Moran, D.A. Wesley, T.J. Lee, and J.H. Copeland, 1992: A comprehensive meteorological modeling system – RAMS. *Meterol. and Atmospheric Physics,,* **49**, 69-91.

Siler, R. K., 1980: A diffusion climatology for Cape Canaveral Florida. NASA Tech. Memo. 58224, April 1980, 43 pp.

Taylor, T.E., M.K. Atchison and C.R. Parks, 1990: The Kenndey Space Center Atmospheric Boundary Layer Experiment (KABLE) - Phase II final Report. ENSCO, Contract NAS10-11544, ARS-90-120.

Tremback, C.J., W.A. Lyons, W.P. Thorson, and R.L. Walko, 1994: An emergency response and local weather forecasting software systeml. *Preprints, 8th Joint Conf. of Air Pollution Meteorology with AWMA,* Nashville, TN, Amer. Meteor. Soc., Boston, 5 pp.

APPENDIX A

Graphs comparing the winds observed at three towers (black) with winds predicted by RAMS (gray) for July and August 1994. The top graph shows wind direction (deg.), the middle graph shows wind speed (ms^{-1}), and the bottom graph shows observed sky cover in tenths (gray diamonds) and observed weather (black asterisks) at the SLF. RAMS data were produced by daily RAMS runs which were initialized at 1200 UTC and which ran for 24 hours. The towers presented in the Appendix are Tower 110, Tower 805, and Tower 303.

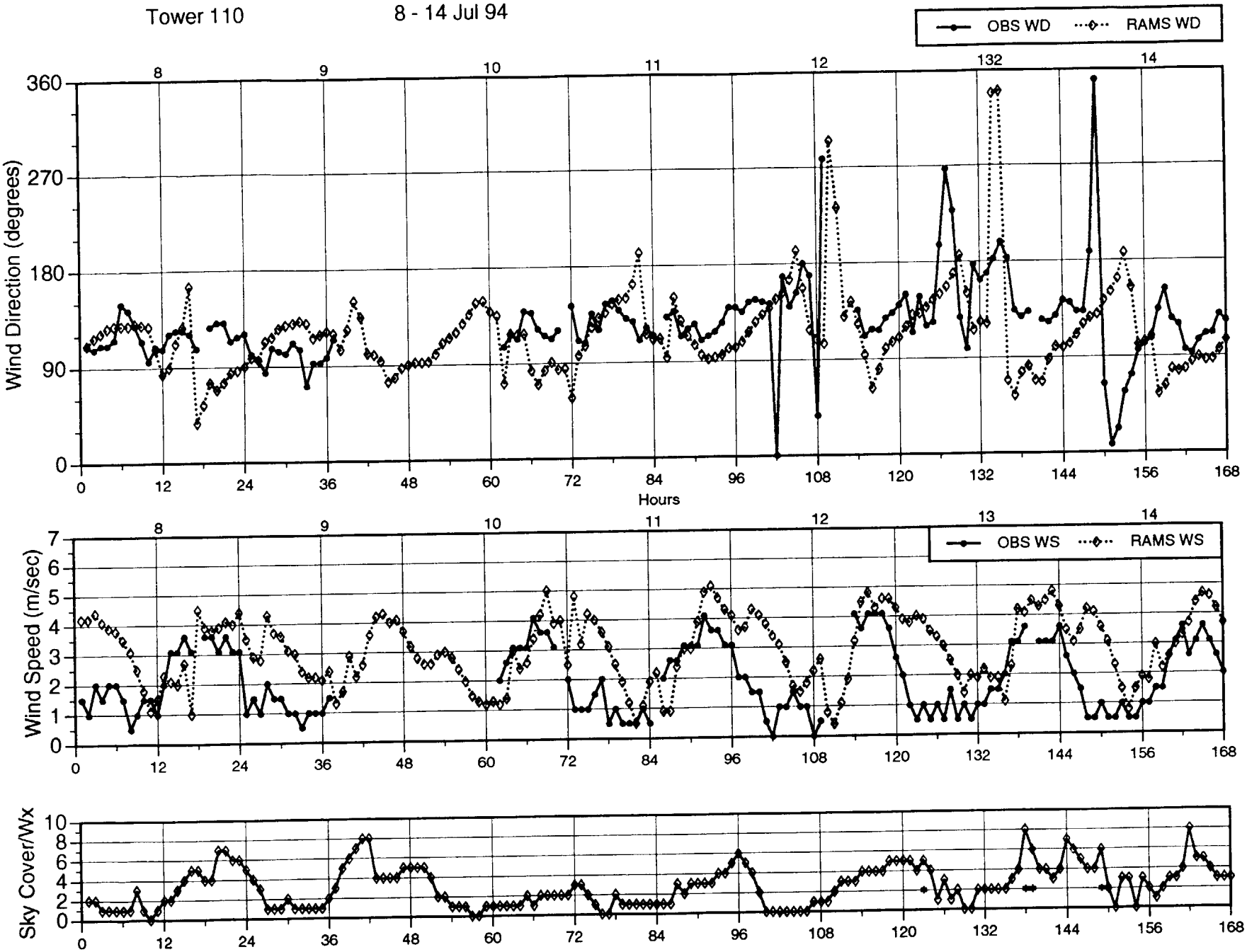
Tower 110
8 - 14 Jul 94
OBS WD
RAMS WD
Wind Direction (degrees)
360
270
180
90
0
8
9
10
11
12
132
14
0
12
24
36
48
60
72
84
96
108
120
132
144
156
168
Hours
OBS WS
RAMS WS
Wind Speed (m/sec)
7
6
5
4
3
2
1
0
13
Sky Cover/Wx
10
8
6
4
2
0

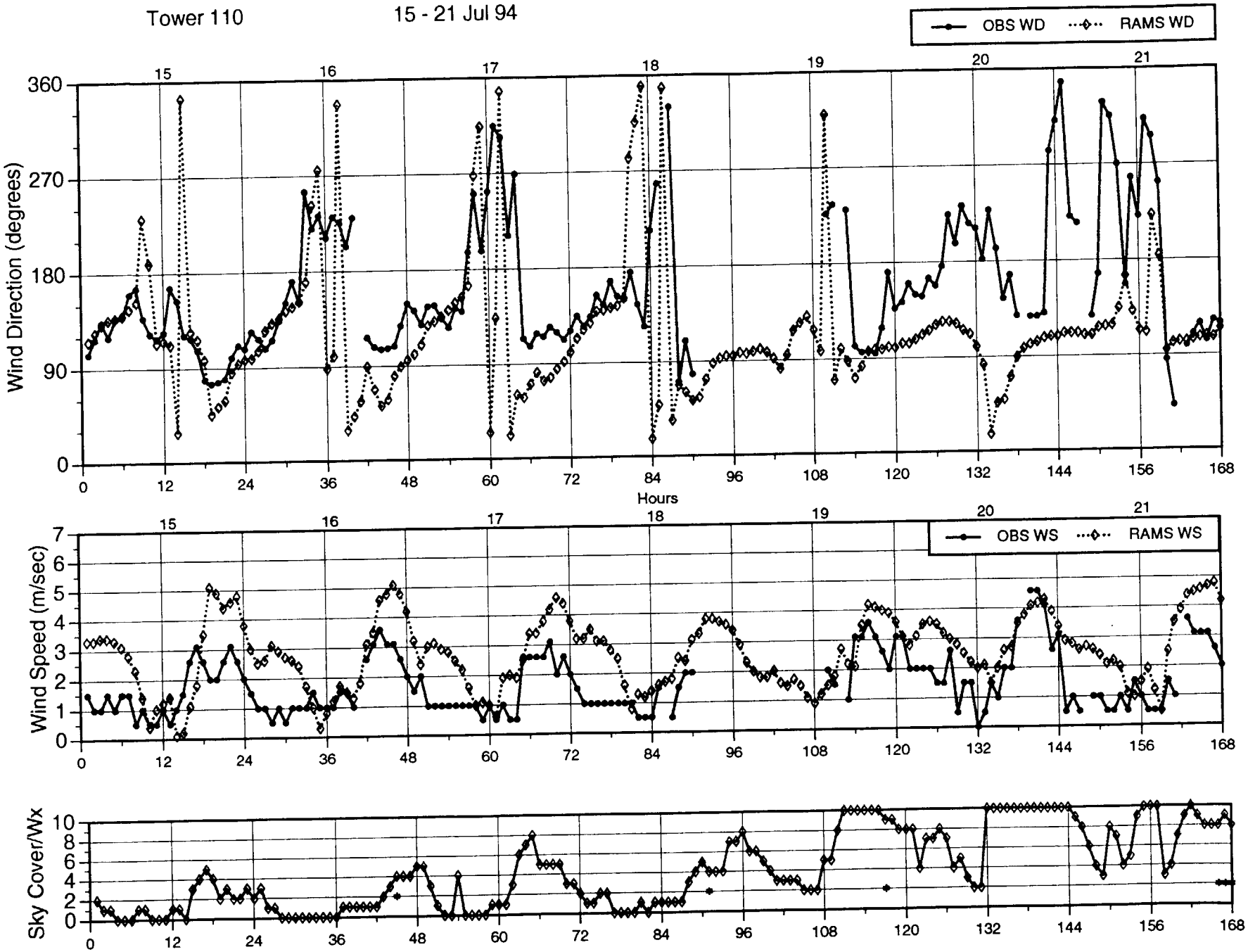
Tower 110
15 - 21 Jul 94
OBS WD
RAMS WD
Wind Direction (degrees)
360
270
180
90
0
15
16
17
18
19
20
21
0
12
24
36
48
60
72
84
96
108
120
132
144
156
168
Hours
OBS WS
RAMS WS
Wind Speed (m/sec)
7
6
5
4
3
2
1
0
Sky Cover/Wx
10
8
6
4
2
0

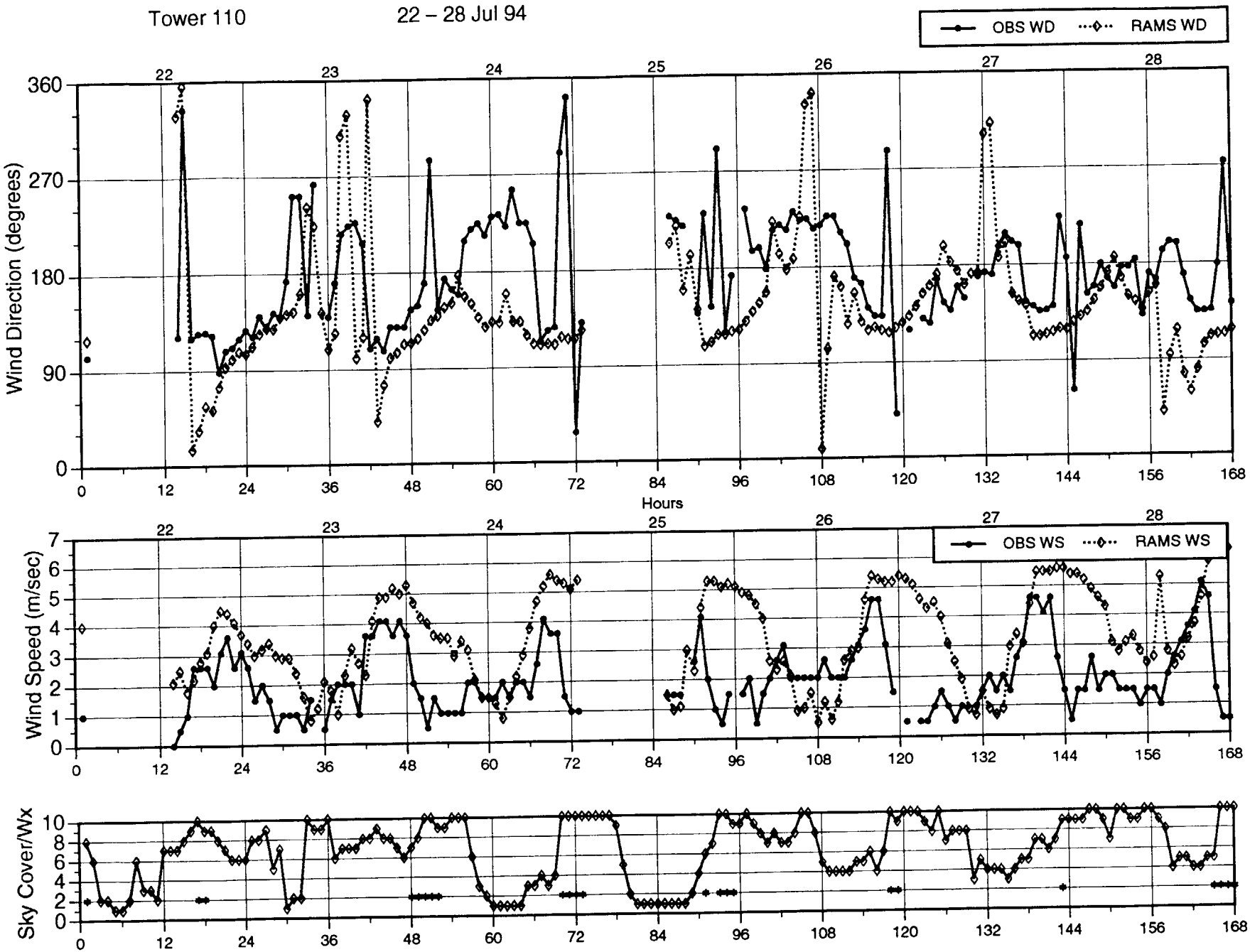
Tower 110
22 – 28 Jul 94
OBS WD
RAMS WD
Wind Direction (degrees)
360
270
180
90
0
22
23
24
25
26
27
28
0
12
24
36
48
60
72
84
96
108
120
132
144
156
168
Hours
OBS WS
RAMS WS
Wind Speed (m/sec)
7
6
5
4
3
2
1
0
Sky Cover/Wx
10
8
6
4
2
0

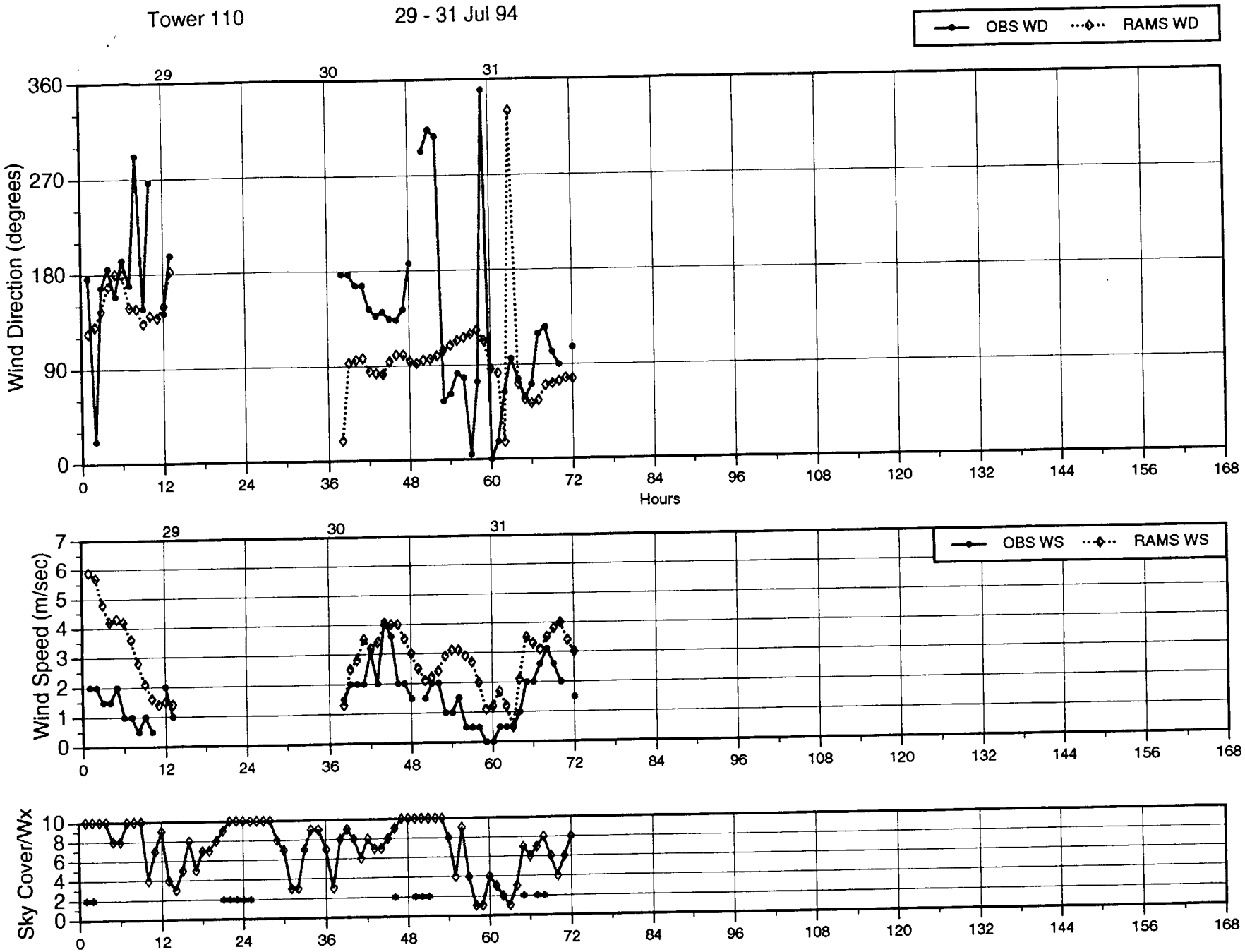
Tower 110
29 - 31 Jul 94
OBS WD
RAMS WD
Wind Direction (degrees)
360
270
180
90
0
29
30
31
0
12
24
36
48
60
72
84
96
108
120
132
144
156
168
Hours
OBS WS
RAMS WS
Wind Speed (m/sec)
7
6
5
4
3
2
1
0
Sky Cover/Wx
10
8
6
4
2
0

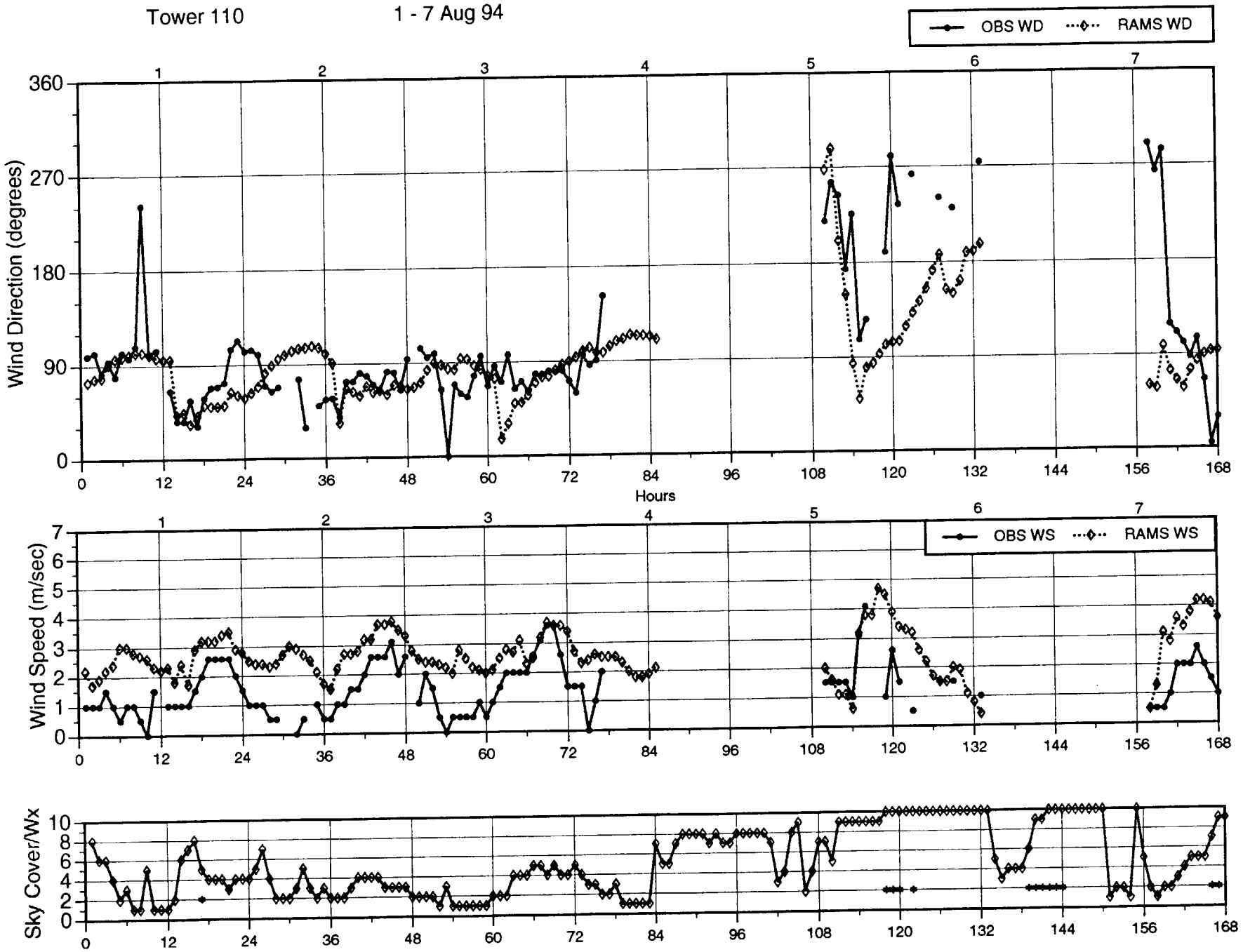
Tower 110
1 - 7 Aug 94
OBS WD
RAMS WD
Wind Direction (degrees)
360
270
180
90
0
1
2
3
4
5
6
7
0
12
24
36
48
60
72
84
96
108
120
132
144
156
168
Hours
OBS WS
RAMS WS
Wind Speed (m/sec)
7
6
5
4
3
2
1
0
Sky Cover/Wx
10
8
6
4
2
0

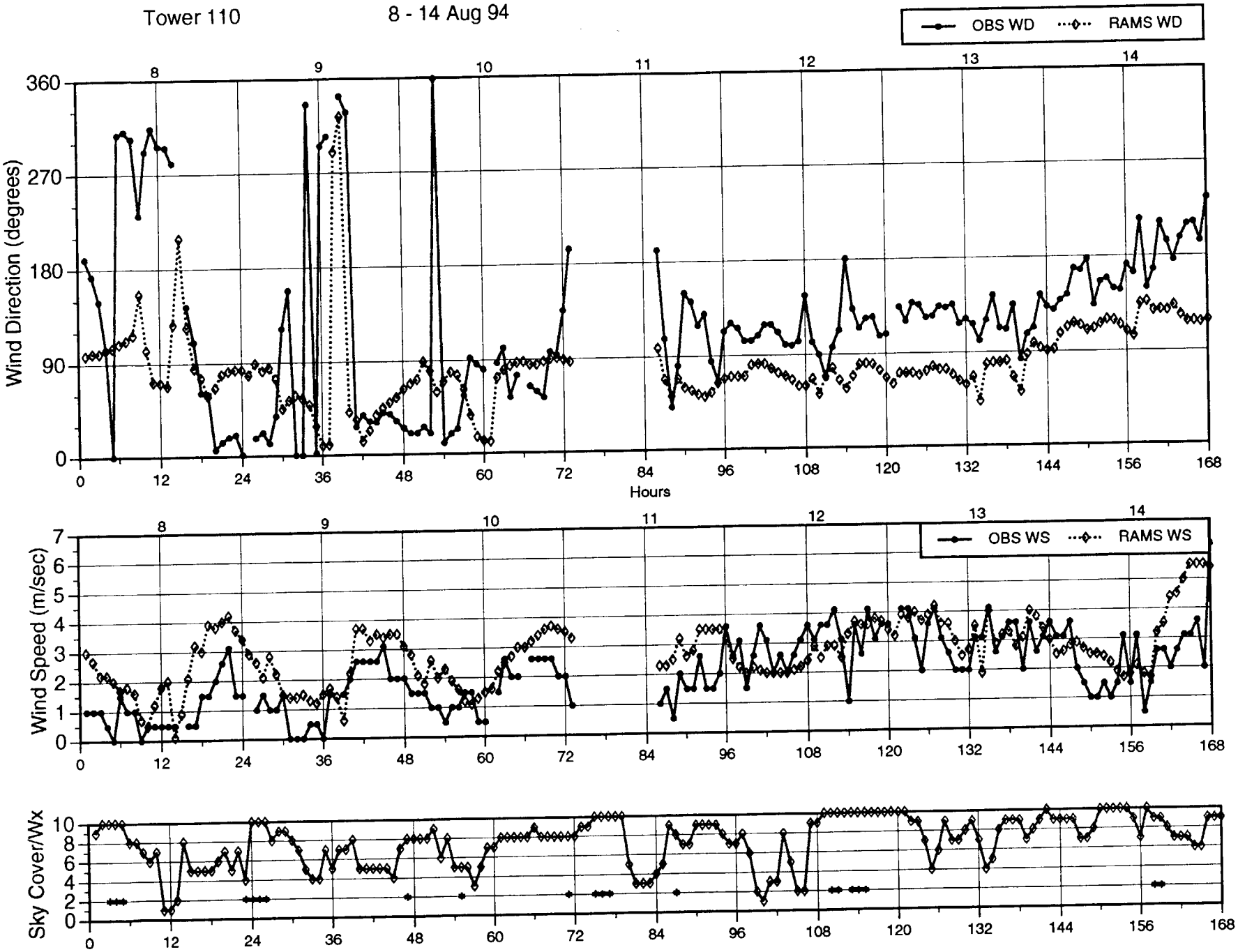
Tower 110
8 - 14 Aug 94
OBS WD
RAMS WD
Wind Direction (degrees)
360
270
180
90
0
8
9
10
11
12
13
14
0
12
24
36
48
60
72
84
96
108
120
132
144
156
168
Hours
OBS WS
RAMS WS
Wind Speed (m/sec)
7
6
5
4
3
2
1
0
Sky Cover/Wx
10
8
6
4
2
0

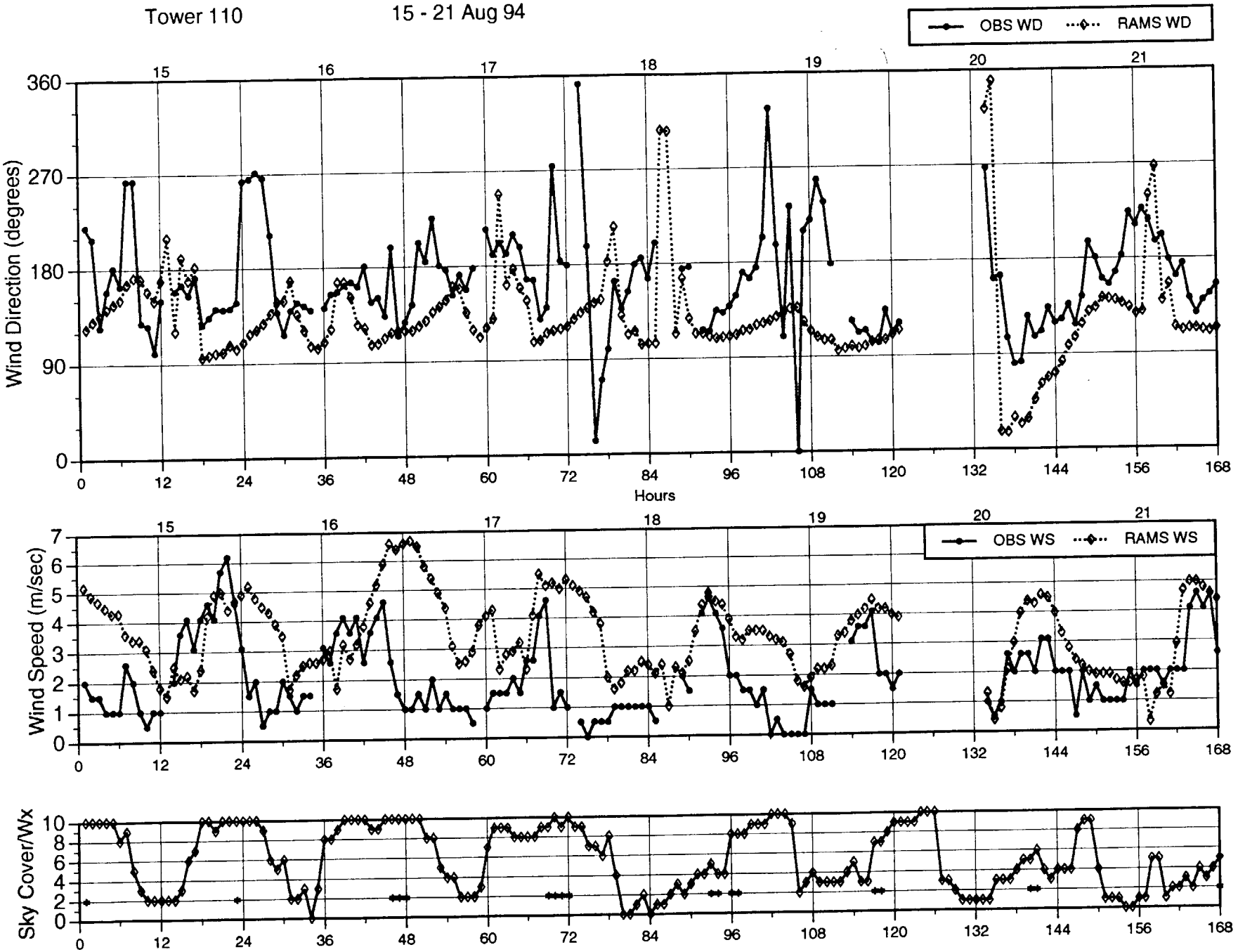
Tower 110
15 - 21 Aug 94
OBS WD
RAMS WD
Wind Direction (degrees)
360
270
180
90
0
15
16
17
18
19
20
21
0
12
24
36
48
60
72
84
96
108
120
132
144
156
168
Hours
OBS WS
RAMS WS
Wind Speed (m/sec)
7
6
5
4
3
2
1
0
Sky Cover/Wx
10
8
6
4
2
0

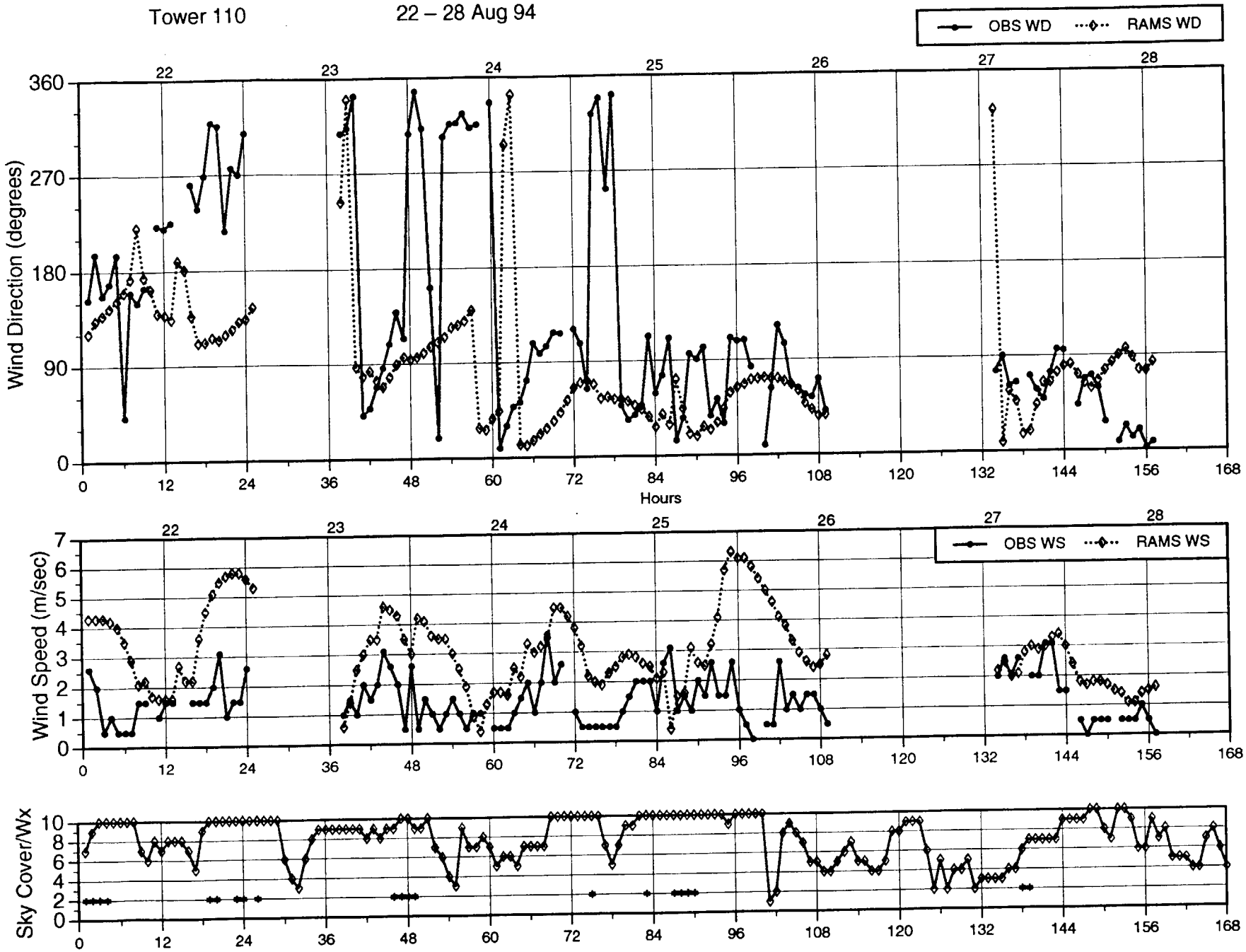
Tower 110
22 – 28 Aug 94
OBS WD
RAMS WD
Wind Direction (degrees)
Hours
OBS WS
RAMS WS
Wind Speed (m/sec)
Sky Cover/Wx

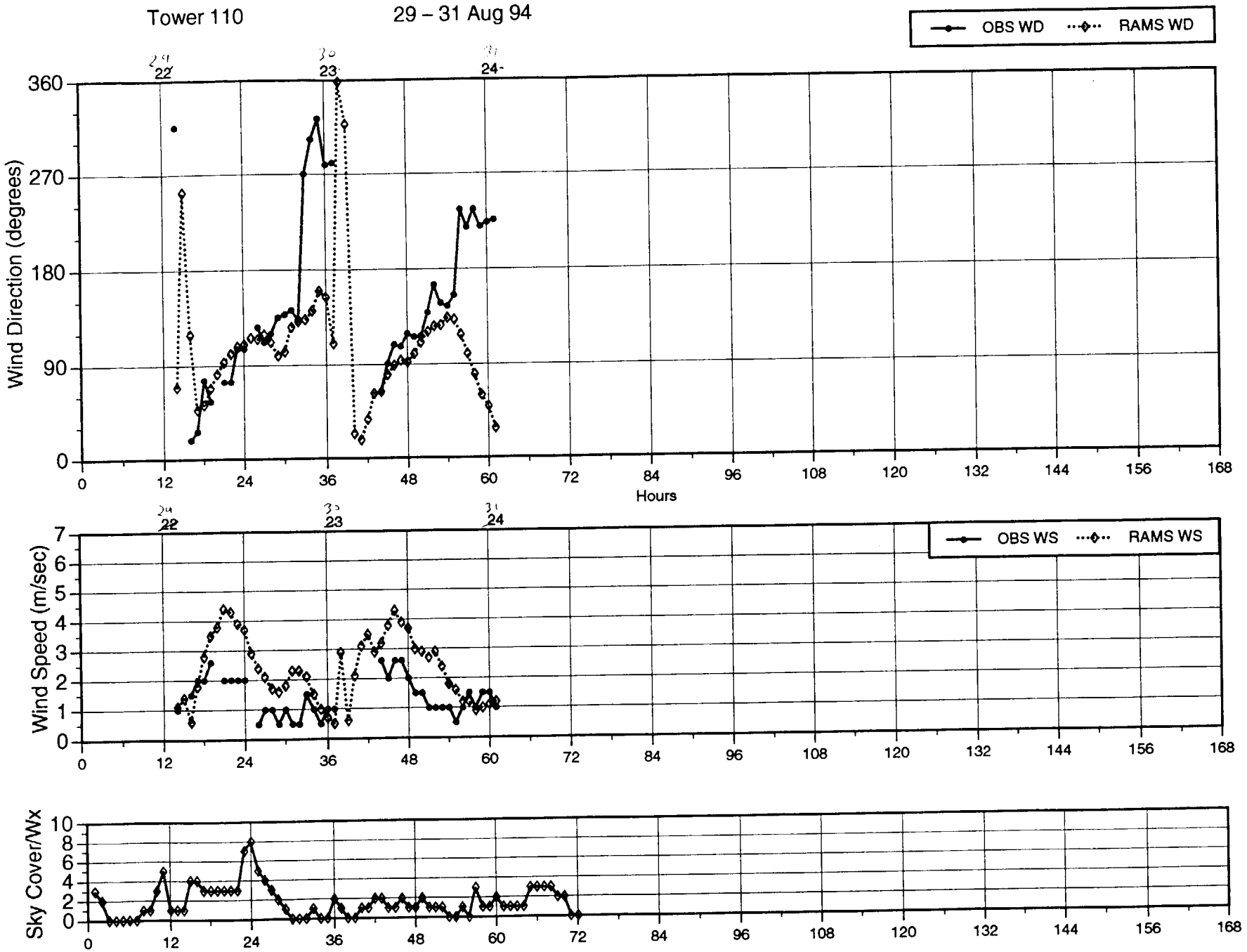
Tower 110
29 – 31 Aug 94
OBS WD
RAMS WD
Wind Direction (degrees)
360
270
180
90
0
22
23
24
0
12
24
36
48
60
72
84
96
108
120
132
144
156
168
Hours
OBS WS
RAMS WS
Wind Speed (m/sec)
7
6
5
4
3
2
1
0
Sky Cover/Wx
10
8
6
4
2
0

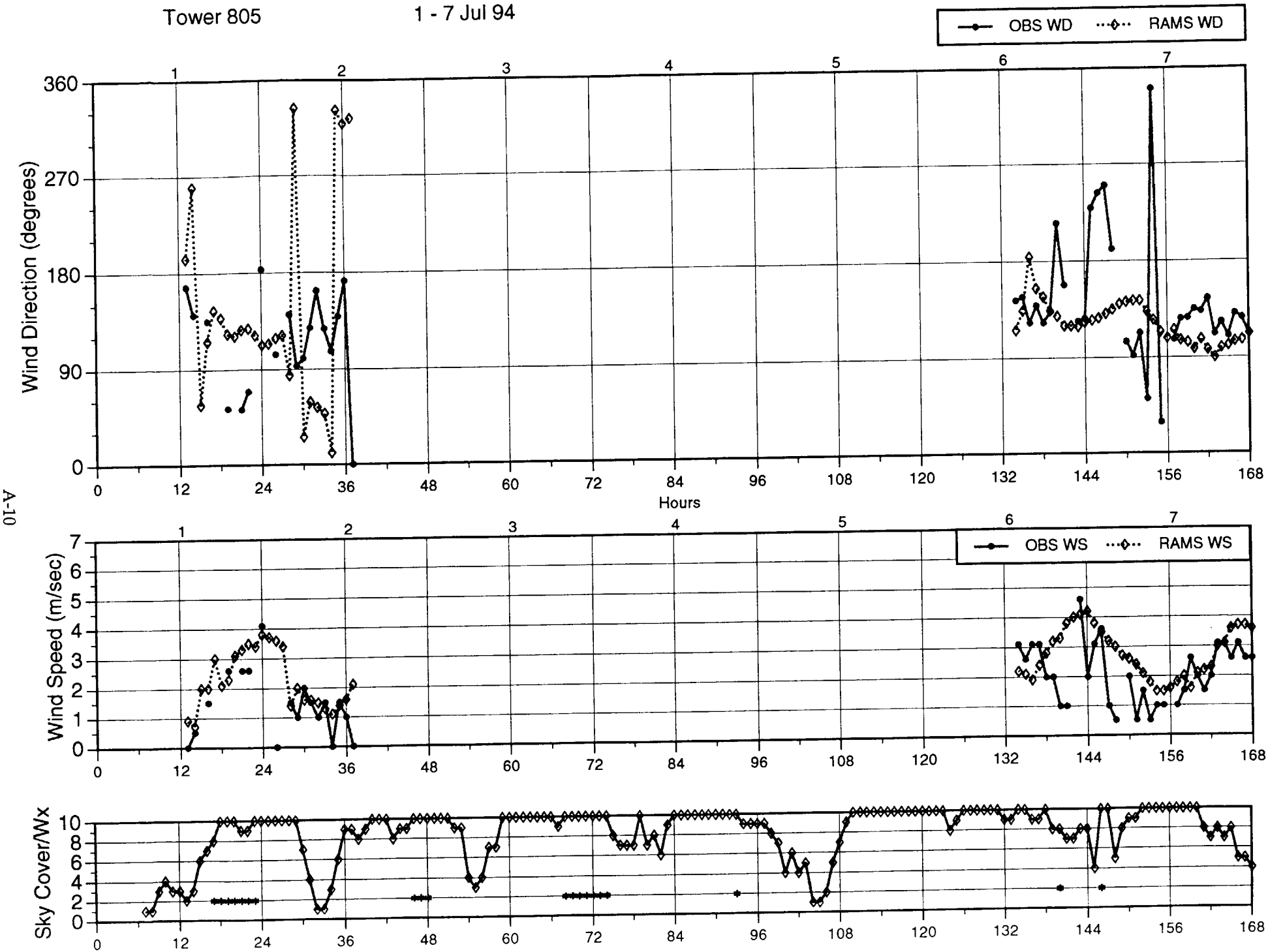
Tower 805
1 - 7 Jul 94
OBS WD
RAMS WD
Wind Direction (degrees)
360
270
180
90
0
1
2
3
4
5
6
7
0
12
24
36
48
60
72
84
96
108
120
132
144
156
168
Hours
OBS WS
RAMS WS
Wind Speed (m/sec)
7
6
5
4
3
2
1
0
Sky Cover/Wx
10
8
6
4
2
0

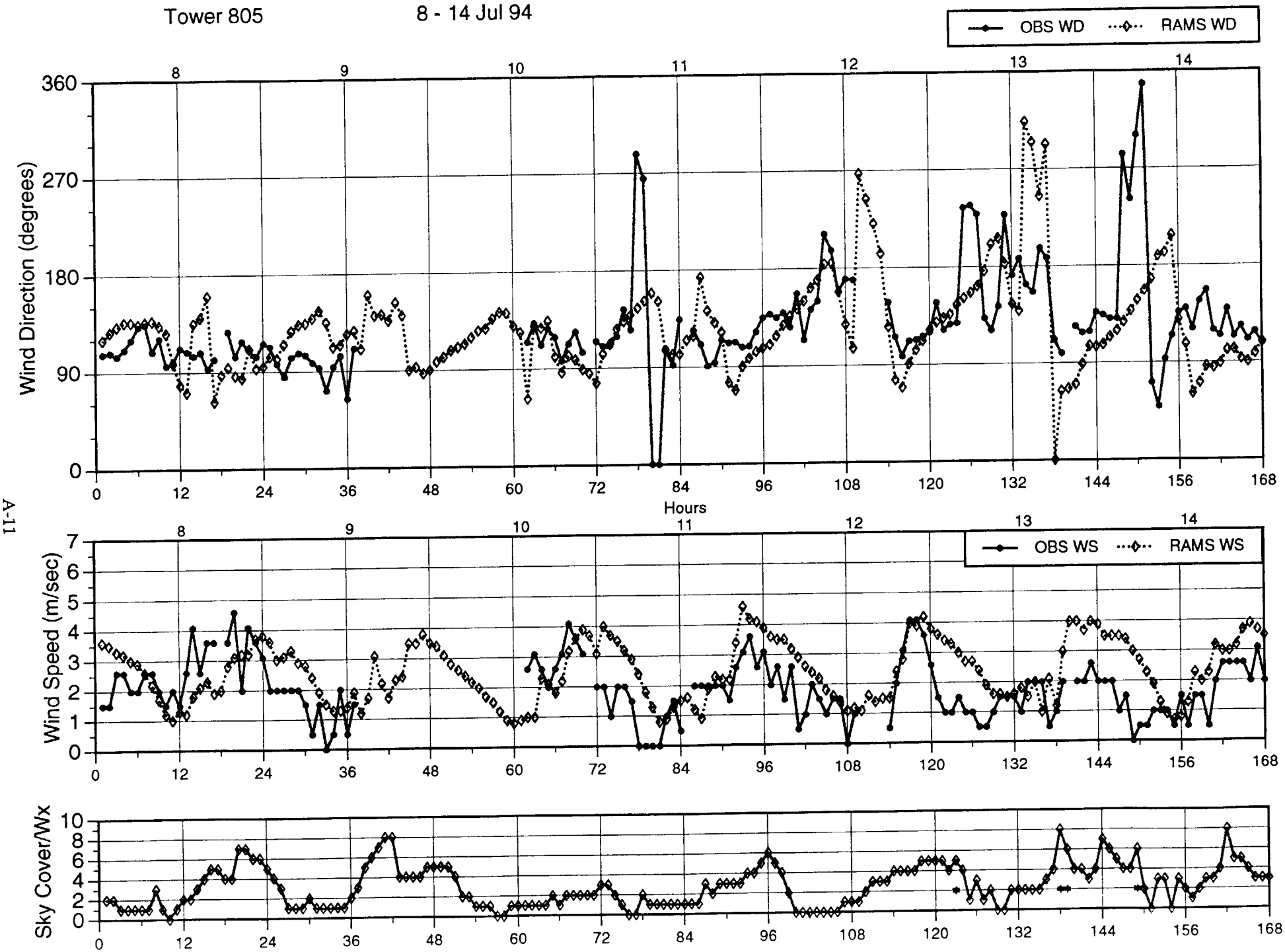
Tower 805
8 - 14 Jul 94
OBS WD
RAMS WD
Wind Direction (degrees)
360
270
180
90
0
8
9
10
11
12
13
14
0
12
24
36
48
60
72
84
96
108
120
132
144
156
168
Hours
OBS WS
RAMS WS
Wind Speed (m/sec)
7
6
5
4
3
2
1
0
Sky Cover/Wx
10
8
6
4
2
0

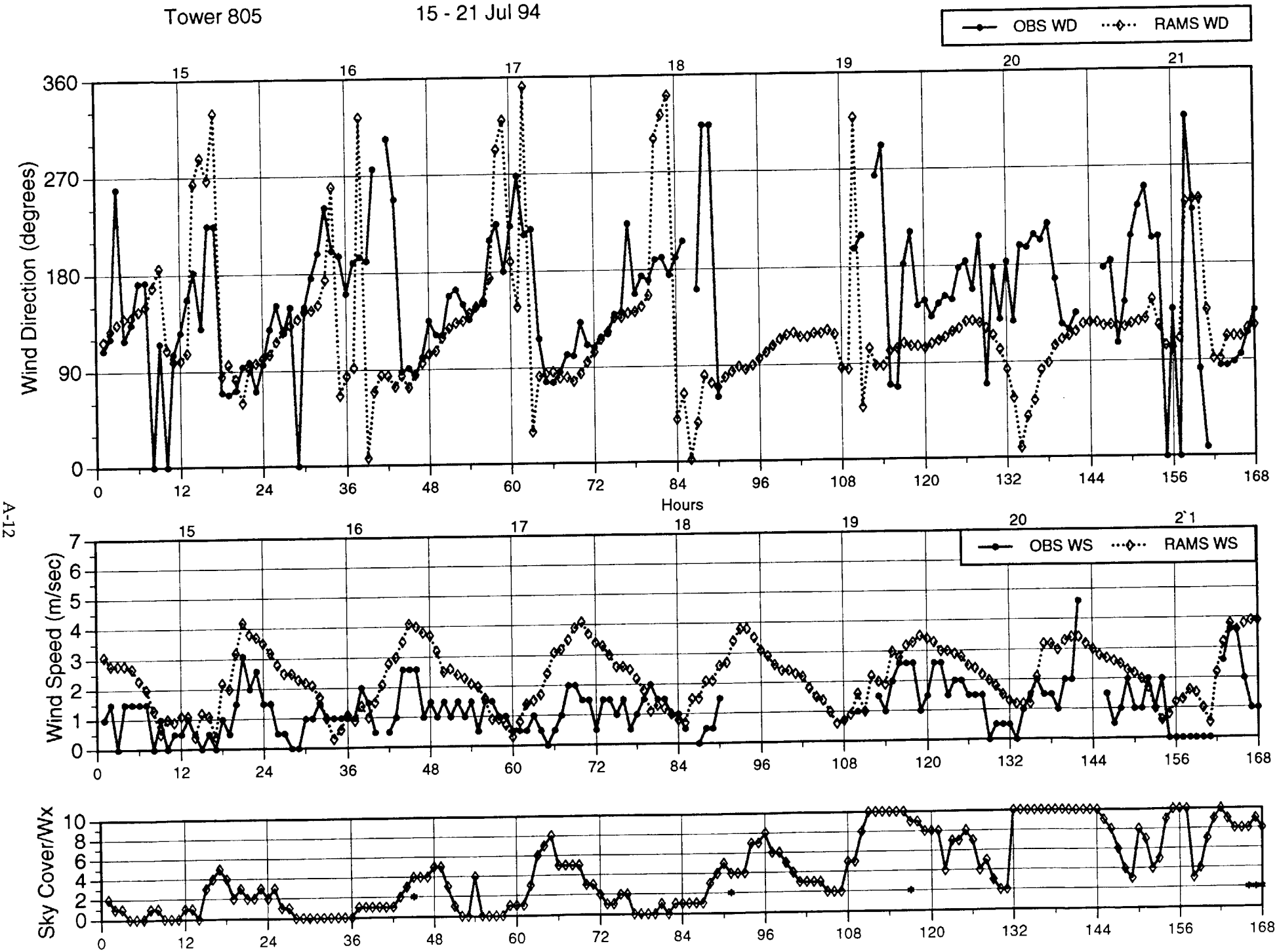
Tower 805
15 - 21 Jul 94
OBS WD
RAMS WD
Wind Direction (degrees)
360
270
180
90
0
15
16
17
18
19
20
21
0
12
24
36
48
60
72
84
96
108
120
132
144
156
168
Hours
OBS WS
RAMS WS
Wind Speed (m/sec)
7
6
5
4
3
2
1
0
Sky Cover/Wx
10
8
6
4
2
0

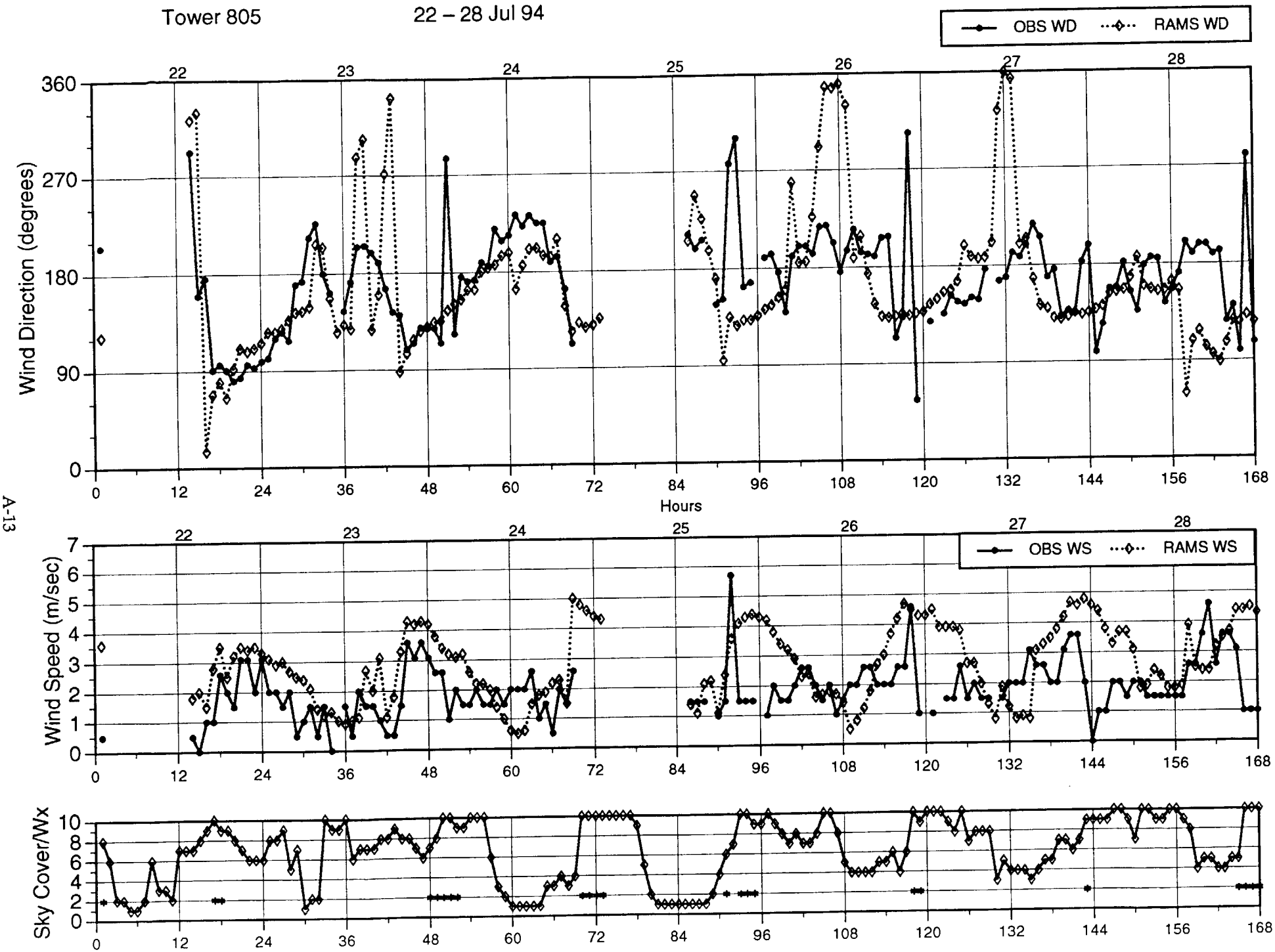
Tower 805
22 – 28 Jul 94
OBS WD
RAMS WD
Wind Direction (degrees)
360
270
180
90
0
22
23
24
25
26
27
28
0
12
24
36
48
60
72
84
96
108
120
132
144
156
168
Hours
OBS WS
RAMS WS
Wind Speed (m/sec)
7
6
5
4
3
2
1
0
Sky Cover/Wx
10
8
6
4
2
0

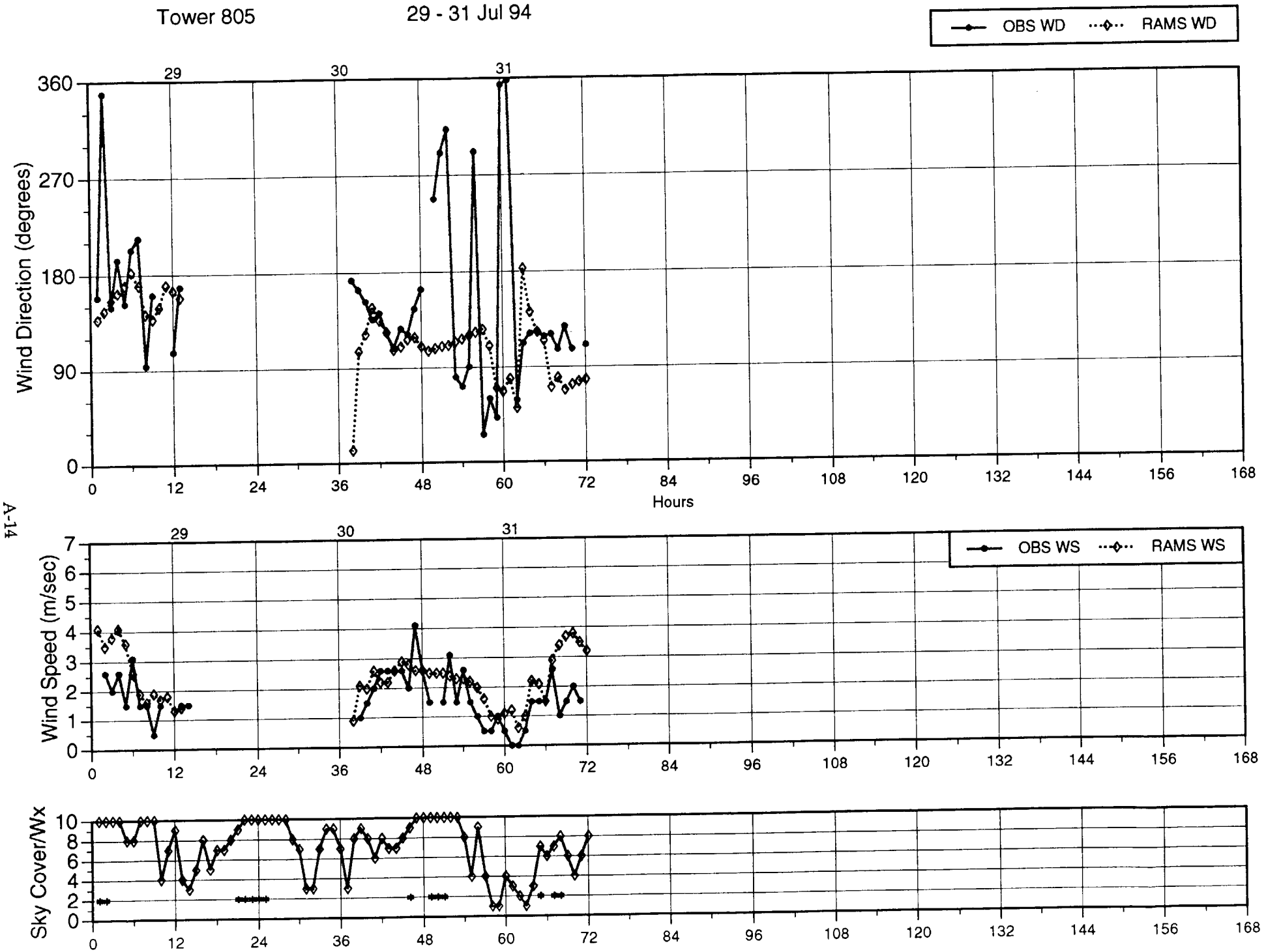
Tower 805
29 - 31 Jul 94
OBS WD
RAMS WD
Wind Direction (degrees)
360
270
180
90
0
29
30
31
0
12
24
36
48
60
72
84
96
108
120
132
144
156
168
Hours
OBS WS
RAMS WS
Wind Speed (m/sec)
7
6
5
4
3
2
1
0
Sky Cover/Wx
10
8
6
4
2
0

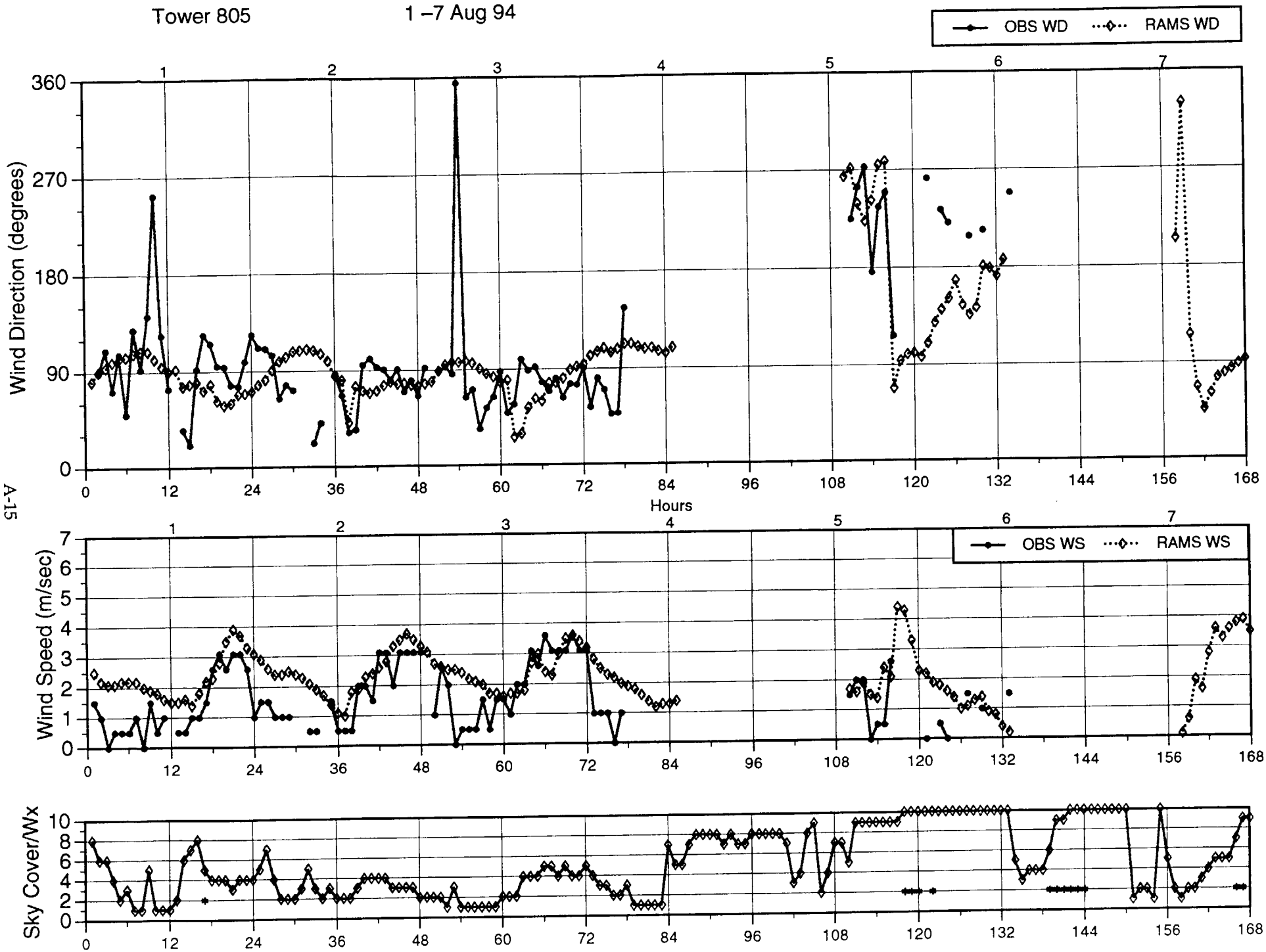
Tower 805
1 –7 Aug 94
OBS WD
RAMS WD
Wind Direction (degrees)
360
270
180
90
0
1
2
3
4
5
6
7
0
12
24
36
48
60
72
84
96
108
120
132
144
156
168
Hours
OBS WS
RAMS WS
Wind Speed (m/sec)
Sky Cover/Wx
10
8
6
4
2

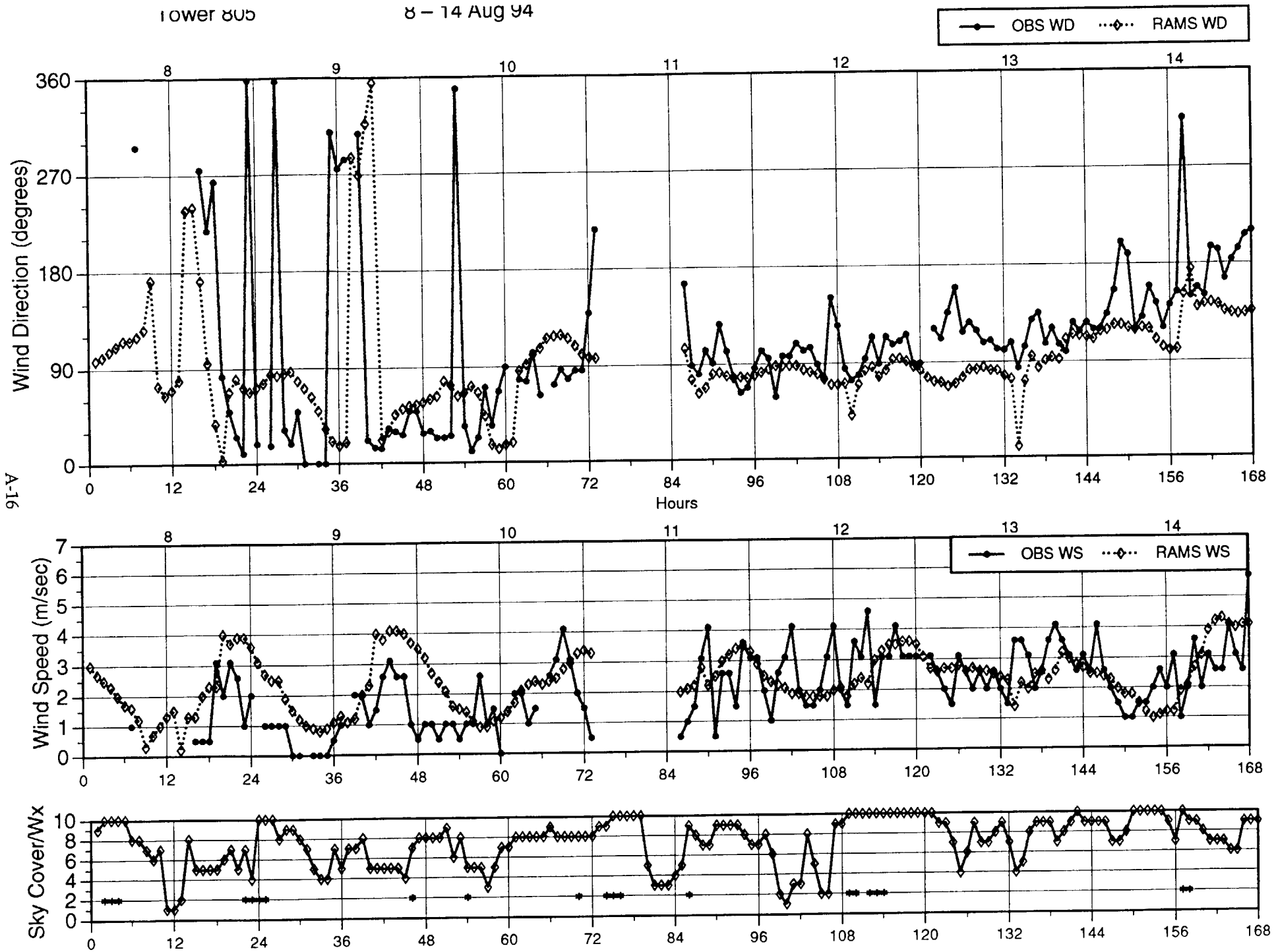
Tower 805
8 – 14 Aug 94
OBS WD
RAMS WD
Wind Direction (degrees)
360
270
180
90
0
8
9
10
11
12
13
14
0
12
24
36
48
60
72
84
96
108
120
132
144
156
168
Hours
OBS WS
RAMS WS
Wind Speed (m/sec)
7
6
5
4
3
2
1
0
Sky Cover/Wx
10
8
6
4
2
0

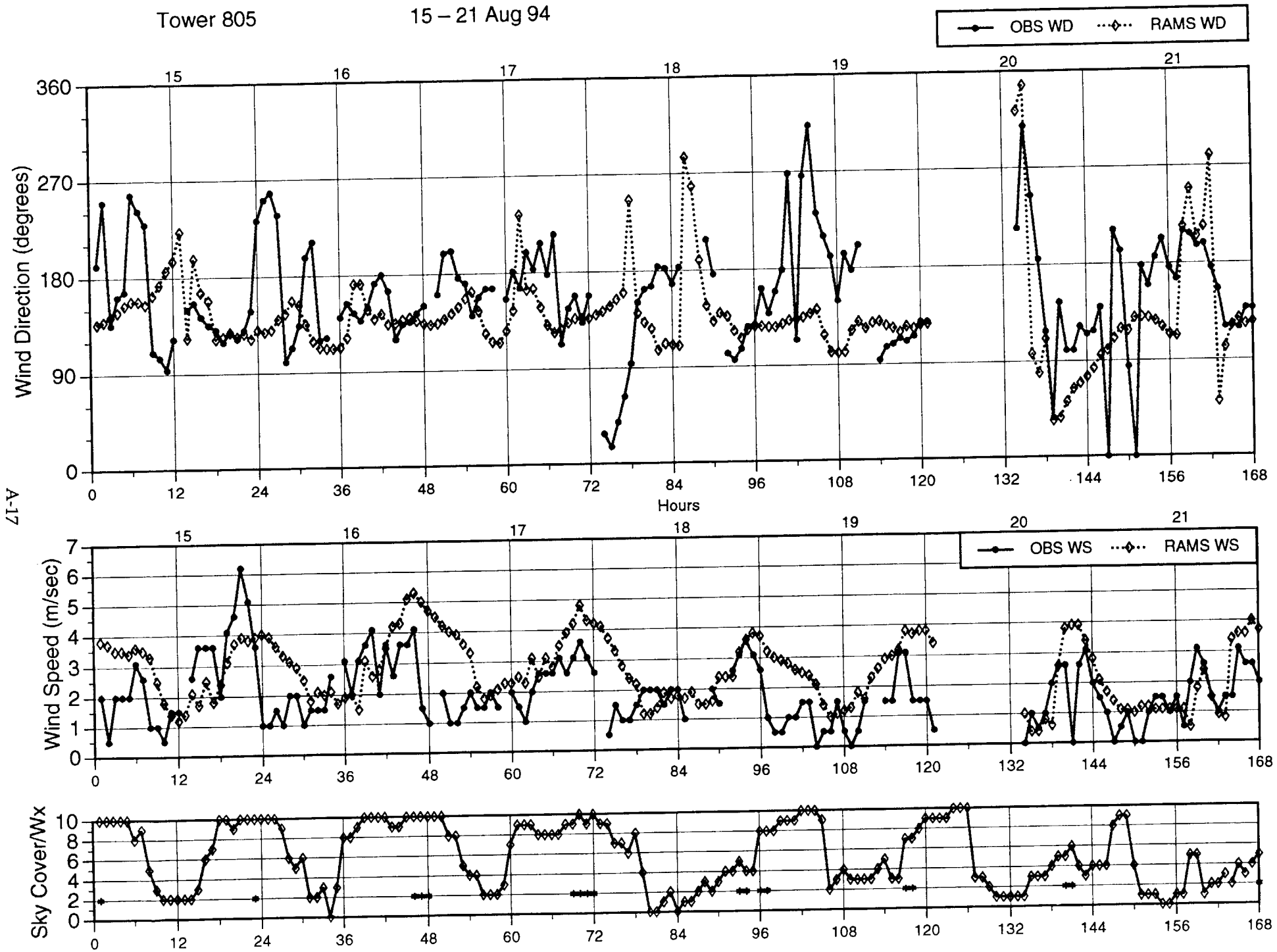
Tower 805
15 – 21 Aug 94
OBS WD
RAMS WD
Wind Direction (degrees)
360
270
180
90
0
15
16
17
18
19
20
21
0
12
24
36
48
60
72
84
96
108
120
132
144
156
168
Hours
OBS WS
RAMS WS
Wind Speed (m/sec)
7
6
5
4
3
2
1
0
Sky Cover/Wx
10
8
6
4
2
0

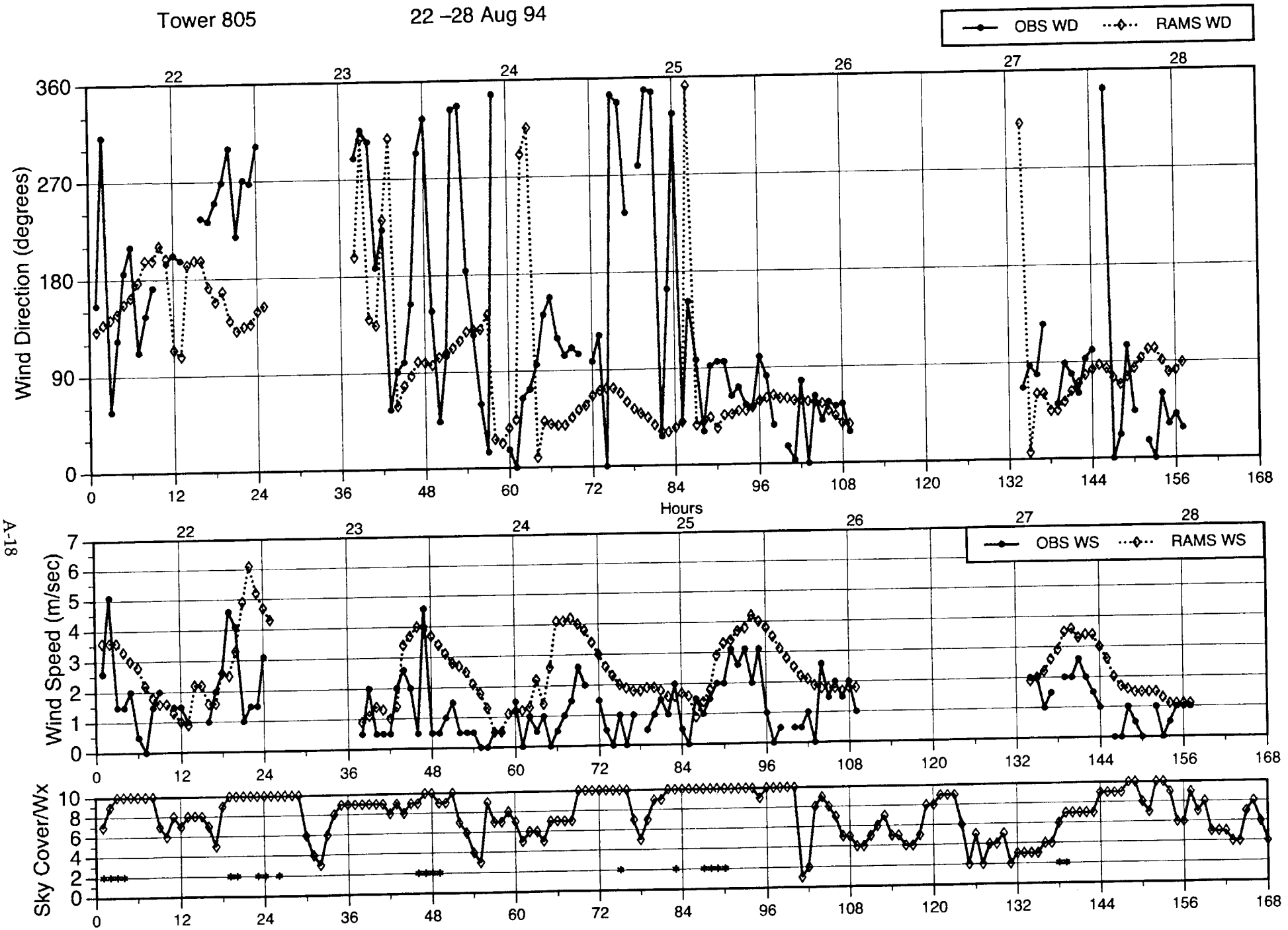
Tower 805
22 –28 Aug 94
OBS WD
RAMS WD
Wind Direction (degrees)
360
270
180
90
0
22
23
24
25
26
27
28
0
12
24
36
48
60
72
84
96
108
120
132
144
156
168
Hours
OBS WS
RAMS WS
Wind Speed (m/sec)
7
6
5
4
3
2
1
0
Sky Cover/Wx
10
8
6
4
2
0

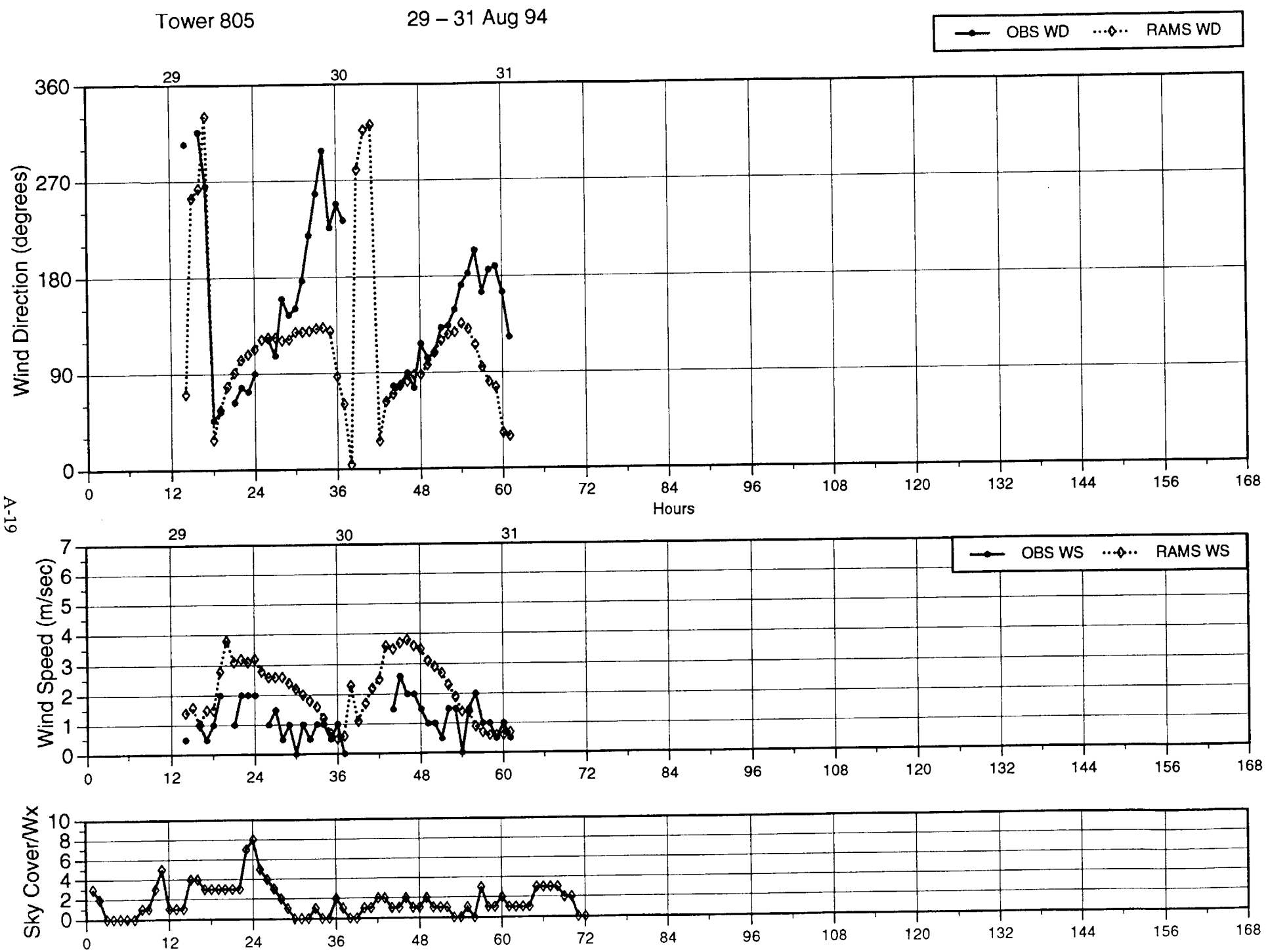
Tower 805
29 – 31 Aug 94
OBS WD
RAMS WD
Wind Direction (degrees)
360
270
180
90
0
29
30
31
0
12
24
36
48
60
72
84
96
108
120
132
144
156
168
Hours
OBS WS
RAMS WS
Wind Speed (m/sec)
7
6
5
4
3
2
1
0
Sky Cover/Wx
10
8
6
4
2
0

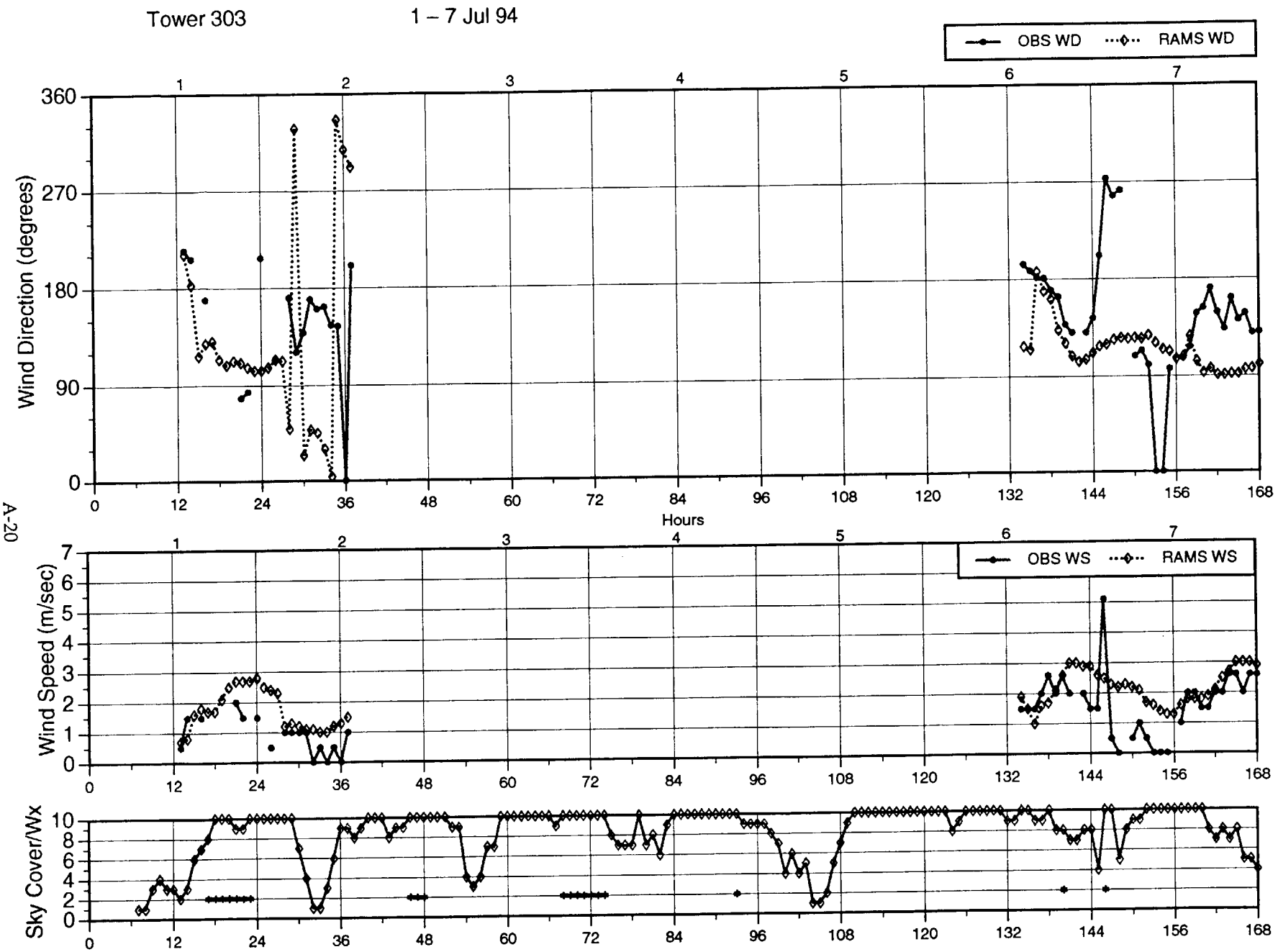
Tower 303
1 – 7 Jul 94
OBS WD
RAMS WD
Wind Direction (degrees)
360
270
180
90
0
1
2
3
4
5
6
7
0
12
24
36
48
60
72
84
96
108
120
132
144
156
168
Hours
OBS WS
RAMS WS
Wind Speed (m/sec)
7
6
5
4
3
2
1
0
Sky Cover/Wx
10
8
6
4
2
0

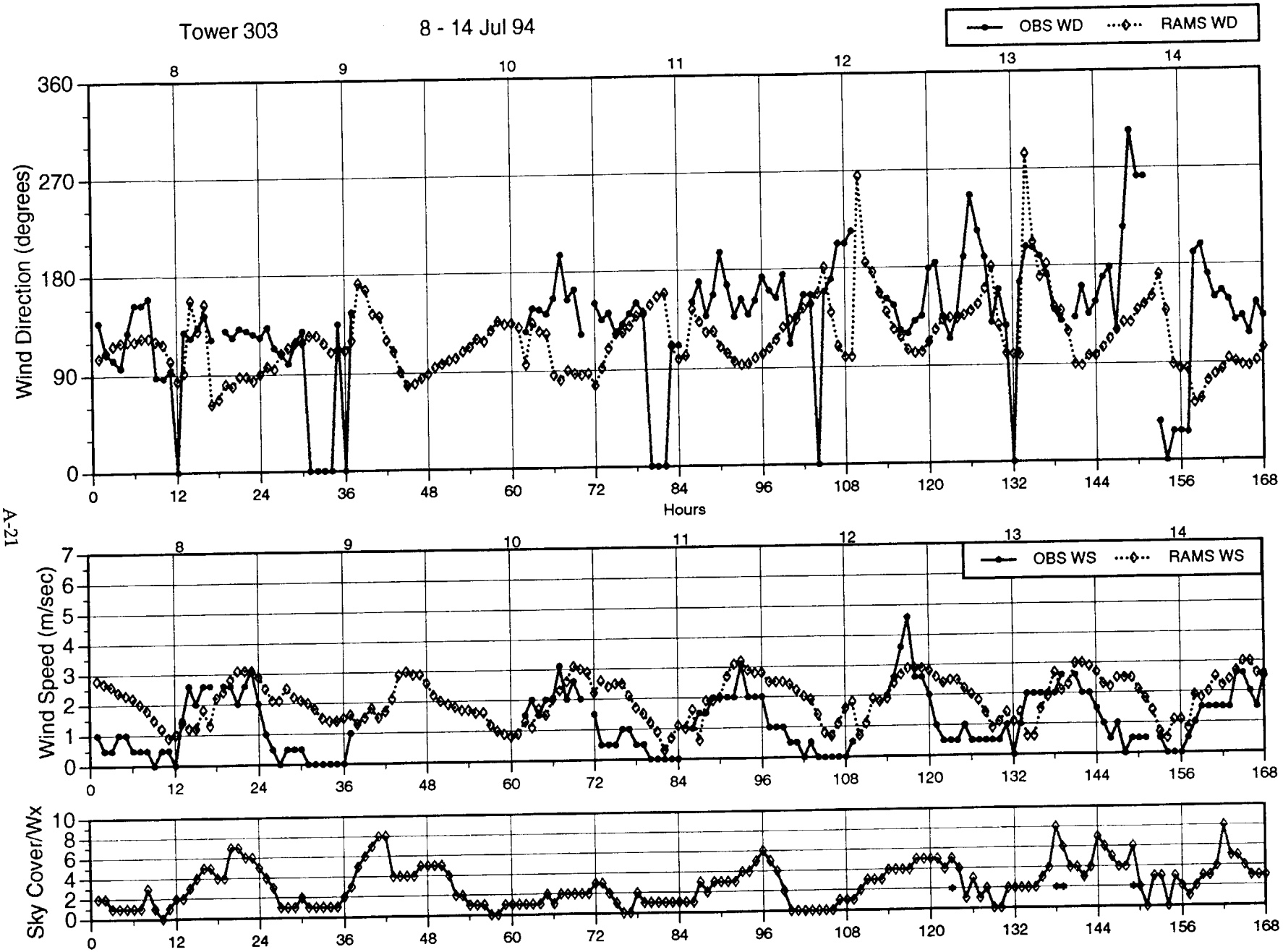
Tower 303
8 - 14 Jul 94
OBS WD
RAMS WD
Wind Direction (degrees)
Hours
OBS WS
RAMS WS
Wind Speed (m/sec)
Sky Cover/Wx

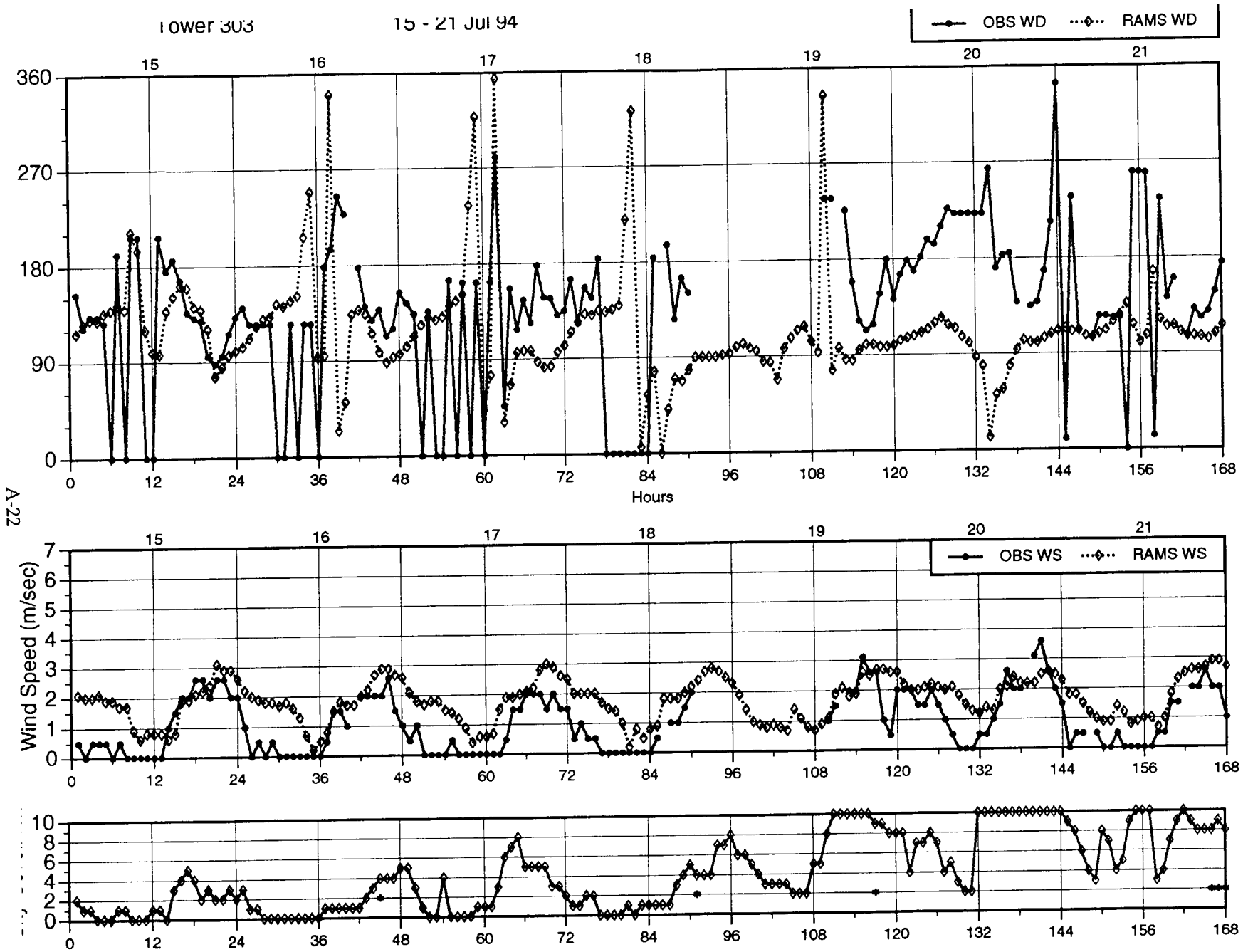
Tower 303
15 - 21 Jul 94
OBS WD
RAMS WD
15
16
17
18
19
20
21
360
270
180
90
0
0
12
24
36
48
60
72
84
96
108
120
132
144
156
168
Hours
OBS WS
RAMS WS
Wind Speed (m/sec)
7
6
5
4
3
2
1
0
10
8
6
4
2
0

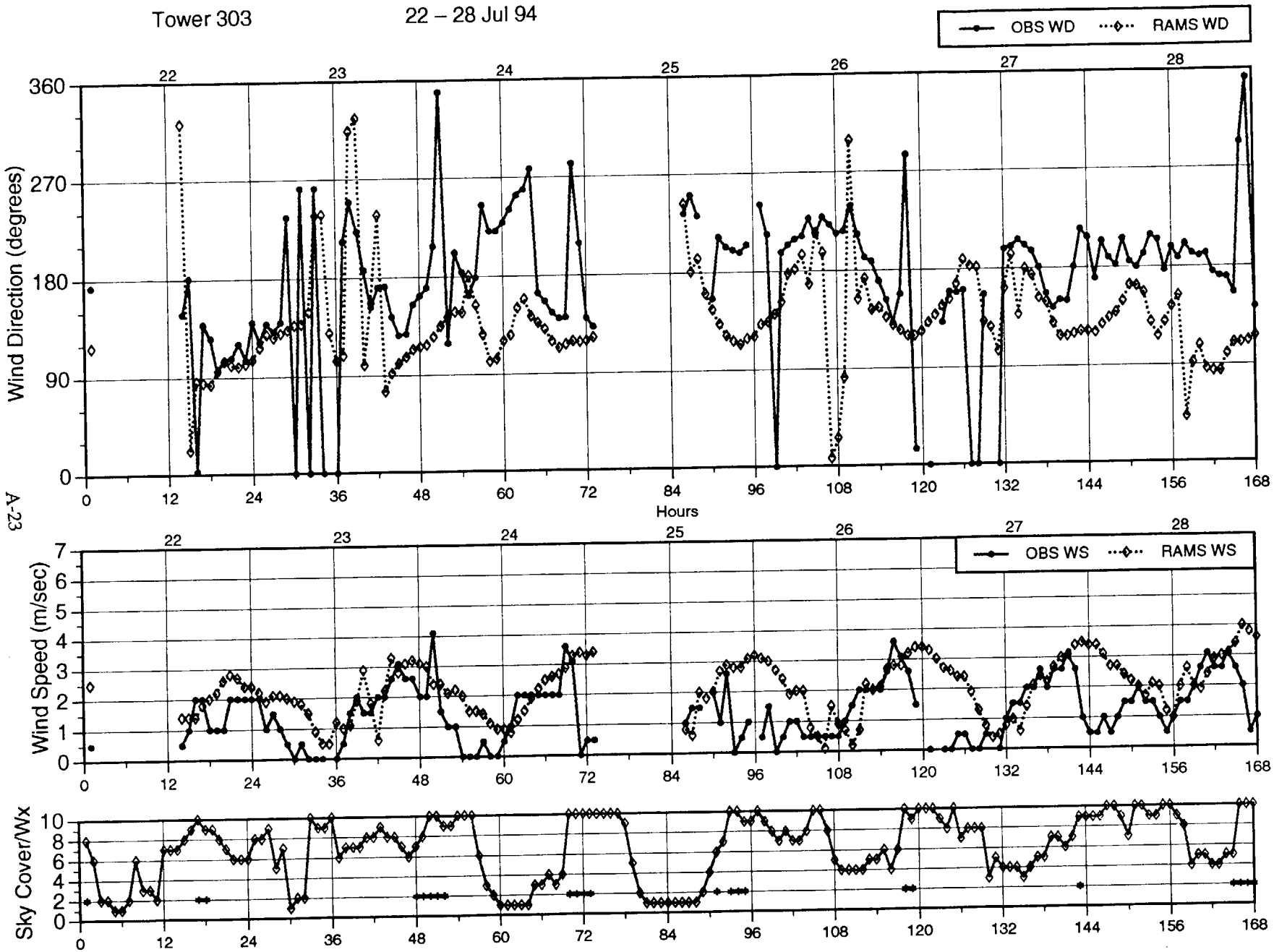
Tower 303
22 – 28 Jul 94
OBS WD
RAMS WD
Wind Direction (degrees)
360
270
180
90
0
22
23
24
25
26
27
28
0
12
24
36
48
60
72
84
96
108
120
132
144
156
168
Hours
OBS WS
RAMS WS
Wind Speed (m/sec)
7
6
5
4
3
2
1
0
Sky Cover/Wx
10
8
6
4
2
0

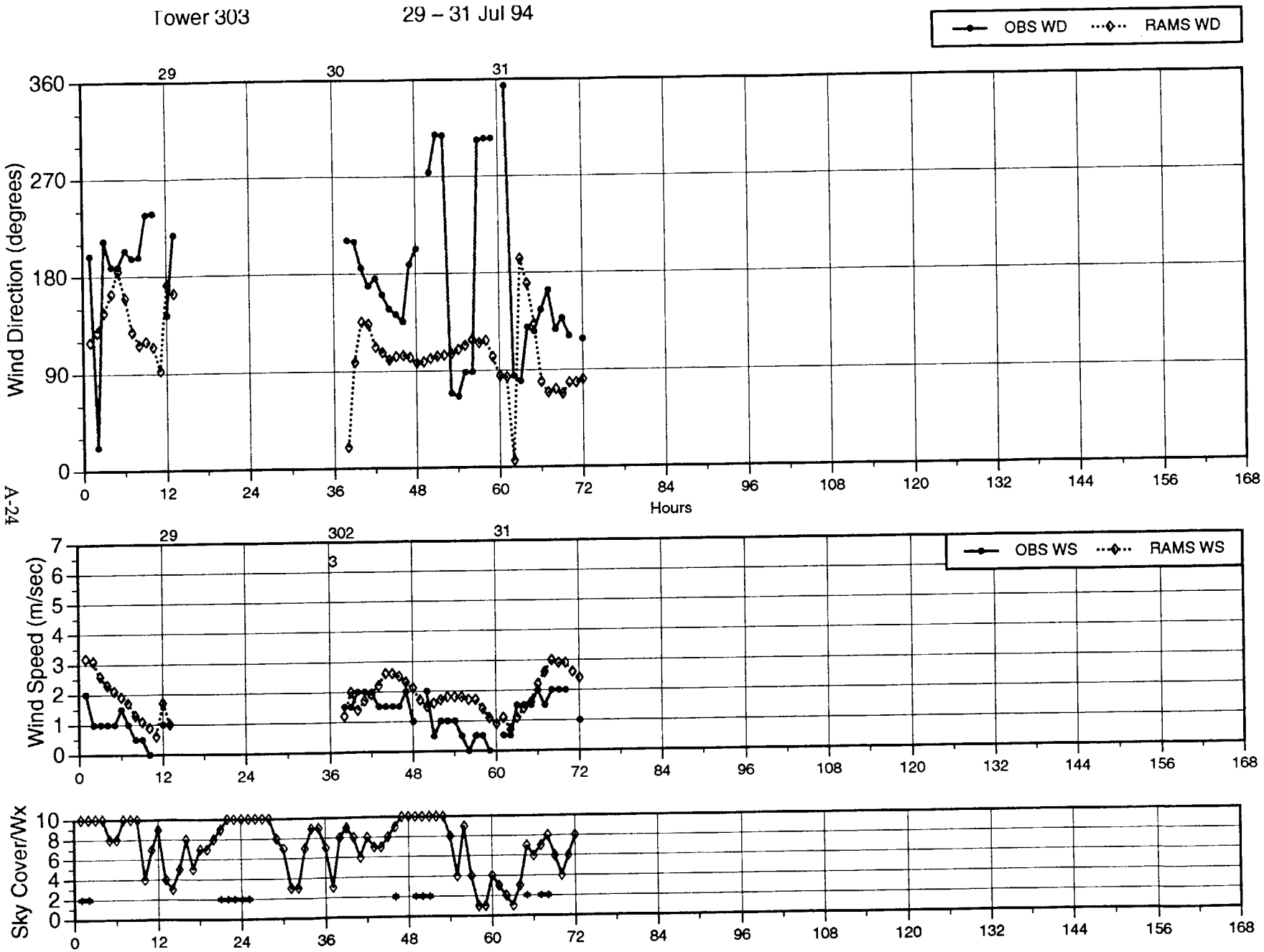
Tower 303
29 – 31 Jul 94
OBS WD
RAMS WD
Wind Direction (degrees)
360
270
180
90
0
29
30
31
0
12
24
36
48
60
72
84
96
108
120
132
144
156
168
Hours
OBS WS
RAMS WS
Wind Speed (m/sec)
7
6
5
4
3
2
1
0
29
302
3
31
Sky Cover/Wx
10
8
6
4
2
0

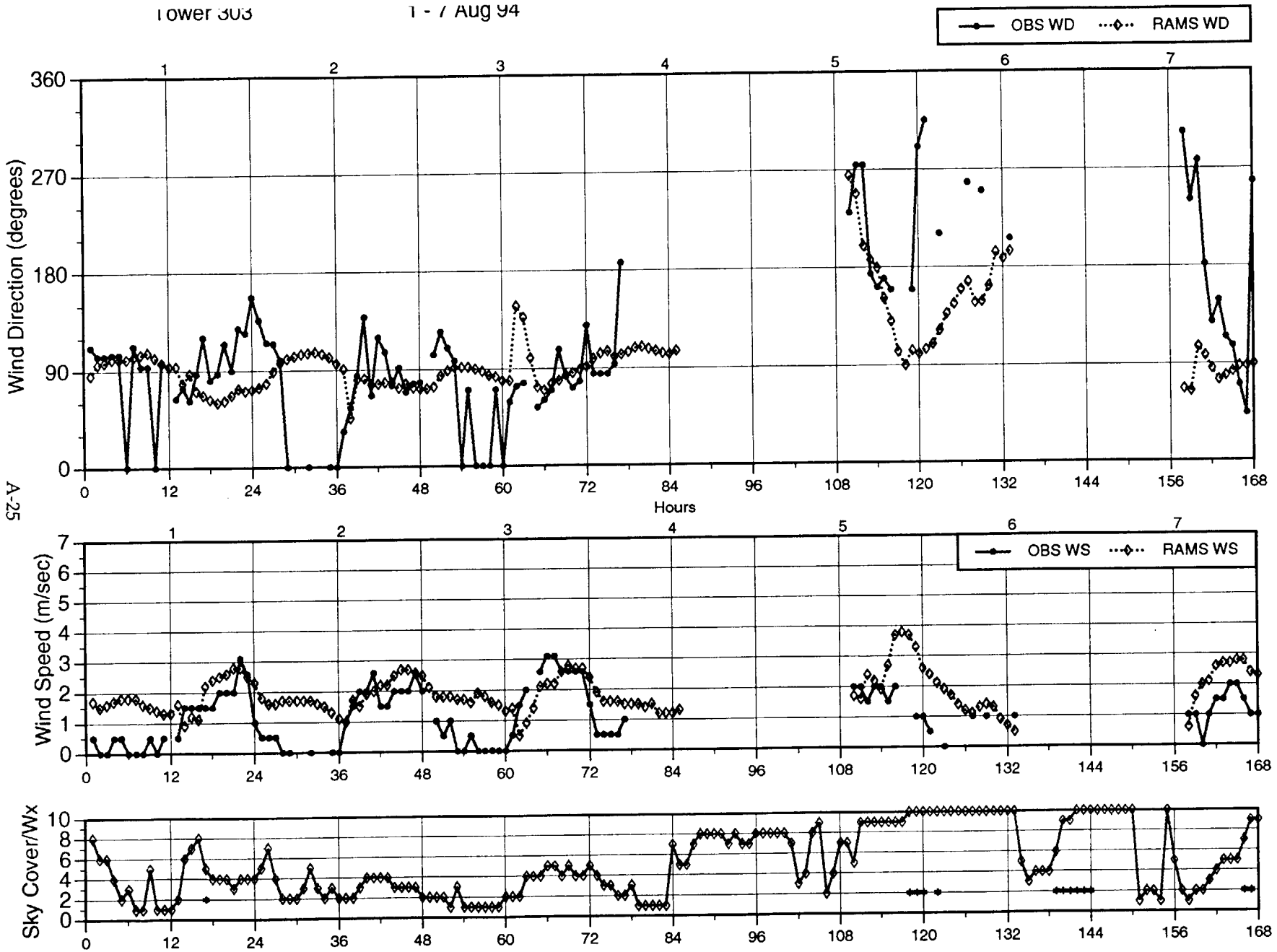
Tower 303
1 - 7 Aug 94
OBS WD
RAMS WD
Wind Direction (degrees)
360
270
180
90
0
1
2
3
4
5
6
7
0
12
24
36
48
60
72
84
96
108
120
132
144
156
168
Hours
OBS WS
RAMS WS
Wind Speed (m/sec)
7
6
5
4
3
2
1
0
Sky Cover/Wx
10
8
6
4
2
0

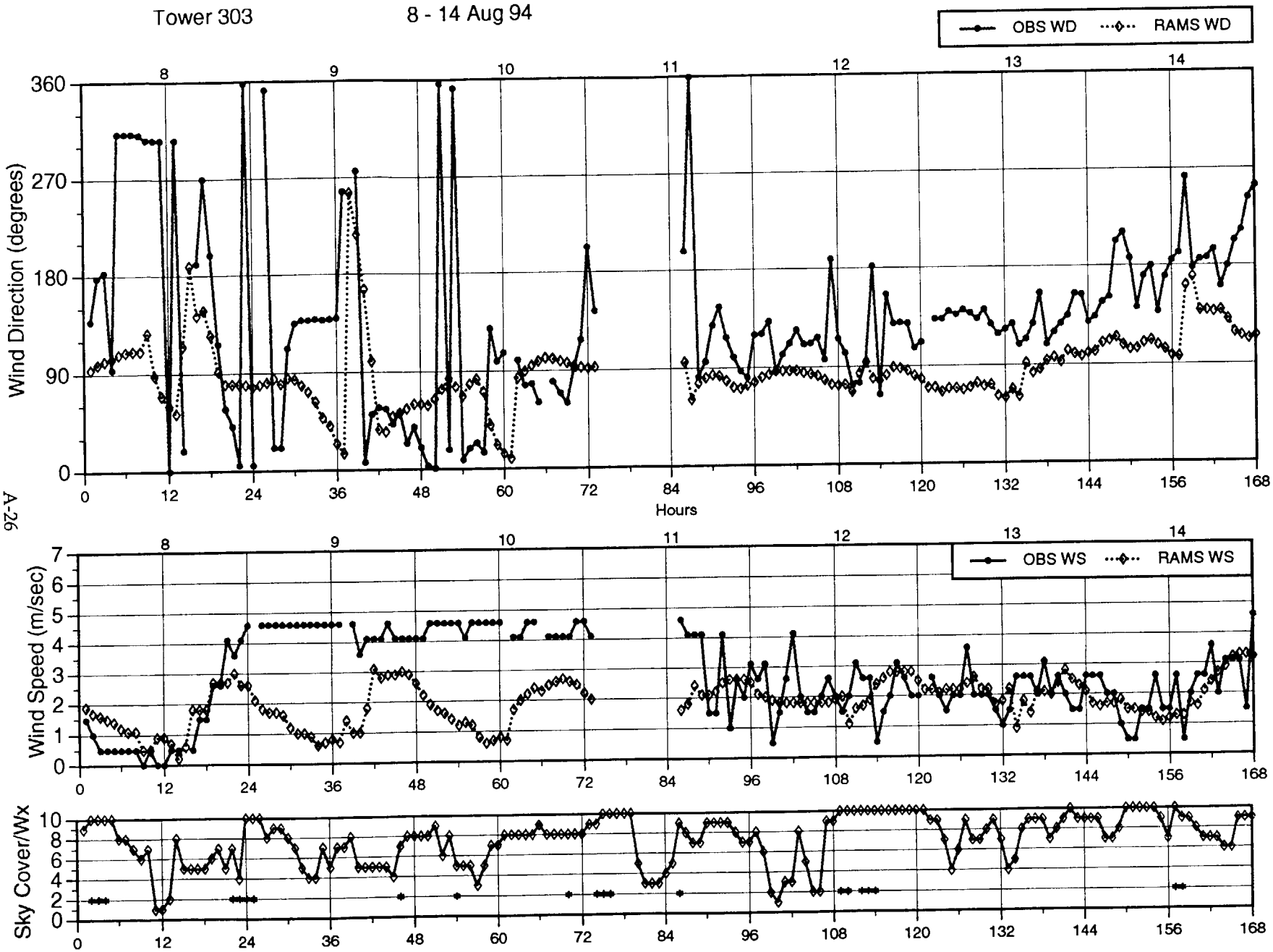
Tower 303
8 - 14 Aug 94
OBS WD
RAMS WD
Wind Direction (degrees)
360
270
180
90
0
8
9
10
11
12
13
14
0
12
24
36
48
60
72
84
96
108
120
132
144
156
168
Hours
OBS WS
RAMS WS
Wind Speed (m/sec)
7
6
5
4
3
2
1
0
Sky Cover/Wx
10
8
6
4
2
0

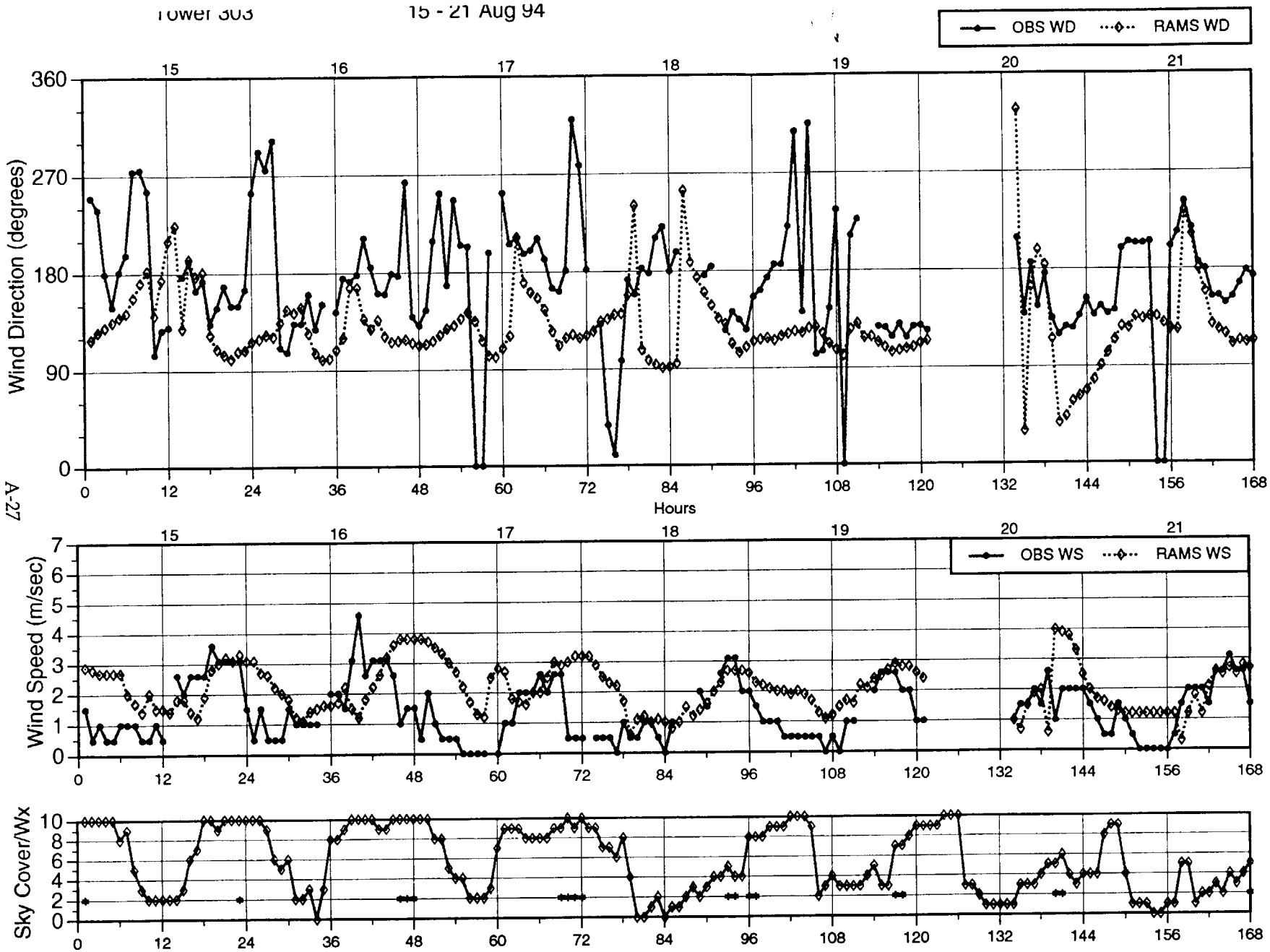
Tower 303
15 - 21 Aug 94
OBS WD
RAMS WD
Wind Direction (degrees)
360
270
180
90
0
15
16
17
18
19
20
21
0
12
24
36
48
60
72
84
96
108
120
132
144
156
168
Hours
OBS WS
RAMS WS
Wind Speed (m/sec)
7
6
5
4
3
2
1
0
Sky Cover/Wx
10
8
6
4
2
0

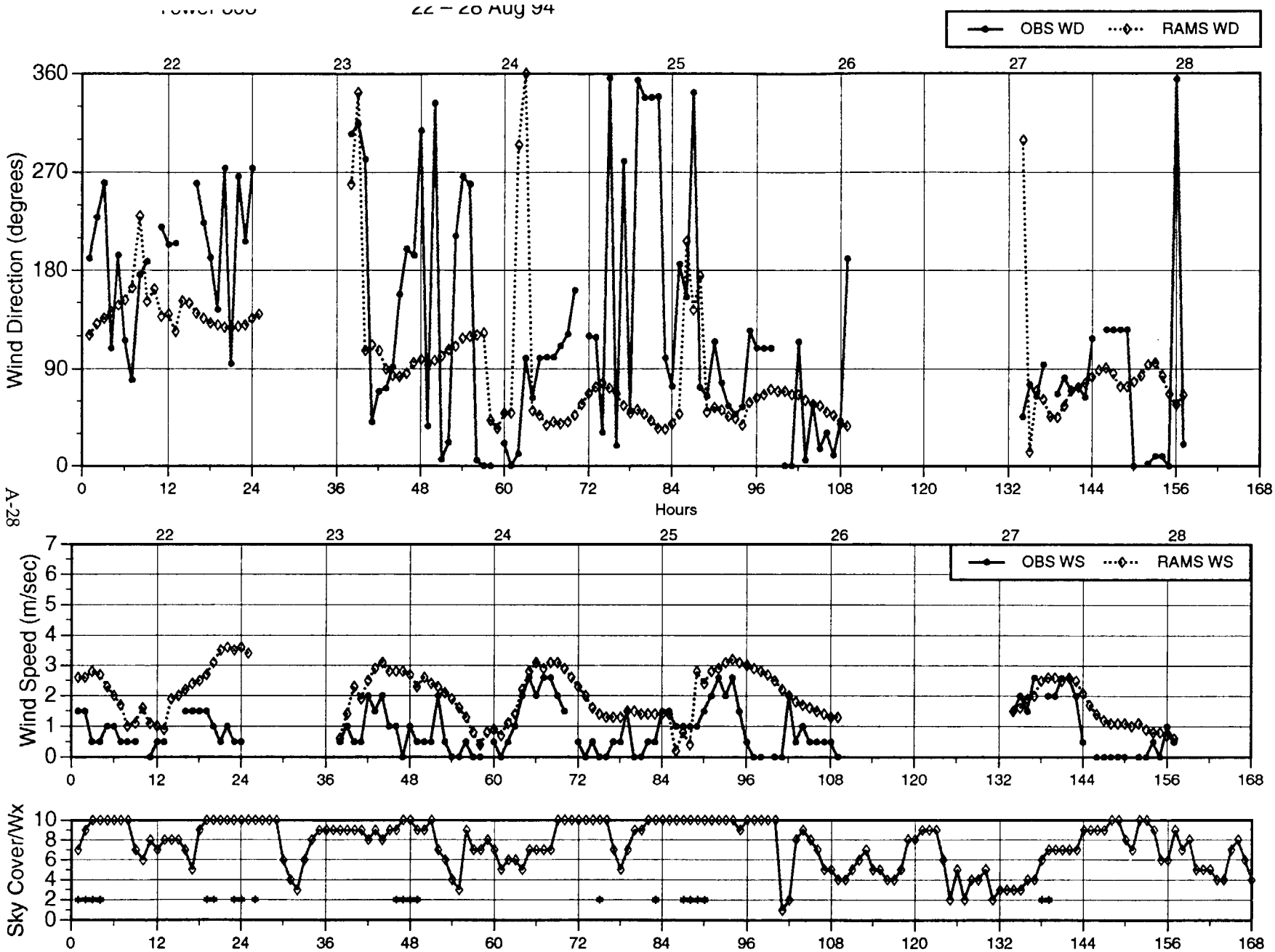
22 – 28 Aug 94
OBS WD
RAMS WD
Wind Direction (degrees)
360
270
180
90
0
22
23
24
25
26
27
28
0
12
24
36
48
60
72
84
96
108
120
132
144
156
168
Hours
OBS WS
RAMS WS
Wind Speed (m/sec)
7
6
5
4
3
2
1
0
Sky Cover/Wx
10
8
6
4
2
0

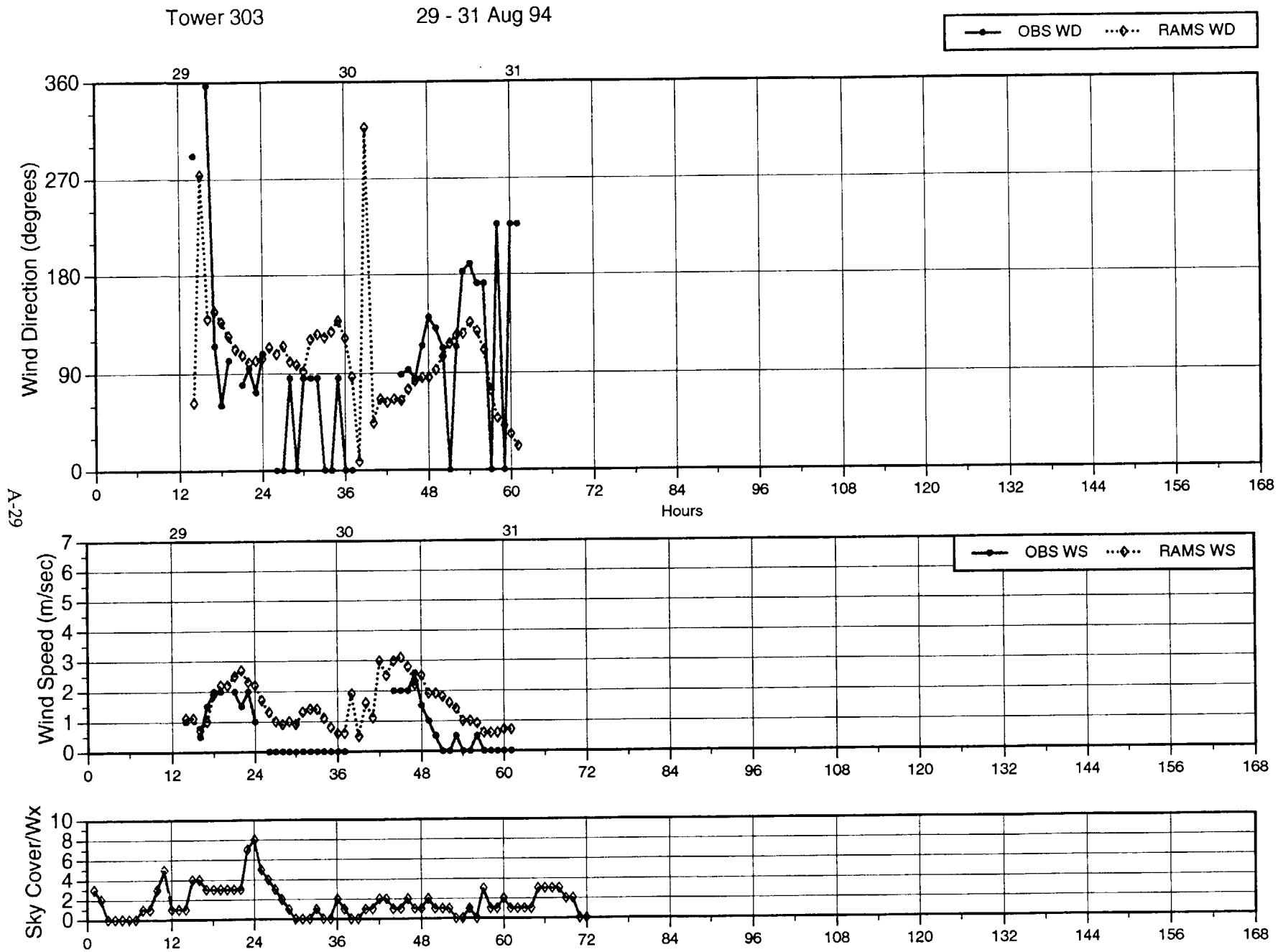
Tower 303
29 - 31 Aug 94
OBS WD
RAMS WD
Wind Direction (degrees)
360
270
180
90
0
29
30
31
0
12
24
36
48
60
72
84
96
108
120
132
144
156
168
Hours
OBS WS
RAMS WS
Wind Speed (m/sec)
7
6
5
4
3
2
1
0
Sky Cover/Wx
10
8
6
4
2
0

NOTICE

Mention of a copyrighted, trademarked or proprietary product, service, or document does not constitute endorsement thereof by the author, ENSCO, Inc., the Applied Meteorology Unit, the National Aeronautics and Space Administration, or the United States Government. Any such mention is solely for the purpose of fully informing the reader of the resources used to conduct the work reported herein.

REPORT DOCUMENTATION PAGE

Form Approved
OMB No. 0704-0188

1. AGENCY USE ONLY (Leave Blank)	2. REPORT DATE	3. REPORT TYPE AND DATES COVERED
	June 1996	Contractor Report

4. TITLE AND SUBTITLE
Final Report on the Evaluation of the Emergency Response Dose Assessment System (ERDAS)

5. FUNDING NUMBERS
C-NAS10-11844

6. AUTHOR(S)
Randolph J. Evans, Winifred Lambert, John Manobianco, Gregory Taylor, Mark Wheeler, and Ann Yersavich

7. PERFORMING ORGANIZATION NAME(S) AND ADDRESS(ES)
ENSCO, Inc., 445 Pineda Court, Melbourne, FL 32940

8. PERFORMING ORGANIZATION REPORT NUMBER
ARS-96-039

9. SPONSORING/MONITORING AGENCY NAME(S) AND ADDRESS(ES)
NASA, John F. Kennedy Space Center, Code PH-B3, Kennedy Space Center, FL 32899

10. SPONSORING/MONITORING AGENCY REPORT NUMBER
NASA CR-201353

11. SUPPLEMENTARY NOTES
Subject Cat.: #47 (Weather Forecasting)

12A. DISTRIBUTION/AVAILABILITY STATEMENT
Unclassified - Unlimited

12B. DISTRIBUTION CODE

13. ABSTRACT (Maximum 200 Words)

This report documents the Applied Meteorology Unit's evaluation of the Emergency Response Dose Assessment System (ERDAS). Mission Research Corporation/ASTER developed ERDAS for the Air Force for the purpose of providing emergency response guidance to operations at KSC/CCAS in case of an accidental hazardous material release or an aborted vehicle launch. ERDAS includes two major software systems: the Regional Atmospheric Modeling System (RAMS), and the Hybrid Particle and Concentration Transport (HYPACT) model. The evaluation of ERDAS included evaluation of the sea breeze predictions, comparison of launch plume location and concentration predictions, case study of a toxic release, evaluation of model sensitivity to varying input parameters, evaluation of the user interface, assessment of ERDAS's operational capabilities, and comparison of the ERDAS models to Ocean Breeze Dry Gulch diffusion model.

Some of the principal conclusions of the ERDAS meteorological model evaluation were: RAMS predicted the 3-dimensional wind field and sea breeze structure reasonably well during non-cloudy conditions. HYPACT-predicted plume trajectory from 3 May 94 Titan launch closely followed the observed trajectory with some variation over time. Comparing diffusion model predictions made by the OBDG model and the ERDAS models in the limited comparison study showed that using the ERDAS models for non-continuous spill scenarios improves launch processing availability in 19 of 29 cases. The report list enhancements required for ERDAS as the system is transitioned to operations.

14. SUBJECT TERMS
Dispersion, Diffusion, Emergency Response, Mesoscale Modeling, Sea Breeze, Launch Plume, 3-Dimensional Winds, RAMS, HYPACT, ERDAS

15. NUMBER OF PAGES 184

16. PRICE CODE

17. SECURITY CLASSIFICATION OF REPORT	18. SECURITY CLASSIFICATION OF THIS PAGE	19. SECURITY CLASSIFICATION OF ABSTRACT	20. LIMITATION OF ABSTRACT
UNCLASSIFIED	UNCLASSIFIED	UNCLASSIFIED	NONE